



Scattering Amplitudes and Form Factors in Effective Field Theories

STEFANO DE ANGELIS

Supervisors

PROF. ANDREAS BRANDHUBER

PROF. GABRIELE TRAVAGLINI

November 29, 2022

Centre for Theoretical Physics
School of Physical and Chemical Sciences
Queen Mary University of London

I, Stefano De Angelis, confirm that the research included within this thesis is my own work or that where it has been carried out in collaboration with or supported by others, that this is duly acknowledged below and my contribution indicated. Previously published material is also acknowledged below.

I attest that I have exercised reasonable care to ensure that the work is original, and does not to the best of my knowledge break any UK law, infringe any third party's copyright or other Intellectual Property Right, or contain any confidential material.

I accept that the College has the right to use plagiarism detection software to check the electronic version of the thesis.

I confirm that this thesis has not been previously submitted for the award of a degree by this or any other university.

The copyright of this thesis rests with the author and no quotation from it or information derived from it may be published without the prior written consent of the author.

Details of collaboration and publications

This thesis covers the original research that I carried out during my PhD program in collaboration with my supervisors, together with Manuel Accettulli Huber, and is based on the four papers where the results were originally presented. These are

- M. Accettulli Huber, A. Brandhuber, S. De Angelis and G. Travaglini, “Complete Form Factors in Yang-Mills from Unitarity and Spinor Helicity in Six Dimensions,” *Phys. Rev. D* **101** (2020) no.2, 026004 [arXiv:1910.04772 [hep-th]],
- M. Accettulli Huber, A. Brandhuber, S. De Angelis and G. Travaglini, “Eikonal phase matrix, deflection angle and time delay in effective field theories of gravity,” *Phys. Rev. D* **102** (2020) no.4, 046014 [arXiv:2006.02375 [hep-th]],
- M. Accettulli Huber and S. De Angelis, “Standard Model EFTs via on-shell methods,” *JHEP* **11** (2021), 221 [arXiv:2108.03669 [hep-th]],
- S. De Angelis, “Amplitude bases in generic EFTs,” [arXiv:2202.02681 [hep-th]].

In addition to the above, during my PhD program, I have also worked on projects which are connected to the main line of research presented in this thesis but have not been included in the text

- M. Accettulli Huber, A. Brandhuber, S. De Angelis and G. Travaglini, “Note on the absence of R^2 corrections to Newton’s potential,” *Phys. Rev. D* **101** (2020) no.4, 046011 [arXiv:1911.10108 [hep-th]],
- M. Accettulli Huber, A. Brandhuber, S. De Angelis and G. Travaglini, “From amplitudes to gravitational radiation with cubic interactions and tidal effects,” *Phys. Rev. D* **103** (2021) no.4, 045015 [arXiv:2012.06548 [hep-th]],

and an additional project, in collaboration with Lorenzo Bianchi and Marco Meineri, with a fairly disconnected focus

- L. Bianchi, S. De Angelis and M. Meineri, “Radiation, entanglement and islands from a boundary local quench,” [arXiv:2203.10103 [hep-th]].

Acknowledgements

First of all, I would like to thank my advisors, Andi and Gab, for introducing me to the world of scattering amplitudes, and for the continuous support both on the scientific and personal side throughout the last four years. Thank you for everything!

I would like to thank everybody at QMUL for the great environment during the four years of my PhD: all my colleagues, Joe, Rodolfo, Arnau, Chris, Ray, Zoltan, Linfeng, Luigi, Nadia, Nejc, Ricardo, David, Enrico, Gergely, Marcel, Rajath, Rashid, Shun-Qing, Adrian, George, Sam, Lewis, Chinmaya, Kymani, Tancredi and Mitchell, all the academics Bill, Chris, Congkao, Costis, David, David, Matthew, Ricardo, Rodolfo, Sanjaye, Steve and all the postdocs with whom I had the pleasure of interacting Gianluca, Jung-Wook and Silvia.

Special thanks go to all the people I had the pleasure to work with over the past years, Christophe, Gang, Gauthier, Graham, Yael, Marco, Micheal, and Josh. In particular, I would like to thank two people who I must regard as mentors: my master thesis advisor Gianguido, for having introduced me to the world of research in theoretical physics, and Lorenzo, for introducing me to the fantastic world of CFTs, teaching me about various aspects of scattering amplitudes, guiding me in every step of my PhD and supporting me in the darkest moments. Finally, I want to thank Manuel, my buddy throughout my first three years of research, who put up with my rough manners more than anyone else, supported me at any time in the past four years and has been the best flatmate I have ever had.

Thanks to my friends Andrea, Giulia, Lorenzo and Lorenzo, with whom I shared the years of my master's degree and were always there when I needed advice or I had questions. We are still waiting for Madrid...

I would like to thank all of the SAGEX PhD students, Andreas, Anne, Canxin, Davide, Gabriele, Ingrid, Kays, Lorenzo, Luke, Marco, Nikolai, Riccardo, Sebastian, for the fun at every meeting, but also for the physics chats. Everything is still fine!

My projects have received funding from the European Unions Horizon 2020 research and innovation programme under the Marie Skłodowska-Curie grant agreement No. 764850 "SAGEX". I would like to thank everyone who helped run this network and organise all the virtual and in-person events.

Non posso non ringraziare anche tutte le persone che mi sono state vicine prima e durante il dottorato, e probabilmente ci saranno ancora per molto. Prima di tutto, la mia famiglia: i miei nonni e mia madre, che sono stati il faro che ha guidato la mia vita col sudore, l'onestà e l'amore, i miei cuginetti Nico, Emanuele, Sara, Matteo e Lavinia, e i miei zii Fiorenzo e Milena, che sono la mia gioia ogni volta che torno a casa.

Voglio ringraziare tutti i miei amici, che mi hanno sostenuto in ogni mia scelta, mi hanno spronato a credere di poter fare sempre di più e, soprattutto, mi hanno fatto vivere momenti indimenticabili e continuano a farlo tutti i giorni. Prima di tutto a Davide, che per noi ha dato ogni cosa e che io non sarò mai capace di ripagare neanche minimamente, grazie! A Bumbum, Chicco e Picetto, che nei momenti più bui mi hanno fatto capire cosa significa l'amicizia, grazie! A Makako, Paolo, Sellicchia e Riccardo, che mi hanno fatto capire che l'amicizia è immutabile anche quando non ci si sente così spesso, grazie! A Alex, Spillo e Umberto, che non riescono a capire quando è il momento di andare a casa e non lasciano andare neanche me, grazie! Ai piccoli Naser e Saverio, che mi mantengono giovane, grazie! A Sara, che mi ha insegnato a vedere il

bello e apprezzare la vita in ogni sua aspetto e che ha illuminato i miei periodi più bui con i suoi sorrisi, grazie! A tutti i ragazzi e le ragazze della Casa del Popolo di Teramo, a tutti i miei amici e le mie amiche di Teramo, grazie!

Abstract

The central theme of the thesis is the application of modern on-shell techniques to compute Scattering Amplitudes and Form Factors in various Effective Field Theories. In particular, we apply such techniques in the context of the Standard Model Effective Field Theories, focusing on the renormalisation group evolution of irrelevant operators, and the study of the classical binary problem in gravitational theories, beyond General Relativity including higher derivative interactions.

We first show how to find a basis of EFT interactions from a purely on-shell point of view. From these EFT building blocks, any tree-level amplitude can be computed using a recursive algorithm which requires only the knowledge of lower-point amplitudes. Starting from these results, modern (generalised) unitarity techniques allow for the computations of higher loop amplitudes which can be used to characterise precision observables both for gravitational waves and for collider experiments. We will focus on the computation of form factors in the context of Standard Model Effective Field Theory which allowed us to compute for the first time the one-loop mixing matrix for all the dimension-eight operators in the theory. Then, we will show how to compute the deflection angle and the time delays induced by higher-derivative corrections to the Einstein-Hilbert action from the eikonal form of gravitational scattering amplitudes.

Contents

1	Introduction to Scattering Amplitudes	11
1.1	A definition for the S-matrix	11
1.2	Unitarity and locality of the S-matrix	13
1.2.1	Tree-level amplitudes from BCFW-like recursion relations	15
1.2.2	Loop-level amplitudes from generalised unitarity	17
1.3	Form factors and low energy expansion	19
1.4	Applications of BCFW-like recursion relations	20
1.5	Modern applications	23
1.6	Summary of the thesis	25
2	Minimal Amplitudes Bases for EFTs	27
2.1	The massless basis	28
2.1.1	Kinematic structures from graphs	28
2.1.2	Schouten identities	29
2.1.3	Momentum conservation	31
2.1.4	A summary of the algorithm	33
2.1.5	Checking the algorithm	35
2.2	The massive basis	36
2.2.1	The Massive Little Group	36
2.2.2	Equations of Motion	37
2.2.3	Momentum Conservation	40
2.2.4	A summary of the algorithm	43
2.3	Applications	44
2.3.1	The on-shell classification of SMEFT operators	45
2.3.2	$D^{2n}F^4$ interactions in gauge theories	49
2.3.3	Five-point interactions between W , Z and γ	51
2.3.4	Spin-tidal interactions in gravitational EFTs	53
3	Bootstrapping Tree-Level Amplitudes	57
3.1	The Standard Model from on-shell techniques	57

3.1.1	Lie Algebras from Tree-Level Unitarity	58
3.2	Bootstrapping the tree-level amplitudes	60
3.2.1	Higher-point Amplitudes without Recursion Relations	61
3.2.2	Generalisations and application to the heavy-mass EFT	69
3.3	Anomalies from Amplitudes \Leftarrow Locality and Unitarity	72
4	Form Factors from Unitarity in 6D	77
4.1	The Dimensional Reconstruction Technique	79
4.1.1	One-Loop Dimensional Reconstruction	79
4.1.2	An L -loop Generalisation	81
4.2	Tree-Level Amplitudes and Form Factors	85
4.2.1	$\text{Tr } F^2$ Form Factors	86
4.2.2	$\text{Tr } F^3$ Form Factors	88
4.2.3	$\text{Tr } F^4$ and Higher Dimensional Form Factors	90
4.3	One-Loop Form Factors	92
4.3.1	The Minimal $\text{Tr } F^2$ Form Factors	92
4.3.2	The Non-Minimal $\text{Tr } F^2$ Form Factor	94
4.3.3	The Minimal $\text{Tr } F^3$ Form Factors	96
4.3.4	The Non-Minimal $\text{Tr } F^3$ Form Factor	97
4.3.5	The Minimal $\text{Tr } F^4$ Form Factors	100
5	One-Loop Anomalous Dimensions in the SMEFT	105
5.1	The UV anomalous mass dimension matrix at leading order	106
5.1.1	Infrared collinear anomalous dimensions in the Standard Model	107
5.2	The Higgs production in association with a W boson	109
6	Gravitational EFTs and the Eikonal Limit	121
6.1	Gravity with higher-derivative couplings	122
6.2	Physical observables from the eikonal phase matrix	124
6.2.1	Kinematics of the scattering	124
6.2.2	Eikonal phase, deflection angle and time delay	126
6.3	The relevant scattering amplitudes	127
6.3.1	Four-point scalar/graviton scattering in EH gravity	128
6.3.2	Four-point scalar/graviton scattering in $\text{EH} + R^3$	129
6.3.3	Four-point scalar/graviton scattering in $\text{EH} + R^4$	129
6.3.4	Scattering with the FFR interaction	132
6.4	Eikonal phase matrix, deflection angle and time delay	135
6.4.1	Graviton deflection angle and time delay in Einstein-Hilbert gravity	136
6.4.2	Graviton deflection angle and time delay in $\text{EH} + R^3$	138

6.4.3	Graviton deflection angle and time delay in $\text{EH} + R^4$	141
6.4.4	Graviton deflection angle and time delay in $\text{EH} + FFR$	142
6.4.5	Photon deflection angle and time delay in $\text{EH} + FFR$	143
7	Conclusions and outlook	147
A	Spinor Helicity Formalism	151
A.1	Four-Dimensional Spinor Helicity Formalism	151
A.2	Six-Dimensional Spinor Helicity Formalism	153
A.3	Momentum Twistors and Rational Kinematics	156
A.4	Finite Field Arithmetic	157
B	SMEFT Conventions and Notations	161
B.1	The Standard Model gauge group	161
B.2	Three-point amplitudes in the Standard Model	162
C	Tree-level Amplitudes in 6D	165
C.1	Six-Dimensional Scattering Amplitudes	165
C.1.1	Non-Minimal Form Factors	167
D	Feynman Integrals	171

Chapter 1

Introduction to Scattering Amplitudes

In this chapter, we are going to introduce the definition of the S-matrix and its main properties, which will be fundamental in understanding the topics presented in the following chapters of this thesis. In particular, the elements of the S-matrix, which are called Scattering Amplitudes, are mathematical objects encoding the observables in scattering experiments.

The typical set-up of collider experiments consists of two collections of particles (non-interacting within each cluster), *in states*, which are initially separated on a macroscopic scale and are made to interact at microscopic scales. The nature of the initial particles can be completely different from the results of this scattering experiment, which is the third bunch of (non-interacting) particles, *out states*. The mathematical object which describes the probability that, given an initial state, we find a final state in a specific kinematic configuration is what we called the Scattering Amplitude. This definition makes manifest that such objects encode most of the features of relativistic quantum mechanics which is relevant for experiments in high-energy physics.

The last thirty years have seen a great development of computational techniques and more theoretical structure in the study of the S-matrix, in perturbation theory. Some of these new results are the main subject of this thesis and are collectively referred to as *on-shell methods*. For a comprehensive review of this topic, we refer to [1–7].

1.1 A definition for the S-matrix

Following [8], the elements of the S-matrix are the overlap between an *in* and an *out states*:

$$S_{\alpha \rightarrow \beta} = \langle \Psi_{\beta}^{\text{out}} | \Psi_{\alpha}^{\text{in}} \rangle, \quad (1.1)$$

where such states (in the Heisenberg picture) are defined in terms of Møller operators $\Omega(t)$, which intertwine states in a free theory with those of an interacting theory. In particular,

$$|\Psi_{\alpha}^{\text{in/out}}\rangle = \Omega(\mp\infty)|\Phi_{\alpha}\rangle, \quad (1.2)$$

where

$$\Omega(t) = e^{iHt} e^{-iH_0 t}, \quad (1.3)$$

where H is the Hamiltonian of the full theory, H_0 is the Hamiltonian of the free theory and $|\Phi_\alpha\rangle$ are eigenstates of the H_0 :

$$\begin{aligned} H_0|\Phi_\alpha\rangle &= E_\alpha|\Phi_\alpha\rangle, \\ \langle\Phi_\beta|\Phi_\alpha\rangle &= \delta(E_\alpha - E_\beta), \end{aligned} \quad (1.4)$$

where we ignored additional quantum numbers identifying the multi-particle states and

$$E_\alpha = \sum_{i \in \alpha} E_{\vec{p}_i} = \sum_{i \in \alpha} \sqrt{m_i^2 + \vec{p}_i^2}. \quad (1.5)$$

In particular, the $|\Phi_\alpha\rangle$ can be defined as vectors in a Fock space with a Lorentz-invariant vacuum $|0\rangle$ (of the free theory, with $\langle 0|0\rangle = 1$). For example, if we are dealing only with bosons we can write vacuum and the one-particle states in terms of annihilation and creation operators $a_\sigma(p)$ and $a_\sigma^\dagger(p)$ which satisfy canonical commutation relations

$$\left[a_\sigma(p), a_{\sigma'}^\dagger(q) \right] = (2\pi)^{(d-1)} 2E_{\vec{p}} \delta_{\sigma\sigma'} \delta^{(d-1)}(\vec{p} - \vec{q}), \quad (1.6)$$

where σ refers to the quantum number characterising the state. The annihilation and creation operators act on the vacuum as follow:

$$a_\sigma(p)|0\rangle = 0, \quad (1.7)$$

and

$$|p^\sigma\rangle = a_\sigma^\dagger(p)|0\rangle. \quad (1.8)$$

The full Hilbert space of the theory is described by the Fock space of multi-particle states, which is the direct sum of n -particle states obtained acting multiple times with creating operators. Then the completeness relation read:

$$\mathbf{1} = |0\rangle\langle 0| + \sum_{n=1}^{\infty} \sum_{\{\sigma\}} \int d\mu_n |p_1^{\sigma_1}, \dots, p_n^{\sigma_n}\rangle \langle p_1^{\sigma_1}, \dots, p_n^{\sigma_n}|, \quad (1.9)$$

where $d\mu_n$ is the Lorentz-invariant phase space measure

$$d\mu_n = \frac{1}{s_1! \dots s_m!} \prod_{i=1}^n \frac{d^d p_i}{(2\pi)^{d-1}} \Theta(E_{\vec{p}_i}) \delta(p_i^2 - m_i^2), \quad (1.10)$$

$s_i!$ are some Bose symmetry factors and Θ is the Heaviside theta.

A number of properties follow immediately from this definition of the S-matrix, most of which have a long history and go back to the seminal works of Wheeler [9], Heisenberg [10] and the S-matrix bootstrap approach (for a review, see [11–13]). We are not going to present an extended review of the topic, but only mention those properties which will be essential to understanding the following chapters.

- The S-matrix is a Poincaré invariant object. In particular, translation invariance implies *momentum conservation* and the elements of the S-matrix can always be written as

$$S_{\alpha \rightarrow \beta} = (2\pi)^d \delta^{(d)} \left(\sum_{i \in \beta} p_i - \sum_{j \in \alpha} p_j \right) \mathcal{S}(\alpha \rightarrow \beta), \quad (1.11)$$

where $\mathcal{S}(\alpha \rightarrow \beta)$ should always be thought as a function defined of the support of the momentum-conserving delta function.

- *Lorentz invariance* also implies that the S-matrix elements are functions only of invariant quantities, like the Mandelstam invariants $s_{i_1 \dots i_n} = \left(\sum_{j=1}^n p_{i_j} \right)^2$ and the masses of the asymptotic states $p_i^2 = m_i^2$.
- Scattering amplitudes are covariant under *little group transformations* of the asymptotic states, in case we are dealing with spinning particles. Then any scattering amplitude can be written as

$$\mathcal{S}(\alpha \rightarrow \beta) = \sum_i \mathcal{R}_{\alpha \rightarrow \beta}^{(i)} \cdot \mathcal{T}_{\alpha \rightarrow \beta}^{(i)}, \quad (1.12)$$

where $\mathcal{R}_{\alpha \rightarrow \beta}^{(i)}$ are rational function of some spinorial variables which encodes the correct transformation properties under little group transformations, while $\mathcal{T}_{\alpha \rightarrow \beta}^{(i)}$ can include polylogarithms, elliptic or more complicated functions of the Mandelstam invariants and the masses. The correct variables to describe $\mathcal{R}_{\alpha \rightarrow \beta}^{(i)}$ are commonly referred to as Spinor Helicity variables and they are specific to the space-time dimensions d (see Appendix A for an introduction to spinor helicity formalism in four and six dimensions). The little group is defined as the subgroup of $\text{SO}(1, d-1)$ which leaves the momentum of the corresponding particle invariant. We can write momenta in a form which makes this invariance manifest. Indeed, we can always write a momentum in terms of two spinors

$$\not{p} = p_\mu \gamma^\mu = \lambda^I \tilde{\lambda}_I, \quad (1.13)$$

where the γ -matrices generate a Clifford algebra $\{\gamma^\mu, \gamma^\nu\} = \eta^{\mu\nu} \mathbf{1}$. The spinors λ and $\tilde{\lambda}$ are matrices transforming in some (spin) representations of the (double) covering of the Lorentz group and of the little group (the latter labelled by the index I). These spinor helicity variables, properly symmetrised to form the correct little group representations, define the rational terms $\mathcal{R}_{\alpha \rightarrow \beta}^{(i)}$.

- In natural units, the *mass dimension* of an n -point scattering amplitude, is

$$[\mathcal{A}_n] = d - n. \quad (1.14)$$

This property will be fundamental in the following chapter, where we consider a perturbative expansion of the scattering amplitudes and we focus on the tree level. Indeed, tree-level scattering amplitudes are particularly simple rational functions as we will show in the following section. By definition, we have $[p^\mu] = 1$, $[\lambda] = \frac{1}{2}$ and $[\tilde{\lambda}] = \frac{1}{2}$.

1.2 Unitarity and locality of the S-matrix

Although the properties we mentioned in the previous section and many other features of the scattering amplitude hold at the non-perturbative level, in the following we will focus only on perturbation theory around a free theory. In particular, in this section, we are going to mention two of the fundamental properties of scattering amplitudes, namely *unitarity* and *locality*. Such properties are made manifest in the standard approach to perturbation theory in QFT, through the Feynman diagrams approach. On the other hand, the ordinary formulation of QFT suffers from a number of *gauge redundancies*

when we introduce particles with spin higher than one-half, which are not present in the fully on-shell approach. In fact, as we will review in Chapter 3, gauge symmetries are recovered from the above-mentioned principles of unitarity and causality.

Unitarity is one of the axioms of quantum mechanics and states that the time-evolution of a system is governed by a unitarity operator, *i.e.* which preserves the inner product of physical states. On the other hand, locality has no unique definition. One possibility is to identify it with the *cluster decomposition principle* [8], which is the requirement that the results of two independent experiments far apart from each other must be uncorrelated (unless we put some special effort into preparing them in an entangled state). In the scattering amplitudes, these two properties appear hand-in-hand: in fact, locality dictates the position of the singularities of the amplitudes, while unitarity fixes the “value” of the amplitudes across the singularities. In particular, long-range interactions correspond to non-analytic terms in the scattering amplitudes, which in turn must correspond to some propagating internal particle going on shell. When a single exchanged particle goes on-shell, the amplitude develops a simple pole, while an intermediate multi-particle state corresponds to a branch point. The residues and the discontinuities are given by properly multiplying the corresponding lower-point and/or lower loop amplitudes, in the perturbative expansion, and integrating over the Lorentz-invariant phase space of the internal particles.

In the following, we show how such properties arise in the scattering amplitudes and, in particular, we focus on the single particle exchange, which is all we need for tree-level amplitudes, *i.e.* usually the leading terms in the perturbative expansion. Beyond leading order, old-fashion unitarity is not the most efficient method to construct loop-level amplitudes. Indeed, such an approach can be improved if we combine the structures of scattering amplitudes with some insights coming from Feynman diagrams (and Feynman integrals), as we will show in the next sections.

We start considering the S-operator

$$S = \Omega(+\infty)^\dagger \Omega(-\infty) , \quad (1.15)$$

which is unitary

$$S^\dagger S = \mathbf{1} . \quad (1.16)$$

We can also write the S-operator as a trivial contribution, which keeps track of disconnected terms in the scattering¹, plus a *transition operator* T which yields the non-trivial part of the scattering matrix:

$$S = \mathbf{1} + iT . \quad (1.17)$$

A *scattering amplitude* $\mathcal{A}(\alpha \rightarrow \beta)$ is defined as the expectation value of iT (up to a momentum conserving delta function):

$$i\langle \Phi_\beta | T | \Phi_\alpha \rangle = (2\pi)^d \delta^{(d)} \left(\sum_{i \in \beta} p_i - \sum_{j \in \alpha} p_j \right) \mathcal{A}(\alpha \rightarrow \beta) . \quad (1.18)$$

The unitarity of the S-operator can be written in terms of the T operator as

$$-i (T - T^\dagger) = T^\dagger T , \quad (1.19)$$

¹For example, when we consider a $3 \rightarrow 3$ scattering, the S-matrix must include the possibility to have disconnected $1 \rightarrow 1$ and $2 \rightarrow 2$ scattering processes.

which encodes most of the analytic structures of the scattering amplitudes. In particular, if we consider the expectation value of both the LHS and RHS and we insert the completeness relation in the product $T^\dagger T$ discarding all the multi-particle contributions we find

$$i\langle\Phi_\beta|T|\Phi_\alpha\rangle - i\langle\Phi_\beta|T^\dagger|\Phi_\alpha\rangle = -\sum_\sigma \int d\mu_1 \langle\Phi_\beta|T^\dagger|p^\sigma\rangle \langle p^\sigma|T|\Phi_\alpha\rangle + \dots \quad (1.20)$$

Using *crossing* (for example, see [11]) on the LHS, this equation brings to

$$\text{Re } \mathcal{A}(\alpha \rightarrow \beta) = -\pi \sum_\sigma \delta(s_\alpha - M_\sigma^2) \mathcal{A}(\alpha \rightarrow p^\sigma) \mathcal{A}^*(\beta \rightarrow p^\sigma) + \dots, \quad (1.21)$$

where $s_\alpha = (\sum_{i \in \alpha} p_i)^2$ and M_σ is the mass of the intermediate state $|p_\sigma\rangle$. A delta-function real part can be obtained from a simple pole (see, for example, the Chapter 24 of [14]):

$$\frac{i}{s_\alpha - M_\sigma^2 + i\epsilon} = \text{P} \frac{i}{s_\alpha - M_\sigma^2} + \pi \delta(s_\alpha - M_\sigma^2), \quad (1.22)$$

where P is the principal value² ³. Then, the residues on these simple poles are given by

$$\text{Res}_{s_{1\dots m}=M_\sigma^2} \mathcal{A}_n(p_1^{h_1} \dots p_n^{h_n}) = i f \sum_{s_I, h_I} \mathcal{A}_{m+1}(p_1^{h_1} \dots p_m^{h_m}, p_I^{h_I}) \mathcal{A}_{n-m+1}(p_I^{h_I} \rightarrow p_{m+1}^{h_{m+1}} \dots p_n^{h_n}), \quad (1.23)$$

where $f = (-1)^{\Delta s}$ with Δs the respective signature of the fermion ordering between the LHS and the RHS, s_I and h_I are the type and the helicity of the intermediate state propagating⁴. This equation will be fundamental in Chapter 3 in the bootstrap of tree-level amplitudes in generic Effective Field Theories (EFTs)⁵.

1.2.1 Tree-level amplitudes from BCFW-like recursion relations

In the following, we consider for simplicity massless theory in four dimensions and amplitudes in the perturbative expansion, unless otherwise specified.

In general, all the three-point scattering amplitudes can be fixed by symmetry, helicity weight and mass dimension considerations, up to an overall *coupling constant* [16]. In particular, the kinematic part of any massless three-point amplitude can be written as

$$\mathcal{A}(1^{h_1}, 2^{h_2}, 3^{h_3}) = \begin{cases} i \mathfrak{g} \langle 12 \rangle^{h_1+h_2-h_3} \langle 23 \rangle^{h_2+h_3-h_1} \langle 31 \rangle^{h_3+h_1-h_2} & \sum_i h_i = -n \\ i \mathfrak{g} & h_1 = h_2 = h_3 = 0 \\ i \mathfrak{g} [12]^{h_1+h_2-h_3} [23]^{h_2+h_3-h_1} [31]^{h_3+h_1-h_2} & \sum_i h_i = n \end{cases}, \quad (1.24)$$

²A possible definition of the principal value is $\text{P} \frac{1}{x} = \frac{1}{2} \left(\frac{1}{x+i\epsilon} + \frac{1}{x-i\epsilon} \right)$, such that $\int_{-\Lambda}^{\Lambda} \text{P} \frac{1}{x} = 0$.

³To be more precise, equation (1.22) is only true $\mathcal{O}((s_\alpha - M_\sigma^2)^0)$. These propagators are exact only when we restrict to tree-level amplitudes in theories with two-derivative kinetic terms.

⁴We adopt the following convention: we indicate with $\mathcal{A}_n^{(L)}(p_1^{h_1} \dots p_n^{h_n})$ an L -loop n -point scattering amplitude with all the momenta outgoing and with $\mathcal{A}_n^{(L)}(p_1^{h_1} \dots p_m^{h_m} \rightarrow p_{m+1}^{h_{m+1}} \dots p_n^{h_n})$ an L -loop n -point amplitude with m incoming and $n-m$ outgoing states. If the superscript (L) is absent, we mean tree-level.

⁵Equation (1.23) works under the assumption that we are dealing with a well-defined basis of asymptotic states. This is true in gapped theories, but it is not guaranteed to hold for theories with massless particles (and infrared divergences), which introduce extra factorising terms [15].

where $n = 1, 2, \dots$ and the mass dimension of the coupling constant is $[\mathbf{g}] = 0$ in the first and last case or $[\mathbf{g}] = 1$ for the purely scalar case. In general, \mathbf{g} must be thought of as a tensor describing the non-kinematic quantum numbers of the asymptotic states.

This classification exhausts all the relevant and marginal couplings in relativistic QFTs with only massless particles, once we consider the four-scalar interaction $\mathcal{A}(1^0, 2^0, 3^0, 4^0) = i\lambda$. For example, a list of all the three-point amplitudes in the Standard Model, with the proper colour and flavour structures, is presented in Appendix B.2. The on-shell classification of relevant and marginal couplings for theories with massive particles can be found in [17–19]. While the most general classification of irrelevant interactions in four-dimension EFTs has been presented [20] and will be discussed in Chapter 2. We will argue that, in principle, the knowledge of such minimal amplitudes is enough to fix any higher-point and higher-loop amplitude and, in this section, we will show how higher-point tree-level amplitudes are usually computed using BCFW-like recursion relations.

Before going to the higher-point amplitudes, some comments are in order about three-point amplitudes. First, such amplitudes do not receive any loop correction and, then, are tree-level exact. Such a feature will be fundamental in Section 3.3. Second, the three-point amplitudes are defined only in complex Minkowski space. In fact, massless three-point kinematics is not allowed in real Minkowski space because we are forced to have $s_{ij} = 0$, for $i, j = 1, 2, 3$. Then, we can consider λ and $\tilde{\lambda}$ spinors as independent (not related by complex conjugation). Then, $s_{ij} = 0$ implies either $\langle ij \rangle = 0$ or $[ij] = 0$ for all i, j . If we consider, for example, the three-vector amplitude in the so-called maximal-helicity-violating (MHV) configuration, we have $\tilde{\lambda}_1 \propto \lambda_2 \propto \lambda_3$ and momentum conservation becomes equivalent to Schouten identity ($\langle 12 \rangle \lambda_3 + \langle 23 \rangle \lambda_1 + \langle 31 \rangle \lambda_2 = 0$).

In the amplitudes literature, the computation of higher-point tree-level amplitudes from on-shell data is usually performed through BCFW recursion relation [21–23] or its generalisations [24–28]. The strategy of BCFW-like recursion relations is the following:

- l momenta are shifted introducing a complex parameter z (l -line shift) in a way which preserves momentum conservation and on-shell conditions, and the real kinematics is recovered when we set $z = 0$.
- The original amplitude is computed as a contour integral in the complex z -plane

$$\mathcal{A}_n(0) = \frac{1}{2\pi i} \oint_{z=0} \frac{\mathcal{A}_n(z)}{z}, \quad (1.25)$$

using Cauchy's theorem knowing that, under the assumption of good behaviour in the $z \rightarrow \infty$ limit (*i.e.* $\mathcal{A}_n(z) \rightarrow z^\gamma$ with $\gamma \leq -1$), the other poles of the amplitude correspond to factorisation channels and can be computed from (1.23).

These recursion relations are particularly well-suited for the computation of amplitudes involving vectors and gravitons in four dimensions (thanks to the especially simple massless spinor helicity formalism), for which the BCFW (two-line) shift gives rather compact results summing over a small subset of the actual factorisation channels. The most general criteria for the shifted amplitude to be well-behaved in the $z \rightarrow \infty$ limit are given in [29]: all renormalisable theories are shown to be five-line constructible and, in particular, theories involving fermions and scalars charged under a $U(1)$ are three-line constructible, as in the case of the Standard Model. Moreover, non-renormalisable amplitudes with no-derivative operator insertions are on-shell constructible, but it is not generally true for operators with derivatives.

On the other hand, recursion relations have some drawbacks. For n -line shifts with $n \geq 3$, we have to introduce non-physical reference spinors and the final result does not depend on the choice of it. On the other hand, eliminating such dependence is usually a non-trivial task. In general, they also give rather cumbersome results and, in no case, locality is manifest in the final amplitude, because of the presence of spurious poles. The residues over such poles are always zero, but re-writing the amplitude such that this property becomes manifest is in general very non-trivial. Moreover, this is an unpleasant feature because, when we use such tree-level amplitude to construct integrands at loop level (through generalised unitarity, which will be explained in the next section), all sorts of unphysical singularities seem to be present in the analytic results of the integrand. Finally, general recursion relations are defined only in four dimensions, while BCFW shift has been generalised in six dimensions [30]. On the other hand, a generalisation to generic d dimensions, which would be necessary for (conventional) dimensional regularisation at higher loops [31–33], is not known. In Chapter 3, we will show how to overcome these issues at the cost of some efficiency, while keeping the recursive features of the on-shell methods (which is the key difference with respect to Feynman diagrams calculations). In particular, the method we will present can be applied to any EFT, even with the insertion of irrelevant operators with derivative interactions.

1.2.2 Loop-level amplitudes from generalised unitarity

While tree-level amplitude has at most simple pole singularities, at loop level we can find all sorts of branch-point singularities associated with multiparticle unitarity. The simplest singularities of this kind are *normal thresholds* and the unitarity constraint (1.19) fixes the discontinuities across the corresponding branch cuts in terms of the product of two (lower-loop) amplitudes, integrated over a n -particle Lorentz-invariant phase space integral. Such discontinuities can be further analytically continued to non-physical values of Mandelstam invariants and present branch points on some specific kinematic points called *Landau singularities* [34]. In general, such discontinuities can be computed by putting a certain number of internal propagators on-shell

$$\frac{i}{s - M_\sigma^2} \rightarrow \pi \delta(s - M_\sigma^2) , \quad (1.26)$$

after glueing the resulting lower-loop amplitudes (*i.e.* summing over all the possible states with mass M_σ which can be exchanged in the propagator) and integrating over the phase space of the internal on-shell states.

These unitarity methods allow constructing recursively loop amplitudes from on-shell tree amplitudes. In gauge or gravity theories, this also allows working only with gauge-invariant quantities at every step, in contrast to Feynman diagrams. However, the old-fashioned approach from the S-matrix bootstrap programme [11] suffered from many problems: the reconstruction of the full amplitudes from the discontinuities is not unique (indeed, we find subtraction terms which are left undetermined), and a generalisation beyond four-point amplitudes had many technical issues and it was not clear how to deal with massless particles. These difficulties have been overcome in the perturbative approach by modern generalised unitarity, introduced in the seminal paper [35], and powerful new methods were discussed in [21, 36–43] to refine generalised unitarity at one loop (a review of generalised unitarity techniques, even beyond one loop, can be found in [44–47]). Indeed, while the old-fashioned approach heavily relied on

non-perturbative properties of the S-matrix, the modern generalised unitarity combines unitarity properties with the knowledge of the structures appearing in the amplitudes in the Feynman diagrammatic perturbative analysis.

An L-loop amplitude can be written schematically as

$$\mathcal{A}_n^{(L)} = \sum_i \int \prod_{j=1}^L \frac{d^4 l_j}{(2\pi)^4} \frac{1}{S_i} \frac{n_i c_i}{\prod_{\alpha_i} d_{\alpha_i}}, \quad (1.27)$$

where i labels all possible L -loop Feynman diagrams, l_j are the l loop momenta, α_i label the propagators and S_i some symmetry factor. The factors n_i are polynomials of Lorentz-invariant contractions of external and loop momenta and polarization vectors. The constants c_i capture all the information about coupling and gauge group structure.

There are new effects at loop level with respect to the analysis at tree level. The first is *ultraviolet* (UV) divergences, which arise due to the bad high energy behaviour of the loop integrals. They can be absorbed through a redefinition (*renormalization*) of the bare parameters appearing in the Lagrangian. The standard way to deal with these divergences is by defining the theory in $d = 4 - 2\epsilon$ dimensions (*dimensional regularization*):

$$\frac{d^4 l_j}{(2\pi)^4} \longrightarrow \frac{d^d l_j}{(2\pi)^d}. \quad (1.28)$$

Then, after the appropriate parameters are renormalized, one can study the limit $\epsilon \rightarrow 0$. A second complication has to do with those theories involving massless particles, they are *infrared* (IR) divergences. These divergences can also be dealt with in the framework of dimensional regularization, analytically continuing to negative ϵ . IR divergences cancel in the IR safe cross-sections against corresponding divergences from real emissions. The integrand is still a rational function which at most simple poles in specific kinematic points, but the loop integration gives rise to the additional branch point singularities mentioned above.

In this thesis, we will only present one-loop computations in four dimensions. Then, in the remaining part of this section, we will briefly review one-loop generalised unitarity. In general, if one is interested only in obtaining a result for scattering amplitudes up to $O(\epsilon)$ terms, it can be shown [48, 49] that one can reduce a generic one-loop integral to a linear combination of one-loop scalar integrals of four, three, two and one point type, plus terms which are *rational* in the external variables and we will denote them as \mathcal{R} . This is the so-called Passarino-Veltman reduction and the result reads:

$$I_N = \sum_{i_4} c_{4,i_4} I_4^{i_4} + \sum_{i_3} c_{3,i_3} I_3^{i_3} + \sum_{i_2} c_{4,i_2} I_2^{i_2} + \sum_{i_1} c_{1,i_1} I_1^{i_1} + \mathcal{R} + O(\epsilon), \quad (1.29)$$

where I_M^i denotes the scalar M -point integral and i refers to the possible distribution of external momenta p_j on the M vertices of I_M^i . The coefficients $c_{M,i}$ are algebraic four-dimensional quantities related to the tree-level amplitudes and fixed by the unitarity methods. For example, let us consider the triangles:

$$I_3(p_1^2, p_2^2, p_3^2) = i \int \frac{d^d l}{(2\pi)^d} \frac{1}{d_1 d_2 d_3}, \quad (1.30)$$

where

$$d_k = (l + \sum_{j=1}^{k-1} p_j)^2 - m_k^2 + i\varepsilon, \quad (1.31)$$

where p_i is the sum of external momenta in the j -th vertex and $\sum_{i=1}^3 p_i = 0$, because of momentum conservation. We shall also mention that UV divergences only occur in the tadpoles and bubbles, IR divergences can only occur in some configurations of triangles and boxes.

The idea behind modern generalized unitarity is to go beyond double cuts and to construct the one-loop amplitude by applying also triple and quadrupole cuts. One starts from the *maximal* number of cuts in order to find the corresponding box coefficients in terms of four tree-level amplitudes, by matching the RHS and LHS in equation (1.29). From this one proceeds to triple, double and single cuts to reconstruct the lower integral coefficients, subtracting carefully the contributions from higher cuts. Rational terms \mathcal{R} are not captured by four-dimensional generalised unitarity, but they can be computed, for example, from locality considerations [50, 51] (see discuss in Section 3.3), four-dimensional recursion relations [52–54] or through d -dimensional unitarity [55–60], as discussed in Chapter 4.

1.3 Form factors and low energy expansion

Scattering amplitudes are fully on-shell quantities, in contrast with correlation functions which are vacuum expectation values of multiple insertions of some operators. A natural question is whether it would be possible to extend on-shell techniques to off-shell quantities, in the perturbative expansion [61]. As an intermediate step, we consider an interpolating quantity between completely off-shell and on-shell quantities, namely the *form factors*. This is defined as the transition matrix between the vacuum as in state and a n -particle out state, with an insertion of a local gauge-invariant operator $\mathcal{O}(x)$.

$$\int d^d x e^{i q \cdot x} \langle p_1^{\sigma_1} \dots p_n^{\sigma_n} | \mathcal{O}(x) | 0 \rangle = (2\pi)^d \delta^{(d)} \left(q - \sum_{i=1}^n p_i \right) \langle p_1^{\sigma_1}, \dots, p_n^{\sigma_n} | \mathcal{O}(0) | 0 \rangle, \quad (1.32)$$

where

$$\mathcal{F}_{\mathcal{O}, n}(p_1^{\sigma_1}, \dots, p_n^{\sigma_n}; q) = \langle p_1^{\sigma_1}, \dots, p_n^{\sigma_n} | \mathcal{O}(0) | 0 \rangle \quad (1.33)$$

is the form factor.

Furthermore, form factors are also relevant in the context of EFTs. Indeed, form factors can be physically interpreted as small perturbations of the S-matrix: setting $q^\mu = 0$, equation (1.32) can be interpreted as the linear term in the expansion of the exponential in the path-integral with a deformed action

$$S = S_0 + \alpha \int d^d x \mathcal{O}(x). \quad (1.34)$$

Such deformations are common in EFTs when we integrate out massive modes whose mass Λ is much bigger than the scales involved in the processes under consideration. In particular, if we consider the large-mass expansion of a propagator

$$\frac{i}{s - \Lambda^2} = -\frac{i}{\Lambda^2} \sum_{i=0}^{\infty} \left(\frac{s}{\Lambda^2} \right)^i. \quad (1.35)$$

in an amplitude, we find that each contribution is equivalent to an irrelevant deformation of the action with a local operator (involving derivatives at higher order in the expansion). This is equivalent to considering insertions in the amplitude of a local

gauge-invariant operator (at $q^\mu = 0$) with the correct field content (fixed by the interaction vertices connected by the expanded propagator). In particular, if we consider the free theory limit of S_0 , using Wick's theorem, we see that there is only one non-vanishing form factor for the operator $\mathcal{O}(x)$ and it is completely local (polynomial) in the kinematic variables. Such quantities are called *minimal form factors* (for $q^\mu = 0$ or $n = 2$, we will also refer to these polynomial terms as *contact terms* or *minimal amplitudes*) and the one-to-one correspondence between its leading order term in perturbation theory and kinematically independent (relevant, marginal or irrelevant) deformations of an EFT action can be exploited to classify EFT operators. Such correspondence has been first used in the context of Standard Model Effective Field Theory (SMEFT) in [62], as there are several technical advantages in the on-shell classification:

- Invariance under field redefinition and the definition of field strengths $[D_\mu, D_\nu] \sim F_{\mu\nu}$, where D_μ are covariant derivatives, are automatically taken into account.
- Fierz identities and Bianchi identities correspond to Schouten identities for the spinor helicity variables.
- Integration-by-part identities $\int d^d x \partial_\mu \mathcal{O}^\mu = 0$ correspond simply to momentum conservation.

Then, a basis of linear independent polynomial structures is equivalent to a basis of EFT operators. Such classification will be the subject of Chapter 2.

1.4 Applications of BCFW-like recursion relations

Before moving to more advanced topics, we present some explicit computations of BCFW recursion relations to clarify the role of the quantities needed in the computations. Then, in this section, we will present two examples, to show both the power and the limits of this method to bootstrap tree-level amplitudes from the knowledge of few on-shell data which are the seeds of the recursion. These are three-point amplitudes or amplitudes which are polynomial in the kinematic variables which will name in the following as *minimal amplitudes*, which will be classified in Chapter 2.

The colour-ordered MHV amplitude in Yang-Mills theories

First, we consider the *colour-ordered maximal-helicity-violating* (MHV) amplitude with n gluons.

Any n -gluon tree-level amplitude in Yang-Mills theory can be decomposed into simpler amplitudes [63, 64]:

$$\mathcal{A}_n \left(1^{h_1, A_1}, \dots, n^{h_n, A_n} \right) = \sum_{\sigma \in \mathbf{S}_n / \mathbf{Z}_n} \tau^{A_{\sigma(1)} \dots A_{\sigma(n)}} A_n \left(\sigma(1)^{h_{\sigma(1)}}, \dots, \sigma(n)^{h_{\sigma(n)}} \right), \quad (1.36)$$

where h_i and A_i are the helicities and the color indices of the gluons, \mathbf{S}_n is the set of all permutations of n elements and \mathbf{Z}_n are the cyclic permutations, $\tau^{A_{i_1} \dots A_{i_n}}$ are the traces of n generators of the fundamental representation of the gauge group and $A_n(i_1^{h_{i_1}}, \dots, i_n^{h_{i_n}})$ are the color-ordered amplitudes. Such amplitudes satisfy a number of properties, which are reviewed, for example, in [65]. Among such properties, it is

important to stress that these amplitudes have poles only in adjacent channels: *e.g.* $A_n(1^{h_1}, \dots, n^{h_n})$ have poles only at $s_{i,i+1, \dots, i+m} = 0$, where the sum of the indices is modulo n , and they only depend on kinematic variables (all the information about colour has been factorised away).

In this section, we will apply BCFW recursion relation to determine the color-ordered MHV amplitudes $A_n(1^-, 2^-, 3^+, \dots, n^+)$. All the amplitudes in Yang-Mills theories in perturbation theory can be reconstructed from the (two) *minimal* three-point amplitudes describing the interaction of three gluons (in a complex kinematic space) which are fixed from little group, mass dimension and parity considerations in equation (1.24) (with some constraints imposed by locality and unitarity as we will show in Chapter 3):

$$A_3(1^-, 2^-, 3^+) = ig \frac{\langle 12 \rangle^4}{\langle 12 \rangle \langle 23 \rangle \langle 31 \rangle}, \quad (1.37)$$

$$A_3(1^-, 2^+, 3^+) = -ig \frac{[23]^4}{[12][23][31]}. \quad (1.38)$$

We want now to prove that the MHV colour-ordered amplitude we are interested in can be written for any n as

$$A_n(1^-, 2^-, 3^+, \dots, n^+) = ig^{n-2} \frac{\langle 12 \rangle^4}{\langle 12 \rangle \langle 23 \rangle \cdots \langle n-1n \rangle \langle n1 \rangle}. \quad (1.39)$$

We can consider the BCFW shift

$$\begin{aligned} \tilde{\lambda}_1 &\rightarrow \tilde{\lambda}_1 - z \tilde{\lambda}_n, \\ \lambda_n &\rightarrow \lambda_n + z \lambda_1, \end{aligned} \quad (1.40)$$

and any other spinor is left untouched in the shifted (complex) kinematics. In particular, we can notice that such deformation preserves momentum conservation and the on-shell condition. Using now Cauchy theorem in (1.25) and factorisation we have

$$\begin{aligned} A_n(1^-, 2^-, 3^+, \dots, n^+) &= A_n(\hat{1}^-, 2^-, 3^+, \dots, \hat{n}^+) \Big|_{z=0} = \\ &= \sum_{m=2}^{n-2} A_{m+1}(\hat{1}^-, \dots, m^{h_m}, \hat{P}_{I_m}^\pm) \frac{i}{P_{I_m}^2} A_{n-m+1}(\hat{P}_{I_m}^\pm \rightarrow (m+1)^+, \dots, \hat{n}^+) \Big|_{z=z_{P_{I_m}}} \\ &= A_{n-1}(\hat{1}^-, \dots, (n-2)^+, \hat{P}_{n-1,n}^+) \frac{i}{s_{n-1,n}} A_3(-\hat{P}_{n-1,n}^-, (n-1)^+, \dots, \hat{n}^+) \Big|_{z=z_{n-1,n}} \\ &= ig^{n-2} \frac{\langle 12 \rangle^4}{\langle 12 \rangle \langle 23 \rangle \cdots \langle n-1n \rangle \langle n1 \rangle}, \end{aligned} \quad (1.41)$$

where in the third step we used the fact that the all-plus (for any n) and single-minus (for $n > 3$) amplitudes vanish at tree-level for pure Yang-Mills theories, while in the last step we needed the amplitudes (1.39) (with $n-1$ gluons) and (1.37), with $z_{n-1,n} = \frac{\langle n-1n \rangle}{\langle 1n-1 \rangle}$ and⁶

$$\hat{P}_{n-1,n} \Big|_{z=z_{n-1,n}} = \lambda_{n-1} \left(\tilde{\lambda}_{n-1} - \frac{\langle 1n \rangle}{\langle 1n-1 \rangle} \tilde{\lambda}_n \right). \quad (1.42)$$

Then, we showed recursively that the colour-ordered MHV amplitude takes the form presented in (1.39). As we said, the BCFW recursion relations are particularly well

⁶We also adopted the convention $\lambda_{-p\alpha} = i \lambda_{p\alpha}$ and $\tilde{\lambda}_{-p\dot{\alpha}} = i \tilde{\lambda}_{p\dot{\alpha}}$, such that $\lambda_{-p\alpha} \tilde{\lambda}_{-p\dot{\alpha}} = -p_{\alpha\dot{\alpha}}$.

suited to compute tree-level amplitudes in Yang-Mills theories and Einstein-Hilbert gravity. Already at this stage, we can notice that the alternative shift

$$\begin{aligned}\lambda_1 &\rightarrow \lambda_1 - z\lambda_n, \\ \tilde{\lambda}_n &\rightarrow \tilde{\lambda}_n + z\tilde{\lambda}_1\end{aligned}\tag{1.43}$$

would give an amplitude which does not fall off as $z \rightarrow \infty$:

$$A_n(\hat{1}^-, 2^-, 3^+, \dots, \hat{n}^+) \underset{z \rightarrow \infty}{\sim} z^3.\tag{1.44}$$

In particular, one could show that in Yang-Mills theories, even beyond the simplest MHV configuration, any other two-line shift

$$\begin{aligned}\lambda_a &\rightarrow \lambda_a - z\lambda_b, \\ \tilde{\lambda}_b &\rightarrow \tilde{\lambda}_b + z\tilde{\lambda}_a\end{aligned}\tag{1.45}$$

gives the correct boundary behaviour if and only if we a and b do not correspond to a helicity-minus and a helicity-plus gluons respectively [22]. Moreover, Yang-Mills tree-level amplitudes can also be determined, for example, using MHV rules [66] (which can be extended even to one-loop [67]), corresponding to the (three-line) Risager shift [24].

The dipole contribution to the $\mathcal{A}_4(\bar{\psi}^+, \psi^+, \gamma^+, \gamma^+)$ amplitude

We now consider a different scattering amplitude and, in particular, we want to focus on the dipole contribution in the SMEFT to the $\bar{\psi}^+\psi^+ \rightarrow \gamma^-\gamma^-$ process. For the moment, we will only define the relevant minimal amplitude: we need two types of three-point amplitudes⁷

$$\mathcal{A}(1_{\bar{\psi}}^-, 2_{\psi}^+, 3_{\gamma}^-) = i Q_{\psi} \frac{\langle 13 \rangle^2}{\langle 12 \rangle}, \quad \mathcal{A}(1_{\bar{\psi}}^-, 2_{\psi}^+, 3_{\gamma}^+) = i Q_{\psi} \frac{[23]^2}{[12]},\tag{1.46}$$

$$\mathcal{A}(1_{\bar{\psi}}^+, 2_{\psi}^+, 3_{\gamma}^+) = i \frac{a_6 v}{\Lambda^2} [13][23], \quad \mathcal{A}(1_{\bar{\psi}}^-, 2_{\psi}^-, 3_{\gamma}^-) = i \frac{a_6 v}{\Lambda^2} \langle 13 \rangle \langle 23 \rangle,\tag{1.47}$$

where the first line is the renormalisable U(1) coupling of fermions with photons, with Q_{ψ} the charge of the fermion, and in the second line we have the dipole coupling. Although this will not be relevant in the following, we specify that v is the vacuum expectation value of the Higgs field, Λ is some energy scale typical of new physics states and a_6 is a numerical *Wilson coefficient*. In general, a method to classify a basis of minimal amplitudes in the a generic EFT (and, in particular, in the SMEFT) will be presented in Chapter 2.

For the computation of this amplitude, we consider the so-called *all-line shift* [25]

$$\lambda_i \rightarrow \hat{\lambda}_i = \lambda_i + z w_i \lambda_X,\tag{1.48}$$

where the w_i have to satisfy

$$\sum_{i=1}^4 w_i \tilde{\lambda}_i = 0,\tag{1.49}$$

which guarantees momentum conservation in the shifted (complex) kinematics.

⁷In principle, we would need also the colour and flavour structures but, since these are only trivial δ factors, we will ignore them in the following computations.

Using the BCFW recursion formula, we find

$$\begin{aligned}
\mathcal{A}_4(1_\psi^+, 2_\psi^+, 3_\gamma^+, 4_\gamma^+) &= \mathcal{A}_3(\hat{1}_\psi^+, (\hat{P}_{14})_\psi^+, \hat{4}_\gamma^+) \frac{i}{P_{14}^2} \mathcal{A}_3((\hat{P}_{14})_\psi^+ \rightarrow \hat{2}_\psi^+, \hat{3}_\gamma^+) \Big|_{z=z_{14}} + \\
&\quad \mathcal{A}_3(\hat{1}_\psi^+, (\hat{P}_{14})_\psi^-, \hat{4}_\gamma^+) \frac{i}{P_{14}^2} \mathcal{A}_3((\hat{P}_{14})_\psi^- \rightarrow \hat{2}_\psi^+, \hat{3}_\gamma^+) \Big|_{z=z_{14}} + (3 \leftrightarrow 4) \\
&= i Q_\psi \frac{a_6 v}{\Lambda^2} \frac{[14][23]}{t} \left([14] \frac{\langle 1X \rangle}{\langle 3X \rangle} - [23] \frac{\langle 2X \rangle}{\langle 4X \rangle} \right) + (3 \leftrightarrow 4) .
\end{aligned} \tag{1.50}$$

Here we can notice some unpleasant features of BCFW-like recursion relations. The amplitude is written in terms of some arbitrary spinor λ_X and one can check (for example, numerically) that the former does not depend on the latter. In particular, the result in (1.50) has some fake (spurious) poles at $\langle 3X \rangle = 0$ and $\langle 4X \rangle = 0$. In fact, one can show that the result just obtained is equivalent to

$$\mathcal{A}_4(1_\psi^+, 2_\psi^+, 3_\gamma^+, 4_\gamma^+) = -2i Q_\psi \frac{a_6 v}{\Lambda^2} \frac{\langle 12 \rangle [13] [14] [23] [24]}{tu} , \tag{1.51}$$

but showing the equivalence of these two quantities is already non-trivial, and it becomes a hopeless problem when we go beyond four points. Such spurious poles are particularly disadvantageous when we use tree-level amplitude to construct the integrands of loop amplitudes through generalised unitarity. Moreover, one can show that no BCFW (two-line) shift can reproduce correctly such amplitude. This situation becomes even worse if we would have considered interactions with explicit derivative insertions in the minimal amplitudes [28] and such a shift could even not exist. Finally, we emphasise that the method we will present in Chapter 3 will bring directly to the result (1.51), for which locality is manifest.

1.5 Modern applications

In recent years, on-shell methods have proved to be extremely powerful in the study of EFTs. Among other applications, they appeared as prominent tools in the study of the SMEFT and (classical) gravitational binary systems.

The SMEFT is a systematic and model-independent framework to characterise both experimental deviation from predictions of the Standard Model (SM) and its possible extensions (for a review, see [68] and references therein), assuming that the light degrees of freedom are all those of the SM. Indeed, up to now, most of the measurements in accelerator experiments of cross-sections are compatible with SM theoretical predictions and no new physics has been observed. Nonetheless, the SM is expected to be an incomplete description of Nature: many theoretical puzzles are still unsolved, including but not limited to the hierarchy problem, the magnitude of the quartic λ coupling of the Higgs, the origin of CP violation in the quark sector, or the unnatural pattern of the Yukawa couplings. More recently, also an experimental deviation from SM predictions has been measured in the $g_\mu - 2$ experiment. [69–71].

Then, how should we look for new physics beyond the SM? When considering extensions of the SM, additional heavy modes with mass Λ can be integrated out at electro-weak energy scales $E_{\text{EW}} \ll \Lambda$. In the Lagrangian formalism, we have some effective interac-

tions which can be organised in terms of their mass dimension as

$$\mathcal{L}_{\text{SMEFT}} = \mathcal{L}_{\text{SM}} + \sum_{i,j} \frac{c_i^{(j)}}{\Lambda^{j-4}} \mathcal{O}_i^{(j)}. \quad (1.52)$$

The first example is the dimension-five Weinberg operators [72] which generate light Majorana-like neutrino masses:

$$\mathcal{L}_{\text{SMEFT}} = \mathcal{L}_{\text{SM}} + \frac{C_{mn}}{\Lambda_L} \left(\epsilon_{ik} \epsilon_{jl} L_m^i L_n^j H^k H^l + \epsilon^{ik} \epsilon^{jl} \bar{L}_{mi} \bar{L}_{nj} \bar{H}_k \bar{H}_l \right), \quad (1.53)$$

where $m, n = 1, 2, 3$ are flavour indices and i, j are $SU(2)$ indices, and Λ_L is the natural cut-off of the effective theory. More precisely Λ_L is the cut-off scale for effective interactions which violate lepton and baryon numbers, as opposed to the scale Λ associated with lepton/baryon number preserving interactions. Experimental constraints on the neutrino masses put the lower bound on the cut-off scale at $\Lambda_L/C_{mn} \gtrsim 10^{15}$ GeV, which are scales currently impracticable for the observation of new physics.

In fact, the leading contributions to the SMEFT come from dimension-six operators [73–79], but there are interesting processes for which the dominant contribution comes from even higher-dimensional operators. Some examples include the light-by-light scattering [80], the light production via gluon fusion [81] and the neutral bosons production [82] and even, in some scenarios, the $g_\mu - 2$ [83] and Higgs production in association with a W boson [84], which receives the first contribution from dimension-eight operators. Dimension-eight operators can play a relevant role even when appearing as subleading contributions [85], and recent studies of their impact on SMEFT have been performed [86–90].

In this context, on-shell methods are acquiring a prominent role. They have been used to discover non-interference theorems between dimension-six operators and the SM [91], to study positivity bounds on Wilson coefficients [92–96] and natural zeros for Wilson coefficient in the matching between UV and IR theory [97]. Crucially, on-shell techniques played a key role in the study of the anomalous dimensions of irrelevant interactions in the SMEFT [98–107], to understand the patterns of zeros in the one-loop anomalous dimension matrix for dimension-six operators in the SMEFT [108–110] and, as we have already mentioned, in the classification of SMEFT interactions [20, 111–122].

The breakthroughs in gravitational-wave science, with the observations by the LIGO and Virgo collaborations [123, 124], has opened new windows to observations in astronomy, cosmology, and particle physics. Gravitational waves can be the key to answering longstanding questions in these areas and offers an observational test of gravitational processes involving huge energy scales, which could have never been probed by experiment. The LIGO and Virgo detectors precision will grow further in future upgrades, and this demands very accurate theoretical predictions, which will be encoded in waveform templates utilized for the gravitational-wave detection and the extraction of source parameters. This calls for high-energy physicists to develop a new theoretical framework to study signals with more and more accuracy.

Traditionally, this is approached using effective one-body, numerical relativity, gravitational self-force, and perturbation theory in the post-Newtonian (PN), post-Minkowskian (PM)⁸, and non-relativistic general relativity frameworks. In the context of on-shell

⁸The PN and PM are complementary perturbative expansions. The former is a double expansion

techniques and scattering amplitudes, the new discoveries started a program for understanding the nature of gravitational wave sources by the collapse of binary systems of celestial objects (black holes and neutron stars, mostly in the inspiral phase of the merging). Although some studies in this context can be traced back to the seventies [125, 126] with some more recent developments [127–129], the program for understanding the nature of gravitational-wave sources is based on tools from scattering amplitudes and effective field theory (EFT) exploded in the last five-ten years [130–143]. These ideas culminated with advancing the state-of-the-art computation to order in the PM expansion to $\mathcal{O}(G^3)$ [144, 145]. This result has been confirmed in a number of studies [146–150], including radiation [151–155]. Moreover, scattering amplitude techniques allowed to compute the conservative two-body scattering dynamics up to $\mathcal{O}(G^4)$ in all orders in velocity [156, 157], and to lower orders in G including spin effects [158–167], tidal effects [168–172] and higher-derivative interactions [173, 174]⁹.

Besides the above-mentioned line of research, there are other important topics which are very important in the development of on-shell methods which we will not mention in this thesis: for example, the strong hint for hidden geometric structures in perturbative scattering amplitudes [189] (for a review, see [190, 191] and references therein), the colour-kinematics duality and the double copy map which links amplitudes in scalar, gauge and gravitational theories [192, 193] (see [65, 194] and references therein), the study and analytic calculation of Feynman integrals (for a modern and comprehensive review, see [195–197]), the study of cosmological correlators in de Sitter spacetime using on-shell inspired methods [198] (see also [199]), or the $\mathcal{N} = 4$ Super-Yang-Mills high-loop computations [200–206].

1.6 Summary of the thesis

This thesis is structured according to the following order:

- First, we consider amplitudes which are polynomial in the kinematic variables, *i.e.* contact terms.
- Second, we show how to glue such contact terms to produce tree-level amplitudes.
- We show how d -dimensional generalised unitarity is enough to construct amplitudes and form factors at loop level.
- Finally, we apply on-shell methods to study relevant (loop) amplitudes in the context of SMEFT and classical General Relativity (GR).

In particular, the material in the various chapters is organised as follows:

1. In Chapter 2, we show the classification of the simplest scattering amplitudes, *i.e.* contact terms. First, we introduced a new strategy for purely massless theories,

in the velocity squared and the inverse separation in units of the Schwarzschild radius, which are of the same order due to the virial theorem ($\vec{v}^2 \sim \frac{Gm}{|r|}$). In contrast, the PM expansion is organized differently, including instead contributions to all orders in velocity at fixed order in G , and the n PM order corresponds to $\mathcal{O}(G^n)$. On-shell methods are intrinsically relativistic, then we will always work in the PM expansion.

⁹There is an PM alternative to the fully on-shell methods, which combines Feynman rules in the worldline formalism with high-loop integration which is also giving promising results in this direction [175–188].

which can be generalised to give a basis of contact terms in any EFT in four dimensions, with masses and higher-spin particles. This chapter is based on [20].

2. In Chapter 3, we present a recursive on-shell alternative to BCFW-like recursion relations, which is valid for any theory. In particular, we first review how Lie algebra structures follow from tree-level unitarity of four-point amplitudes in gauge theories. Then, we show how to generalise the algorithm to higher-point tree-level amplitudes. Finally, we show how unitarity and locality fix anomaly cancellation conditions in the Standard Model. Most of this chapter is based on the work presented in [104].
3. In Chapter 4, we show how Dimensional Reconstruction Techniques allow computing loop amplitudes, including rational terms, from d -dimensional generalised unitarity. We generalised these techniques to form factors which are relevant to the Higgs decay into gluons, following the paper [207].
4. In Chapter 5, we present the techniques needed to compute the full mixing matrix between dimension-eight operators in the SMEFT. Partial results are shown explicitly for the operators relevant for the Higgs production in association with a W -boson through pp scattering. The complete result is given in the ancillary files of [104].
5. In Chapter 6, we present the calculations of the corrections to the deflection angle and the time delay of light and gravitons from a heavy source (like a black hole), induced by higher-derivative interactions beyond GR, using the eikonal (exponential) form of the corresponding two-to-two gravitational scattering amplitude. These results were presented in [174].
6. Finally, some appendices are presented. In Appendix A, we review (massless and massive) spinor helicity formalism in four dimensions, massless spinor helicity formalism in six dimensions, and some basics of momentum twistors relevant for the generation of rational kinematics and some basic concepts of finite field arithmetic. In Appendix B, we fix our conventions in the SMEFT and we provide the three-point amplitudes of the Standard Model. In Appendix C, we give some details on the computation of six-dimensional tree-level amplitudes relevant for computations in Chapter 4. Finally, in Appendix D, we provide the analytic results of the one-loop Feynman integrals appearing in this thesis.

Chapter 2

Minimal Amplitudes Bases for EFTs

In general, the classification of irrelevant operators in an EFT is a complicated task. The counting of non-redundant operators can be performed via the Hilbert series method, as shown in [208–210], however, explicit construction of the SMEFT operators is rather involved. Traditional techniques require taking care separately of many sources of redundancy, *e.g.* Bianchi identities and IBP identities of operators with derivative insertions, field redefinitions and Fierz identities. More recently, as discussed in the introduction, a more direct way of constructing this basis has been proposed, which relies on the classification of the independent effective interactions directly from their S-matrix elements, and has been used to classify all the SMEFT operators up to mass dimension nine [117, 118]. Indeed, in the context of weakly coupled EFTs, the on-shell program provides us with an alternative to the standard Lagrangian EFTs, where the information of the theory beyond the IR physics is encoded by adding irrelevant operators. In particular, it exists a one-to-one correspondence between irrelevant independent operators and minimal amplitudes, *i.e.* terms in the low-energy expansion of the S-matrix which are polynomial in the kinematic variables (and are linear in the Wilson coefficients). This means that from the S-matrix perspective the classification and enumeration of independent operators [208–212] are equivalent to finding a basis of kinematically independent polynomial structures in the amplitudes [62, 213]. From these “building blocks”, higher-point tree-level amplitudes can be constructed from the knowledge of the factorisation channels.

The classification program was carried out mainly in four dimensions where we take advantage of the simplicity of both massless [214–217] and massive [18] spinor helicity formalism. Generic techniques to classify fully massless interactions have been worked out in previous works mentioned in the introduction. For massive particles, the authors of [19, 116] introduced an *unbolding/bolding* procedure to classify massive structures from their massless counterparts, and they presented a strategy to tackle this problem for four-point contact terms and particles with spin $S \leq 1$. An alternative strategy valid for any multiplicity and any spin has been presented in [218], but this method does not allow for a clear one-to-one correspondence between independent structures and operators. A general method for massive particles with any mass, spin and multiplicity has only been developed recently [20, 121]

In this chapter, we present the method to classify generic contact terms in four-dimension of [20], for any mass, spin and multiplicity ($n \geq 4$, the classification for $n = 3$ is known [16–19]), starting from the graph method presented in [104], strengthened by the *unbolding/bolding* procedure of [19, 116] which we implement at the level of

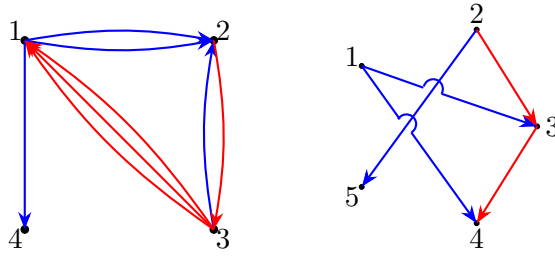


Figure 2.1: The graph associate to the kinematic structures $\langle 23 \rangle \langle 31 \rangle^3 [12]^2 [14] [32]$ and $\langle 23 \rangle \langle 34 \rangle [13] [14] [25]$ respectively.

graphs. In this algorithm, structures involving powers of any mass are always regarded as kinematically independent from structures with fewer powers of mass. This allows for a clear one-to-one correspondence between independent contact terms and operators in massive EFTs.

This chapter is organised as follows. In Section 2.1 we review the graph method introduced in [104], giving more details on the algorithm and its implementation. In Section 2.2 we will extend the method to the structures involving massive spinor variables. In Section 2.3, we work out explicitly four examples: the classification of SMEFT operators (with some details about the identical particles and the Lie algebra structures), the classification of $D^{2n}F^4$ operators in $SU(N)$ Yang-Mills theories, of dimension-six interactions between (charged and uncharged) massive and massless vectors and of quadratic-in-spin (spin-)tidal interactions in gravity.

2.1 The massless basis

2.1.1 Kinematic structures from graphs

A simple way to find all possible Lorentz invariant structures in four dimensions is to identify them with an oriented graph with two types of edges, where each vertex is associated with a particle, and the edges correspond to angle (red) or square (blue) brackets, as shown in Figure 2.1. The orientation of the edges then keeps track of the ordering in the spinor brackets and thus provides potential minus signs.

The valency of each vertex is given by two natural numbers $v^i = (v_a^i, v_s^i)$ such that $v_s^i - v_a^i = 2h_i$ is the helicity of the i^{th} particle. In general, we consider polynomial structures with an arbitrary number of momentum insertions $n_\partial \geq 0$. Each momentum in the structure can be assigned to any of the n states, which increases the valency of the corresponding vertex by $(1, 1)$. Then the number of momenta associated with each vertex is $\min\{v_a^i, v_s^i\}$. Moreover, for reasons which will become clear in the next section, it is crucial to consider a circular embedding for our graphs, *i.e.* we take all the vertices to be ordered points on a circle.

We can associate to each graph a couple of $n \times n$ adjacency matrices (\mathbf{A}, \mathbf{S}) , whose elements are non-negative integer numbers: each element $A_{ij} \geq 0$ (or $S_{ij} \geq 0$) indicates the number of red (or blue) edges going from the i^{th} -vertex to the j^{th} -vertex. Finally, there is a trivial map \mathbb{M} from the adjacency matrices to the corresponding polynomial

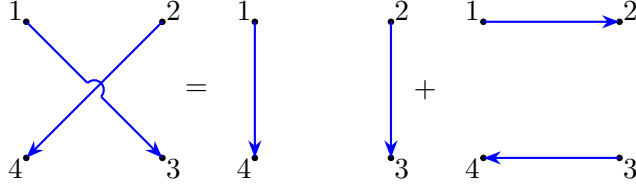


Figure 2.2: Graphical representation of the relation $[13][24] = [14][23] + [12][34]$. Then Schouten identities are equivalent to untying crossings for both the two kinds of edges (red and blue) in the graph.

spinor structure:

$$\mathbb{M}(\mathbf{A}, \mathbf{S}) = \prod_{i,j=1}^n \langle ij \rangle^{A_{ij}} [ij]^{S_{ij}} . \quad (2.1)$$

This map is in general non-invertible, because the spinor brackets are antisymmetric ($\langle ij \rangle = -\langle ji \rangle$, $[ij] = -[ji]$). Then we restrict without loss of generality to upper-half triangular adjacency matrices ($A_{ij} = 0$ and $S_{ij} = 0$ if $i \geq j$), in order to make the correspondence between polynomial structures and graphs one-to-one.

At this point, we are interested in finding a basis of structures that are independent up to Schouten identity and momentum conservation. Notice that the former acts separately on the angle and square invariants, while the latter mixes the two structures. In the following sections, we will show how to deal with these identities in terms of the graphs mentioned above.

2.1.2 Schouten identities

Schouten identities for angle and square brackets read

$$\begin{aligned} \langle i_1 i_2 \rangle \langle i_3 i_4 \rangle + \langle i_2 i_3 \rangle \langle i_1 i_4 \rangle + \langle i_3 i_1 \rangle \langle i_2 i_4 \rangle &= 0 , \\ [i_1 i_2] [i_3 i_4] + [i_2 i_3] [i_1 i_4] + [i_3 i_1] [i_2 i_4] &= 0 . \end{aligned} \quad (2.2)$$

Thinking of the kinematic structures in terms of graphs, specifically using the circular embedding already mentioned, if (i_1, i_2, i_3, i_4) are arranged in cyclic order, we notice that $\langle i_1 i_3 \rangle \langle i_2 i_4 \rangle$ correspond to intersecting edges in the graph, while $\langle i_1 i_2 \rangle \langle i_3 i_4 \rangle$ and $\langle i_2 i_3 \rangle \langle i_1 i_4 \rangle$ do not (the same is true for the square brackets). This is illustrated in Figure 2.2. In a generic graph, this relation can be applied recursively a finite number of times until we end up with a sum over graphs that do not have any crossings. It is then clear that a basis for kinematic structures that are independent under Schouten identity can be obtained by classifying all *planar graphs* associated with a polynomial kinematic structure.

It is easy to see that the planarity of the graph translates into a sharp condition on the adjacency matrices associated with it:

$$\text{if } A_{ij} \neq 0 , \quad A_{kl} = 0 \text{ for } i < k < j < l \leq n , \quad (2.3)$$

for any $i = 1, \dots, n$ and $j = i+2, \dots, n-1$. Indeed, to have an intersection between the edges (i, j) and (k, l) , the vertices must have the order specified above. In particular,

the number of crossings of a graph is given by the sum

$$n_{\times} = \sum_{i=1}^{n-1} \sum_{j=i+1}^n A_{ij} \sum_{l=j+1}^n \sum_{k=i+1}^{j-1} A_{kl} , \quad (2.4)$$

where the extrema of the sums are consistent with the restriction to upper-half triangular adjacency matrices.

This also provides an algorithmic method to write any non-planar structure in terms of planar ones. Indeed, if we consider a graph (\mathbf{A}, \mathbf{S}) for which, for example, the red edges are non-planar, *i.e.* if in (2.3) any of the $A_{kl} \neq 0$, then we can recursively untie the corresponding crossing(s) using

$$\mathbb{M}(\mathbf{A}, \mathbf{S}) = \mathbb{M}(\mathbf{A} + \mathbf{E}_{(kl)}^{(ij)}, \mathbf{S}) + \mathbb{M}(\mathbf{A} + \mathbf{F}_{(kl)}^{(ij)}, \mathbf{S}) , \quad (2.5)$$

where

$$E_{(kl), ab}^{(ij)} = -\delta_{a,i} \delta_{b,j} - \delta_{a,k} \delta_{b,l} + \delta_{a,i} \delta_{b,k} + \delta_{a,j} \delta_{b,l} , \quad (2.6)$$

$$F_{(kl), ab}^{(ij)} = -\delta_{a,i} \delta_{b,j} - \delta_{a,k} \delta_{b,l} + \delta_{a,i} \delta_{b,l} + \delta_{a,j} \delta_{b,k} . \quad (2.7)$$

Applying such decomposition a finite number of times, every non-planar structure can be written as a linear combination of planar ones. A proof of this statement is given at the end of this section.

This algorithm can be used to find a basis of SU(2) singlets in the tensor product of any finite-dimensional representation of the SU(2) group. In fact, any tensor that transforms in a representation $\mathbf{2q} + \mathbf{1}$ can be written as a totally symmetric tensor $T^{a_1 \dots a_q} = T^{(a_1 \dots a_q)}$, where a_i are indices in the fundamental of SU(2). The singlets are given by contractions of any product of tensors of this kind with $\epsilon_{a_1 a_2} = -\epsilon_{a_2 a_1}$ and the Schouten identities are equivalent to

$$\epsilon_{[a_1 a_2} \epsilon_{a_3] a_4} = 0 . \quad (2.8)$$

Then to any tensor T we can associate a vertex with valency q , and the edges correspond to contractions of two SU(2) indices through an $\epsilon_{a_i a_j}$. Any loop is then automatically zero because

$$T^{a_1 \dots a_i \dots a_j \dots a_n} \epsilon_{a_i a_j} = 0 . \quad (2.9)$$

This observation is useful if we want to apply our method to select a basis of independent SU(2) gauge structures (see for example [104]), or when we will consider polynomial structures with masses involved because the little group for massive particles in four dimensions is exactly SU(2). This could also be applied to the Lorentz group SL(2, \mathbb{C}), because the finite-dimensional representations are in one-to-one correspondence with those of SU(2) \times SU(2).

Reduction to the planar basis

In this section, we give details on the algorithm to decompose spinor structures corresponding to a non-planar graph into our basis, given by the set of structures related to planar graphs. Such decomposition amounts to repeatedly applying Schouten identities, which act separately on angle and square invariants. Then for simplicity, we are going

to consider Lorentz invariant structures with only angle invariants ($S_{ij} = 0 \forall i, j$). The condition that identifies a crossing between the edges (i, j) and (k, l) is

$$A_{ab} \neq 0, \quad A_{cd} \neq 0, \quad a < c < b < d. \quad (2.10)$$

Obviously, there are a finite number of edges (and crossings) associated with each vertex. We can consider the total number of crossings of the matrices \mathbf{A} and $\mathbf{A} + \mathbf{E}_{(c,d)}^{(a,b)}$, which we call n_{\times} and n'_{\times} , respectively. Then, proving that

$$n'_{\times} - n_{\times} < 0, \quad (2.11)$$

is equivalent to the statement that every non-planar graph can be decomposed as a sum of planar ones in a finite number of steps. We have

$$n'_{\times} - n_{\times} = \sum_{i=1}^{n-1} \sum_{j=i+1}^n \sum_{l=j+1}^n \sum_{k=i+1}^{j-1} \left(A_{ij} E_{(cd),kl}^{(ab)} + E_{(cd),ij}^{(ab)} A_{kl} + E_{(cd),ij}^{(ab)} E_{(cd),kl}^{(ab)} \right), \quad (2.12)$$

where

$$\sum_{i=1}^{n-1} \sum_{j=i+1}^n \sum_{l=j+1}^n \sum_{k=i+1}^{j-1} A_{ij} E_{(cd),kl}^{(ab)} = \left(- \sum_{i=c}^{b-1} \sum_{j=c+1}^n - \sum_{i=c+1}^b \sum_{j=d+1}^n + \sum_{i=a+1}^{b-1} \sum_{j=c+1}^b \right) A_{ij}, \quad (2.13)$$

$$\sum_{i=1}^{n-1} \sum_{j=i+1}^n \sum_{l=j+1}^n \sum_{k=i+1}^{j-1} E_{(cd),ij}^{(ab)} A_{kl} = \left(- \sum_{i=1}^{a-1} \sum_{j=c}^{b-1} - \sum_{i=1}^{c-1} \sum_{j=c+1}^b + \sum_{i=c}^{b-1} \sum_{j=b+1}^{d-1} \right) A_{ij}, \quad (2.14)$$

$$\sum_{i=1}^{n-1} \sum_{j=i+1}^n \sum_{l=j+1}^n \sum_{k=i+1}^{j-1} E_{(cd),ij}^{(ab)} E_{(cd),kl}^{(ab)} = 1. \quad (2.15)$$

Summing these contributions, we find

$$n'_{\times} - n_{\times} \leq -A_{ab} - A_{cd} + 1 < 0. \quad (2.16)$$

The same is true for the difference between the total number of crossings of \mathbf{A} and $\mathbf{A} + \mathbf{F}_{(c,d)}^{(a,b)}$.

Then, we need to choose a recursive way of eliminating all the crossings. We select a, b, c, d so that we have (2.10) and they are the smallest (in the selected order). We apply the decomposition in equation (2.5) $\min\{A_{ab}, A_{cd}\}$ times and we repeat this step until we end up with a sum of planar structures. Obviously, this choice is not always the fastest route, but the decomposition into planar graphs does not require an optimised strategy.

2.1.3 Momentum conservation

Momentum conservation is more subtle and does not have a clear graph-based interpretation. On the other hand, the classification above allows for a massive simplification and the conditions to find a basis of spinor structures independent, up to both Schouten identity and momentum conservation, are easy to implement.

We can take into account most of the relations coming from momentum conservation simply by excluding the momentum of the n^{th} -particle from the previous assignment.

Then the n^{th} -vertex will have valency $(\frac{|h_n|+h_n}{2}, \frac{|h_n|-h_n}{2})^1$. This is equivalent to imposing the constraint

$$p_n = - \sum_{i=1}^{n-1} p_i , \quad (2.17)$$

and we can *discard* from our basis any graph whose adjacency matrix *does not* satisfy the conditions

$$A_{in} = 0 \quad \text{or} \quad S_{jn} = 0 , \quad (2.18)$$

for any $i, j = 1, \dots, n-1$.

However, this is not the end of the story, because there are in general n additional momentum conservation conditions that do not involve any insertions of the momentum of the n^{th} particles:

$$0 = \begin{cases} \sum_{j=1}^{n-1} \langle ij \rangle [jn] & h_n > 0 \\ \sum_{j=1}^{n-1} \langle nj \rangle [ji] & h_n < 0 \end{cases} \quad (2.19)$$

which are a consequence of the equation of motion for free particles $p_{n\alpha\dot{\alpha}} \tilde{\lambda}_n^{\dot{\alpha}} = 0 = \lambda_n^\alpha p_{n\alpha\dot{\alpha}}$. If $h_n = 0$ the valency of the n^{th} vertex is $(0, 0)$ and there is only one additional condition to consider:

$$\left(\sum_{i=1}^{n-1} p_{i\alpha\dot{\alpha}} \right)^2 = \sum_{i=1}^{n-2} \sum_{j=i+1}^{n-1} s_{ij} = p_n^2 = 0 . \quad (2.20)$$

As already noticed in the previous section, Schouten identities do not change the valency of vertices in the multigraph, so they do not change the number of momenta associated with each vertex. Then, we have to find a set of elements in our planar basis which can be written as a linear combination of the others via momentum conservation. Once we have discarded all the polynomial structures in which we find the momentum of the n^{th} -particle, we need to carefully discard the structures that *maximise* their appearance in conditions (2.19) and (2.20). Since the edges $(1, n)$ and $(n-1, n)$ are always planar, the natural choice is to isolate terms where either p_1 or p_{n-1} appears

¹Fully eliminating the momentum of the n^{th} -particle is a matter of choices and in principles we could choose any other particle.

and to write the additional momentum conservation conditions as ²

$$\begin{cases} \langle i(n-1) \rangle [(n-1)n] = - \sum_{j=1}^{n-2} \langle ij \rangle [jn] \\ \langle (n-1)1 \rangle [1n] = - \sum_{j=2}^{n-2} \langle (n-1)j \rangle [jn] \\ s_{1n-1} = - \sum_{j=2}^{n-2} s_{1j} - \sum_{i=2}^{n-2} \sum_{j=i+1}^{n-1} s_{ij} \end{cases} \quad \begin{matrix} h_n > 0, \\ \\ h_n = 0, \end{matrix} \quad (2.21)$$

$$\begin{cases} \langle n(n-1) \rangle [(n-1)i] = - \sum_{j=1}^{n-2} \langle nj \rangle [ji] \\ \langle n1 \rangle [1(n-1)] = - \sum_{j=2}^{n-2} \langle nj \rangle [j(n-1)] \end{cases} \quad h_n < 0.$$

Notice that also the structures $\langle (n-1)1 \rangle [1n]$ (for $h_n > 0$, or s_{1n-1} and $\langle n1 \rangle [1n-1]$ in the other cases) are *always* planar, because any source of non-planarity would come from $\langle in \rangle$ invariants, which are always excluded by our choice of eliminating any momentum insertions of the n^{th} -particle. In other words, the valency of the n^{th} -vertex is $(h_n, 0)$ and $(0, h_n)$ for $h_n \leq 0$ and $h_n > 0$, respectively.

The conditions on the adjacency matrices for the polynomial structures to be in our basis are trivial. We are going to write them in the case $h_n < 0$ for simplicity:

$$\begin{aligned} A_{n-1n} &= 0 \quad \text{or} \quad S_{in-1} = 0, \\ A_{1n} &= 0 \quad \text{or} \quad S_{1n-1} = 0, \end{aligned} \quad (2.22)$$

Moreover, equations (2.21) provide an algorithmic way of writing linear relations of the structures in terms of the elements of our basis.

2.1.4 A summary of the algorithm

In this section, we elaborate on the algorithms that follow from the considerations discussed in the previous sections. In particular, we present, step-by-step, how to find a basis of kinematically independent minimal amplitudes associated with a given particle content (or field content of the associated irrelevant operators) and a specified mass dimension. For the moment, we will ignore complications coming from colour structures, which will be discussed briefly later in this chapter (for an extended discussion see for example [117]).

1. We start with an initial trivial assignment of nodes valencies determined by the field content of the operators we want to consider. In this step, we choose the arbitrary ordering of the particles in the circular embedding.

²This is an actual choice between momenta of the 1st and the $n-1^{\text{th}}$ momenta. We could choose an equivalent basis by writing (2.19) as

$$\begin{cases} \langle i1 \rangle [1n] = - \sum_{j=2}^{n-1} \langle ij \rangle [jn] \\ \langle 1(n-1) \rangle [(n-1)n] = - \sum_{j=2}^{n-2} \langle 1j \rangle [jn] \end{cases} \quad h_n > 0,$$

$$\begin{cases} \langle n1 \rangle [1i] = - \sum_{j=2}^{n-1} \langle nj \rangle [ji] \\ \langle n(n-1) \rangle [(n-1)1] = - \sum_{j=2}^{n-2} \langle nj \rangle [j1] \end{cases} \quad h_n < 0.$$

2. Accordingly to their mass dimension, such operators can have a number n_∂ of derivatives. These derivatives correspond to momenta insertions in the associated minimal amplitudes. Then, we must consider all the permutations of the partitions of n_∂ momentum insertions into at most $n - 1$ integers. By doing so, we have already taken into account the conditions (2.18) coming from momentum conservation, *i.e.* we exclude any insertion of n^{th} momentum.
3. Each momentum insertion modifies the valency of nodes, as explained in 2.1.1. Then, we have a set of possible valency assignations for the graphs and we need to generate the corresponding structures which are kinematically independent:
 - (a) We classify all the planar graphs with the valency assignment just found.
 - (b) From this set of graphs, we exclude those *not* satisfying the conditions (2.22).
 - (c) Using the map \mathbb{M} , we write down our basis of kinematically independent spinor structures³.
4. Operators may involve multiple insertions of the same field, *i.e.* we have identical particles in the minimal amplitude. For a detailed discussion see [212, 219]. In these cases, the set of kinematically independent structures does not correspond to an independent basis of EFT operators. In practice, we consider all the previously classified independent structures and we act on them with a proper Young projector over the labels of the identical states, as explained in Section 2.3.1. When summing over permutations we introduce terms which are not elements of our planar basis and we need an algorithm to write them as a linear combination of such elements⁴.
 - (a) The inverse map \mathbb{M}^{-1} gives the graphs associated with such structures.
 - (b) We apply recursively (2.5) (both for the angles and squares invariants) a finite number of times to write such graph as a sum of planar terms.
 - (c) We might end up with terms which do not satisfy (2.18) or (2.22). Such terms must also be decomposed in our basis and the graph operations, equivalent to (2.17), is

$$\mathbb{M}(\mathbf{A}, \mathbf{S}) = - \sum_{k=1}^{n-1} \mathbb{M}(\mathbf{A} + \mathbf{G}_{(k)}^{(i)}, \mathbf{S} + \mathbf{G}_{(k)}^{(j)}), \quad (2.23)$$

where

$$G_{(j), ab}^{(i)} = -\delta_{a,i}\delta_{b,n} + \delta_{a,i}\delta_{b,j}. \quad (2.24)$$

Similarly we take into account the relations (2.21). Obviously, such operations never introduce negative powers of the Lorentz invariant structures, by construction.

- (d) After applying momentum conservation identities, the terms in the sum might not be all planar and we have to recursively apply (2.5) again.

³Each of the previous steps can be visualised in the `Mathematica` package `MassiveGraphs`, using the function `HelicityCategoryBasis` (which perform the classification) and setting the option `Echos` to `True`.

⁴This second part of the algorithm has not been made publicly available in the `MassiveGraphs` code yet. On the other hand, an older version (valid only for purely massless structures) can be found in the `Mathematica` package `HelicityStructures` and the function is called `AllIdentities`.

5. After this decomposition we end up with linear combinations of terms in the chosen basis and transforming properly under permutations of the particles.
6. Finally we check whether there is a linear relation between such terms.

2.1.5 Checking the algorithm

We performed several non-trivial checks on the algorithm just presented.

1. The procedure seems to rely a lot on the cyclic order chosen for the vertices of the graphs and the momenta which we want to eliminate (using momentum conservation and equation of motion). Different choices correspond simply to different but equivalent bases for the kinematic structures. We checked that the number of elements in the basis does not depend on these choices in many non-trivial examples, involving several particles, also with higher helicity, and a high number of momenta insertions.
2. Generating all the graphs we classify all the corresponding structures. We verified numerically (on rational kinematic, as explained in Appendix A.3) that the relations we find through our algorithm are correct and that they are all.

- (a) In particular, once the basis $\{\mathbf{b}_i\}_{i=1,\dots,N}$ is generated, we might ask whether additional identities exist, which have not been considered in our approach. If such relation exist, we can find rational non-zero coefficients $\{\alpha_i\}_{i=1,\dots,N}$ such that

$$\sum_{i=1}^N \alpha_i \mathbf{b}_i = 0 . \quad (2.25)$$

We generate N independent rational kinematics and evaluate the RHS of the previous equation. By doing so we obtain a homogeneous linear system of N equations in N variables and, if its solution is $\alpha_i = 0 \ \forall i$, we checked the full independence of the elements of the basis.

- (b) In a similar way we can check completeness. It is easy to generate all the graph corresponding to the helicity assignments and distribution of momentum insertions $\{\mathbf{c}_i\}_{i=1,\dots,M}$ and we want to find numerically the rational coefficients $\{\beta_{ij}\}_{i=1,\dots,N, j=1,\dots,M}$ such that

$$\mathbf{c}_i = \sum_{j=1}^N \beta_{ij} \mathbf{b}_j . \quad (2.26)$$

We evaluate $N + 1$ times both LHS and RHS on random rational kinematics and we obtain an inhomogeneous linear system of $M \times (N + 1)$ equations in $M \times N$ variables. If a solution exists, we have verified completeness. We can also check the solution against the linear relations found from the graphic decomposition described in detail in the previous section.

We always found that the bases were complete and their elements independent in several non-trivial cases. The linear relations match with the results of the graphic decomposition.

2.2 The massive basis

The classification of independent structures in massive theories involves more technical considerations, but a generalisation of the method presented above for fully massless theories is possible. There are two sources of such additional complications:

1. The little group structures,
2. The equations of motion involving mass terms.

Indeed, when classifying irrelevant interactions for massive theories, we have to be careful about the mass ordering of the independent structures, *i.e.* we should not consider the operators \mathcal{O}_Δ and $\mathcal{O}_{\Delta+2} = m_i^2 \mathcal{O}_\Delta$ as independent when listing operators of dimension Δ and $\Delta + 2$, for example.

In Section 2.1, we identified a basis of structures $\mathcal{B} = \{\mathbf{b}_i\}$ such that any other combination of spinors with the proper mass dimension and helicity configuration can be written as a linear combination of \mathbf{b}_i 's.

When dealing with massive particles, we fix the *helicity category*⁵ and the mass dimension of the structures. We can identify a set of structures such that any element within the above-mentioned helicity category can be written as a linear combination in this basis. On the other hand, the latter will contain terms proportional to m_i , \tilde{m}_i (through the equation of motion) and p_i^2 , which are redundant when we exploit the correspondence between polynomial kinematic structures and irrelevant operators.

Then, for a specified helicity category (S_1, \dots, S_n) and mass dimension Δ , we will identify different bases that are relevant for different purposes:

- *Kinematic basis*: any spinorial structures within the chosen helicity category and mass dimension can be written as a linear combination of the terms in the basis. This basis contains also structures in different helicity categories, multiplied by powers of the masses. Such basis is the relevant one when we test our method numerically on rational kinematics as explained in Section 2.1.5 or we are interested in building an ansatz for amplitudes (for example, see [104]).
- *Helicity category basis*: any term proportional to m_i or \tilde{m}_i is ruled out. This gives a basis of structures that are kinematically independent of each other modulo identities across different helicity categories. This basis is the relevant one when we classify independent minimal amplitudes in order of the mass dimension of the corresponding EFT operators. For example, when classifying terms of mass dimension Δ , any terms proportional to m_i or \tilde{m}_i have already been considered with arbitrary coefficients in the basis for terms with mass dimension $\Delta - 1$. This will allow us to work effectively up to terms proportional to any power of the masses.

2.2.1 The Massive Little Group

When dealing with combinations of massive spinors, we must distinguish between spinors whose little group indices are contracted and those with free indices (to which

⁵The helicity category [116] of a minimal amplitude is the helicity configurations of the structures obtained *unbolding* the massive spinors [18, 19].

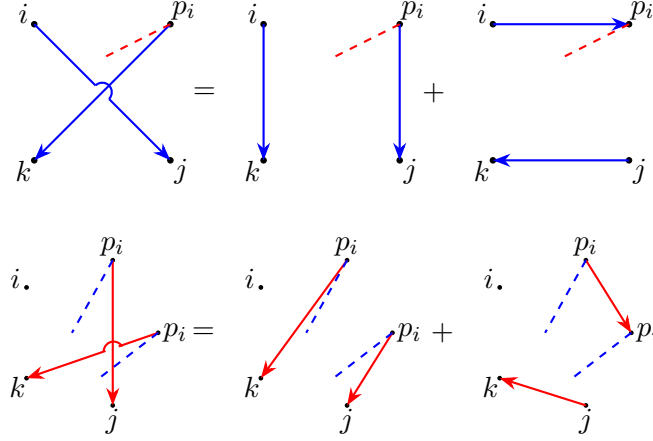


Figure 2.3: Schouten identities w.r.t. LG indices (2.27) are again equivalent to untying crossings of edges anchored to the spin and momentum vertices associated with the same particle.

we will refer as *free spinors*). Since we are interested in structures that transform under irreducible representations of the little group, the free indices associated with a particle will automatically be fully symmetric⁶. This distinction suggests that we have to associate different vertices in the graph with each momentum (*momentum vertices*) and free spinor (*spin vertex*).

Schouten identities for the little group can involve either a momentum or a free spinor ($p_{i\alpha\dot{\alpha}} \tilde{\lambda}_{i\dot{\beta}}^I$ or $p_{i\alpha\dot{\alpha}} \lambda_{i\dot{\beta}}^I$) or two momenta $p_{i\alpha\dot{\alpha}} p_{i\beta\dot{\beta}}$. We will show in detail that Schouten identities are again equivalent to untying the crossing of two edges, both anchored to momentum vertices and/or to the spin vertices. Indeed, considering the combinations mentioned above, with $p_{i\alpha\dot{\alpha}} = \lambda_{i\alpha}^I \lambda_{i\dot{\alpha}I}$ and antisymmetrising over two little group indices, we find

$$\begin{aligned} p_{i\alpha\dot{\alpha}} \tilde{\lambda}_{i\dot{\beta}}^I &= p_{i\alpha\dot{\beta}} \tilde{\lambda}_{i\dot{\alpha}}^I - \epsilon_{\dot{\alpha}\dot{\beta}} p_{i\alpha\dot{\gamma}} \tilde{\lambda}_{i\dot{\gamma}}^I, \\ p_{i\alpha\dot{\alpha}} p_{i\beta\dot{\beta}} &= p_{i\beta\dot{\alpha}} p_{i\alpha\dot{\beta}} - \epsilon_{\alpha\beta} p_{i\gamma\dot{\alpha}} p_{i\dot{\beta}}^\gamma, \end{aligned} \quad (2.27)$$

and their “conjugates”, which are identical to the relations one would find applying the antisymmetrisation directly over the $SL(2, \mathbb{C})$ indices. We show their graph representation in Figure 2.3.

We should emphasise a crucial point: since we are looking for a basis of polynomial structures with a *well-defined notion of mass ordering*, momentum vertices must be all succeeding (or all preceding) the spin vertex. Indeed, we want the combinations which are proportional to higher powers of the mass to be always planar. This is not guaranteed if the condition mentioned above is lifted, as shown in Figure 2.4.

2.2.2 Equations of Motion

So far we find a proliferation of vertices, each particle is associated with a vertex carrying both helicity weight and momentum insertions for massless particles and only spin

⁶For those spinors we will use the bold notation introduced in [18].

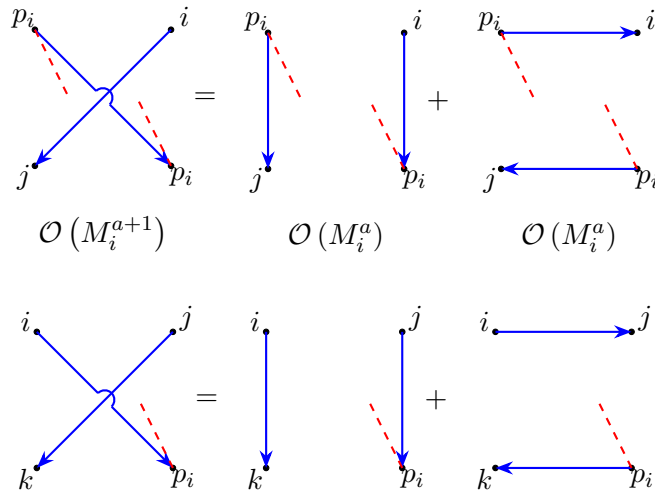


Figure 2.4: The notion of mass ordering requires that momentum vertices succeed (or precede) the spin vertex, as dictated by the on-shell conditions $p_{i\dot{\alpha}}\tilde{\lambda}_i^{\dot{\alpha}I} = \tilde{m}_i\lambda_{i\alpha}^I$ and $p_{i\dot{\alpha}}p_i^{\dot{\alpha}\beta} = M_i^2\delta_\alpha^\beta$.

weight for a massive one. Besides, in the latter case, we need to add a vertex next to the spin vertex of the corresponding particle for each insertion of massive momenta. The order of momentum vertices among themselves is irrelevant, even though it seems crucial when we are dealing with planar graphs only.

In this section, we will show how the Dirac equation for the spinors allows mapping our problem to a finite set of fully massless classifications. Then, before dealing with momentum conservation identities, we simplify our problem by using the graph equivalent of the *unbolding-bolding* procedure presented in [116].

In the previous section, we have shown that choosing carefully the arrangement of the momentum vertices in the circular embedding is essential to guarantee that any polynomial structure can be written as a linear combination of structures in our basis which have the same number of explicit mass powers or higher. This suggests that there could be a way to classify independent spinor structures with fixed powers of mass, *i.e.* a classification modulo equations of motion, excluding all the graphs where any momentum vertex is connected to the corresponding spin vertex. The key observation is the following: *unbolded* graphs, *i.e.* graphs for which we do not distinguish between momentum and spin vertices, are in *one-to-one correspondence* with planar “massive”-*bolded* graphs for which no momentum vertex is linked to the corresponding spin vertex and between themselves, and the edges are not crossing. An example of this is illustrated in Figure 2.5.

When we deal with massive structures, we have to introduce a notion of *transversality*, because the spins characterise our structures only partially. Indeed, when we consider, for example, a spin-1 particle, its polarisation tensor (that we define to be dimensionless) could in principle be defined in several ways:

$$\frac{\lambda_\alpha^{(I}\lambda_\beta^{J)}}{m}, \quad \frac{\lambda_\alpha^{(I}\tilde{\lambda}_{\dot{\alpha}}^{J)}}{M}, \quad \frac{\tilde{\lambda}_{\dot{\alpha}}^{(I}\tilde{\lambda}_{\dot{\beta}}^{J)}}{\tilde{m}}, \quad (2.28)$$

which correspond to transversality -1 , 0 , and $+1$ in our notation. In general, the

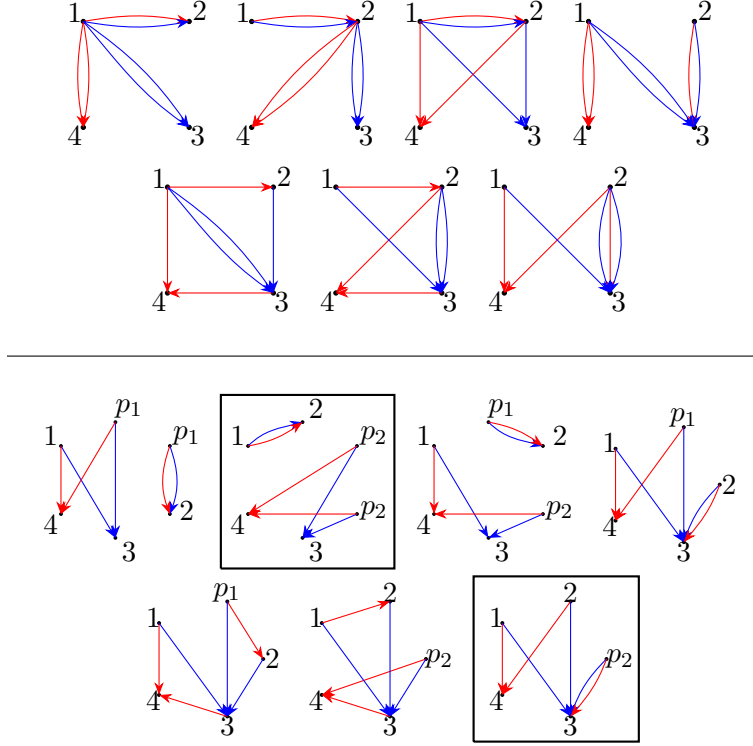


Figure 2.5: We considered the planar graphs associated terms in the helicity category $(1^{1_0}, 2^{1_0}, 3^{+1}, 4^{-1})$ and mass dimension 6. For simplicity, we did not consider a priori the ones with insertions of p_4 and those proportional to any insertion of M_1 and M_2 . We are showing both the unbolded and the bolded versions of the graphs to make the one-to-one correspondence evident. The two framed graphs correspond to our basis after taking into account momentum conservation.

transversality can take the values $C = -J, -J + 1, \dots, J$ and we will specify it as J_C . The set of transversalities and helicities identify the helicity category of the structure.

Any edge, linking a momentum vertex with its respective spin vertex, gives a power of the mass and changes the transversality of the structure:

$$p_{i\alpha\dot{\alpha}} \tilde{\lambda}_i^{\dot{\alpha}I} = \tilde{m}_i \lambda_{i\alpha}^I, \quad p_i^{\dot{\alpha}\alpha} \lambda_{i\alpha}^I = m_i \tilde{\lambda}_i^{\dot{\alpha}I}, \quad (2.29)$$

or graphically

$$\begin{array}{c} i \\ \diagup \quad \diagdown \\ \vdots \quad \vdots \\ \vdots \quad \vdots \\ \vdots \quad \vdots \end{array} \begin{array}{c} \xrightarrow{p_i} \\ | \\ \vdots \end{array} = m_i \begin{array}{c} i \\ \diagup \quad \diagdown \\ \vdots \quad \vdots \\ \vdots \quad \vdots \\ \vdots \quad \vdots \end{array}, \quad \begin{array}{c} i \\ \diagup \quad \diagdown \\ \vdots \quad \vdots \\ \vdots \quad \vdots \\ \vdots \quad \vdots \end{array} \begin{array}{c} \xrightarrow{p_i} \\ | \\ \vdots \end{array} = \tilde{m}_i \begin{array}{c} i \\ \diagup \quad \diagdown \\ \vdots \quad \vdots \\ \vdots \quad \vdots \\ \vdots \quad \vdots \end{array}.$$

Indeed, given the valency of the spin vertex of the i^{th} -particle (v_a^i, v_s^i) , then $J = v_a^i + v_s^i$ and $C = v_s^i - v_a^i$. When we classify the combinations in the helicity category $(\{i^{S_i}\}_{i=1,\dots,n})$ (with $S_i = J_{iC_i}$ or $S_i = h_i$ for massive and massless particles, respectively) and mass dimension Δ , the number of momentum insertions is $\Delta - \sum_{i=1}^n |S_i|$. Then, if we are interested in the *kinematic basis*, in addition to the structures with the chosen transversality and no mass insertion (*helicity category basis*), we need to consider also the terms in which the equations of motion change the transversality. We consider the example shown in Figure 2.5, i.e. $(1^{1_0}, 2^{1_0}, 3^{+1}, 4^{-1})_6$: we also need to classify

$(1^{1+1}, 2^{10}, 3^{+1}, 4^{-1})_5$, $(1^{1-1}, 2^{10}, 3^{+1}, 4^{-1})_5$, $(1^{10}, 2^{1+1}, 3^{+1}, 4^{-1})_5$, $(1^{10}, 2^{1-1}, 3^{+1}, 4^{-1})_5$
(multiplied by \tilde{m}_1 , m_1 , \tilde{m}_2 , m_2 respectively) and $(1^{1+1}, 2^{1+1}, 3^{+1}, 4^{-1})_4$, $(1^{1-1}, 2^{1+1}, 3^{+1}, 4^{-1})_4$,
 $(1^{1+1}, 2^{1-1}, 3^{+1}, 4^{-1})_4$, $(1^{1-1}, 2^{1-1}, 3^{+1}, 4^{-1})_4$ (all multiplied by $\tilde{m}_1 \tilde{m}_2$, $m_1 \tilde{m}_2$, $\tilde{m}_1 m_2$,
 $m_1 m_2$)⁷:

$$\begin{aligned} & \{ \langle \mathbf{12} \rangle [\mathbf{12}] \langle 4 | p_2 | 3 \rangle^2, -\langle \mathbf{14} \rangle \langle \mathbf{24} \rangle [\mathbf{13}] [\mathbf{23}] \langle 3 | p_2 | 3 \rangle, \\ & -\tilde{m}_1 \langle \mathbf{12} \rangle \langle \mathbf{14} \rangle [\mathbf{23}] \langle 4 | p_2 | 3 \rangle, -m_1 [\mathbf{12}] \langle \mathbf{24} \rangle [\mathbf{13}] \langle 4 | p_2 | 3 \rangle \\ & -\tilde{m}_2 \langle \mathbf{12} \rangle \langle \mathbf{24} \rangle [\mathbf{13}] \langle 4 | p_2 | 3 \rangle, -m_2 [\mathbf{12}] \langle \mathbf{14} \rangle [\mathbf{23}] \langle 4 | p_2 | 3 \rangle, \\ & \tilde{m}_1 m_2 \langle \mathbf{14} \rangle^2 [\mathbf{23}]^2, m_1 \tilde{m}_2 \langle \mathbf{24} \rangle^2 [\mathbf{13}]^2 \} . \end{aligned} \quad (2.30)$$

and the structures $(1^{10}, 2^{10}, 3^{+1}, 4^{-1})_4$, multiplied by both M_1^2 and M_2^2 :

$$\{ M_1^2 \langle \mathbf{14} \rangle \langle \mathbf{24} \rangle [\mathbf{13}] \langle \mathbf{23} \rangle, M_2^2 \langle \mathbf{14} \rangle \langle \mathbf{24} \rangle [\mathbf{13}] \langle \mathbf{23} \rangle \} . \quad (2.31)$$

Such terms are generated by the contractions $p_{i\alpha\dot{\alpha}} p_i^{\dot{\alpha}\beta} = M_i^2 \delta_\alpha^\beta$ and $p_i^{\dot{\alpha}\alpha} p_{i\alpha\dot{\beta}} = M_i^2 \delta_{\dot{\beta}}^{\dot{\alpha}}$, or graphically

$$\begin{array}{c} p_i \quad p_i \\ \color{red}{\longrightarrow} \\ \color{blue}{\downarrow} \quad \color{blue}{\downarrow} \\ k \quad j \end{array} = M_i^2 \color{blue}{\longleftarrow} \begin{array}{c} k \quad j \\ \color{blue}{\longleftarrow} \end{array} , \quad \begin{array}{c} p_i \quad p_i \\ \color{blue}{\longrightarrow} \\ \color{red}{\downarrow} \quad \color{red}{\downarrow} \\ k \quad j \end{array} = M_i^2 \color{red}{\longleftarrow} \begin{array}{c} k \quad j \\ \color{red}{\longleftarrow} \end{array} .$$

The total power of the masses cannot exceed the number of momentum insertions in the original structure. In particular, the maximum power of the i^{th} -particle mass in the kinematic basis is

$$\min \left\{ \max \{ |C_i - J_i|, |C_i + J_i| \}, \Delta - \sum_{i=1}^n |S_i| \right\} . \quad (2.32)$$

2.2.3 Momentum Conservation

When dealing with massive structures, momentum conservation identities involve more subtleties. First, we can always choose a particle whose momentum does never appear in the structure: for example, the n^{th} -state. Then, we can write the remaining momentum

⁷We have already taken into account momentum conservation identities, which will be described in the next section. The reader might notice that in the example shown, with the fourth particle being massless, momentum conservation identities are identical to the fully massless case, once we consider the unbolded graphs.

conservation identities as

$$\begin{aligned}
p_{n-1}|n^I] &= - \sum_{i=1}^{n-2} p_i|n^I] - p_n|n^I] , \\
\langle n^I|p_{n-1} &= - \sum_{i=1}^{n-2} \langle n^I|p_i - \langle n^I|p_n , \\
\langle n^I|p_1|(n-1)^J] &= - \sum_{i=2}^{n-2} \langle n^I|p_i|(n-1)^J] \\
&\quad - \langle n^I|p_n|(n-1)^J] - \langle n^I|p_{n-1}|(n-1)^J] , \\
\langle (n-1)^I|p_1|n^J] &= - \sum_{i=2}^{n-2} \langle (n-1)^I|p_i|n^J] \\
&\quad - \langle (n-1)^I|p_n|n^J] - \langle (n-1)^I|p_{n-1}|n^J] , \\
2 p_1 \cdot p_{n-1} &= M_n^2 - \sum_{i=1}^{n-2} \sum_{j=i+1}^{n-1} 2 p_i \cdot p_j - \sum_{i=1}^{n-1} M_i^2 ,
\end{aligned} \tag{2.33}$$

where the LG indices can be either contracted or not, or not be present at all (as the corresponding particle could be massless). We write these identities such that the terms with higher powers of the masses are independent, *i.e.* they can only be written as a linear combination of the structures with the same or higher mass powers. This allows us to effectively set them to zero and work modulo equations of motion ($\stackrel{D}{\simeq}$), as explained in the previous section. For example, some of the equations in (2.33) look like

$$\begin{aligned}
p_{n-1}|n^I] &\stackrel{D}{\simeq} - \sum_{i=1}^{n-2} p_i|n^I] , \\
\langle (n-1)^I|p_1|n^J] &\stackrel{D}{\simeq} - \sum_{i=2}^{n-2} \langle (n-1)^I|p_i|n^J] , \\
2 p_1 \cdot p_{n-1} &\stackrel{D}{\simeq} - \sum_{i=1}^{n-2} \sum_{j=i+1}^{n-1} 2 p_i \cdot p_j ,
\end{aligned} \tag{2.34}$$

which resemble fully massless identities (2.21). Classifying the structures up to equations of motion means that we can put forward the identification

$$\langle j^J|p_i|k^K] \lambda_{i\alpha}^I \stackrel{D}{\simeq} \langle j^J i^I \rangle p_i|k^K]_\alpha , \tag{2.35}$$

and its “conjugate”. This is equivalent to stating that the momentum conservation conditions for unbolded graphs are identical to the fully massless case, *i.e.* that we should not distinguish between spin and momentum vertices but only keep track of the number of momentum insertions for each particle. In particular, if the n^{th} particle is either massless or $J_n \leq \frac{1}{2}$, momentum conservation identities for unbolded graphs are identical to the fully massless case, once we check if there are insertions of p_1 or p_{n-1} .

On the other hand, there is a subtlety when we consider fully massive structures or, in general, we choose to fully eliminate the momentum of a spin- J massive particle whose transversality $C \neq -J$, J and $J \geq 1$. In particular, in these cases, the structures $\langle n^I|p_1|(n-1)^J]$ and $\langle (n-1)^I|p_1|n^J]$ are not guaranteed to be planar because the spin

vertex of the n^{th} -particle has non-vanishing valency for the edges corresponding to both squares and angles, even if there are no momentum insertions associated to it. Nevertheless, these non-planar structures give additional momentum conservation constraints which should be taken into account.

An *ad hoc* solution to overcome this problem is the following:

- 1) We classify and count the number m of independent structures, or planar graphs after redefining the valencies of the vertices as

$$\begin{aligned} (v_a^1, v_s^1) &\rightarrow (v_a^1 - l, v_s^1 - l) , \\ (v_a^{n-1}, v_s^{n-1}) &\rightarrow (v_a^{n-1} - l_1, v_s^{n-1} - l_2) , \\ (v_a^n, v_s^n) &\rightarrow (v_a^n - l_2, v_s^n - l_1) , \end{aligned} \quad (2.36)$$

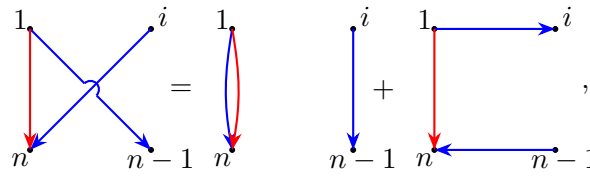
where $l = l_1 + l_2$. In this way, we classify the independent structures for which we *factorise* the product $\langle (n-1)^{I_1} | p_1 | n^{J_1} \rangle^{l_1} \langle n^{J_2} | p_1 | (n-1)^{I_2} \rangle^{l_2}$.

- 2) If we restore the *factorised* edges in the graphs obtained in this classification as

$$\begin{aligned} A_{i,1n-1} &\rightarrow A_{i,1n-1} + l_1 , \\ A_{i,1n} &\rightarrow A_{i,1n} + l_2 , \\ S_{i,1n-1} &\rightarrow S_{i,1n-1} + l_2 , \\ S_{i,1n} &\rightarrow S_{i,1n} + l_1 , \end{aligned} \quad (2.37)$$

for $i = 1, \dots, m$, we obtain a series of planar and non-planar graphs. The structures corresponding to planar graphs in this classification must be removed from our basis.

- 3) Non-planar structures must be treated separately. There is a unique source of non-planarity in these graphs and, using iteratively Schouten identities, we can write these non-planar structures as linear combinations of planar ones. In particular, we find



$$\begin{aligned} & \begin{array}{c} 1 \\ \downarrow \\ n \end{array} \begin{array}{c} i \\ \downarrow \\ n-1 \end{array} = \begin{array}{c} 1 \\ \downarrow \\ n \end{array} \begin{array}{c} i \\ \downarrow \\ n \end{array} + \begin{array}{c} i \\ \downarrow \\ n-1 \end{array} \begin{array}{c} 1 \\ \downarrow \\ n \end{array} \begin{array}{c} i \\ \downarrow \\ n-1 \end{array} , \end{aligned} \quad (2.38)$$

and its “conjugate”. Using momentum conservation on the LHS we can trade p_1 insertions with a sum of structures which do not depend on neither p_1 , p_{n-1} nor p_n . This means that each non-planar structure gives a linear constraint for terms appearing on the RHS.

- 4) Then, we can *discard* a number m of graphs whose adjacency matrices satisfy the conditions

$$A_{1n} > 0 , \quad S_{1n} > 0 , \quad \exists i \text{ s.t. } S_{in-1} > 0 , \quad (2.39)$$

or

$$A_{1n} > 0 , \quad S_{n-1n} > 0 , \quad \exists i \text{ s.t. } S_{1i} > 0 , \quad (2.40)$$

or their “conjugates”.

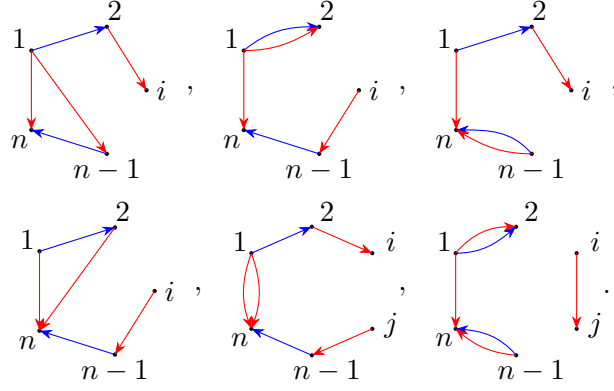


Figure 2.6: Planar structures to eliminate corresponding to the factorised term $\langle \mathbf{1n} | [(\mathbf{n}-1)\mathbf{n}] \langle (\mathbf{n}-1) | p_2 | \mathbf{1}]$.

Surprisingly, if we consider cases in which $J_i \geq 1$ and $C_i \neq -J_i, J_i$ for $i = 1, n-1, n$, there is an additional relation to take into account:

$$\langle \mathbf{1n} | [(\mathbf{n}-1)\mathbf{n}] \langle (\mathbf{n}-1) | \sum_{i=2}^{n-2} p_i | \mathbf{1}] \stackrel{D}{\simeq} [\mathbf{1n}] \langle (\mathbf{n}-1)\mathbf{n} | \langle \mathbf{1} | \sum_{i=2}^{n-2} p_i | \mathbf{n}-1] \quad (2.41)$$

In order for the terms in this additional relation to be independent from the momentum conservation conditions already considered, the momenta p_1, p_{n-1} , and p_n must be massive and none of them can appear in the structures in (2.41). The algorithm to eliminate this additional constraint is identical to the one just presented, except for the factorised structure, which we choose to be $\langle \mathbf{1n} | [(\mathbf{n}-1)\mathbf{n}] \langle (\mathbf{n}-1) | p_2 | \mathbf{1}]$, and the corresponding planar structures that we need to eliminate are shown in Figure 2.6.

These algorithms give the basis of the independent kinematic structures we are looking for, modulo Schouten identities, momentum conservation, and equation of motion. To find the complete *kinematic basis* we need to consider all the *helicity categories bases* with lower mass dimensions multiplied by proper mass powers, as shown in Section 2.2.2.

2.2.4 A summary of the algorithm

We now present a summary of the algorithm for minimal amplitudes, including massive particles. The general structure is the same presented for fully massless amplitudes, with few key differences.

1. We start with an initial trivial assignment of vertex valencies determined by the field content of the operators and the distribution of momentum insertions (*i.e.* mass dimensions).
2. We are interested in the helicity category basis, then we will work up to terms with explicit powers of the masses, *i.e.* we do not distinguish free spinors and momentum vertices in the graphs.
3. We generate the corresponding structures which are kinematically independent⁸:

⁸As in the massless case, this classification correspond to the `HelicityCategoryBasis` function in the `MassiveGraphs` code. If we are also interested in the terms proportional to powers of the masses, *i.e.* to the kinematic basis, the function to use is `KinematicBasis`.

- (a) We classify all the planar graphs.
- (b) From this set of graphs, we exclude some of the graphs thanks to momentum conservation, as explained in Section 2.2.3.
- (c) To each of the remaining graphs, we can associate a unique planar massive graph⁹.
- (d) Using the massive generalisation of the map \mathbb{M} , we write down our basis of kinematically independent spinor structures in the helicity category basis. It is quite hard to write down an explicit (and clear) closed formula for such a map, then we provide a couple of examples from Figure 2.5:

$$\begin{array}{c}
 \begin{array}{c}
 \begin{array}{c}
 \text{1} \quad \text{2} \\
 \nearrow \quad \searrow \\
 \text{4} \quad \text{3}
 \end{array} \\
 \text{M} \circ
 \end{array}
 = \langle \mathbf{12} \rangle [\mathbf{12}] \langle 4 | p_2 | 3 \rangle^2 , \\
 \\
 \begin{array}{c}
 \begin{array}{c}
 \text{1} \quad \text{2} \\
 \nearrow \quad \searrow \\
 \text{4} \quad \text{3}
 \end{array} \\
 \text{M} \circ
 \end{array}
 = \langle \mathbf{14} \rangle \langle \mathbf{24} \rangle [\mathbf{13}] [\mathbf{23}] \langle 3 | p_2 | 3 \rangle .
 \end{array}$$

- 4. When dealing with identical particles, we also need to decompose some structures which do not appear in our basis. Since our algorithm relies on the unbolding/bolding procedure at the level of graphs, we can find linear relations only up to terms with masses, like equations (2.34), (2.35) or (2.41). The details can be extrapolated from point (4) in Section 2.1.4 and the discussion of Section 2.2.3. Even if such linear relations are not complete, the information they provide is enough, as the missing terms are proportional for minimal amplitude with the same field content, but a smaller mass dimension.
- 5. After this decomposition we end up with linear combinations of terms in the chosen basis and transforming properly under permutations of the particles.
- 6. Finally we check whether there are linear relations between such terms.
- 7. The checks on the algorithm are exactly the same presented in Section 2.1.5.

2.3 Applications

In this section, we are going to present some applications of our method for the classification of irrelevant interactions in effective theories. The fully massless algorithm has been used in [104] to list the SMEFT irrelevant operators up to dimension eight.

The method presented in this thesis can be applied to any number of particles with arbitrary helicity and spin. In particular, we will show some details needed for the construction of our SMEFT basis, the classification of $D^{2n}F^4$ effective interactions in $SU(N)$ Yang-Mills theories, five-point effective interactions involving W , Z and γ vector

⁹For the interested reader, the bolding map at the level of graphs is not shown in this thesis, but it can be found explicitly coded in the [MassiveGraphs](#) package.

bosons and spin-tidal interactions in gravity. In particular, in the last case, we will show how our method is related to the strategy presented in [116], explicitly showing the mass-complete relations relevant to the case considered.

In the first part, we will briefly mention how to treat identical particles and colour structures, which have been extensively studied in the literature [116, 117, 210, 212, 219, 220].

All algorithms for massive particles have been implemented in the `Mathematica` package `MassiveGraphs`, which make use of the `SpinorHelicity` package. An older version of this code, working only in the fully massless case and focusing on the construction of a SMEFT basis of irrelevant interactions, is `SMEFT-operators`, which make use of the package `SpinorHelicity6D` to deal with spinor helicity structures.

2.3.1 The on-shell classification of SMEFT operators

In this section we are going to extend the on-shell methods to the classification of effective interactions [62, 113, 116] in the SMEFT [19, 111, 112, 114], corresponding in the Lagrangian formalism to insertions of irrelevant operators [211, 221–223]. First, we are going to classify all the independent kinematic structures in a generic theory in four dimensions introducing a new algorithm in terms of graphs and then we will consider the specific case of the Standard Model, combining these with the colour structures¹⁰. A subset of the contact term basis for dimension-six and dimension-eight irrelevant interactions, relevant for the study of deviation from the Standard Model in the process $pp \rightarrow Wh$, is shown explicitly in the next chapter, in Table 5.1 and 5.2. The full list up to dimension-eight can be found in the ancillary files of [104].

Mass dimension and minimal amplitudes in massless gauge theories

As we explained in the previous sections, each effective interaction will be identified by its *minimal* amplitude, *i.e.* the amplitude at leading order which does not vanish in free theory (if we switch off all the other interactions). This has to be a contact term, *i.e.* no intermediate modes are propagating.

As a first step in the classification procedure, we fix the mass-dimension $[\mathcal{O}]$ of the irrelevant operators for which we want to find a complete basis. From the minimal amplitudes, we strip off the coupling of the effective interaction, which is related to the dimension of the corresponding irrelevant operator by

$$[g_{\mathcal{O}}] = 4 - [\mathcal{O}] . \quad (2.42)$$

What we are looking for are the kinematic structures which have mass dimension

$$[\mathcal{O}] - n \geq 0 , \quad (2.43)$$

where n is the number of external legs in the corresponding minimal amplitude. Equation (2.43) provides a constraint on n which can be further refined by taking into account which types of particles are found in the amplitudes. In fact, to get helicity weights right, each vector in the minimal amplitude will contribute with at least two spinor

¹⁰The approach presented in this section has been coded in `Mathematica`. The code and an example notebook are available at the link <https://github.com/StefanoDeAngelis/SMEFT-operators>.

$(n_{g^-}, n_{g^+}, n_{f^-}, n_{f^+}, n_s)$	Independent structures
(0, 0, 0, 0, 6)	1
(0, 0, 0, 0, 4)	$[12]\langle 12 \rangle, [23]\langle 23 \rangle$
(0, 0, 0, 2, 3)	$[12]$
(0, 0, 0, 4, 0)	$[12][34], [14][23]$
(0, 0, 1, 1, 2)	$[23]\langle 13 \rangle$
(0, 0, 2, 0, 3)	$\langle 12 \rangle$
(0, 0, 2, 2, 0)	$[34]\langle 12 \rangle$
(0, 0, 4, 0, 0)	$\langle 12 \rangle \langle 34 \rangle, \langle 14 \rangle \langle 3 \rangle$
(0, 1, 0, 2, 1)	$[12][13]$
(0, 2, 0, 0, 2)	$[12]^2$
(0, 3, 0, 0, 0)	$[12][13][23]$
(1, 0, 2, 0, 1)	$\langle 12 \rangle \langle 13 \rangle$
(2, 0, 0, 0, 2)	$\langle 12 \rangle^2$
(3, 0, 0, 0, 0)	$\langle 12 \rangle \langle 13 \rangle \langle 23 \rangle$

Table 2.1: All the independent structures and possible particle content for minimal amplitudes corresponding to irrelevant operators of mass dimension six.

variables and each fermion with at least one. This leads to the stronger constraint¹¹

$$[\mathcal{O}] - n \geq 2 \times \frac{1}{2} \times n_g + \frac{1}{2} \times n_f \quad \Longrightarrow \quad 2n_g + \frac{3}{2}n_f + n_s \leq [\mathcal{O}] \quad , \quad (2.44)$$

where n_g , n_f and n_s are respectively the number of vectors, fermions and scalars and clearly $n = n_g + n_f + n_s$. Next, we need to take into account the constraints coming from the condition that our kinematic structures must be $SL(2, \mathbb{C})$ invariant. This requires to further distinguish between helicities of the different particles, and to find all the $(n_{g^-}, n_{g^+}, n_{f^-}, n_{f^+}, n_s)$ ¹² compatible with the constraint (2.44). Once n_g , n_f and n_s are fixed, we take into account that every state can contribute to the kinematic structures with powers of its momentum, which correspond to derivatives in the operator language. The total number of momenta n_∂ is fixed by saturating the mass dimension constraint to

$$n_\partial = [\mathcal{O}] - 2n_g - \frac{3}{2}n_f - n_s \quad . \quad (2.45)$$

This algorithm classifies efficiently all the $SL(2, \mathbb{C})$ -invariant structures which are polynomial in the spinor variables with fixed mass dimension and helicity configuration, associated to each $(n_{g^-}, n_{g^+}, n_{f^-}, n_{f^+}, n_s)$. We notice that this algorithm can be applied also beyond gauge theories and massless states. As an example, in Table 2.1 we show all the possible particle configurations for minimal amplitudes corresponding to irrelevant operators of mass dimension six in generic gauge theories.

The classification of the helicity structures is completely theory-independent and is indeed not limited to gauge theories, but can be applied to effective field theories of gravity, with (massive and spinning) matter as well. Information about the Standard Model enters only in the $SU(3) \times SU(2) \times U(1)$ (invariant) structures associated with the chosen set of particles.

¹¹This condition is not only necessary but also sufficient for having local interactions.

¹²The superscript of the subscript specify the helicity of the particles: $n_g = n_{g^-} + n_{g^+}$ and $n_f = n_{f^-} + n_{f^+}$.

The gauge group structures

The classification of the invariant structures of the gauge groups can be worked out using standard group theory techniques. In particular

- $U(1)$: to each $(n_{g^-}, n_{g^+}, n_{f^-}, n_{f^+}, n_s)$ structure we associate all the possible combinations of Standard Model states for which the total hypercharge is zero.
- $SU(2)$: we notice that the algorithm presented in the previous section can be generalised to the case of $SU(2)$ invariants with a single graph associated with the invariants. Each oriented edge from the n^{th} to the m^{th} vertices correspond to an $\epsilon^{i_n i_m}$ tensors and the valence of each vertex v_i is fixed by the representation of the i^{th} -particle, labelled by its dimension $\mathbf{v}_i + \mathbf{1}$. The indices associated with the same vertex must be taken as completely symmetric. In the case of the $SU(2)$ group there is no analogous of momentum conservation, so the independent structures can be taken to be in one-to-one correspondence with planar graphs.
- $SU(3)$: the $SU(N)$ invariants have been studied a lot both in mathematic and physic literature (see, for example, [224–226]), so we will not go into further details here. In our algorithm we adopt the standard Littlewood-Richardson rule [227, 228] as suggested in [117, 118].

Once the kinematic structures associated to $(n_{g^-}, n_{g^+}, n_{f^-}, n_{f^+}, n_s)$ have been generated and a compatible set of gauge singlets was found, we combine all the invariants to find a basis of independent structures enclosing information about both the kinematics and the colour. If no identical fields are present, these structures coincide with the minimal amplitudes, else one needs to impose Bose-Einstein and Dirac-Fermi statistics as explained in the next section.

Repeated fields and Young projectors

There are cases for which the minimal amplitude involves identical states, for example for $[g_{\mathcal{O}}] = -2$ we could have minimal amplitudes with (G^+, G^+, G^+) or (Q, Q, u, d) . The treatment of this subtlety has been systematically taken into account in [117, 219]. Starting from their classification, we take a slightly different approach, since we deal with minimal amplitudes and not with operators. We distinguish between identical bosons and fermions at the level of the minimal amplitude and impose the Bose-Einstein statistic for the former and Dirac-Fermi statistic for the latter. In practice, we consider all the previously classified independent structures and we act on them with a proper Young projector over the labels of the identical states:

- in the case of n identical bosons we act on the structures with the symmetriser projector

$$\mathcal{Y}_{\overline{\mathbb{1}} \cdot \overline{\mathbb{1}}} = \frac{1}{n!} \sum_{i=1}^{n!} p_i, \quad (2.46)$$

where p_i are all the permutations of the n labels associated with the identical bosons.

- in the case of n identical fermions we act on the structures with the total anti-symmetriser projector

$$\mathcal{Y}_{\begin{array}{|c|} \hline \mathbb{1} \\ \hline \mathbb{n} \\ \hline \end{array}} = \frac{1}{n!} \sum_{i=1}^{n!} s_i p_i , \quad (2.47)$$

where s_i is the signature of the permutations p_i .

Once, we apply the Young projectors to the independent minimal amplitudes, we will end up with a sum over terms which will not necessarily belong to the basis of independent structures chosen. To find the minimal amplitudes, we need to re-write these symmetrised amplitudes in terms of elements of our structure basis and check if they are linearly independent of each other (which in general will not be the case, some structures will even be automatically zero after projection).

A further subtlety arises in the case of the Standard Model, due to the *flavour* of fermions: to each particle, we can associate a further $SU(N_f)$ index, where N_f is the number of flavours. The independent minimal amplitudes can then be classified in terms of inequivalent irreducible representations of $SU(N_f)$, which are in one-to-one correspondence with the irreducible representations of the symmetric group S_n , where n is the number of identical fermions in the same family. For example, for dimension 6 operators we can consider the baryon number violating effective interactions with (Q, Q, Q, L) ($n = 3$). Then we have a basis of four independent structures:

$$\epsilon^{a_1 a_2 a_3} \epsilon^{i_1 i_4} \epsilon^{i_2 i_3} \langle 12 \rangle \langle 34 \rangle , \quad (2.48)$$

$$\epsilon^{a_1 a_2 a_3} \epsilon^{i_1 i_2} \epsilon^{i_3 i_4} \langle 12 \rangle \langle 34 \rangle , \quad (2.49)$$

$$\epsilon^{a_1 a_2 a_3} \epsilon^{i_1 i_4} \epsilon^{i_2 i_3} \langle 14 \rangle \langle 23 \rangle , \quad (2.50)$$

$$\epsilon^{a_1 a_2 a_3} \epsilon^{i_1 i_2} \epsilon^{i_3 i_4} \langle 14 \rangle \langle 23 \rangle . \quad (2.51)$$

There are three inequivalent representations of S_3 , corresponding to the Young diagrams $\square\square\square$, $\square\square$ and \square . Then we can act on the independent structure with the projectors associated to the standard Young tableaux $\begin{array}{|c|c|} \hline \mathbb{1} & \mathbb{2} & \mathbb{3} \\ \hline \end{array}$, $\begin{array}{|c|} \hline \mathbb{1} & \mathbb{2} \\ \hline \end{array}$ and $\begin{array}{|c|} \hline \mathbb{1} \\ \hline \end{array}$ ¹³. There is a unique linearly independent structure associated with each irreducible representation:

$$C_{m_1 m_2 m_3, m_4}^{\{3\}, \{1\}} \mathcal{Y}_{\begin{array}{|c|} \hline \mathbb{1} & \mathbb{2} & \mathbb{3} \\ \hline \end{array}} \circ \epsilon^{a_1 a_2 a_3} \epsilon^{i_1 i_4} \epsilon^{i_2 i_3} \langle 12 \rangle \langle 34 \rangle , \quad (2.52)$$

$$C_{m_1 m_2 m_3, m_4}^{\{2,1\}, \{1\}} \mathcal{Y}_{\begin{array}{|c|} \hline \mathbb{1} & \mathbb{2} \\ \hline \mathbb{3} \\ \hline \end{array}} \circ \epsilon^{a_1 a_2 a_3} \epsilon^{i_1 i_4} \epsilon^{i_2 i_3} \langle 12 \rangle \langle 34 \rangle , \quad (2.53)$$

$$C_{m_1 m_2 m_3, m_4}^{\{1,1,1\}, \{1\}} \mathcal{Y}_{\begin{array}{|c|c|} \hline \mathbb{1} & \mathbb{2} & \mathbb{3} \\ \hline \end{array}} \circ \epsilon^{a_1 a_2 a_3} \epsilon^{i_1 i_4} \epsilon^{i_2 i_3} \langle 12 \rangle \langle 34 \rangle , \quad (2.54)$$

where $C_{m_1 m_2 m_3, m_4}^{\pi, \{1\}}$ is a Wilson coefficient tensor associated with each effective minimal amplitude, with π being the integer partition corresponding to the Young diagram for the Q fields. Notice that Dirac-Fermi statistics forces the Wilson coefficient tensor to have the ‘‘opposite’’ symmetry properties with respect to the Young tableau associated to the projector: *e.g.* $C_{m_1 m_2 m_3, m_4}^{\{3\}, \{1\}} = C_{(m_1 m_2 m_3), m_4}^{\{3\}, \{1\}}$, $C_{m_1 m_2 m_3, m_4}^{\{2,1\}, \{1\}} = C_{[m_1 m_2] m_3, m_4}^{\{2,1\}, \{1\}}$,

¹³The fourth standard tableau $\begin{array}{|c|} \hline \mathbb{1} & \mathbb{3} \\ \hline \mathbb{2} \\ \hline \end{array}$ would not give an independent minimal amplitude, because it could be obtained from the second one by relabelling: $\mathcal{Y}_{\begin{array}{|c|} \hline \mathbb{1} & \mathbb{3} \\ \hline \mathbb{2} \\ \hline \end{array}} = (2\ 3) \circ \mathcal{Y}_{\begin{array}{|c|} \hline \mathbb{1} & \mathbb{2} \\ \hline \mathbb{3} \\ \hline \end{array}} \circ (2\ 3)$, where $(2\ 3)$ is the permutation of the labels 2 and 3.

$C_{[m_1 m_2 m_3], m_4}^{\{2,1\}, \{1\}} = 0$ and $C_{[m_1 m_2 m_3], m_4}^{\{1,1,1\}, \{1\}} = C_{[m_1 m_2 m_3], m_4}^{\{1,1,1\}, \{1\}}$. The number of independent operators for this specific case is ¹⁴ $\frac{(N_f+2)(N_f+1)N_f}{6}$, $\frac{(N_f+1)N_f(N_f-1)}{3}$ and $\frac{N_f(N_f-1)(N_f-2)}{6}$ for each tensor respectively.

2.3.2 $D^{2n}F^4$ interactions in gauge theories

We consider now a simple example in which all the particles are massless vector bosons in $SU(N)$ Yang-Mills theory with $N > 3$. We will consider in order the three independent helicity configurations $(+++)$, $(+++-)$ and $(++--)$.

All-plus configuration

The algorithm provides us with a basis of kinematically independent structures which are compatible with the mass dimension $4 + 2n$ and the chosen helicity configuration. In particular, we find

$$s_{12}^n [12]^2 [34]^2, s_{12}^n [14]^2 [23]^2, s_{12}^n [12][23][34][41], \{s_{23}^{n-k} s_{12}^k [14]^2 [23]^2\}_{k=0, \dots, n-1}, \quad (2.55)$$

which correspond to the only $n + 3$ graphs that meet all the requirements stated in Section 2.1. A basis of independent colour structures for $N > 3$ is

$$\mathcal{C} = \{\delta^{A_1 A_4} \delta^{A_2 A_3}, \delta^{A_1 A_3} \delta^{A_2 A_4}, \delta^{A_1 A_2} \delta^{A_3 A_4}\} \cup \{\tau^{A_1 A_i A_j A_k}\}_{(i,j,k)=\mathcal{P}_3(2,3,4)}, \quad (2.56)$$

where $\mathcal{P}_3(2, 3, 4)$ corresponds to the permutations of $(2, 3, 4)$, and $\tau^{A_1 A_2 A_3 A_4}$ is the trace of four $SU(N)$ generators τ^A .

These two bases must be combined to find the effective interactions we are looking for. At this point, we have $9 \times (3 + n)$ terms and, as we are dealing with identical particles, we need to sum over all the permutations of the external legs in these structures. For example, we can consider $\delta^{A_1 A_4} \delta^{A_2 A_3} s_{12}^n [12]^2 [34]^2$:

$$\begin{aligned} \mathcal{Y}_{\overline{1234}} \circ \delta^{A_1 A_2} \delta^{A_3 A_4} s_{12}^n [12]^2 [34]^2 &\equiv \frac{1}{3} \delta^{A_1 A_2} \delta^{A_3 A_4} s_{12}^n [12]^2 [34]^2 + \frac{1}{3} \delta^{A_1 A_3} \delta^{A_2 A_4} s_{13}^n [13]^2 [24]^2 \\ &+ \frac{1}{3} \delta^{A_1 A_4} \delta^{A_2 A_3} s_{23}^n [14]^2 [23]^2. \end{aligned} \quad (2.57)$$

The structure $s_{13}^n [13]^2 [24]^2$ does not belong to our basis and we have to rewrite it as a linear combination of elements of our basis. We can do this using the algorithm presented in Section 2.1 and we always verify such relations on rational kinematics, as presented in Appendix A.3. This means that, after symmetrisation, not all the $9 \times (3 + n)$ structures are kinematically independent. Indeed, it turns out that only $4 + 2 \lfloor \frac{n}{2} \rfloor$ structures actually are. We are going to present a basis of effective interactions

¹⁴The counting can be performed using the Hook Content Formula.

for $n \leq 8$, which we will denote by \mathcal{B}_{4+2n} :

$$\begin{aligned}
\mathcal{B}_4 &= ([14]^2[23]^2 \times \mathcal{C}_1) \cup ([14]^2[23]^2 \times \mathcal{C}_2) , \\
\mathcal{B}_6 &= s_{23} \times \mathcal{B}_4 , \\
\mathcal{B}_8 &= (s_{12} \times \mathcal{B}_6) \cup (s_{12}s_{23}[14]^2[23]^2 \times \mathcal{C}_3), \\
\mathcal{B}_{10} &= s_{23} \times \mathcal{B}_8 , \\
\mathcal{B}_{12} &= (s_{12} \times \mathcal{B}_{10}) \cup (s_{12}s_{23}^3[14]^2[23]^2 \times \mathcal{C}_1) , \\
\mathcal{B}_{14} &= s_{23} \times \mathcal{B}_{12} , \\
\mathcal{B}_{16} &= (s_{12}^2s_{23}^2 \times \mathcal{B}_8) \cup (s_{12}^2s_{23}^4 \times \mathcal{B}_4) , \\
\mathcal{B}_{18} &= s_{23}\mathcal{B}_{16} , \\
\mathcal{B}_{20} &= (s_{12}^4s_{23}^4 \times \mathcal{B}_8) \cup (s_{12}^3s_{23}^5 \times \mathcal{B}_8) ,
\end{aligned}$$

where

$$\begin{aligned}
\mathcal{C}_1 &= \{\delta^{A_1A_4}\delta^{A_2A_3}, \tau^{A_1A_2A_3A_4}\} , \\
\mathcal{C}_2 &= \{\delta^{A_1A_3}\delta^{A_2A_4}, \tau^{A_1A_2A_4A_3}\} , \\
\mathcal{C}_3 &= \{\delta^{A_1A_2}\delta^{A_3A_4}, \tau^{A_1A_3A_2A_4}\} ,
\end{aligned}$$

and the symmetrisation is understood for each element in the lists. For example, the first element in \mathcal{B}_4 is

$$\begin{aligned}
\delta^{A_1A_4}\delta^{A_2A_3}[14]^2[23]^2 &\rightarrow \frac{1}{3}\delta^{A_1A_2}\delta^{A_3A_4}[12]^2[34]^2 + \frac{1}{3}\delta^{A_1A_3}\delta^{A_2A_4}[13]^2[24]^2 \\
&\quad + \frac{1}{3}\delta^{A_1A_4}\delta^{A_2A_3}[14]^2[23]^2 .
\end{aligned} \tag{2.58}$$

Single-minus configuration

In this case, the basis of kinematically independent structures consists of n elements:

$$\{s_{12}^{n-k-1}s_{23}^k\langle 24 \rangle^2[12]^2[23]^2\}_{k=0,\dots,n-1} . \tag{2.59}$$

After combining with the colour basis and symmetrising over the $(1, 2, 3)$ we end up with $\lfloor \frac{3n+1}{2} \rfloor$ independent contact terms:

$$\begin{aligned}
\mathcal{B}_6 &= (\langle 24 \rangle^2[12]^2[23]^2 \times \mathcal{C}_1) , \\
\mathcal{B}_8 &= (s_{23} \times \mathcal{B}_6) \cup \{\tau^{A_1A_2A_4A_3}s_{23}\langle 24 \rangle^2[12]^2[23]^2\} , \\
\mathcal{B}_{10} &= s_{12}s_{23}\langle 24 \rangle^2[12]^2[23]^2 \times (\mathcal{C}_1 \cup \mathcal{C}_2) \cup \{\tau^{A_1A_3A_4A_2}s_{12}s_{23}\langle 24 \rangle^2[12]^2[23]^2\} , \\
\mathcal{B}_{12} &= s_{23} \times \mathcal{B}_{10} \cup \{\tau^{A_1A_3A_2A_4}s_{12}s_{23}^2\langle 24 \rangle^2[12]^2[23]^2\} , \\
\mathcal{B}_{14} &= s_{12} \times \mathcal{B}_{12} \cup s_{12}s_{23}^3\langle 24 \rangle^2[12]^2[23]^2 \times \mathcal{C}_1 , \\
\mathcal{B}_{16} &= s_{12}^2s_{23}^3\langle 24 \rangle^2[12]^2[23]^2 \times \mathcal{C} , \\
\mathcal{B}_{18} &= s_{12}^2s_{23}^2 \times \mathcal{B}_{10} \cup s_{12}s_{23}^2 \times \mathcal{B}_{12} , \\
\mathcal{B}_{20} &= s_{12}s_{23} \times \mathcal{B}_{16} \cup s_{12}^2s_{23}^4 \times \mathcal{B}_8 ,
\end{aligned}$$

where the symmetrisation is understood for each element in the lists.

MHV configuration

In this configuration the basis of kinematically independent structures consists of $n + 1$ elements:

$$s_{12}^n [12]^2 \langle 34 \rangle^2, s_{12}^{n-1} [12]^2 \langle 34 \rangle \langle 3|p_2 p_1|4 \rangle, \{s_{23}^{n-k-2} s_{12}^k [12]^2 \langle 3|p_2 p_1|4 \rangle^2\}_{k=0, \dots, n-2}, \quad (2.60)$$

where the negative powers of the Mandelstam invariants for $n = 0, 1$ mean that such a structure is not in the basis.

The number of effective interactions in the $SU(N)$ gauge theories is $4 + \lfloor \frac{7n}{2} \rfloor$ and the choice of basis is given by

$$\begin{aligned} \mathcal{B}_4 &= [12]^2 \langle 34 \rangle^2 \times (\mathcal{C}_1 \cup \mathcal{C}_3), \\ \mathcal{B}_6 &= s_{12} \times \mathcal{B}_4 \cup [12]^2 \langle 34 \rangle \langle 3|p_2 p_1|4 \rangle \times \mathcal{C}'_1, \\ \mathcal{B}_8 &= s_{12}^2 \times \mathcal{B}_4 \cup [12]^2 \langle 3|p_2 p_1|4 \rangle^2 \times (\mathcal{C}_1 \cup \mathcal{C}_2 \cup \mathcal{C}_3 \cup \{\tau^{A_1 A_4 A_2 A_3}\}), \\ \mathcal{B}_{10} &= s_{12} \times \mathcal{B}_8 \cup s_{23} [12]^2 \langle 3|p_2 p_1|4 \rangle^2 \times \mathcal{C}'_1, \\ \mathcal{B}_{12} &= s_{12} \times \mathcal{B}_{10} \cup s_{23}^2 [12]^2 \langle 3|p_2 p_1|4 \rangle^2 \times (\mathcal{C}_1 \cup \mathcal{C}_3), \\ \mathcal{B}_{14} &= s_{12} \times \mathcal{B}_{12} \cup s_{23}^3 [12]^2 \langle 3|p_2 p_1|4 \rangle^2 \times \mathcal{C}'_1, \\ \mathcal{B}_{16} &= s_{12}^2 \times \mathcal{B}_{12} \cup s_{23}^3 [12]^2 \langle 3|p_2 p_1|4 \rangle^2 \times (\mathcal{C}_1 \cup \mathcal{C}_2 \cup \mathcal{C}_3 \cup \{\tau^{A_1 A_4 A_2 A_3}\}), \\ \mathcal{B}_{18} &= s_{12}^3 \times \mathcal{B}_{12} \cup s_{23} \times (\mathcal{B}_{16} \setminus s_{12}^2 \times \mathcal{B}_{12}) \cup s_{12}^2 s_{23}^3 [12]^2 \langle 3|p_2 p_1|4 \rangle^2 \times \mathcal{C}'_1, \\ \mathcal{B}_{20} &= s_{12}^4 \times \mathcal{B}_{12} \cup s_{23}^2 \times (\mathcal{B}_{16} \setminus s_{12}^2 \times \mathcal{B}_{12}) \cup s_{12}^3 s_{23}^3 [12]^2 \langle 3|p_2 p_1|4 \rangle^2 \times \mathcal{C}'_1 \\ &\quad \cup s_{12}^3 s_{23}^3 [12]^2 \langle 3|p_2 p_1|4 \rangle^2 \times (\mathcal{C}_1 \cup \mathcal{C}_3), \end{aligned}$$

where

$$\mathcal{C}'_1 = \mathcal{C}_1 \cup \{\tau^{A_1 A_3 A_2 A_4}\}. \quad (2.61)$$

Clearly, the basis we found is not the most symmetric and recursive. In this section, we wanted to show how our method can systematically deal with this problem of classification. But it is easy to start from our basis and find more symmetric ones, as we will show explicitly in Section 2.3.4.

2.3.3 Five-point interactions between W , Z and γ

In this section we show how our algorithm can be applied beyond the results of [116] (beyond four-point and purely massive amplitudes), classifying the effective interaction corresponding to dimension-six operators at five-point, with massive (both charged and uncharged) and $U(1)$ massless vector bosons, which we call W^\pm , Z and γ . Such operators can appear in various combinations: $D(W^+)^2(W^-)^2 Z$, $DW^+W^-Z^3$, DZ^5 , $F_\gamma(W^+)^2(W^-)^2$, $F_\gamma W^+W^-Z^2$ and $F_\gamma Z^4$. Now we will deal with the purely massive cases and the mixed case separately, as the purely kinematic structures are common in the two cases.

Five-point massive effective interactions

First, we need to classify all possible contact terms using the algorithm presented in Section 2.2: we need terms with mass dimension 6 and in the helicity category $(1^{10}, 2^{10}, 3^{10}, 4^{10}, 5^{10})$, and terms with mass dimension 5 in the various helicity categories $(1^{1\pm 1}, 2^{10})$,

$3^{10}, 4^{10}, 5^{10}$), plus the permutations needed to distinguish different particles. We are not going to write all the structures explicitly as they are of order 10^2 . As in the purely massless case, after symmetrising over identical particles we find structures that are not in our basis of kinematic independent structures. Nevertheless, we can use our algorithm to write down explicitly the decomposition of such structures. When doing so, it is important to distinguish between m_i , \tilde{m}_i , and M_i , and only at the very end set $m_i = \tilde{m}_i = M_i$, as explained in the Appendix A.3.

It is important to note that in the massive case, such relations contain terms across different helicity categories, which enter in the relations multiplied by powers of the masses. Then, the linear independence of the symmetrised terms can be checked by either setting all the masses to zero and working with a fixed helicity category, or by keeping the masses and considering the independence across the different categories in order of increasing mass dimension.

The number of independent contact terms in the three cases under consideration $D(W^+)^2(W^-)^2Z$, $DW^+W^-Z^3$, DZ^5 are, respectively, 20, 14 and 0:

$$\begin{aligned} \mathcal{B}_6^{W^4Z} = & \{M_Z \langle \mathbf{15} \rangle \langle \mathbf{23} \rangle \langle \mathbf{45} \rangle [\mathbf{14}] [\mathbf{23}], M_W \langle \mathbf{15} \rangle \langle \mathbf{24} \rangle \langle \mathbf{34} \rangle [\mathbf{15}] [\mathbf{23}], M_W \langle \mathbf{14} \rangle \langle \mathbf{23} \rangle \langle \mathbf{45} \rangle [\mathbf{15}] [\mathbf{23}], \\ & M_W \langle \mathbf{12} \rangle \langle \mathbf{34} \rangle \langle \mathbf{45} \rangle [\mathbf{15}] [\mathbf{23}], M_W \langle \mathbf{25} \rangle \langle \mathbf{34} \rangle [\mathbf{14}] [\mathbf{15}] [\mathbf{23}], M_W \langle \mathbf{23} \rangle \langle \mathbf{45} \rangle [\mathbf{14}] [\mathbf{15}] [\mathbf{23}], \\ & M_W \langle \mathbf{13} \rangle \langle \mathbf{45} \rangle [\mathbf{15}] [\mathbf{23}] [\mathbf{24}], M_W \langle \mathbf{12} \rangle \langle \mathbf{25} \rangle \langle \mathbf{34} \rangle [\mathbf{15}] [\mathbf{34}], M_W \langle \mathbf{15} \rangle \langle \mathbf{24} \rangle [\mathbf{15}] [\mathbf{23}] [\mathbf{34}], \\ & M_W \langle \mathbf{12} \rangle \langle \mathbf{45} \rangle [\mathbf{15}] [\mathbf{23}] [\mathbf{34}], M_W \langle \mathbf{15} \rangle \langle \mathbf{23} \rangle \langle \mathbf{24} \rangle [\mathbf{13}] [\mathbf{45}], M_W \langle \mathbf{12} \rangle \langle \mathbf{23} \rangle \langle \mathbf{45} \rangle [\mathbf{13}] [\mathbf{45}], \\ & M_W \langle \mathbf{15} \rangle \langle \mathbf{24} \rangle [\mathbf{13}] [\mathbf{23}] [\mathbf{45}], M_Z \langle \mathbf{14} \rangle \langle \mathbf{23} \rangle [\mathbf{15}] [\mathbf{23}] [\mathbf{45}], \langle \mathbf{13} \rangle \langle \mathbf{45} \rangle [\mathbf{15}] [\mathbf{34}] \langle \mathbf{2} | p_1 | \mathbf{2} \rangle, \\ & \langle \mathbf{13} \rangle \langle \mathbf{45} \rangle [\mathbf{13}] [\mathbf{45}] \langle \mathbf{2} | p_1 | \mathbf{2} \rangle, \langle \mathbf{12} \rangle \langle \mathbf{45} \rangle [\mathbf{15}] [\mathbf{24}] \langle \mathbf{3} | p_2 | \mathbf{3} \rangle, \langle \mathbf{15} \rangle \langle \mathbf{24} \rangle [\mathbf{15}] [\mathbf{24}] \langle \mathbf{3} | p_2 | \mathbf{3} \rangle, \\ & \langle \mathbf{15} \rangle \langle \mathbf{23} \rangle [\mathbf{15}] [\mathbf{23}] \langle \mathbf{4} | p_3 | \mathbf{4} \rangle, \langle \mathbf{15} \rangle \langle \mathbf{23} \rangle [\mathbf{23}] [\mathbf{45}] \langle \mathbf{4} | p_3 | \mathbf{1} \rangle \} , \end{aligned}$$

and

$$\begin{aligned} \mathcal{B}_6^{W^2Z^3} = & \{M_Z \langle \mathbf{15} \rangle \langle \mathbf{25} \rangle \langle \mathbf{34} \rangle [\mathbf{14}] [\mathbf{23}], M_Z \langle \mathbf{15} \rangle \langle \mathbf{23} \rangle \langle \mathbf{45} \rangle [\mathbf{14}] [\mathbf{23}], M_Z \langle \mathbf{12} \rangle \langle \mathbf{35} \rangle \langle \mathbf{45} \rangle [\mathbf{14}] [\mathbf{23}], \\ & M_W \langle \mathbf{25} \rangle \langle \mathbf{34} \rangle [\mathbf{14}] [\mathbf{15}] [\mathbf{23}], M_W \langle \mathbf{13} \rangle \langle \mathbf{45} \rangle [\mathbf{15}] [\mathbf{23}] [\mathbf{24}], M_W \langle \mathbf{12} \rangle \langle \mathbf{25} \rangle \langle \mathbf{34} \rangle [\mathbf{15}] [\mathbf{34}], \\ & M_Z \langle \mathbf{15} \rangle \langle \mathbf{24} \rangle [\mathbf{15}] [\mathbf{23}] [\mathbf{34}], M_Z \langle \mathbf{12} \rangle \langle \mathbf{45} \rangle [\mathbf{15}] [\mathbf{23}] [\mathbf{34}], M_W \langle \mathbf{14} \rangle \langle \mathbf{15} \rangle \langle \mathbf{23} \rangle [\mathbf{25}] [\mathbf{34}], \\ & M_Z \langle \mathbf{15} \rangle \langle \mathbf{24} \rangle [\mathbf{12}] [\mathbf{34}] [\mathbf{35}], \langle \mathbf{13} \rangle \langle \mathbf{45} \rangle [\mathbf{15}] [\mathbf{34}] \langle \mathbf{2} | p_1 | \mathbf{2} \rangle, \langle \mathbf{12} \rangle \langle \mathbf{45} \rangle [\mathbf{12}] [\mathbf{45}] \langle \mathbf{3} | p_2 | \mathbf{3} \rangle, \\ & \langle \mathbf{15} \rangle \langle \mathbf{24} \rangle [\mathbf{15}] [\mathbf{24}] \langle \mathbf{3} | p_2 | \mathbf{3} \rangle, \langle \mathbf{15} \rangle \langle \mathbf{23} \rangle [\mathbf{15}] [\mathbf{23}] \langle \mathbf{4} | p_3 | \mathbf{4} \rangle \} . \end{aligned}$$

All elements of these lists are understood to be properly symmetric under permutations: the elements of the former must be symmetric in (1, 2) and (3, 4) and the latter in (3, 4, 5). For example, if we consider the first element of $\mathcal{B}_6^{W^4Z}$, we have:

$$\begin{aligned} M_Z \langle \mathbf{15} \rangle \langle \mathbf{23} \rangle \langle \mathbf{45} \rangle [\mathbf{14}] [\mathbf{23}] \rightarrow & \frac{M_Z}{4} \langle \mathbf{14} \rangle \langle \mathbf{25} \rangle \langle \mathbf{35} \rangle [\mathbf{14}] [\mathbf{23}] + \frac{M_Z}{4} \langle \mathbf{15} \rangle \langle \mathbf{23} \rangle \langle \mathbf{45} \rangle [\mathbf{14}] [\mathbf{23}] \\ & + \frac{M_Z}{4} \langle \mathbf{15} \rangle \langle \mathbf{24} \rangle \langle \mathbf{35} \rangle [\mathbf{13}] [\mathbf{24}] + \frac{M_Z}{4} \langle \mathbf{13} \rangle \langle \mathbf{25} \rangle \langle \mathbf{45} \rangle [\mathbf{13}] [\mathbf{24}] . \end{aligned}$$

Finally, keeping in mind the definition of the polarisation tensor for massive vectors (2.28), we need to divide these polynomial structures by $M_W^4 M_Z$ and $M_W^2 M_Z^3$ to obtain contact terms with the correct mass dimension.

$F_\gamma W^4$, $F_\gamma W^2 Z^2$, $F_\gamma Z^4$ contact terms

This example is easier to follow than the previous one because there is only one helicity category involved when we consider dimension-six operators. The kinematic basis has

only six elements:

$$\begin{aligned} & \{ \langle \mathbf{12} \rangle \langle \mathbf{34} \rangle [\mathbf{12}] [\mathbf{53}] [\mathbf{54}], \langle \mathbf{12} \rangle \langle \mathbf{34} \rangle [\mathbf{23}] [\mathbf{51}] [\mathbf{54}], \langle \mathbf{12} \rangle \langle \mathbf{34} \rangle [\mathbf{34}] [\mathbf{51}] [\mathbf{52}], \\ & \langle \mathbf{14} \rangle \langle \mathbf{23} \rangle [\mathbf{12}] [\mathbf{53}] [\mathbf{54}], \langle \mathbf{14} \rangle \langle \mathbf{23} \rangle [\mathbf{23}] [\mathbf{51}] [\mathbf{54}], \langle \mathbf{14} \rangle \langle \mathbf{23} \rangle [\mathbf{34}] [\mathbf{51}] [\mathbf{52}] \} . \end{aligned} \quad (2.62)$$

After the proper symmetrisations, we find that the number of contact terms for the operators we are considering are 1, 3 and 0, respectively. In particular, we find

$$\mathcal{B}_6^{\gamma W^4} = \left\{ \frac{1}{M_W^4} \mathcal{Y}_{\mathbf{112}} \circ \mathcal{Y}_{\mathbf{34}} \circ \langle \mathbf{14} \rangle \langle \mathbf{23} \rangle [\mathbf{23}] [\mathbf{51}] [\mathbf{54}] \right\} ,$$

and

$$\mathcal{B}_6^{\gamma W^2 Z^2} = \left\{ \frac{1}{M_Z^2 M_W^2} \mathcal{Y}_{\mathbf{34}} \circ \langle \mathbf{12} \rangle \langle \mathbf{34} \rangle [\mathbf{12}] [\mathbf{53}] [\mathbf{54}], \frac{1}{M_Z^2 M_W^2} \mathcal{Y}_{\mathbf{34}} \circ \langle \mathbf{14} \rangle \langle \mathbf{23} \rangle [\mathbf{12}] [\mathbf{53}] [\mathbf{54}], \right. \\ \left. \frac{1}{M_Z^2 M_W^2} \mathcal{Y}_{\mathbf{34}} \circ \langle \mathbf{14} \rangle \langle \mathbf{23} \rangle [\mathbf{23}] [\mathbf{51}] [\mathbf{54}] \right\} .$$

2.3.4 Spin-tidal interactions in gravitational EFTs

In this section, we will apply our algorithm to classify the operators that encode spin-tidal interactions for spin $S_i = 1$ in gravitational systems. This work has been carried out for $S_i = 0, \frac{1}{2}$ in [169, 172]. In this section, we will massage the original basis such that the terms appearing are easily recursive when going up in mass dimension. Furthermore, we will highlight the difference between our strategy and the existing procedure presented in [116]. We will study the helicity category $(1^{1_0}, 2^{1_0}, 3^{+2}, 4^{+2})$ in detail and present the general result in Table 2.2 and 2.3.

The minimal mass dimension for such helicity category is 6, and the basis is

$$\mathcal{B}_6 = \{ \langle \mathbf{12} \rangle [\mathbf{12}] [\mathbf{34}]^4, \langle \mathbf{12} \rangle [\mathbf{14}] [\mathbf{23}] [\mathbf{34}]^3 \} . \quad (2.63)$$

A *helicity category basis* for higher mass dimensions is

$$\mathcal{B}_{6+2n} \stackrel{\text{D}}{\simeq} \{ \langle \mathbf{12} \rangle [\mathbf{12}] [\mathbf{34}]^4 \tilde{s}_{12}^{n-k} \tilde{s}_{23}^k \}_{k=0, \dots, n} \cup \{ \langle \mathbf{12} \rangle [\mathbf{14}] [\mathbf{23}] [\mathbf{34}]^3 \tilde{s}_{23}^n \} , \quad (2.64)$$

where $\tilde{s}_{ij} = s_{ij} - M_i^2 - M_j^2$ and $\stackrel{\text{D}}{\simeq}$ means that these bases have been found from the original basis from the algorithm Section 2.2, working on the graphs modulo terms with powers of the masses (and different helicity categories). Terms of the form $\langle \mathbf{12} \rangle [\mathbf{14}] [\mathbf{23}] [\mathbf{34}]^3 \tilde{s}_{12}^k \tilde{s}_{23}^{n-k}$ with $k \neq 0$ are not kinematically independent from those in our basis. In particular, we have the (mass completed) relation:

$$\begin{aligned} & \tilde{s}_{12} \langle \mathbf{12} \rangle [\mathbf{23}] [\mathbf{14}] [\mathbf{34}]^3 - \tilde{s}_{23} \langle \mathbf{12} \rangle [\mathbf{12}] [\mathbf{34}]^4 = \\ & - \tilde{m}_2 \langle \mathbf{12} \rangle [\mathbf{14}] [\mathbf{34}]^3 \langle \mathbf{2} | p_1 | \mathbf{3} \rangle - \tilde{m}_1 \langle \mathbf{12} \rangle [\mathbf{24}] [\mathbf{34}]^3 \langle \mathbf{1} | p_2 | \mathbf{3} \rangle + M_2^2 \langle \mathbf{12} \rangle [\mathbf{12}] [\mathbf{34}]^4 . \end{aligned} \quad (2.65)$$

In the strategy of [116], in the helicity categories $(1^{1-1}, 2^{1_0}, 3^{+2}, 4^{+2})$ and $(1^{1_0}, 2^{1-1}, 3^{+2}, 4^{+2})$ we would allow only (anti-symmetrised) spinor structures

$$\tilde{m}_2 \langle \mathbf{12} \rangle [\mathbf{14}] [\mathbf{34}]^3 \langle \mathbf{2} | p_1 | \mathbf{3} \rangle - \tilde{m}_1 \langle \mathbf{12} \rangle [\mathbf{24}] [\mathbf{34}]^3 \langle \mathbf{1} | p_2 | \mathbf{3} \rangle , \quad (2.66)$$

such that we could consider $\tilde{s}_{12} \langle \mathbf{12} \rangle [\mathbf{23}] [\mathbf{14}] [\mathbf{34}]^3$ and $\tilde{s}_{23} \langle \mathbf{12} \rangle [\mathbf{12}] [\mathbf{34}]^4$ as independent. On the other hand, our algorithm regards the two structures in the different helicity categories as independent and excludes the terms mentioned above.

Helicity category	$\mathcal{B}_{d_{\text{dim}}}$	$\mathcal{B}_{d_{\text{dim}}+2n}$
$(1^{1+1}, 2^{1+1}, 3^{+2}, 4^{+2})$	$[\mathbf{12}]^2[34]^4$ $[14]^2[\mathbf{23}]^2[34]^4$ $[\mathbf{12}][14][\mathbf{23}][34]^4$	$\{[\mathbf{12}]^2[34]^4 s_{12}^{n-k} s_{23}^k\}_{k=0,\dots,n}$ $[14]^2[\mathbf{23}]^2[34]^4 s_{12}^{n-1} s_{23}$ $[14]^2[\mathbf{23}]^2[34]^4 s_{23}^n$
$(1^{1+1}, 2^{10}, 3^{+2}, 4^{+2})$	$\langle 2 p_1 2\rangle[\mathbf{13}][14][34]^3$ $\langle 2 p_1 3\rangle[14]^2[\mathbf{23}][34]^2$	$\{\langle 2 p_1 2\rangle[\mathbf{13}][14][34]^3 s_{12}^{n-k} s_{23}^k\}_{k=0,\dots,n}$ $\langle 2 p_1 3\rangle[14]^2[\mathbf{23}][34]^2 s_{23}^n$
$(1^{1+1}, 2^{1-1}, 3^{+2}, 4^{+2})$	$\langle 2 p_1 3\rangle^2[14]^2[34]^2$	$\{\langle 2 p_1 3\rangle^2[14]^2[34]^2 s_{12}^{n-k} s_{23}^k\}_{k=0,\dots,n}$
$(1^{10}, 2^{1+1}, 3^{+2}, 4^{+2})$	$\langle 1 p_2 3\rangle[\mathbf{12}][\mathbf{24}][34]^3$ $\langle 1 p_2 3\rangle[14][\mathbf{23}][\mathbf{24}][34]^2$	$\{\langle 1 p_2 3\rangle[\mathbf{12}][\mathbf{24}][34]^3 s_{12}^{n-k} s_{23}^k\}_{k=0,\dots,n}$ $\langle 1 p_2 3\rangle[14][\mathbf{23}][\mathbf{24}][34]^2 s_{23}^n$
$(1^{10}, 2^{10}, 3^{+2}, 4^{+2})$	$\langle \mathbf{12}\rangle[\mathbf{12}][34]^4$ $\langle \mathbf{12}\rangle[14][\mathbf{23}][34]^3$	$\{\langle \mathbf{12}\rangle[\mathbf{12}][34]^4 s_{12}^{n-k} s_{23}^k\}_{k=0,\dots,n}$ $\langle \mathbf{12}\rangle[14][\mathbf{23}][34]^3 s_{23}^n$
$(1^{10}, 2^{1-1}, 3^{+2}, 4^{+2})$	$\langle 2 p_1 3\rangle[\mathbf{12}][14][34]^3$	$\{\langle 2 p_1 3\rangle[\mathbf{12}][14][34]^3 s_{12}^{n-k} s_{23}^k\}_{k=0,\dots,n}$
$(1^{1-1}, 2^{1+1}, 3^{+2}, 4^{+2})$	$\langle 1 p_2 3\rangle^2[\mathbf{24}]^2[34]^2$	$\{\langle 1 p_2 3\rangle^2[\mathbf{24}]^2[34]^2 s_{12}^{n-k} s_{23}^k\}_{k=0,\dots,n}$
$(1^{1-1}, 2^{10}, 3^{+2}, 4^{+2})$	$\langle 1 p_2 3\rangle[\mathbf{12}][\mathbf{24}][34]^3$	$\{\langle 1 p_2 3\rangle[\mathbf{12}][\mathbf{24}][34]^3 s_{12}^{n-k} s_{23}^k\}_{k=0,\dots,n}$
$(1^{1-1}, 2^{1-1}, 3^{+2}, 4^{+2})$	$\langle \mathbf{12}\rangle^2[34]^4$	$\{\langle \mathbf{12}\rangle^2[34]^4 s_{12}^{n-k} s_{23}^k\}_{k=0,\dots,n}$
$(1^{1+1}, 2^{1+1}, 3^{+2}, 4^{-2})$	$\langle 4 p_2 3\rangle^4[\mathbf{12}]^2$	$\{\langle 4 p_2 3\rangle^4[\mathbf{12}]^2 s_{12}^{n-k} s_{23}^k\}_{k=0,\dots,n}$
$(1^{1+1}, 2^{10}, 3^{+2}, 4^{-2})$	$\langle 4 p_2 3\rangle^3\langle \mathbf{24}\rangle[\mathbf{12}][\mathbf{13}]$	$\{\langle 4 p_2 3\rangle^3\langle \mathbf{24}\rangle[\mathbf{12}][\mathbf{13}] s_{12}^{n-k} s_{23}^k\}_{k=0,\dots,n}$
$(1^{1+1}, 2^{1-1}, 3^{+2}, 4^{-2})$	$\langle 4 p_2 3\rangle^2\langle \mathbf{24}\rangle^2[\mathbf{13}]^2$	$\{\langle 4 p_2 3\rangle^2\langle \mathbf{24}\rangle^2[\mathbf{13}]^2 s_{12}^{n-k} s_{23}^k\}_{k=0,\dots,n}$
$(1^{10}, 2^{1+1}, 3^{+2}, 4^{-2})$	$\langle 4 p_2 3\rangle^3\langle \mathbf{14}\rangle[\mathbf{12}][\mathbf{23}]$	$\{\langle 4 p_2 3\rangle^3\langle \mathbf{14}\rangle[\mathbf{12}][\mathbf{23}] s_{12}^{n-k} s_{23}^k\}_{k=0,\dots,n}$
$(1^{10}, 2^{10}, 3^{+2}, 4^{-2})$	$\langle 4 p_2 3\rangle^2\langle \mathbf{14}\rangle\langle \mathbf{24}\rangle[\mathbf{13}][\mathbf{23}]$	$\{\langle 4 p_2 3\rangle^2\langle \mathbf{14}\rangle\langle \mathbf{24}\rangle[\mathbf{13}][\mathbf{23}] s_{12}^{n-k} s_{23}^k\}_{k=0,\dots,n}$
$(1^{10}, 2^{1-1}, 3^{+2}, 4^{-2})$	$\langle 4 p_2 3\rangle^3\langle \mathbf{12}\rangle\langle \mathbf{24}\rangle[\mathbf{13}]$	$\{\langle 4 p_2 3\rangle^3\langle \mathbf{12}\rangle\langle \mathbf{24}\rangle[\mathbf{13}] s_{12}^{n-k} s_{23}^k\}_{k=0,\dots,n}$
$(1^{1-1}, 2^{1+1}, 3^{+2}, 4^{-2})$	$\langle 4 p_2 3\rangle^2\langle \mathbf{14}\rangle^2[\mathbf{23}]^2$	$\{\langle 4 p_2 3\rangle^2\langle \mathbf{14}\rangle^2[\mathbf{23}]^2 s_{12}^{n-k} s_{23}^k\}_{k=0,\dots,n}$
$(1^{1-1}, 2^{10}, 3^{+2}, 4^{-2})$	$\langle 4 p_2 3\rangle^3\langle \mathbf{12}\rangle\langle \mathbf{14}\rangle[\mathbf{23}]$	$\{\langle 4 p_2 3\rangle^3\langle \mathbf{12}\rangle\langle \mathbf{14}\rangle[\mathbf{23}] s_{12}^{n-k} s_{23}^k\}_{k=0,\dots,n}$
$(1^{1-1}, 2^{1-1}, 3^{+2}, 4^{-2})$	$\langle 4 p_2 3\rangle^4\langle \mathbf{12}\rangle^2$	$\{\langle 4 p_2 3\rangle^4\langle \mathbf{12}\rangle^2 s_{12}^{n-k} s_{23}^k\}_{k=0,\dots,n}$

Table 2.2: The helicity category bases for the spin-tidal interactions at $S = 1$.

Until now, we have dealt with gravitons and spinning massive particles as different between themselves. The basis is further restricted when we consider identical particles:

$$\mathcal{B}_{6+4m}^{\text{id}} = \{\langle \mathbf{12}\rangle[\mathbf{12}][34]^4 \tilde{s}_{12}^{2m-2k} \tilde{s}_{23}^{2k}\}_{k=0,\dots,m}, \quad (2.67)$$

and

$$\mathcal{B}_{6+4m+2}^{\text{id}} = \{\langle \mathbf{12}\rangle[\mathbf{12}][34]^4 \tilde{s}_{12}^{2m+1-2k} \tilde{s}_{23}^{2k}\}_{k=0,\dots,m} \cup \{\langle \mathbf{12}\rangle[14][\mathbf{23}][34]^3 \tilde{s}_{23}^{2m+1}\}, \quad (2.68)$$

where the elements of the bases are always understood as properly symmetrised.

Helicity category	$\mathcal{B}_{d_{\min}+2n}^{\text{id}}$
(++, ++)	$\mathcal{Y}_{\underline{12}} \circ \mathcal{Y}_{\underline{34}} \circ [\mathbf{12}]^2 [34]^4 \tilde{s}_{12}^{n-2k} \tilde{s}_{23}^{2k} \quad k = 0, \dots, \lfloor \frac{n}{2} \rfloor$ $\mathcal{Y}_{\underline{12}} \circ \mathcal{Y}_{\underline{34}} \circ [\mathbf{14}]^2 [\mathbf{23}]^2 [34]^4 s_{12} s_{23}^{n-1}$
(+0, ++)	$\mathcal{Y}_{\underline{12}} \circ \mathcal{Y}_{\underline{34}} \circ \langle \mathbf{2} p_1 \mathbf{2} \rangle [13] [14] [34]^3 s_{12}^{n-k-1} s_{23}^{k+1} \quad k = 0, \dots, \lfloor \frac{n}{2} \rfloor - 1$ $\mathcal{Y}_{\underline{12}} \circ \mathcal{Y}_{\underline{34}} \circ \langle \mathbf{2} p_1 3 \rangle [14]^2 [\mathbf{23}] [34]^2 s_{23}^n \quad n \text{ even}$
(+-, ++)	$\mathcal{Y}_{\underline{12}} \circ \mathcal{Y}_{\underline{34}} \circ \langle \mathbf{2} p_1 3 \rangle^2 [\mathbf{14}]^2 [34]^2 s_{12}^{n-k} s_{23}^k \quad k = 0, \dots, \lfloor \frac{n}{2} \rfloor$
(0-, ++)	$\mathcal{Y}_{\underline{12}} \circ \mathcal{Y}_{\underline{34}} \circ \langle \mathbf{2} p_1 3 \rangle \langle \mathbf{12} \rangle [14] [34]^3 s_{12}^{n-k-1} s_{23}^{k+1} \quad k = 0, \dots, \lfloor \frac{n}{2} \rfloor - 1$
(--, ++)	$\mathcal{Y}_{\underline{12}} \circ \mathcal{Y}_{\underline{34}} \circ \langle \mathbf{12} \rangle^2 [34]^4 \tilde{s}_{12}^{n-2k} \tilde{s}_{23}^{2k} \quad k = 0, \dots, \lfloor \frac{n}{2} \rfloor$
(++, +-)	$\mathcal{Y}_{\underline{12}} \circ \langle 4 p_2 3 \rangle^4 [\mathbf{12}]^2 \tilde{s}_{12}^{n-2k} \tilde{s}_{23}^{2k} \quad k = 0, \dots, \lfloor \frac{n}{2} \rfloor$
(+0, +-)	$\mathcal{Y}_{\underline{12}} \circ \langle 4 p_2 3 \rangle^3 \langle \mathbf{24} \rangle [\mathbf{12}] [\mathbf{13}] \tilde{s}_{12}^{n-k} \tilde{s}_{23}^k \quad k = 0, \dots, n$
(+-, +-)	$\mathcal{Y}_{\underline{12}} \circ \langle 4 p_2 3 \rangle^2 \langle \mathbf{24} \rangle^2 [\mathbf{13}]^2 \tilde{s}_{12}^{n-k} \tilde{s}_{23}^k \quad k = 0, \dots, n$
(00, +-)	$\mathcal{Y}_{\underline{12}} \circ \langle 4 p_2 3 \rangle^2 \langle \mathbf{14} \rangle \langle \mathbf{24} \rangle [\mathbf{13}] [\mathbf{23}] \tilde{s}_{12}^{n-2k} \tilde{s}_{23}^{2k} \quad k = 0, \dots, \lfloor \frac{n}{2} \rfloor$
(0-, +-)	$\mathcal{Y}_{\underline{12}} \circ \langle 4 p_2 3 \rangle^3 \langle \mathbf{12} \rangle \langle \mathbf{24} \rangle [\mathbf{13}] \tilde{s}_{12}^{n-k} \tilde{s}_{23}^k \quad k = 0, \dots, n$
(--, +-)	$\mathcal{Y}_{\underline{12}} \circ \langle 4 p_2 3 \rangle^4 \langle \mathbf{12} \rangle^2 \tilde{s}_{12}^{n-2k} \tilde{s}_{23}^{2k} \quad k = 0, \dots, \lfloor \frac{n}{2} \rfloor$

Table 2.3: The *amplitude bases* for the different helicity categories, after taking into account that we are dealing with identical bosons. On the right-hand side, we wrote only the transversality and the helicity of each particle, separating massive and massless states with a comma.

Chapter 3

Bootstrapping Tree-Level Amplitudes

In the previous chapter, we have introduced a systematic algorithm to classify polynomial terms in four-dimensional scattering amplitudes. From such contact terms, we can in principle compute any tree-level amplitude. In Section 1.2.1, we introduced the strategy of BCFW-like recursion relations, emphasising their limits. In particular, when it comes to effective field theories, such relations cannot fix amplitudes with insertions of irrelevant interactions with derivative insertions and locality is never manifest in the final result. Since in our approach we should consider all kinds of operators, we have to find an alternative approach to recursion relations, which is anyway completely on-shell, and in the following chapter we are going to argue that in our framework any effective field theory is fully on-shell constructible from unitarity and locality. In particular, the singularity structure will be manifest in the final result.

In this chapter, we will focus mainly on the Standard Model in the unbroken phase¹ and the SMEFT as a playground for the development of the new recursive method. But we will mention some possible extensions beyond fully massless theories and four dimensions.

In particular, in Section 3.1 we will show, in the context of the Standard Model, how consistent factorisation of four-point tree-level amplitudes constrains the (matrix) couplings \mathfrak{g} in (1.24). Then, in Section 3.2, we will generalise the tree-level bootstrap to higher-point amplitudes, constructing an ansatz consistent with locality and unitarity and fixing all the unknown coefficients using factorisation of the tree level on finite fields. Finally, in Section 3.3, we will move to one loop using generalised unitarity and show that unitarity and locality also fix the anomaly cancellation conditions, from a purely on-shell point of view.

3.1 The Standard Model from on-shell techniques

All the four-point amplitudes in the Standard Model, but $\mathcal{A}(\bar{H}^i, \bar{H}^j, H^k, H^l)$, can be completely fixed by factorisation. This will be proven in Section 3.2.1 but we assume

¹The mixing of EFT operators, discussed in Chapter 5, is a UV phenomenon, then we can work at energies which are much larger than the electroweak scale ($\sim 100\text{GeV}$). Effectively, we will ignore the higgs vacuum expectation value in the SM Lagrangian and work with states transforming under the full $U(1) \times SU(2) \times SU(3)$ symmetry.

it for the moment. Consistency between different factorisation channels at tree-level for four-point amplitudes then constrains many of the structures in the three-point amplitude. These constraints fix the (gauge-invariant) structures appearing and impose relations between couplings [16].

The constraints imposed by factorisation are completely equivalent to those found when we construct a consistent gauge-invariant Lagrangian describing a unitary QFT of self-interacting vector bosons [229] and their minimal coupling to fermions and scalars, *i.e.* the Lie algebra structures and the universality of Yang-Mills coupling (see, for example, [230]). Moreover, we generalise this argument and find that factorisation also imposes relations between the hypercharges associate to the minimal coupling of matter with (non-self-interacting) $U(1)$ -vectors, which are equivalent from a Lagrangian perspective to the requirement that the Yukawa interactions are $U(1)_Y$ invariant, *i.e.* scattering amplitudes are non zero only for hypercharge-conserving processes. Similar arguments have been applied to supersymmetric theories and gravitational amplitudes [18] and recently also to massive gauge theories [231].

3.1.1 Lie Algebras from Tree-Level Unitarity

Jacobi identities from factorisation

In this subsection we review the observations in [16], from a somewhat different perspective. We consider the three-gluon amplitudes²

$$\mathcal{A}(G_-^A, G_-^B, G_+^C) = g_3 f^{ABC} \frac{\langle 12 \rangle^3}{\langle 23 \rangle \langle 31 \rangle}, \quad \mathcal{A}(G_-^A, G_+^B, G_+^C) = -g_3 f^{BCA} \frac{[23]^3}{[12][31]}, \quad (3.1)$$

where $f^{ABC} = f^{[ABC]}$ ³ to satisfy Bose-Einstein symmetry of the three-point amplitude and we try to bootstrap the four-gluon amplitude from factorisation. The most generic (slightly redundant) ansatz for the four-point amplitude which is compatible with locality and unitarity is

$$\begin{aligned} \frac{\mathcal{A}(G_-^A, G_-^B, G_+^C, G_+^D)}{i\langle 12 \rangle^2 [34]^2} &= \frac{f^{ABE} f^{CDE}}{s_{12}} \left(\frac{c_1}{s_{13}} + \frac{c_2}{s_{14}} \right) + \frac{f^{ACE} f^{BDE}}{s_{13}} \left(\frac{c_3}{s_{12}} + \frac{c_4}{s_{14}} \right) \\ &+ \frac{f^{ADE} f^{BCE}}{s_{14}} \left(\frac{c_5}{s_{12}} + \frac{c_6}{s_{13}} \right). \end{aligned} \quad (3.2)$$

The coefficients c_i can be fixed from factorisation using (1.23) which in the 4-point case reduces to⁴

$$-i \operatorname{Res}_{s_{ij}=0} \mathcal{A}_4 = \mathcal{A}_3 \cdot \mathcal{A}_3. \quad (3.3)$$

Imposing this constraint for all the three distinct channels, we find

$$\begin{cases} f^{ABE} f^{CDE} (c_1 - c_2) + f^{ACE} f^{BDE} c_3 - f^{ADE} f^{BCE} c_5 = -g_3^2 f^{ABE} f^{CDE} \\ f^{ABE} f^{CDE} c_1 + f^{ACE} f^{BDE} (c_3 - c_4) - f^{ADE} f^{BCE} c_6 = -g_3^2 f^{ACE} f^{BDE} \\ f^{ABE} f^{CDE} c_2 - f^{ACE} f^{BDE} c_4 + f^{ADE} f^{BCE} (c_5 - c_6) = -g_3^2 f^{ADE} f^{BCE} \end{cases}. \quad (3.4)$$

²The relative minus sign between the so called MHV and $\overline{\text{MHV}}$ amplitudes is fixed by requiring parity invariance of the theory.

³In principle, this assumption could be lifted and would follow from factorisation as well if the gauge group is compact, but for simplicity we assume it from the beginning.

⁴We remind the reader that when fermions are present in the amplitudes, the RHS of (3.3) might get a minus sign contribution from fermion reordering and a further factor of $-i$ when crossing a fermion from initial to final state. This subtlety will be relevant in the computations of the following sections.

This linear system in general has no solutions, unless we impose the following quadratic relations among the constants f^{ABC} :

$$f^{ABE} f^{CDE} + f^{BCE} f^{ADE} + f^{CAE} f^{BDE} = 0, \quad (3.5)$$

which can be recognised as the Jacobi identities for the structure constants of a Lie algebra.

Lie algebras from factorisation

We can apply the same reasoning to scalars and fermions coupled to the non-abelian spin-1 particles and find that also their minimal coupling is tightly constrained by locality and unitarity [18]. We consider as an example the four-point amplitude $\mathcal{A}(G_-^A, G_+^B, \bar{u}^a, u^b)$. The three-point minimal coupling is fixed by little group and in principle can take the general form

$$\mathcal{A}(G_-^A, \bar{u}^a, u^b) = i g_{3,m} \tau^{Aa}_b \frac{\langle 12 \rangle^2}{\langle 23 \rangle}, \quad \mathcal{A}(G_+^A, \bar{u}^a, u^b) = i g_{3,m} \tau^{Aa}_b \frac{[13]^2}{[23]}, \quad (3.6)$$

where, for the moment, τ^{Aa}_b is some generic matrix encoding the interaction properties of the fermions u^a (\bar{u}^a) and the vector bosons, and we factored out an overall numerical coefficient. The most general ansatz for the four-point is then

$$\begin{aligned} \frac{\mathcal{A}(G_-^A, G_+^B, \bar{u}^a, u^b)}{i \langle 13 \rangle^2 [23] [24]} &= \frac{f^{ABC} \tau^{Ca}_b}{s_{12}} \left(\frac{c_1}{s_{13}} + \frac{c_2}{s_{14}} \right) + \frac{\tau^{ABa}_b}{s_{13}} \left(\frac{c_3}{s_{12}} + \frac{c_4}{s_{14}} \right) \\ &+ \frac{\tau^{BAa}_b}{s_{14}} \left(\frac{c_5}{s_{12}} + \frac{c_6}{s_{13}} \right) \end{aligned} \quad (3.7)$$

where $\tau^{ABa}_b = \tau^{Aa}_c \tau^{Bc}_b$. Again taking the residues and matching with the factorisation channels as in equation (3.3), we find:

$$\begin{cases} f^{ABC} \tau^{Ca}_b (c_1 - c_2) + \tau^{ABa}_b c_3 - \tau^{BAa}_b c_5 = i g_3 g_{3,m} f^{ABC} \tau^{Ca}_b \\ f^{ABC} \tau^{Ca}_b c_1 + \tau^{ABa}_b (c_3 - c_4) - \tau^{BAa}_b c_6 = g_{3,m}^2 \tau^{ABa}_b \\ f^{ABC} \tau^{Ca}_b c_2 - \tau^{ABa}_b c_4 + \tau^{BAa}_b (c_5 - c_6) = g_{3,m}^2 \tau^{BAa}_b \end{cases}, \quad (3.8)$$

This linear system has solutions if and only if

$$g_{3,m} = g_3, \quad (3.9)$$

$$\tau^{ABa}_b - \tau^{BAa}_b = i f^{ABC} \tau^{Ca}_b, \quad (3.10)$$

i.e. iff the coupling constant of the interaction is universal and the matrices τ^{Aa}_b are representations of the elements of a Lie algebra, with f^{ABC} the structure constants.

Charge conservation and Yukawa coupling

Last we generalise the procedure of the previous sections to the minimal coupling of the abelian vectors with scalars and fermions interacting via Yukawa coupling. Unitarity and locality will then imply that the hypercharge associated to the minimal coupling of

the matter states to the abelian vector is conserved. The relevant three-point amplitudes are

$$\mathcal{A}(B_-, \bar{e}, e) = i g_1 Y_e \frac{\langle 12 \rangle^2}{\langle 23 \rangle}, \quad (3.11)$$

$$\mathcal{A}(B_-, \bar{L}^i, L^j) = i g_1 Y_L \delta_i^j \frac{\langle 12 \rangle^2}{\langle 23 \rangle}, \quad (3.12)$$

$$\mathcal{A}(B_-, \bar{H}^i, H^j) = i g_1 Y_H \delta_i^j \frac{\langle 12 \rangle \langle 31 \rangle}{\langle 23 \rangle}, \quad (3.13)$$

$$\mathcal{A}(L^i, e, \bar{H}^j) = i \bar{\mathcal{Y}}^{(3)} \delta_j^i [12], \quad (3.14)$$

where Y_i is the hypercharge associated to the i -th state, and $\mathcal{Y}^{(3)}$ is the Yukawa coupling matrix for the electron family, with $\bar{\mathcal{Y}}^{(3)} = (\mathcal{Y}^{(3)})^\dagger$. The most generic ansatz consistent with locality and unitarity is

$$\frac{\mathcal{A}(B_-, L^i, e, \bar{H}^j)}{i \langle 12 \rangle \langle 13 \rangle [23]^2} = \delta_j^i \left(\frac{c_1}{s_{12} s_{13}} + \frac{c_2}{s_{12} s_{14}} + \frac{c_3}{s_{13} s_{14}} \right), \quad (3.15)$$

and probing the three different factorisation channels we find the system:

$$\begin{cases} c_1 - c_2 = -g_1 \bar{\mathcal{Y}}^{(3)} Y_L \\ c_1 - c_3 = +g_1 \bar{\mathcal{Y}}^{(3)} Y_e, \\ c_2 - c_3 = +g_1 \bar{\mathcal{Y}}^{(3)} Y_H \end{cases} \quad (3.16)$$

which has solutions if and only if we impose the hypercharge conserving condition:

$$Y_L = Y_H - Y_e. \quad (3.17)$$

Analogously, one can also find the charge conservation conditions for the processes involving quarks, instead of leptons:

$$Y_Q = Y_H - Y_d, \quad (3.18)$$

$$Y_Q = -Y_H - Y_u. \quad (3.19)$$

3.2 Bootstrapping the tree-level amplitudes

The strategy presented for four-point amplitudes can be generalised to higher-point amplitudes in generic massless effective field theories, keeping in mind the particular example of the SMEFT. While the four-point cases can be worked out by hand analytically, the same procedure become rather cumbersome for higher points. In particular, the number of terms in the ansatz grows and the relations between spinor helicity structures make the matching procedure on the cuts exponentially difficult. On the other hand, generating the ansatz with computer algebra software and fixing the coefficients evaluating the kinematics numerically make the following algorithm definitely more efficient than summing over all the Feynman diagrams and writing the amplitude in a form which manifests both gauge invariance and locality.

At the end of this sections we will show a possible generalisation of the algorithm (which relies heavily on four-dimensional spinor helicity formalism, so far) to d -dimensional scattering amplitudes, which are essential for generalised unitarity when we go beyond one-loop [32, 33]. As an example, we will compute analytically the one-gluon amplitude in the HEFT with two heavy sources, from the single-heavy-source amplitudes presented in [232].

3.2.1 Higher-point Amplitudes without Recursion Relations

The procedure can be roughly divided into two parts: the construction of an ansatz and the matching procedure on the single-particle cuts to fix the free-parameters, which we perform numerically over finite fields to speed up the computation.

Constructing an ansatz

A generic tree-level amplitude can be schematically written as

$$\mathcal{A}_n(p_1^{a_1, h_1}, \dots, p_n^{a_n, h_n}) = \sum_{i,j,k} \frac{C_{i,j}^{a_1 \dots a_n}}{\mathcal{D}_i} c_{i,j,k} \mathcal{N}_{i,j,k} + \mathcal{P}^{a_1 \dots a_n}, \quad (3.20)$$

where $p_i^{a_i, h_i}$ represents a generic state with helicity h_i and gauge-group index a_i . The tensors $C_{i,j}^{a_1 \dots a_n}$ are the gauge-group invariant structure of the amplitude, whereas \mathcal{D}_i and $\mathcal{N}_{i,j,k}$ are kinematic denominators and numerators respectively, where the latter carry the dependence on the helicity structure. The $c_{i,j,k}$ are rational coefficients associated to the different helicity structures $\mathcal{N}_{i,j,k}$. Finally, the $\mathcal{P}^{a_1 \dots a_n}$ are terms with polynomial dependence in the kinematic variables, in other words contact terms, which vanish whenever we probe any factorisation channel. We will show that in our framework the contact terms are irrelevant and the tree-level amplitudes are fully determined by lower-point amplitudes from factorisation.

First we motivate this assumption for renormalisable theories through a simple dimensional analysis consideration: due to (1.14), for $n > 4$ we have $[\mathcal{A}_n] < 0$. Moreover, all the couplings in the SM are dimensionless, we are considering only massless states (there are no dimension-full parameters in the amplitude) and by construction $[\mathcal{P}^{a_1 \dots a_n}] \geq 0$. These considerations imply necessarily that for renormalisable massless theories for $n > 4$ $\mathcal{P}^{a_1 \dots a_n} = 0$ and every term in the amplitude must possess some kinematic denominators \mathcal{D}_i . This means that the amplitudes can be fully determined from factorisation, through a recursive procedure described below in this section.

This argument is somehow subtle for $n = 4$, because it is possible to build terms of mass dimension zero which are ratios of spinor variables but vanish on any cut. An example of such a structure for the all-plus four-gluon amplitudes is

$$\frac{[12]^2[34]^2}{s_{12}^2} = \frac{[13]^2[24]^2}{s_{13}^2} = \frac{[14]^2[23]^2}{s_{14}^2}, \quad (3.21)$$

whose residue is zero on any of the three configuration $s_{12}=0$, $s_{13}=0$ or $s_{14}=0$. These structures do not introduce any correction to the factorisation channels of four-point amplitudes (*i.e.* they are polynomial in the kinematic variables, thanks to the permutation symmetry). We will systematically ignore such contact terms at four points, except for the four-scalar contact term (corresponding in the Lagrangian formalism to the $\lambda\phi^4$ interaction). Indeed, such terms are usually computed through d -dimensional generalised unitarity techniques as one-loop finite rational terms [233, 234], hence they must be vanishing at tree-level⁵. In particular, in the case of the four-scalar amplitude we will add to the factorisable part a contact term whose kinematic dependence is trivial:

⁵For example, we know that such terms can never be generated by any local Lagrangian interaction at tree-level.

$$\mathcal{A}_4(\bar{H}^{i_1} \bar{H}^{i_2} H^{i_3} H^{i_4}) = - \left(g_1^2 Y_H^2 \delta_{i_1}^{i_3} \delta_{i_2}^{i_4} + g_2^2 \sigma^{I i_3}_{i_1} \sigma^{I i_4}_{i_2} \right) \frac{s_{12} - s_{14}}{s_{13}} - \lambda \delta_{i_1}^{i_3} \delta_{i_2}^{i_4} + (3 \leftrightarrow 4) . \quad (3.22)$$

We stress that for $n > 4$ non-singular terms such as (3.21) cannot appear: by dimensional analysis considerations, there must be a singularity for renormalisable amplitudes with more than four external particles.

This argument cannot be generalised to the case of scattering amplitudes with insertions of effective interactions. For example, consider the six-scalar amplitude with an insertion of a $\partial^2 \phi^4$ interaction, call it $\mathcal{F}_{6,6,\partial^2 \phi^4}$. There is no equivalent argument to discard a ϕ^6 -like contact term contribution arising in the calculation of this amplitude. On the other hand, any physical process which gets a contribution from $\mathcal{F}_{6,6,\partial^2 \phi^4}$ will also get one from $\mathcal{F}_{6,6,\phi^6}$ which is the contact interaction due to the operator ϕ^6 itself. Physically, the two contact term contributions cannot be disentangled, because they provide the same description for the interaction between scalars. As a consequence, if we are already considering an effective field theory with both $\partial^2 \phi^4$ and ϕ^6 interactions in our operator basis, neglecting the ϕ^6 -like contact term in $\mathcal{F}_{6,6,\partial^2 \phi^4}$ can be compensated by appropriately shifting the Wilson coefficient of the ϕ^6 operator.

This argument can be generalised to more generic theories, like the SMEFT in our case. What we wanted to convey is that, as long as we consider a complete basis of operators up to a given dimension, contact terms can only contribute shifting the Wilson coefficients of a different operator. Then we *choose* our basis of EFT interactions such that it does not generate polynomial terms when computing higher-multiplicity amplitudes and thus we can effectively neglect them in the computations, so $\mathcal{P}^{a_1 \dots a_n} = 0$.

Now we present the algorithm to compute higher-point tree-level amplitudes from factorisation.

1. We begin by enumerating all the possible singularity structures of the amplitude consistent with locality, which are provided by all the possible ways the amplitude can consistently factorise into tree graphs⁶. First, we enumerate all the possible tree graphs with trivalent and quadrivalent internal vertices, and then we apply a selection criterion to discard channels which are not compatible with the particles associated to the external vertices and the Standard Model interactions.
2. We associate to each tree graph a unique kinematic denominator \mathcal{D}_i , which is the product of the propagators corresponding to internal edges in the graphs, *i.e.* it is a product of the Mandelstam invariants characterising the channels.
3. Unitarity also fixes the colour structures associated to each graph $\{C_{i,j}^{a_1 \dots a_n}\}_{j=1, \dots, s}$. In particular, different colour structures correspond to different particles propagating in the internal lines. Once the internal particles are determined, the colour structures are obtained from the contraction of the colour structures in the three-point amplitudes associated to each vertex.
4. Finally, the kinematic numerators are generated with the algorithm presented in

⁶The nodes of the tree graph must be either the Standard Model three-point interactions (plus the quadrivalent scalar interaction $-\lambda(\bar{H}H)^2/4$) or, if we are considering amplitudes with effective operator insertions, also any of the relevant effective interaction classified in Section 2.3.1.

Section 2.1.1⁷. The $\{\mathcal{N}_{i,j,k}\}_{k=1,\dots,h}$ are h independent spinor structures in our basis, and a set of these numerators is associated to each of the colour structure $C_{i,j}^{a_1\dots a_n}$ corresponding to the denominator \mathcal{D}_i . The latter fixes the mass dimension of the numerators through $[\mathcal{N}_{i,j,k}] = [\mathcal{A}_n] + [\mathcal{D}_i]$ whereas the helicity weights are given by the external particles. Each of the $\mathcal{N}_{i,j,k}$ is multiplied by arbitrary (rational) coefficients $c_{i,j,k}$ which will be fixed by the matching procedure over the different factorisation channels described in detail later in the section. Notice that the basis of numerators does obviously not depend on the colour structures, but only on the mass dimension of the denominator structure: *i.e.* $\mathcal{N}_{i_1,j_1,k} = \mathcal{N}_{i_2,j_2,k}$ if $[\mathcal{D}_{i_1}] = [\mathcal{D}_{i_2}]$ for any colour structure labelled by j_1 and j_2 . This fact has been exploited heavily to speed up the numerical evaluation of the ansatz when solving for the coefficients $\{c_{i,j,k}\}$.

5. Some of the coefficients can be fixed before the matching procedure by demanding that the ansatz is not redundant. In particular, the simplifying observation is that the various coefficients cannot combine in such a way that the sum over the related structures is proportional to any of the Mandelstam invariants appearing in the denominators, which are associate to a physical intermediate one-particle state.
6. Finally we solve for the $\{c_{i,j,k}\}$ by matching over the different factorisation channels as described below. The matching usually fixes all the coefficients $\{c_{i,j,k}\}$, but there are cases where the ansatz is redundant. We have already encountered the first example in the previous section: in fact, when we have particles with helicity $|h_i| \geq 1$ we are forced to introduce some redundancy in the ansatz, as we will explain later in this section.

We consider, as an example, the five-point amplitude $\mathcal{A}_5(Q^{a_1,i_1}, u^{a_2}, \bar{H}^{i_3}, H^{i_4}, H^{i_5})$. There are 21 trivalent graphs compatible with this process, and some of them are shown in Figure 3.1. Most of the graphs do not involve the scalar quadrivalent interaction, except the last one. Indeed, we then have $[\mathcal{D}_i] = 4$ for $i = 1, \dots, 20$ and $[\mathcal{D}_{21}] = 2$ with:

$$\{\mathcal{D}_i\}_{i=1,\dots,21} = \{s_{12}s_{35}, s_{14}s_{35}, s_{24}s_{35}, s_{12}s_{34}, s_{15}s_{34}, s_{25}s_{34}, s_{13}s_{25}, s_{14}s_{25}, s_{25}s_{34}, s_{13}s_{24}, \\ s_{15}s_{24}, s_{24}s_{35}, s_{15}s_{24}, s_{15}s_{34}, s_{14}s_{25}, s_{14}s_{35}, s_{13}s_{24}, s_{13}s_{25}, s_{12}s_{34}, s_{12}s_{35}, s_{12}\}$$
(3.23)

Next we build the kinematic numerators whose structure is fixed by the helicity of the external particles along with the mass dimension of the amplitude and of the denominators as

$$[\mathcal{A}_n] = [\mathcal{N}_{i,j,k}] - [\mathcal{D}_j] \quad \Rightarrow \quad [\mathcal{N}_{i,j,k}] = 4 - n + [\mathcal{D}_j] . \quad (3.24)$$

In our example we have then

$$\{\mathcal{N}_{i,j,k}\}_{k=1,\dots,6} = \{s_{12}[12], s_{13}[12], s_{23}[12], s_{24}[12], s_{34}[12], \langle 34 \rangle [14][23]\} , \quad (3.25)$$

for $i = 1, \dots, 20$ and any j , and

$$\{\mathcal{N}_{21,j,k}\}_{k=1} = \{[12]\} . \quad (3.26)$$

⁷The full algorithm presented in this section can be applied to the case of form factors as well. If this was the case we were interested in, we should consider at this point a simplified version of the algorithm presented in Section 2.1.1, in which we ignore momentum conservation.

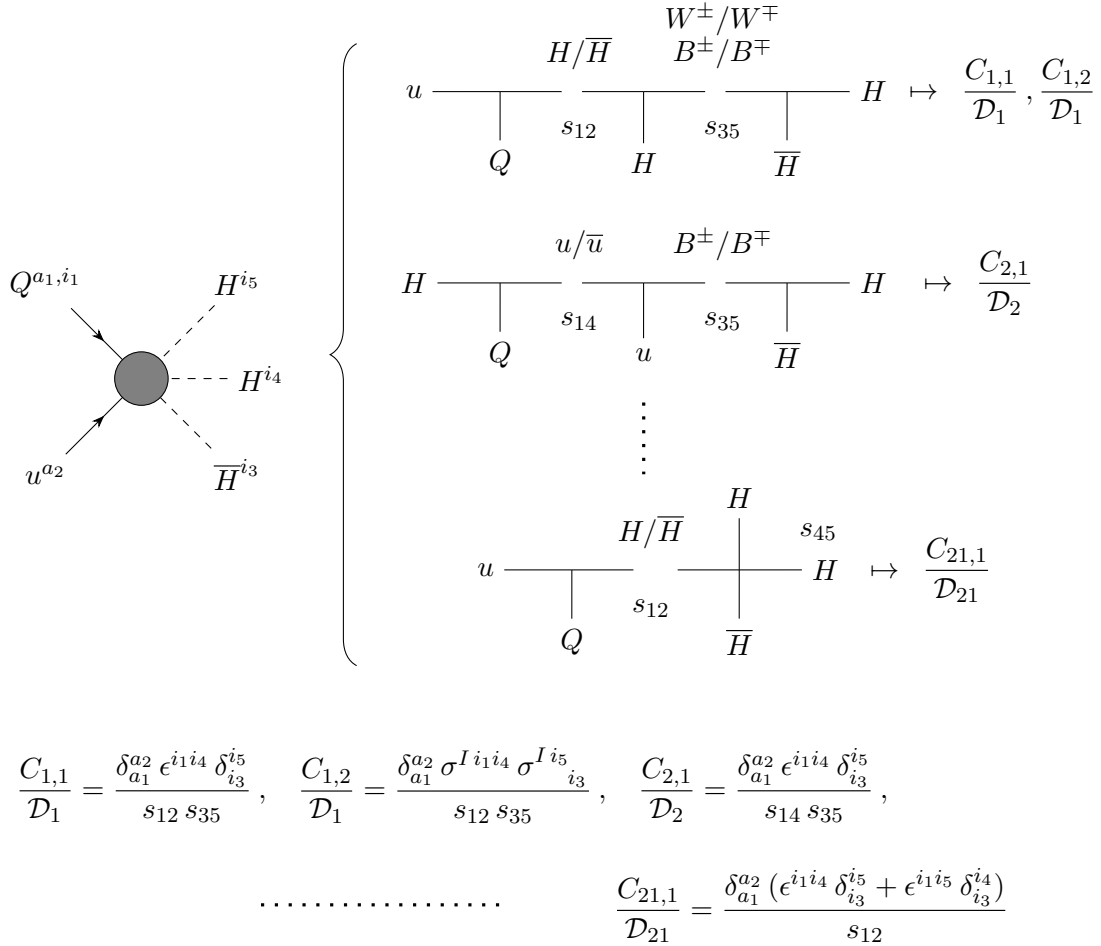


Figure 3.1: The splitting of $\mathcal{A}_5(Q^{a_1, i_1}, u^{a_2}, \overline{H}^{i_3}, H^{i_4}, H^{i_5})$ into trivalent graphs and the associated colour factors and kinematic denominators. There are a total of 21 possible trivalent graphs associated with this amplitude, we showed explicitly the first, the second and the last, as significant examples. The second is a trivial instance of trivalent graphs and there is a unique choice compatible with the Standard Model interactions of internal particle propagating. The same is not true for the first factorisation channel, for which we can have both B s and W s propagating, which give us two different colour structures $C_{1,1}$ and $C_{2,1}$, respectively. The last channel is the only one for this amplitude which involves an insertion of the quadrivalent Higgs interaction.

Computing the amplitude then reduces to fixing the rational coefficients $c_{i,j,k}$ multiplying each of these numerators.

In fact, before proceeding with the system solution we can fine tune the ansatz in order to remove combinations which would lead to cancellations in the denominators. In particular, since there are two Mandelstam invariants for the first twenty denominators, this would fix a priori two coefficients for each denominator and for each colour structures. We consider, for example, the first two trivalent graphs, shown in Figure 3.1. The general algorithm to fix the coefficient is the following:

- We have a set of independent helicity structures with a specified mass dimension d , *i.e.* $\{\mathcal{N}_{i,j,k}\}_{k=1,\dots,h_1}$, and we assume the existence of a set of structures with the same helicity configuration and mass dimension $d-2$, *i.e.* $\{\mathcal{M}_{i,j,l}\}_{l=1,\dots,h_2}$. If the latter do not exist, this procedure can be skipped, as in the case of $\mathcal{N}_{21,1,1}$.
- For each Mandelstam invariant $s_{i_1\dots i_n}$ appearing in the denominator \mathcal{D}_i we fix some coefficients $d_{i,j,k}^{(p)}$ through

$$\sum_{k=1}^{h_1} d_{i,j,k}^{(p)} \mathcal{N}_{i,j,k} = s_{i_1\dots i_n} \mathcal{M}_{i,j,l} \quad \forall l. \quad (3.27)$$

These conditions provide us with $p = 1, \dots, \lfloor \frac{\mathcal{D}_i}{2} \rfloor \cdot h_2$ vectors $d_{i,j,k}^{(p)}$.

- Finally, we impose the orthogonality condition for the c 's with respect to the d 's

$$\sum_{k=1}^{h_1} c_{i,j,k} d_{i,j,k}^{(p)} = 0 \quad \forall p, \quad (3.28)$$

which fixes some of the $c_{i,j,k}$, as anticipated. In our specific example, for \mathcal{D}_1 we find $c_{1,j,1} = 0$ and $c_{1,j,5} = -c_{1,j,2} - c_{1,j,3}$ with $j = 1, 2$ and for \mathcal{D}_2 we find $c_{2,1,4} = -c_{2,1,1}$ and, again, $c_{2,1,5} = -c_{2,1,2} - c_{2,1,3}$.

The case of external vector bosons

The procedure described so far works very well when we are dealing with amplitudes with only scalars and fermions as external particles. But when vector bosons are involved, or more in general massless particles with $|h| \geq 1$, an extension of the method is required. One has to take into account that these particles provide further kinematic denominators which are not due to intermediate particle exchanges. A simple example has already been shown in Section 3.1.1, where we considered the four-gluon amplitude. Indeed, the four-point amplitude has mass-dimension zero, the helicity structure with the smallest mass dimension is $\langle 12 \rangle^2 [34]^2$ which has mass-dimension four, and consequently a single $\frac{1}{s_{ij}}$ (associated to a trivalent graph) is not enough to get the mass-dimensions right⁸. Typically, once a set of denominators has been generated as described in the

⁸When we think of the problem in terms of a Feynman diagrammatic approach for $|h| = 1$, this additional kinematic dependence is hidden in the polarisation vectors which in terms of spinor-helicity variables can be written as

$$\epsilon_{\alpha\dot{\alpha}}^+(p, \xi) = \sqrt{2} \frac{\xi_{\alpha} \tilde{\lambda}_{\dot{\alpha}}}{\langle \xi \lambda \rangle}, \quad \epsilon_{\alpha\dot{\alpha}}^-(p, \xi) = \sqrt{2} \frac{\lambda_{\alpha} \tilde{\xi}_{\dot{\alpha}}}{[\tilde{\lambda} \tilde{\xi}]}, \quad (3.29)$$

previous section, we need to add at least one Mandelstam invariant to each denominator or possibly more in case of higher-point amplitudes. This is done in iterated steps: we first add to every denominator a single Mandelstam invariant s_{ij} in all the possible ways compatible with locality⁹, then we build the complete ansatz and try to solve it. If the number of invariants considered for the denominators is insufficient we will find no solution for the c 's, so we add all the possible terms with a further invariant in the denominator and try to solve again. At every step clearly the number of possible denominators grows quite drastically, and so does the number of possible numerators since higher and higher mass-dimensions become available. The latter effect is however counteracted by discarding those numerators which cancel any power of Mandelstam invariants from the denominator, which would indeed reproduce a term of the ansatz already present from previous iterations.

This part of the method proves to be the bottleneck when it comes to computing higher-multiplicity amplitudes, because we did not implement any systematic way of combining different factorisation channels. Such combinations may be better understood in connection with the color-kinematic duality [192, 193] and/or geometries described by the singularity structures [189, 235].

This procedure of adding Mandelstam invariants to the kinematic denominators is clearly responsible for the ‘‘mixing’’ process between different factorisation channels which brought us to the identities between colour structures at the level of the four-point amplitudes in Section 3.1 and it is strictly related to gauge invariance.

Solution of the ansatz

So far we have built an ansatz of the form (3.20), where each of the $\mathcal{N}_{i,j,k}$ has an associated coefficient $c_{i,j,k}$. In order to fix these coefficients we impose the validity of (1.23) in every single kinematic channel, and we do so through repeated numerical evaluations:

$$-i \operatorname{Res}_{s_{i_1 \dots i_m}} \underbrace{\mathcal{A}_n(p_1^{h_1} \dots p_n^{h_n})}_{\text{ansatz}} = f \sum_{s_I, h_I} \underbrace{\mathcal{A}_{m+1}(p_{i_1}^{h_{i_1}} \dots p_{i_m}^{h_{i_m}}, p_I^{h_I}) \mathcal{A}_{n-m+1}(p_I^{h_I} \rightarrow p_{i_{m+1}}^{h_{i_{m+1}}} \dots p_{i_n}^{h_{i_n}})}_{\text{lower point on-shell amplitudes}} . \quad (3.30)$$

The lower point amplitudes in the RHS of (3.30) is known, because our algorithm is recursive. On the LHS we take the residue on the ansatz, which selects a subset of the denominator structures. Next we decompose, through the algorithms described in Section 2.3.1, the colour structures on both sides of (3.30) in a suitable basis $\{C_l^{a_1 \dots a_n}\}$:

$$C_{i,j}^{a_1 \dots a_n} = \sum_l b_{i,j,l} C_l^{a_1 \dots a_n} . \quad (3.31)$$

We impose the matching of the coefficients of the colour structures in this basis on both sides of the equality (3.30) so we end up with a set of equations of the type

$$-i \sum_{i',j,k} \frac{b_{i',j,l}}{\widetilde{\mathcal{D}}_{i'}} c_{i',j,k} \mathcal{N}_{i',j,k} = \mathcal{K}_l . \quad (3.32)$$

where $p_{\alpha\dot{\alpha}} = \lambda_\alpha \tilde{\lambda}_{\dot{\alpha}}$ and ξ is an arbitrary reference spinor. In our approach, it is either a simple dimensional analysis as for the four-gluon amplitude which forces us to add more denominators, or for higher-point amplitudes it will be unitarity itself that does so.

⁹By this we mean exhausting the combinatorics of possible invariants without however adding those already present in the denominator, which would of course lead to unphysical higher-order poles.

Here i' runs over the tree graphs in which the specified Mandelstam invariant $s_{i_1\dots i_m}$ appears, the $\tilde{\mathcal{D}}_{i'}$ are the $\mathcal{D}_{i'}$ stripped of a factor $s_{i_1\dots i_m}$ and the $c_{i',j,k}$ are the rational coefficients to be fixed. The \mathcal{K}_l are kinematic coefficients defined by the product of lower point amplitudes as

$$f \sum_{s_I, h_I} \mathcal{A}_{m+1}(p_{i_1}^{h_{i_1}} \dots p_{i_m}^{h_{i_m}}, p_I^{h_I}) \mathcal{A}_{n-m+1}(p_I^{h_I} \rightarrow p_{i_{m+1}}^{h_{i_{m+1}}} \dots p_{i_n}^{h_{i_n}}) := \sum_l C_l^{a_1\dots a_n} \mathcal{K}_l \quad (3.33)$$

where the colour structures $C_l^{a_1\dots a_n}$ are elements of the chosen colour basis. The \mathcal{K}_l are known analytic functions of the spinor invariants and Mandelstam invariants, and they also contain the dependence on the couplings g_k , $\mathcal{Y}^{(f)}$ and λ . Each equation (3.32) now only contains kinematic invariants, the $c_{i',j,k}$ for which we want to solve and products of couplings. Thus we repeatedly evaluate the kinematics numerically and so obtain a linear system in the $c_{i',j,k}$ which upon solution yields a subset of the $c_{i',j,k}$ as functions of the couplings and possibly other c 's. Since numerical evaluations are performed on very special kinematic points where intermediate states go on-shell, some of the coefficients $c_{i',j,k}$ might in principle drop out of the system. These coefficients are identified by an a priori numerical evaluation, which then allows to only solve the system in the actually relevant variables.

Repeating this procedure in every kinematic channel might still not completely fix the ansatz, since some of the $c_{i',j,k}$ might be spurious in the sense that using momentum conservation and Schouten identities appropriately they actually drop out altogether from the final result. In particular this happens when we consider amplitudes with external vectors. At the very end of the calculation, we take advantage of the arbitrary nature of these coefficients to set them, for example, either to a value which makes the final result more compact or to zero.

In order to get exact solutions and avoid possible issues tied to precision loss in floating point arithmetic, we make use of finite fields arithmetic¹⁰ which is made possible by the fact that at tree-level the kinematic dependence of the amplitudes in the spinor variables is rational. More specifically for each subamplitude we generate a set of momentum-twistors [238, 239], as explained in Appendix A.3, with components on \mathbb{Z}_p , where twistors associated to different subamplitudes but to the same internal momentum are by construction taken to be on the same plane¹¹. From these components then we compute the kinematic invariants and from there the products of the tree-amplitudes, all of which naturally live on the field \mathbb{Z}_p . This approach in general greatly speeds up the calculations, having as single minor drawback the fact that to obtain the solution to the linear system on \mathbb{Q} once it has been computed on \mathbb{Z}_p would generally require repeated sampling for different values of the prime p (see appendix A.4). However, since the coefficients involved in our calculations are typically very small compared to the prime p we consider, the use of a single field is usually enough, further strengthened by checking the solutions a posteriori on rational kinematic points. The system solution itself is done through row reduction: the matrix A to be reduced is obtained from numerically evaluating (3.32) $t + 1$ times, with t being the number of $c_{i',j,k}$ appearing in the latter linear equation¹², and can be schematically written as

¹⁰The use of finite fields in high-energy physics has been introduced in [236] in the context of IBP reductions, and further pioneered in [237] where a much wider range of applications was explored. A brief overview of the topic can be found in Appendix A.4.

¹¹In twistor space, two intersecting lines define a null momentum, and a closed contour with n edges defines n conserved null momenta. When generating kinematics for the two subamplitudes \mathcal{A}_{m+1} and \mathcal{A}_{n-m+1} in (3.33), p_I is defined by the same intersecting lines for both of them.

¹²Generating and solving a system with an additional redundant equation ensures that when a

$$\left\{ \begin{array}{l} \sum_{s=1}^S a_{0,s} m_s = 0 \\ \sum_{s=1}^S a_{1,s} m_s = 0 \\ \vdots \\ \sum_{s=1}^S a_{t+1,s} m_s = 0 \end{array} \right. \mapsto \underbrace{\begin{pmatrix} a_{0,0} & \cdots & a_{0,S} \\ \vdots & & \vdots \\ a_{t+1,0} & \cdots & a_{t+1,S} \end{pmatrix}}_A \underbrace{\begin{pmatrix} m_0 \\ \vdots \\ m_S \end{pmatrix}}_V = 0, \quad (3.34)$$

where the $a_{i,j}$ are numeric constants (from the numerical evaluations of the kinematic parts) and the m_s are the unknowns $c_{i,j,k}$ or monomials in the couplings g , \mathcal{Y} and λ and the imaginary unit i . The explicit mention of the imaginary unit is due to the fact that it needs to be treated with some care when using finite fields. Imaginary units are almost ubiquitous in our construction and we decided to treat them as symbolic objects on the same footing as the coupling constants. Square roots would in principle require a similar treatment, but these are easily removed by choosing appropriate normalisations of the colour factors, and thus are never present in our calculation. Getting back to the system solution, upon row-reducing the numeric matrix A on finite fields one gets to a matrix B in row echelon form, which of course still satisfies $V' \equiv B V = 0$, with V the vector of constants $c_{i,j,k}$ and couplings. The relation $V' = 0$ can then be trivially solved for the couplings $c_{i,j,k}$ corresponding to the leading (the first non-vanishing) entries in each row of B . These relations provide the solution to the system.

It is worth stressing that, differently from either a Feynman diagrammatic approach or a BCFW-like calculation where consistency tests need to be performed a posteriori, through factorisation every step of the calculation is in itself a consistency check on the code. The systems of equations we obtain in the end always have a (possibly vanishing) solution, unless there is some physical obstruction. This is indeed the case when vector bosons are present among the external states (or more in general massless particles with helicity $|h| \geq 1$) and not enough invariants have been considered in the denominator construction. An impossible solution is symptomatic of unitarity breaking telling us that the ansatz was not general enough.

Thanks to many small, but at times significant, expedients¹³ the construction of the numeric system is rather fast despite our use of `Mathematica` rather than dedicated low-level language implementations, for example in C, which are usually better suited for the task. As a consequence, the main bottleneck of the system-solving procedure is the system solution itself. As an aside, we note that our ansatz construction is of course independent of the ansatz solution method. More specifically, if the reader was interested in getting analytic expressions for tree-level amplitudes and already had at her/his disposal a routine for numerically evaluating the amplitude itself, say Berends-Giele [240] recursion for example, then the ansatz solution could be clearly done in one go solving a single large system in all the $c_{i,j,k}$. Despite being viable, we consider our approach far more appealing, not only conceptually because of the use of just on-shell quantities but also practically: solving the ansatz on the different factorisation channels leads to many small systems whose solution is faster than a single large one and furthermore lends itself to effective parallelisation.

determined solution is found this is kinematics-independent and thus a true solution. Impossible systems might still admit determined kinematic-dependent solutions which are clearly unacceptable.

¹³These include, for example, recycling numeric data whenever possible, storing and reusing directly the exact invariant products making up the numerators instead of the single invariants, and generating a minimal parametrization of the kinematic points first, reducing thus the numerical kinematic generation to evaluations of polynomials in one/two variables.

3.2.2 Generalisations and application to the heavy-mass EFT

This method does not apply only to massless theories in four-dimensions, but it can be generalised for amplitudes with massive particles and in any spacetime dimensions. Relaxing the former restriction can be done by simply generating the possible numerators in step (4) of the algorithm as elements of the kinematic basis for massive structures, presented in Section 2.2. The numerical evaluation over finite fields is still possible, generalising the twistor construction to the massive case, as shown in Appendix A.3. But in this case polynomial terms must be treated carefully to preserve unitarity [231] and contrary to the fully-massless case constrains like those presented in Section 3.1 are expected also at higher points in the massive scalar sector of the theory under considerations [241, 242]. On the other hand, in generic space-time dimensions we would need a systematic algorithm to classify kinematically independent numerators and an algorithmic way of generating rational kinematics, but the strategy still works generically for any (effective) theory. As an explicit example, we show how to compute the five-point colour-order amplitudes with two heavy scalars and an external gluon in the HEFT [232, 243–245].

Five-point amplitudes with two heavy sources in the HEFT

The analytic form of the tree-level $(n + 2)$ -point amplitude with n external gluons and one heavy source (two scalars) which makes colour-kinematic duality manifest has been found in [246]. We use the three- and four-point amplitudes from this thesis and the knowledge of the leading soft limit in Yang-Mills theories [247] to determine completely the five-point with two massive sources (four-scalars) and one gluon. The five-point kinematic can be represented as

$$(3.35)$$

In this parametrisation, momentum conservation reads $k^\mu = q_1^\mu + q_2^\mu$ and the on-shell condition for the external scalar, after taking the heavy-mass limit, becomes

$$p_i \cdot q_i = \mathcal{O}(m_i^0). \quad (3.36)$$

In the HEFT, massive propagators are linear and the amplitude is a homogeneous function of the masses of degree 1 (in gauge theories, while is it homogeneous of degree 2 in gravitational theories). This point will be fundamental in constructing an ansatz with a very limited number of terms. Also, the factorisation channels with internal heavy scalars cannot be probed in the heavy-mass limit, because such kinematics lays beyond the regime of validity of the HEFT, as suggested by condition (3.36). Nevertheless, we will show that the knowledge of the massless poles (together with the leading-order soft behaviour) is enough to fully fix the amplitude, thanks to the mixing of channels induced by the presence of the external gluon. Finally, we should mention that gauge

invariance will be always manifest, both in the ansatz and in the factorisation channels because we will use the gauge-invariant amplitudes of [232, 246].

- In the generation of the amplitude a *power counting analysis* is essential. We will perform it in four dimensions for simplicity, but the result is not dependent on this. The five-point amplitude has mass dimension

$$[\mathcal{A}_5] = -1 , \quad (3.37)$$

and the Yang-Mills coupling is dimensionless ($[g] = 0$).

- The massless pole are q_1^2 and q_2^2 . Then, we want to generate an ansatz

$$\frac{\mathcal{A}_5}{ig^3} = \frac{\mathcal{N}_1}{q_1^2} + \frac{\mathcal{N}_2}{q_2^2} + \frac{\mathcal{N}_3}{q_1^2 q_2^2} + \mathcal{N}_c , \quad (3.38)$$

which has *no redundancy*, i.e. $\mathcal{N}_i|_{q_j^2=0} \neq 0$ and they are finite, as we want that all the massless singularities are in the explicit propagators. \mathcal{N}_c is a term which has no massless propagator and we improperly call *contact term*, as it still have (linear) massive propagators, which can be probed by taking the soft- k limit.

- In order to guarantee both *gauge invariance* and little group covariance, we require

$$\mathcal{A}_5 = F_k^{\mu\nu} \mathcal{A}_{5\mu\nu} , \quad (3.39)$$

where $F_k^{\mu\nu} = k_\mu \epsilon_\nu - k_\nu \epsilon_\mu$ is the linearised field strength. Schematically, then we must have

$$\mathcal{N}_i = \frac{F_k \otimes \bigotimes_j p_j^{\otimes n_{i,j}}}{\bigotimes_j p_j^{\otimes m_{i,j}}} , \quad p_j = \{p_1, p_2, q_1, q_2, k\} , \quad (3.40)$$

with

$$\sum_j n_{i,j} - m_{i,j} = 0 , \quad ([\mathcal{N}_i] = 1) , \quad (i = 1, 2) \quad (3.41)$$

$$\sum_j n_{3,j} - m_{3,j} = 2 , \quad ([\mathcal{N}_3] = 3) . \quad (3.42)$$

Trivially $\sum_j n_{i,j}$ and $\sum_j m_{i,j}$ must be even and, since $F_k^\mu = 0$, we must have $\sum_j m_{i,j} \neq 0$. In the denominators only massive propagators are allowed: in particular, only $p_1 \cdot k$ and $p_2 \cdot k$ can appear ($p_1 \cdot q_2 = p_1 \cdot k$ and $p_2 \cdot q_1 = p_2 \cdot k$ in the heavy-mass limit). We will assume that only single powers of these linear propagators can appear (which will be enough for the gauge theory amplitudes, while it would not work for gravity).

- As we have said already, we are computing HEFT amplitudes which are *homogeneous in the mass* and, in particular, *proportional to $m_1 m_2$* .
- First, we consider \mathcal{N}_1 and \mathcal{N}_2 . A single factor $p_i \cdot k$ is not enough, because the homogeneity forces any term to be zero. Then we need both massive propagators and there is a unique term contributing:

$$\mathcal{N}_i = \alpha_i \frac{p_1 \cdot p_2 p_1 \cdot F_k \cdot p_2}{p_1 \cdot k p_2 \cdot k} , \quad i = 1, 2 . \quad (3.43)$$

- \mathcal{N}_3 is more convoluted:

$$\mathcal{N}_3 = \mathcal{N}_3^{(0)} + \frac{\mathcal{N}_3^{(1')}}{p_1 \cdot k} + \frac{\mathcal{N}_3^{(1'')}}{p_2 \cdot k} + \frac{\mathcal{N}_3^{(2)}}{p_1 \cdot k p_2 \cdot k}, \quad (3.44)$$

where

$$\begin{aligned} \mathcal{N}_3^{(0)} &= \beta_1 p_1 \cdot F_k \cdot p_2, \\ \mathcal{N}_3^{(1')} &= \beta_2 p_1 \cdot p_2 q_1 \cdot F_k \cdot p_1 + \beta'_2 p_1 \cdot p_2 q_2 \cdot F_k \cdot p_1, \\ \mathcal{N}_3^{(1'')} &= \beta_3 p_1 \cdot p_2 q_1 \cdot F_k \cdot p_2 + \beta'_3 p_1 \cdot p_2 q_2 \cdot F_k \cdot p_2, \\ \mathcal{N}_3^{(2)} &= \beta_4 q_1 \cdot q_2 p_1 \cdot F_k \cdot p_2 + \beta_5 (p_1 \cdot p_2)^2 q_1 \cdot F_k \cdot q_2. \end{aligned} \quad (3.45)$$

But $q_2 \cdot F_k \cdot p = -q_1 \cdot F_k \cdot p$ and $q_1 \cdot F_k \cdot q_2 = 0$ (from the equation of motion $k_\mu F_k^{\mu\nu} = 0$). Moreover, $q_1 \cdot q_2 \propto q_1^2 + q_2^2$ (from $k^2 = 0$). Then, we can choose $\beta'_2 = \beta'_3 = \beta_4 = \beta_5 = 0$, such that we do not have a redundant ansatz. Anyway, there is still a source of redundancy which we did not consider. Indeed, the following non-trivial identity holds:

$$(q_1^2 - q_2^2) p_1 \cdot F_k \cdot p_2 = 2p_1 \cdot k q_1 \cdot F_k \cdot p_2 - 2p_2 \cdot k q_1 \cdot F_k \cdot p_1. \quad (3.46)$$

Then we can also impose

$$\alpha = \alpha_1 = \alpha_2, \quad (3.47)$$

without any restriction.

- The complete non-redundant ansatz is

$$\begin{aligned} \frac{\mathcal{A}_5}{ig^3} &= \frac{1}{q_1^2 q_2^2} \left[\alpha \frac{(q_1^2 + q_2^2) p_1 \cdot p_2 p_1 \cdot F_k \cdot p_2}{p_1 \cdot k p_2 \cdot k} + \beta_1 p_1 \cdot F_k \cdot p_2 + (p_1 \cdot p_2) \times \right. \\ &\quad \left. \times \left(\beta_2 \frac{q_1 \cdot F_k \cdot p_1}{p_1 \cdot k} + \beta_3 \frac{q_1 \cdot F_k \cdot p_2}{p_2 \cdot k} \right) \right] + \mathcal{N}_c. \end{aligned} \quad (3.48)$$

- We fix these four remaining coefficients ($\alpha, \beta_1, \beta_2, \beta_3$) by matching the residues on the massless poles with the factorisation channels:

$$\begin{aligned} -i \operatorname{Res}_{q_1^2=0} \mathcal{A}_5(p_1, p_2; q_1, q_2, k) &= \mathcal{A}_3(p_1; q_1) \mathcal{A}_4(p_2; k, -q_1)|_{q_1^2=0} \\ &= -\frac{2 p_1 \cdot F_k \cdot p_2}{q_2^2} + \frac{2 p_1 \cdot p_2 q_1 \cdot F_k \cdot p_2}{q_2^2 p_2 \cdot k}, \\ -i \operatorname{Res}_{q_2^2=0} \mathcal{A}_5(p_1, p_2; q_1, q_2, k) &= \mathcal{A}_4(p_1; -q_2, k) \mathcal{A}_3(p_2; q_2)|_{q_2^2=0} = \\ &= -\frac{2 p_1 \cdot F_k \cdot p_2}{q_1^2} + \frac{2 p_1 \cdot p_2 q_1 \cdot F_k \cdot p_1}{q_1^2 p_1 \cdot k}, \end{aligned} \quad (3.49)$$

and solving the resulting linear system we find

$$\begin{cases} \alpha = -\frac{1}{4} \\ \beta_1 = -1 \\ \beta_2 = \frac{1}{2} \\ \beta_3 = \frac{1}{2} \end{cases}. \quad (3.50)$$

- Finally, we notice that homogeneity and mass dimension considerations do not allow for any contact term with a single power of linear propagators at the denominators. On the other hand, higher powers would introduce more singular terms in the soft- k limit which cannot be compensated by any of the terms in (3.48). Then, simple power counting considerations give

$$\mathcal{N}_c = 0 . \quad (3.51)$$

We checked that (3.48) and (3.50) match the computations with Feynman diagrams.

3.3 Anomalies from Amplitudes \Leftarrow Locality and Unitarity

On top of the relations we found so far, it would be nice to be able to further relate Y_e and Y_u as is done by the anomaly cancellation condition $Y_L + 3Y_Q = 0$. Indeed, it has long been known that in gauge theories with chiral fermions anomalies arise from fermion loops [248, 249]. These gauge anomalies impose consistency conditions on the theory, which in the case of the SM translate into relations among the hypercharges of the fermions. Interestingly, as first noticed in [50, 51], the same cancellation conditions are required from a purely on-shell point of view by a clash of unitarity and locality in some one-loop amplitudes. In this section, we apply this method to recover the SM anomaly cancellation conditions.

The core of the idea is that one-loop amplitudes can be computed using generalised unitarity methods, up to rational terms which have no branch points. Such amplitudes by construction are unitary, however locality is not guaranteed (spurious poles can appear in the final result) and needs to be restored by appropriately fixing the rational terms to which the unitarity methods are blind. These rational terms might in turn introduce new corrections to the factorisation of the four-point amplitude, which is inconsistent with the fact that the three-point amplitudes are tree-level exact and fixed by helicity and mass dimension. When this happens additional properties of the theory need to be required for these terms to vanish. In particular, in this section we will show that for the Standard Model this leads to well known anomaly constraints on the fermion hypercharges.

We will specifically consider a fermion loop coupled to four external gauge bosons in the MHV configuration. The full one-loop amplitudes in the Standard Model can be schematically written as

$$\mathcal{A}^{1\text{-loop}} = \mathcal{A}_{\text{vec}}^{1\text{-loop}} + \mathcal{A}_{\text{ferm}}^{1\text{-loop}} + \mathcal{A}_{\text{scal}}^{1\text{-loop}} , \quad (3.52)$$

where the three contributions correspond respectively to vector bosons, fermions or scalars running in the internal loop, the specific type of these particles depending on the external states. We want to focus here on the fermion loop contributions, which are infrared finite and are the only part contributing to the chiral anomaly. The kinematic information of these amplitudes is entirely captured by the coefficients of Figure 3.2 with cyclic rotations providing the other orderings. For later convenience we define the following kinematic combinations, which turn out to be ubiquitous in the one-loop amplitudes

$$K_{\text{even}} := \frac{\langle 24 \rangle^2 [13]^2}{s_{12}s_{14}} \sum_{i,j} (c_{i,j}^f + \bar{c}_{i,j}^f) I_i(j) , \quad K_{\text{odd}} := \frac{\langle 24 \rangle^2 [13]^2}{s_{12}s_{14}} \sum_{i,j} (c_{i,j}^f - \bar{c}_{i,j}^f) I_i(j) , \quad (3.53)$$

Figure 3.2 displays four kinematic diagrams and their corresponding coefficients, arranged in a 2x2 grid. Each diagram shows external legs labeled 1^+ , 2^- , 3^+ , and 4^- , and internal lines with labels $+\frac{1}{2}$ and $-\frac{1}{2}$.

- Top-left diagram: $c_4^f = -\frac{s_{12}^4 s_{14}^2}{2 s_{13}^4}$
- Top-right diagram: $c_4^{\bar{f}} = -\frac{s_{12}^2 s_{14}^4}{2 s_{13}^4}$
- Middle-left diagram: $c_{3,(12)}^f = \frac{s_{12}^4 s_{14}}{2 s_{13}^4}$
- Middle-right diagram: $c_{3,(12)}^{\bar{f}} = \frac{s_{12}^2 s_{14}^3}{2 s_{13}^4}$
- Bottom-left diagram: $c_{2,(12)}^f = \frac{s_{14}(2s_{14}^2 + 11s_{12}^2 + 7s_{12}s_{14})}{6s_{13}^3}$
- Bottom-right diagram: $c_{2,(12)}^{\bar{f}} = \frac{s_{14}(2s_{14}^2 - s_{12}^2 - 5s_{12}s_{14})}{6s_{13}^3}$

Figure 3.2: Kinematic coefficients from generalised unitarity [41], here a kinematic contribution of the type $\frac{\langle 24 \rangle^2 [13]^2}{s_{12} s_{14}}$ has been factored out.

with $i = 2, 3, 4$ and $j = s_{12}, s_{14}$, and I_2, I_3 and I_4 being the bubble, triangle and box integrals given in Appendix D. Notice that in the chosen helicity configuration in the one-loop amplitude there are no discontinuities in the s_{13} channel, because all the tree-amplitudes entering the fermion loop contribution in the generalised unitarity calculation vanish in this channel.

Then we consider as a first example the one-loop amplitude with two W s and two B s as external states, and consequently Q/\bar{Q} and L/\bar{L} as the only possible fermions running through the loop. We find

$$\mathcal{A}_{\text{ferm}}^{1\text{-loop}}(W_+^I, B_-, W_+^J, B_-) \Big|_{\text{cut}} = g_1^2 g_2^2 (Y_L^2 + 3Y_Q^2) \delta^{IJ} K_{\text{even}}. \quad (3.54)$$

The presence of only K_{even} was to be expected due to the interplay of the colour part with the kinematics. The $SU(3)$ colour part is trivial being absent in the case of the L/\bar{L} circulating in the loop and contributing a numeric factor $\delta_a^a = 3$ for the Q/\bar{Q} loop. The $SU(2)$ part on the other hand contributes with a factor of $\text{Tr } \sigma^I \sigma^J = \frac{1}{2} \delta^{IJ}$ in both the s_{12} and s_{14} channels, which then leads to an additive combination of the kinematic parts into K_{even} . Studying the behaviour of K_{even} in the small- s_{13} limit one finds that

$$K_{\text{even}} \xrightarrow{s_{13} \rightarrow 0} \frac{\langle 24 \rangle^2 [13]^2}{s_{12} s_{14}} \left(-\frac{s_{12}^2}{s_{13}^2} - \frac{s_{12}}{s_{13}} + \mathcal{O}(s_{13}^0) \right), \quad (3.55)$$

thus, in order to restore locality, this amplitude requires a rational term whose kinematic part is of the form

$$R_{\text{even}} = -\frac{\langle 24 \rangle^2 [13]^2}{s_{13}^2}, \quad (3.56)$$

which cancels both the spurious poles of (3.55) and does not produce any modification to the residues in the s_{12} and s_{14} channels. Adding together the cut-constructible and rational piece one gets the complete fermion loop contribution

$$\mathcal{A}_{\text{ferm}}^{1\text{-loop}}(W_+^I, B_-, W_+^J, B_-) = g_1^2 g_2^2 (Y_L^2 + 3Y_Q^2) \delta^{IJ} (K_{\text{even}} + R_{\text{even}}). \quad (3.57)$$

On the other hand, considering three external W and a single B , one ends up with

$$\mathcal{A}_{\text{ferm}}^{1\text{-loop}}(W_+^I, W_-^J, W_+^K, B_-) \Big|_{\text{cut}} = \frac{i}{2} g_1 g_2^3 (Y_L + 3Y_Q) \epsilon^{IJK} K_{\text{odd}}, \quad (3.58)$$

where once again the $SU(2)$ colour structure, which is $\text{Tr } \sigma^I \sigma^J \sigma^K = \frac{i}{4} \epsilon^{IJK}$ in the s_{12} channel and $\text{Tr } \sigma^I \sigma^K \sigma^J = -\frac{i}{4} \epsilon^{IJK}$ in the s_{14} channel, is responsible for the relative sign among the kinematic structures and the combination into K_{odd} .

Now K_{odd} in the small- s_{13} limit goes as

$$K_{\text{odd}} \xrightarrow{s_{13} \rightarrow 0} \frac{\langle 24 \rangle^2 [13]^2}{s_{12} s_{14}} \left(-\frac{s_{12}}{s_{13}} + \mathcal{O}(s_{13}^0) \right), \quad (3.59)$$

requiring a compensating rational term of the form

$$R_{\text{odd}} = \langle 24 \rangle^2 [13]^2 \frac{s_{12} - s_{14}}{2s_{12}s_{13}s_{14}}, \quad (3.60)$$

which would lead to a complete fermion loop contribution of

$$\mathcal{A}_{\text{ferm}}^{1\text{-loop}}(W_+^I, W_-^J, W_+^K, B_-) = \frac{i}{2} g_1 g_2^3 (Y_L + 3Y_Q) \epsilon^{IJK} (K_{\text{odd}} + R_{\text{odd}}). \quad (3.61)$$

However, R_{odd} introduces (unphysical) corrections to the residues in the s_{12} and s_{14} channels, because the one-loop four-point amplitude cannot have any factorisation channel and thus it cannot appear in the one loop amplitude¹⁴. In order to get an answer which satisfies both unitarity and locality we must then enforce the coefficient of the amplitude to vanish, which means imposing

$$Y_L + 3Y_Q = 0 . \quad (3.62)$$

In a similar fashion, when looking at the one-loop interaction of three gluons with a single B we get the condition

$$2Y_Q = Y_u + Y_d , \quad (3.63)$$

which is necessary for the fermion-loop contribution to recombine in the physically meaningful form

$$\mathcal{A}_{\text{ferm}}^{1\text{-loop}}(G_+^A, G_-^B, G_+^C, B_-) \Big|_{\tau ABC} = -2g_1 g_3^3 (Y_u + Y_d) (K_{\text{even}} + R_{\text{even}}) . \quad (3.64)$$

On the other hand, it is not clear with amplitudes we need to study in order to obtain the additional textbook constraint on the hypercharges

$$(2Y_L^3 - Y_e^3) + 3(2Y_Q^3 - Y_u^3 - Y_d^3) = 0 , \quad (3.65)$$

and

$$(2Y_L - Y_e) + 3(2Y_Q - Y_u - Y_d) = 0 . \quad (3.66)$$

The former may be found studying unitarity and locality properties of the three-point form factor with a Lagrangian insertion (which is any way reminiscent of the classical treatment of anomalies in perturbative QFT), while for the latter we need to couple the Standard Model to Einstein-Hilbert gravity.

¹⁴Three-point amplitudes are exact at tree-level and fixed by helicity and mass dimensions consideration. This make the poles of four-point amplitudes tree-level exact, *i.e.* there are no loop corrections to the residues of these poles.

Chapter 4

Form Factors from Unitarity in 6D

The aim of this chapter is to construct complete, analytic form factors of gauge-invariant operators at one loop. In supersymmetric theories, four-dimensional unitarity [35, 36] is sufficient to obtain complete answers for amplitudes at one loop. Without supersymmetry or for form factors of non-protected operators this is no longer the case because of the appearance of rational contributions. In the amplitude context, this problem has been addressed in different ways. In one approach, one makes use of factorisation to establish a recursion relation that allows to reconstruct rational terms [52, 53] (see [250, 251] for recent elegant applications to two-loop amplitudes in pure Yang-Mills). Another approach is to shift the dimensionality of internal states in the loop away from four dimensions [55, 252] where rational terms acquire a singularity which can then be detected using unitarity cuts. This method requires that the internal lines, corresponding to virtual particles, are kept in d dimensions, while momenta and polarisation vectors of external particles live in four dimensions.

Having the internal particles in arbitrary, non-integer dimensions introduces complications, since tree amplitudes are no longer simple and the power of the spinor-helicity formalism is lost. Moreover, it is not possible to numerically evaluate d -dimensional amplitudes in non-integer dimensions. A solution to these problems is offered by “dimensional reconstruction” [59, 60, 233, 253, 254]. In this approach, one investigates the dependence of the loop amplitudes on the dimensionality of spacetime, which turns out to be polynomial in pure Yang-Mills theory, at the level of the integrand. Then one computes the amplitudes with virtual particles kept in integer dimension $d > 4$ to fix the coefficients in the polynomial by interpolation, which leads by analytic continuation to an expression valid for any non-integer dimension d . The dimensional reconstruction approach can also be effectively combined with the spinor-helicity formalism in six dimensions of [30], which allows for compact expressions of the on-shell building blocks. At higher loops, these techniques were used in [255] to derive the five-point all-plus gluon amplitude integrand in pure Yang-Mills, while a generalisation to incorporate fermions was carried out in [256]. Recent numerical as well as analytical results for arbitrary helicity configurations of five partons were derived in [257–259]. Six-dimensional unitarity has also been used in [260] to test conjectures about rational terms in two-loop all-plus gluon amplitudes up to nine-points. In this framework, a systematic prescription for complete form factors, including rational terms, have been presented in [207].

As already explained in the general introduction, a form factor is defined as the overlap of an n -particle state and the state produced by an operator $\mathcal{O}(x)$ acting on the vacuum. Notable examples of form factors include the form factor of the hadronic

electromagnetic current with an external hadronic state, which feature in the $e^+e^- \rightarrow$ hadrons and deep inelastic scattering matrix elements, and the form factor of the electromagnetic current, which computes the (electron) $g - 2$. The form factors which will be considered in this thesis are related to scattering processes of the Higgs boson and many gluons. In the large top-quark mass approximation or considering an BSM heavy particle, we find infinite series of higher-dimensional interactions of the Higgs with the gluon field strength and its derivatives, in addition to couplings to light degrees of freedom, which we will consider to be just pure Yang-Mills. More precisely, this effective Lagrangian reads

$$\mathcal{L}_{\text{eff}} = \hat{c}_0 \mathcal{O}_0 + \frac{1}{M^2} \sum_{i=1}^4 \hat{c}_i \mathcal{O}_i + \mathcal{O}\left(\frac{1}{M^4}\right), \quad (4.1)$$

where the leading-order term in the expansion is $\mathcal{O}_0 := h \text{Tr} F^2$ [261–264] and h is the Higgs field, \mathcal{O}_i , $i = 1, \dots, 4$ are dimension-7 operators made of gluon field strengths and covariant derivatives [265–268], M is the mass of the heavy particle integrated out, and \hat{c}_0 , \hat{c}_i are Wilson coefficients¹. In the study of Higgs + gluon processes one replaces q^2 with the squared mass of the Higgs m_{H}^2 to obtain the amplitudes relevant for this process.

In this thesis we will apply the approach discussed so far to form factors of operators of the form $\text{Tr} F^n$, for $n = 2, 3, 4$, both for minimal and non-minimal form factors up to four external gluons. Modern amplitude techniques were applied to form factors of $\text{Tr} F^2$, which compute the leading contribution to Higgs + multi-gluon amplitudes in the effective Lagrangian approach, including MHV diagrams [66, 67] at tree level [269, 270] and one loop [271], and a combination of one-loop MHV diagrams and recursion relations [272]. Recent work [273–277] addressed the computation of the four-dimensional cut-constructible part of Higgs+multi-gluon scattering from operators of mass dimension seven using generalised unitarity applied to form factors [278–290]. The key point of this chapter is that we extend dimensional reconstruction to any form factor of operators involving vector fields, which requires the subtraction of form factors of an appropriate class of scalar operators that we identify. Along the way we have also found a generalisation of this procedure to any loop order, for amplitudes and form factors.

The rest of the chapter is organised as follows. In Section 4.1 we review the dimensional reconstruction technique at one loop and generalise it to form factors involving vector fields. We also discuss its generalisation to any number of loops, which for one and two loops is in agreement with known results. In Section 4.2 we study tree-level form factors for a wide class of operators involving field strengths in four and six dimensions. These quantities are needed in the one-loop unitarity-based calculations of Section 4.3. There, we begin by reproducing the well-know one-loop form factors for $\text{Tr} F^2$ with two and three external gluons. Then we prove that the minimal form factor for $\text{Tr} F^3$ has no rational terms, as argued in the literature. Finally, we calculate for the first time the non-minimal one-loop form factor for $\text{Tr} F^3$ and the minimal form factor for $\text{Tr} F^4$ with different helicity configurations. We also generalise some of these results for a class of form factors of the $\text{Tr} F^n$ operators.

¹The Wilson coefficients are proportional to v the Higgs field vacuum expectation value. If we consider the Wilson coefficients in the EFT after integrating out the top quark in the loops, then they will be proportional to $1/v$. Their precise form will be of no relevance for this thesis.

4.1 The Dimensional Reconstruction Technique

In the first part of the section, we look at DR technique at the one-loop case from a different perspective, which lends itself to a systematic generalisation to form factors in generic Yang-Mills theory. The new viewpoint we adopt presents also a much desirable advantage: it allows for a natural generalisation to any loop order, for both amplitudes and form factors, which will be discussed in the second part of the section.

4.1.1 One-Loop Dimensional Reconstruction

The first step in our study is to identify the dependence of the loop amplitude on the dimensionality of the spacetime. In the literature, a common procedure is to distinguish the two sources of this dependence:

- the first is the number of spin-eigenstates, which is a function of the dimension of the spacetime d_s (for example, gluons have $d_s - 2$ spin degrees of freedom);
- the second is the integration over the loop momentum, which lives in a d -dimensional space.

In the following, we will show how such dependence can be disentangled.

As we said, we consider pure Yang-Mills theory in dimensional regularisation ($d = 4 - 2\epsilon$):

$$\mathcal{L} = -\frac{1}{4}(F_{\mu\nu}^a F^{a\mu\nu})(x), \quad (4.2)$$

and we are interested in calculating amplitudes (and form factors) involving four-dimensional real² external gluons. At one loop it is possible to write a generic ansatz for the amplitude

$$\mathcal{A}_{(d)}^{(1)}(\{p_i, h_i\}) = \int \frac{d^d l}{(2\pi)^d} \frac{\mathcal{N}(\{p_i, h_i\})}{\prod_i D_i}, \quad (4.3)$$

where $\mathcal{N}^d(\{p_i, h_i\})$ depends on d , through the number of spin eigenstates of the gluons and the loop momentum. Since all external momenta are four-dimensional, the latter dependence (*i.e.* the additional components of l) enter the amplitude only through the square of the loop momentum, which can always be written as

$$l^2 := (l^{(4)})^2 - \mu^2. \quad (4.4)$$

The dependence of the amplitude on μ^2 manifests itself in a number of additional integrals with non-trivial numerators, which have to be added to the usual master integral basis. These integrals have the form:

$$\int \frac{d^d l}{(2\pi)^d} \frac{\mu^{2p}}{D_1 \cdots D_n} := I_n^d[\mu^{2p}], \quad (4.5)$$

which can be evaluated as ordinary integrals, but in higher dimensions [55]. The presence of these integrals cannot be probed using four-dimensional unitarity cuts, *i.e.* such terms do not have discontinuities in four dimensions. In particular, such integrals correspond to the rational terms we are looking for.

²Here real is used in contrast with *virtual*, which describes both internal particles propagating and soft emissions, which must be treated on the same footing to preserve unitarity.

Consider now the explicit dependence of the amplitude on spin. One-loop integrands involving only vector bosons are explicitly *linearly* dependent on d . The origin of such dependence is the contraction of the metric tensor, coming from vertices and propagators, in a closed loop. Since we were able to tell these two sources on d , we can write the amplitude as

$$\mathcal{A}_{(d_s, d)}^{(1)}(\{p_i, h_i\}) = \int \frac{d^d l}{(2\pi)^d} \frac{d_s \mathcal{N}_1(\{p_i, h_i\}) - \mathcal{N}_0(\{p_i, h_i\})}{\prod_i D_i}, \quad (4.6)$$

where we distinguished between d and d_s and the physical meaning of such distinction will be clarified in a moment.

By definition d are the dynamical dimensions of the theory and we can always choose $d_s \leq d$, following a procedure reminiscent of dimensional reduction [291]: indeed, it is sufficient to write a d -dimensional vector as $A^{a\mu} = (A^{a\hat{\mu}}, \phi^{a,1}, \dots, \phi^{a, d-d_s})$, where $A^{a\hat{\mu}}$ transforms as a vector under transformations of the Lorentz group in d_s dimensions, and to ignore any contribution to the amplitudes from the $\phi^{a,i}$ scalars. On the other hand, since the dependence of the amplitude on d_s is trivial, we can analytically continue it to $d_s > d$ [292]. Then, it is sufficient to compute the amplitude in two integer dimensions, for example d_0 and $d_1 = d_0 + 1$, and write it in the Four Dimensional Helicity (FDH) scheme [293]. The result of the interpolation is given by [59]:

$$\mathcal{A}_{(4, d)}^{(1)} = (d_1 - 4)\mathcal{A}_{(d_0, d)}^{(1)} - (d_0 - 4)\mathcal{A}_{(d_1, d)}^{(1)}. \quad (4.7)$$

On the other hand, the d_1 -dimensional gluon behaves as a d_0 -dimensional one plus a real scalar. In terms of the Lagrangian, we have

$$\mathcal{L}_{d_1} = \mathcal{L}_{d_0} + \frac{1}{2} D_\mu \phi^a D^\mu \phi^a. \quad (4.8)$$

It is easy to conclude that the one-loop d_1 -dimensional amplitude $\mathcal{A}_{(d_1, d)}^{(1)}$ ³ can be expressed as the sum of two contributions: the first contribution is given by the equivalent one-loop gluon amplitude with internal particles living in d_0 dimensions $\mathcal{A}_{(d_0, d)}$, the second one, denoted in the following as $\mathcal{A}_{(d)}^S$, takes into account also scalar interactions coming from the second term on the right-hand side of (4.8). It is also important to stress that $\mathcal{A}_{(d)}^S$ is a gauge-invariant quantity in its own right and it is the sum of diagrams with a scalar running in the loop and the gluons as external particles. As a result of these observations, (4.7) can be written as:

$$\mathcal{A}_{(4, d)}^{(1)} = \mathcal{A}_{(d_0, d)}^{(1)} - (d_0 - 4)\mathcal{A}_{(d)}^S. \quad (4.9)$$

Up to some additional considerations, the above discussion holds true for form factors as well, and so does (4.9). In particular, the scalar quantity that we have to subtract from the form factor with d_0 -dimensional internal gluons is obtained by trading the gluon loop with a scalar one. However, in contradistinction with the amplitude case, there are two sources for scalars when we are dealing with form factors. Inside the loop, one can have scalars coupled to gluon lines coming from terms of the form $\frac{1}{2} D_\mu \phi^a D^\mu \phi^a$ in the “dimensionally-reduced” Lagrangian (as in the case of amplitudes), but also scalars coming from the same operator as the form factor insertion. This procedure will be clear

³This notation denotes an amplitude for which the virtual gluons have momenta defined in d dimensions, while their polarization vectors live in $d_1 > d$.

in the calculation of the non-minimal $\text{Tr } F^2$ form factor, described in Section 4.3.2, where we will emphasise the role of these two distinct contributions (see also [254]).

We need is to identify such scalar contributions for a generic operator in Yang-Mills theories to extend the DR technique and, again, the procedure is reminiscent of dimensional reduction, as in (4.8). In particular, for the only two operators with mass-dimension six involving solely gluons, namely $\text{Tr}(DF)^2$ and $\text{Tr } F^3$, the scalar contribution comes from

$$D_\mu F_{\nu\rho}^a D^\mu F^{a\nu\rho} \mapsto D_\mu D_\nu \phi^a D^\mu D^\nu \phi^a, \quad (4.10)$$

and

$$f^{abc} F^a{}^\mu{}_\nu F^{b\nu}{}_\rho F^{c\rho}{}_\mu \mapsto f^{abc} D_\mu \phi^a D_\nu \phi^b F^{c\mu\nu}, \quad (4.11)$$

where scalar operators associated to each operator come from the dimensional reduction from $d_s + 1$ to d_s . On the other hand for the $\text{Tr } F^4$ operator, which we will consider later in this thesis, at one-loop we get

$$\text{Tr } F^\mu{}_\nu F^\nu{}_\rho F^\rho{}_\sigma F^\sigma{}_\mu \mapsto \text{Tr } D_\mu \phi D_\nu \phi F^\nu{}_\rho F^{\rho\mu}, \quad (4.12)$$

where in the last equation the trace is in colour space. The proportionality coefficients are still to be fixed and we will give the right prescription for them within the full tree-level calculation in Section 4.2.

4.1.2 An L -loop Generalisation

The arguments leading to (4.7) can be extended to arbitrary loop order. Considering pure Yang-Mills theory, any L -loop amplitude can be written as a degree L polynomial in d_s dimensions⁴,

$$\mathcal{A}_{(d_s, d)}^{(L)} = \sum_{i=0}^L (d_s - 4)^i \mathcal{K}_i, \quad (4.13)$$

where \mathcal{K}_i are quantities to be determined. In particular, note that the four-dimensional amplitude in the FDH scheme [292, 293] coincides with the zero-degree coefficient: $\mathcal{K}_0 = \mathcal{A}_{(4, d)}^{(L)}$. In order to find the coefficients \mathcal{K}_i , we can interpolate the polynomial in $L + 1$ distinct integer dimensions $d_i > d$. Writing the problem in matrix form, one has

$$\begin{pmatrix} \mathcal{A}_{(d_0, d)}^{(L)} \\ \mathcal{A}_{(d_1, d)}^{(L)} \\ \vdots \\ \mathcal{A}_{(d_L, d)}^{(L)} \end{pmatrix} = \begin{pmatrix} 1 & (d_0 - 4) & (d_0 - 4)^2 & \cdots & (d_0 - 4)^L \\ 1 & (d_1 - 4) & (d_1 - 4)^2 & \cdots & (d_1 - 4)^L \\ \vdots & & & & \vdots \\ 1 & (d_L - 4) & (d_L - 4)^2 & \cdots & (d_L - 4)^L \end{pmatrix} \begin{pmatrix} \mathcal{K}_0 \\ \mathcal{K}_1 \\ \vdots \\ \mathcal{K}_L \end{pmatrix}, \quad (4.14)$$

where we recognise the Vandermonde matrix. Inverting this matrix, it is possible to express the \mathcal{K}_i as functions of the higher-dimensional amplitudes $\mathcal{A}_{(d_i, d)}^{(L)}$ for $i = 0, \dots, L$. In particular \mathcal{K}_0 , which is the amplitude in the FDH scheme, can be written as

$$\mathcal{A}_{(4, d)}^{(L)} = \mathcal{K}_0 = \prod_{j=0}^L (d_j - 4) \sum_{i=0}^L \frac{1}{(d_i - 4)} \prod_{\substack{k=0 \\ k \neq i}}^L \frac{1}{(d_k - d_i)} \mathcal{A}_{(d_i, d)}^{(L)}. \quad (4.15)$$

⁴As already mentioned, the d_s dependence comes from traces of η tensors, and there can be at most L closed loops leading to such a trace.

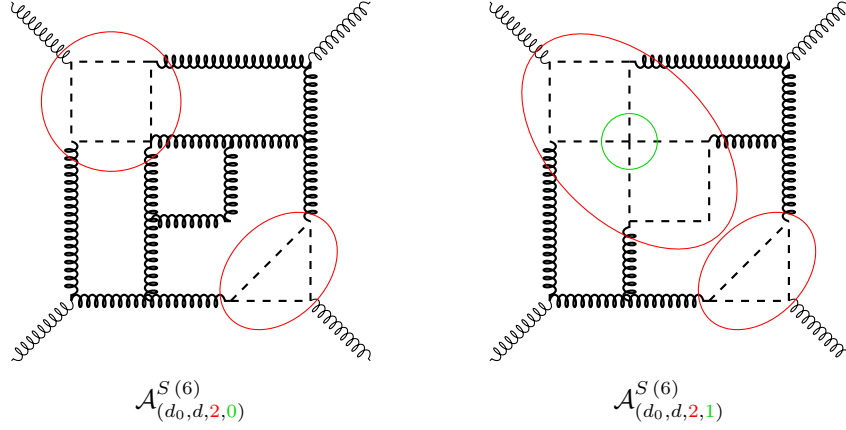


Figure 4.1: Two of the many possible diagrams contributing to the scalar amplitudes at six loops. On the left-hand side an example contribution to $\mathcal{A}_{(d_0, d, 2, 0)}^{S(6)}$ is shown. On the right-hand side the same diagram but with one of the gluon loops involving a four-point interaction replaced by a scalar. The latter diagram contributes to $\mathcal{A}_{(d_0, d, 2, 1)}^{S(6)}$.

We can always choose $d_0 > d$ to be the smallest dimension among the d_i 's, and we know that at most d dimensions are dynamical. Then, we can write the Lagrangian of pure Yang-Mills theory in $d_i > d_0$ dimensions as:

$$\mathcal{L}_{d_i} = -\frac{1}{4} F_{\mu\nu}^a F^{\alpha\mu\nu} + \frac{1}{2} \sum_{i=1}^{d_i-d_0} D_\mu \phi_i^a D^\mu \phi_i^a - \frac{\lambda}{2} f^{abc} f^{ade} \sum_{\substack{i, j=1 \\ j>i}}^{d_i-d_0} \phi_i^b \phi_j^c \phi_i^d \phi_j^e, \quad (4.16)$$

where μ, ν are d_0 -dimensional Lorentz indices, a, b, c are colour indices and f^{abc} are the structure constants of the gauge group. The vector field in d_i dimensions is decomposed in a (d_0 -dimensional) vector A_μ^a and $d_i - d_0$ scalars ϕ_i^a . The coupling of the ϕ^4 interaction is given by

$$\lambda = g^2, \quad (4.17)$$

and we call it λ for reasons that will be clear in a moment.

From (4.16), we can compute the amplitude with only external gluons⁵

$$\mathcal{A}_{(d_i, d)}^{(L)} = \mathcal{A}_{(d_0, d)}^{(L)} + \sum_{m=0}^{L-1} (d_i - d_0 - 1)^m \sum_{n=1}^{L-m} (d_i - d_0)^n \mathcal{A}_{(d_0, d, n, m)}^{S(L)}, \quad (4.18)$$

where $\mathcal{A}_{(d_0, d)}^{(L)}$ is the complete L -loop amplitude where all the internal legs are vectors and $\mathcal{A}_{(d_0, d, n, m)}^{S(L)}$ are specific combinations of diagrams with at least one scalar loop. Specifically, the diagrams contributing to $\mathcal{A}_{(d_0, d, n, m)}^{S(L)}$ are of order λ^m , *i.e.* they contain m four-scalar interactions, and in addition have n distinct purely scalar subdiagrams.

The coefficients for the scalar contributions in (4.18) can be understood as follows.

1. The number of distinct flavours of scalars is $d_i - d_0$ and they all give the same contribution.

⁵In this section, for the sake of clarity, we reserve the word *vector* only for the d_0 -dimensional vector, whereas we refer to the four-dimensional equivalents as gluons.

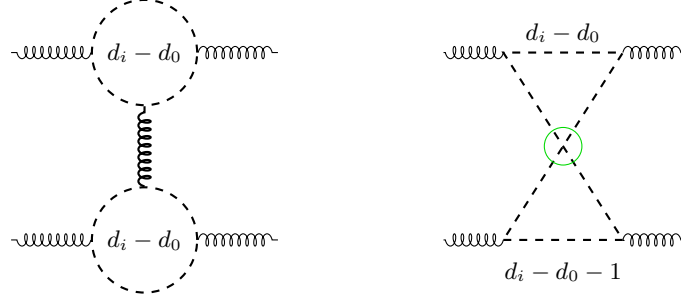


Figure 4.2: Two two-loop diagrams for comparison. In the first case there are two disconnected scalar loops, and every loop admits $d_i - d_0$ different flavours leading to an overall factor $(d_i - d_0)^2$. The second diagram represents two scalar loops connected by a flavour-changing four-scalar vertex (highlighted in green). In this case there are $d_i - d_0$ allowed flavours in one loop but only $d_i - d_0 - 1$ in the second loop, which leads to an overall factor $(d_i - d_0)(d_i - d_0 - 1)$.

2. Given a set of contiguous scalar propagators inside a diagram, when we draw the first scalar propagator, we need to multiply the diagram by a $d_i - d_0$ factor, corresponding to the distinct possible flavours.
3. Inside the same set of contiguous scalar propagators, each vertex with two scalars and one vector must preserve the scalar flavour, while the four-scalar vertex changes it. Thus each power of λ brings a $d_i - d_0 - 1$ factor.
4. Every distinct set of scalar propagators leads to an additional $d_i - d_0$ factor.
5. Since there are no external scalars, the number of distinct sets of scalar propagators plus the number of scalar quartic interactions coincides with the number of scalar loops:

$$n + m = \# \text{ scalar loops} \quad (4.19)$$

6. Clearly the number of scalar loops can be at most L .

We can substitute (4.18) in (4.15) and, for simplicity, we choose

$$d_i = d_0 + i \quad (4.20)$$

with $i = 0, \dots, L$. The final result should not depend on this choice, because the coefficient of a polynomial cannot depend on which point we choose for the fitting. After some manipulations, we find a closed expression which relates complete L -loop four-dimensional amplitudes to the same amplitudes in a higher integer dimension d_0 up to subtractions of scalar contribution:

$$\mathcal{A}_{(4,d)}^{(L)} = \mathcal{A}_{(d_0,d)}^{(L)} + \sum_{m=0}^{L-1} \sum_{n=1}^{L-m} (4 - d_0)^n (3 - d_0)^m \mathcal{A}_{(d_0,d,n,m)}^{S(L)}. \quad (4.21)$$

The whole reasoning can be applied to a more generic scheme where $d_s = 4$ (FDH scheme) is replaced by a generic d_s (e.g. the HV scheme [294] with $d_s = d = 4 - 2\epsilon$). As long as we keep $d_i > d_s$ and $d_i \geq d$, all the previous steps are still applicable, and we arrive at

$$\mathcal{A}_{(d_s,d)}^{(L)} = \mathcal{A}_{(d_0,d)}^{(L)} + \sum_{m=0}^{L-1} \sum_{n=1}^{L-m} (d_s - d_0)^n (d_s - d_0 - 1)^m \mathcal{A}_{(d_0,d,n,m)}^{S(L)}, \quad (4.22)$$

which at first sight is identical to (4.18). The non-trivial difference between the two expressions is that $d_s < d_0$, while we need $d_i > d_0$ ($i = 1, \dots, L$) in order to write (4.18). Moreover, as we stressed before, the quantity $(d_i - d_0)$ has a precise physical meaning: it is the number of distinct flavours of scalars in the dimensional reduced theory (4.16). On the other hand, $(d_s - d_0)$ takes into account the number of extra spin degrees of freedom in dimensional regularisation⁶.

The fact that the two expressions are exactly the same is a consequence of our previous considerations. Indeed, one could have recognised the polynomial dependence of the amplitude on the dimensionality d_s already from (4.18), and further identified (4.22) as its analytic continuation for $d_s - d_0 < 0$. Thus, starting from the ‘‘dimensionally-reduced’’ Lagrangian (4.16), the dependence on the dimensionality d_s emerges naturally, and the preceding considerations relating the d_i to d_s through the Vandermonde matrix may appear redundant. However, starting from the analysis of the dimensional dependence of the amplitudes provides a clear physical picture of the relation between d_s , d and d_i .

Our expression reproduces the known results at one loop [59]

$$\mathcal{A}_{(d_s,d)}^{(1)} = \mathcal{A}_{(d_0,d)}^{(1)} + (d_s - d_0)\mathcal{A}_{(d_0,d,0,1)}^{S(1)}, \quad (4.23)$$

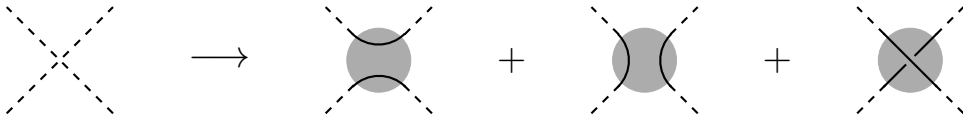
and two loops [255]

$$\mathcal{A}_{(d_s,d)}^{(2)} = \mathcal{A}_{(d_0,d)}^{(2)} + (d_s - d_0)\Delta_{(d_0,d)}^S + (d_s - d_0)^2\Delta_{(d_0,d)}^{2S}, \quad (4.24)$$

where

$$\Delta_{(d_0,d)}^S = \mathcal{A}_{(d_0,d,0,1)}^{S(2)} - \mathcal{A}_{(d_0,d,1,1)}^{S(2)}, \quad \Delta_{(d_0,d)}^{2S} = \mathcal{A}_{(d_0,d,0,2)}^{S(2)} + \mathcal{A}_{(d_0,d,1,1)}^{S(2)}. \quad (4.25)$$

Considering the two-loop expression in more detail, one sees that in [255] the four-scalar vertex is interpreted in terms of three fictitious flavour contributions:



The two continuous lines in the grey blob represent the colour flow inside the vertex. Considering Figure 4.2 we see that, in our interpretation, the only diagram which at two loops involves this vertex contributes with a factor $(d_s - d_0)(d_s - d_0 - 1)$. However, splitting the vertex according to colour flow as above, the contribution of the same diagram can be attributed to terms containing a factor $(d_s - d_0)^2$ as well as $(d_s - d_0)$. Taking into account this different interpretation of the four-scalar vertex, the two methods perfectly match.

We emphasise that individually each $\mathcal{A}_{(d_0,d,n,m)}^{S(L)}$ is a gauge-invariant quantity. Indeed, we know that $\mathcal{A}_{(d_0,d)}^{(L)}$ is gauge invariant by its own right and we might consider a theory for which $\lambda \neq g^2$ and a number of scalars $n_s \neq d_s - d_0$: then, the respective coefficients in the sums in (4.22) would change but the full answer would still be gauge-invariant.

As in the case of the one-loop procedure, (4.21) can be applied also to form factors, as far as we bear in mind that more scalar operators are involved in higher-loop calculations, in addition to those entering already at one loop. These additional terms emerge

⁶There is no dynamics in the dimensions $d_i - d_0$, while this could be not true for the dimensions $d_0 - d_s$.

clearly from (4.16). Indeed, for the operator $\text{Tr } F^2$, beyond one-loop calculations we also need to subtract the scalar contribution from the ϕ^4 operator:

$$F_{\mu\nu}^a F^{a\mu\nu} \mapsto g^2 f^{abd} f^{acd} \phi^b \tilde{\phi}^c \phi^d \tilde{\phi}^e, \quad (4.26)$$

where ϕ and $\tilde{\phi}$ are scalars with different flavour. Its contribution has to be carefully taken into account in the subtraction with the right d_s -dependence. In particular, in the form factor equivalent of (4.18), its insertion brings a $(d_i - d_0)(d_i - d_0 - 1)$ coefficient, because of the flavour changing.

An equivalent reasoning is also valid for higher-dimensional operators. For example, from the dimensional reduction procedure of the $\text{Tr } F^3$ operator, we find that the additional scalar operators entering higher-loop calculations are

$$f^{abc} F^a{}_{\mu}{}_{\nu} F^{b\nu}{}_{\rho} F^{c\rho}{}_{\mu} \mapsto \begin{cases} g f^{abc} f^{ade} D_{\mu} \phi^b D^{\mu} \tilde{\phi}^c \phi^d \tilde{\phi}^e \\ g^3 f^{abc} f^{ade} f^{bfg} f^{chi} \phi^d \tilde{\phi}^e \phi^f \hat{\phi}^g \tilde{\phi}^h \hat{\phi}^i \end{cases}, \quad (4.27)$$

where the former enters the calculation at two-loop level, while the latter from three loops. We stress that ϕ , $\tilde{\phi}$ and $\hat{\phi}$ represent three different scalar flavours. Then, in the generalisation of (4.18) to form factors, the insertion of the scalar operators bring a factor of $(d_i - d_0)(d_i - d_0 - 1)$ and $(d_i - d_0)(d_i - d_0 - 1)(d_i - d_0 - 2)$ respectively. Following the same procedure one can recover the scalar operators for $\text{Tr } F^4$, which we do not write explicitly.

In the following we are going to apply this technique to one-loop calculations for form factors. We will always choose $d_0 = 6$, due to the existence of a powerful Spinor Helicity Formalism in six dimensions [30, 60].

A technical comment is in order here. In performing loop calculations, initially we treat the loop momenta as living in $d_0 = 6$ dimensions, instead of d . This procedure is well defined at the integrand level, as we showed. Indeed, first we have to sum over the helicity states of the internal gluons and reduce to four-dimensional components for the external one. Then, knowing the functional dependence of the integrand on the $d - 4$ components of the loop momenta, which appear only through rational combinations of $l_i^{(-2\epsilon)} \cdot l_j^{(-2\epsilon)}$ and μ_i^2 ⁷, we can identify these combinations and we can treat the loop momenta as being d -dimensional and integrate over them. The choice $d_0 = 6$ is guaranteed to be good enough for the integrands at least up to two loops because we do not introduce any additional Gram determinant identity. Power counting and symmetry arguments may extend the validity of the six-dimensional computations beyond two loops in some special theories, see for example [60].

4.2 Tree-Level Amplitudes and Form Factors

In this section we will provide all the analytic expressions of the tree-level colour-ordered form factors required for loop calculations.

The tensorial structure of the field strength in four dimensions is given by the anti-symmetric product of two vector representations

$$\left(\frac{1}{2}, \frac{1}{2}\right) \wedge \left(\frac{1}{2}, \frac{1}{2}\right) = (1, 0) \oplus (0, 1), \quad (4.28)$$

⁷It is worth mentioning that in terms of the six-dimensional spinor components the quantity mentioned above reads as follows: $l_i^{(-2\epsilon)} \cdot l_j^{(-2\epsilon)} = \frac{1}{2}(m_i \tilde{m}_j + m_j \tilde{m}_i)$ and $\mu_i^2 = m_i \tilde{m}_i$.

where we can choose each component to correspond to the helicity configurations ± 1 . We then define the *self-dual* component of the free field strength as⁸

$$F_{\text{SD},\alpha\dot{\alpha}\beta\dot{\beta}} := \lambda_\alpha \lambda_\beta \epsilon_{\dot{\alpha}\dot{\beta}}, \quad (4.29)$$

which has helicity -1 and transforms in the $(1, 0)$ representation of the Lorentz group⁹. Then, the *anti-self-dual* component, transforming in the $(0, 1)$ representation is

$$F_{\text{ASD},\alpha\dot{\alpha}\beta\dot{\beta}} = \epsilon_{\alpha\beta} \tilde{\lambda}_{\dot{\alpha}} \tilde{\lambda}_{\dot{\beta}}. \quad (4.30)$$

In terms of $\text{SU}^*(4)$ representations, the six-dimensional free field strength transforms in the $\mathbf{6} \wedge \mathbf{6} = \mathbf{15}$, which is the traceless part of $\mathbf{4} \otimes \bar{\mathbf{4}}$. Thus it can be written as [295]

$$F_{a\dot{a}}^{AB}{}_{CD} = \alpha \delta_{[C}^{[A} F_{a\dot{a}}{}^{B]}{}_{D]}, \quad (4.31)$$

where α is a numerical coefficient to be fixed and $F_{a\dot{a}}{}^A{}_B$ is such that $F_{a\dot{a}}{}^A{}_A = 0$ ¹⁰. In spinor helicity variables this quantity is [295]

$$F_{a\dot{a}}{}^A{}_B = \lambda_a^A \tilde{\lambda}_{\dot{a}B}, \quad (4.32)$$

which is indeed traceless thanks to the six-dimensional Dirac equation (A.28). Upon dimensionally reducing, (4.32) down to four dimensions we match it with (4.29) and (4.30), which fixes the proportionality coefficient to be $\alpha = 2$.

4.2.1 Tr F^2 Form Factors

In this section we consider the operator

$$\mathcal{O}_2 := F_{\mu\nu}^a F^{a\mu\nu}. \quad (4.33)$$

In four dimensions \mathcal{O}_2 splits naturally into the sum of the traces of the self-dual and the anti-self-dual components of the field strength:

$$\text{Tr } F^2 = \text{Tr } F_{\text{SD}}^2 + \text{Tr } F_{\text{ASD}}^2. \quad (4.34)$$

It is trivial to identify these two four-dimensional components of the colour-ordered form factor:

$$\begin{aligned} F_{\mathcal{O}_2}^{(0)}(1^+, 2^+; q) &= 2[12][21], \\ F_{\mathcal{O}_2}^{(0)}(1^-, 2^-; q) &= 2\langle 12 \rangle \langle 21 \rangle. \end{aligned} \quad (4.35)$$

On the other hand, the six-dimensional form factor is

$$F_{\mathcal{O}_2}^{(0)}(1_{a\dot{a}}, 2_{b\dot{b}}; q) = 2\langle 1_a 2_{\dot{b}} \rangle \langle 2_b 1_{\dot{a}} \rangle, \quad (4.36)$$

⁸To clarify the abuse of nomenclature, the quantity is the field strength in momentum space corresponding to a polarisation vector of given helicity.

⁹We could have used as definition the following: $F_{\text{SD},\alpha\dot{\alpha}\beta\dot{\beta}} := p_{\alpha\dot{\alpha}} \epsilon_{\beta\dot{\beta}}^- - p_{\beta\dot{\beta}} \epsilon_{\alpha\dot{\alpha}}^- = -\sqrt{2} \lambda_\alpha \lambda_\beta \epsilon_{\dot{\alpha}\dot{\beta}}$. As we can see the only difference is a $-\sqrt{2}$ normalisation factor.

¹⁰ $A, B, \dots = 1, \dots, 4$ are indices in the (anti)fundamental representation of $\text{SU}^*(4)$ and a, \dot{a} are indices of the six-dimensional little group (for a detailed discussion see Appendix A.2).

where the definitions of the spinor brackets, in both four and six dimensions, and the conventions adopted can be found in Appendices A.1 and A.2. Using the particular embedding of the four-dimensional into the six-dimensional space introduced in Appendix A.2 we find that¹¹

$$F_{\mathcal{O}_2}^{(0)}(1_{1i}, 2_{1i}; q) \Big|_{4D} = F_{\mathcal{O}_2}^{(0)}(1^+, 2^+; q), \quad F_{\mathcal{O}_2}^{(0)}(1_{2j}, 2_{2j}; q) \Big|_{4D} = F_{\mathcal{O}_2}^{(0)}(1^-, 2^-; q). \quad (4.37)$$

An analogous statement is true also for tree-level amplitudes, where all the four-dimensional helicity configurations can be recovered from the six-dimensional amplitude.¹²

The scalar form factor is obtained from (4.8), and we find

$$F_{\mathcal{O}_{2,s}}^{(0)}(1, 2; q) = -\langle 1_a, 2_b \rangle \langle 1^a, 2^b \rangle = 2s_{12}, \quad (4.38)$$

where

$$\mathcal{O}_{2,s} \propto (D\phi)^2 := D_\mu \phi^a D^\mu \phi^a. \quad (4.39)$$

The normalisation of (4.38) has been fixed by matching the four-dimensional limit of this operator with that of the scalar components of (4.36) (*i.e.* reducing first to four dimensions and selecting the helicity components $(1, \hat{2})$ or $(2, \hat{1})$), which must yield the same result. An equivalent prescription would be computing the minimal form factors of the two operators with the relative normalisation fixed by the Lagrangian (4.8). But the four-dimensional matching prescription is faster for more complex operators.

It is also important to stress that it would not be possible to implement the scalar subtraction just by excluding the little group components that in four dimensions behave like scalars. Indeed, this would bring us to a result which is not invariant under a little group transformation of the internal (six-dimensional) legs. In particular, for the subtraction we need a quantity that behaves as a scalar in six dimensions and matches the scalar components of the dimensional-reduced gluon in four dimensions, as shown in Appendix C.1.

Using BFCW recursion relation [21, 22] in six dimensions [30] we have derived the six-dimensional non-minimal form factors with three external legs at tree level, both for the gluon and the scalar operators. The results for \mathcal{O}_2 with three gluons reads

$$\begin{aligned} F_{\mathcal{O}_2}^{(0)}(1_{a\hat{a}}, 2_{b\hat{b}}, 3_{c\hat{c}}; q) &= \frac{2}{s_{23}s_{31}} \langle 1_a 2_b \rangle \langle 2_b 1_{\hat{a}} \rangle \langle 3_c | \not{p}_1 \not{p}_2 | 3_{\hat{c}} \rangle + \text{cyclic} \\ &+ 2 \left(\frac{1}{s_{12}} + \frac{1}{s_{23}} + \frac{1}{s_{31}} \right) (\langle 1_a 2_b \rangle \langle 2_b 3_{\hat{c}} \rangle \langle 3_c 1_{\hat{a}} \rangle - [1_{\hat{a}} 2_b] [2_b 3_c] [3_c 1_a]), \end{aligned} \quad (4.40)$$

which agrees with the analogous result computed from Feynman diagrams in [254], upon some algebraic manipulation. As a further consistency check we verified that in the four-dimensional limit the different helicity components match the results of [269].

Furthermore, as it will be clear from the discussion in the next section, in the scalar subtraction we need to take into account both the form factor of the operator \mathcal{O}_2 with two external scalars and one gluon, which is different from zero:

$$F_{\mathcal{O}_2}^{(0)}(1, 2, 3_{c\hat{c}}; q) = -\frac{2}{s_{12}} \langle 3_c | \not{p}_1 \not{p}_2 | 3_{\hat{c}} \rangle, \quad (4.41)$$

¹¹Four-dimensional limit here means choosing appropriate little-group indices corresponding to the desired helicity configuration in four dimensions, and the taking $m_i, \hat{m}_i \rightarrow 0$ for any particle i .

¹²Further details on the relation between four and six-dimensional tree-level quantities can be found in Appendix C.1.

and the non-minimal scalar form factor of $\mathcal{O}_{2,s}$:

$$F_{\mathcal{O}_{2,s}}^{(0)}(1, 2, 3_{c\dot{c}}; q) = -\frac{2q^2}{s_{23}s_{31}} \langle 3_c | \not{p}_1 \not{p}_2 | 3_{\dot{c}} \rangle . \quad (4.42)$$

For a detailed derivation of (4.40)-(4.42) see Appendix C.1.1. The sum of (4.41) and (4.42) agrees with the result of [254].

4.2.2 $\text{Tr } F^3$ Form Factors

Consider now the operator

$$\mathcal{O}_3 := \text{Tr } F^\mu{}_\nu F^\nu{}_\rho F^\rho{}_\mu . \quad (4.43)$$

Similarly to the case of $\text{Tr } F^2$, this operator splits, in four dimensions, into a self-dual and anti-self dual part

$$\mathcal{O}_3 := \text{Tr } F^3 = \text{Tr } F_{\text{SD}}^3 + \text{Tr } F_{\text{ASD}}^3 . \quad (4.44)$$

Consequently, the only possible helicity configurations of the minimal tree-level form factors are all-plus and all-minus:

$$\begin{aligned} F_{\mathcal{O}_3}^{(0)}(1^+, 2^+, 3^+; q) &= -2[12][23][31] , \\ F_{\mathcal{O}_3}^{(0)}(1^-, 2^-, 3^-; q) &= 2\langle 12 \rangle \langle 23 \rangle \langle 31 \rangle . \end{aligned} \quad (4.45)$$

In six dimensions the minimal form factor is given by

$$\begin{aligned} F_{\mathcal{O}_3}^{(0)}(1_{a\dot{a}}, 2_{b\dot{b}}, 3_{c\dot{c}}) &= F_{1_{a\dot{a}} CD}^{AB} F_{2_{b\dot{b}} EF}^{CD} F_{3_{c\dot{c}} AB}^{EF} \\ &= -\langle 1_a 2_{\dot{b}} \rangle \langle 2_b 3_{\dot{c}} \rangle \langle 3_c 1_{\dot{a}} \rangle + [1_{\dot{a}} 2_b] [2_{\dot{b}} 3_c] [3_{\dot{c}} 1_a] , \end{aligned} \quad (4.46)$$

where $F_{a\dot{a}}^{AB}{}_{CD}$ is defined in (4.31). From (4.11), we find the scalar operator associated to the scalar subtraction:

$$\mathcal{O}_{3,s} \propto \text{Tr}(D\phi)^2 F := \text{Tr } D_\mu \phi D_\nu \phi F^{\mu\nu} , \quad (4.47)$$

and

$$F_{\mathcal{O}_{3,s}}^{(0)}(1, 2, 3_{c\dot{c}}) := \frac{1}{2} p_1^{AB} p_{2CD} F_{3_{c\dot{c}}}^{CD}{}_{AB} = \langle 3_c | \not{p}_1 \not{p}_2 | 3_{\dot{c}} \rangle , \quad (4.48)$$

where, once again, the normalisation is fixed by matching the four-dimensional limits of this quantity with the scalar configuration of (4.46).

As a final remark, we point out that \mathcal{O}_3 is not the only mass-dimension six operator which appears in the Yang-Mills theories (also with matter). One also has a contribution from

$$\tilde{\mathcal{O}}_3 := D^\alpha F^{a\mu\nu} D_\alpha F_{\mu\nu}^a . \quad (4.49)$$

However, it is easy to see that the minimal form factor for $\tilde{\mathcal{O}}_3$ can be related to the one of \mathcal{O}_2 as

$$F_{\tilde{\mathcal{O}}_3}^{(0)}(1_{a\dot{a}}, 2_{b\dot{b}}; q) = s_{12} F_{\mathcal{O}_2}^{(0)}(1_{a\dot{a}}, 2_{b\dot{b}}; q) . \quad (4.50)$$

It can be shown that any other contraction for operators built from two covariant derivatives and two field strength, such as $D^\mu F_{\mu\nu}^{a\rho} D^\rho F_{\rho\nu}^a$, are not independent and can be expressed in terms of $\tilde{\mathcal{O}}_3$ up to a normalisation factor. Moreover, we must highlight

that $\tilde{\mathcal{O}}_3$ itself must not be regarded as an independent operator. Indeed, as explained in the introduction of this chapter, the study of this form factors may be relevant in the context of the effective field theory as correction to the jet production through Higgs decay in the Standard Model. Then, the form factor can be thought as the correction to the $h + \text{jets}$ amplitude due to the irrelevant deformation $h\tilde{\mathcal{O}}_3$ and we notice that $s_{12} = q^2 = m_h^2$, in (4.50). Then, from the Lagrangian point of view, it exists a field redefinition which maps $h\tilde{\mathcal{O}}_3$ to $m_h^2 h\mathcal{O}_2$ at leading order in the irrelevant deformation. For a detailed discussion on this point from an off-shell point of view using equation of motion, see [296].

Finally, we provide the tree-level expressions needed for the one-loop computation of the non-minimal form factor of \mathcal{O}_3 which are:

- the non-minimal tree-level form factor of \mathcal{O}_3 with four gluons

$$F_{\mathcal{O}_3}^{(0)}(1_{a\dot{a}}, 2_{b\dot{b}}, 3_{c\dot{c}}, 4_{d\dot{d}}; q) = \mathcal{B}_{a\dot{a}b\dot{b}c\dot{c}d\dot{d}} + \mathcal{C}_{a\dot{a}b\dot{b}c\dot{c}d\dot{d}} + \mathcal{D}_{a\dot{a}b\dot{b}c\dot{c}d\dot{d}}, \quad (4.51)$$

with

$$\begin{aligned} \mathcal{B}_{a\dot{a}b\dot{b}c\dot{c}d\dot{d}} &= (-\langle 1_a 2_b \rangle \langle 2_b 3_c \rangle \langle 3_c 1_a \rangle + [1_{\dot{a}} 2_{\dot{b}}] [2_{\dot{b}} 3_{\dot{c}}] [3_{\dot{c}} 1_{\dot{a}}]) \frac{\langle 4_d | \not{p}_1 \not{p}_3 | 4_d \rangle}{s_{34}s_{41}} + \text{cyclic}, \\ \mathcal{C}_{a\dot{a}b\dot{b}c\dot{c}d\dot{d}} &= \frac{\langle 1_a 2_b \rangle \langle 2_b 4_d \rangle \langle 4_d 3_c \rangle \langle 3_c 1_a \rangle + [1_{\dot{a}} 2_{\dot{b}}] [2_{\dot{b}} 4_{\dot{d}}] [4_{\dot{d}} 3_{\dot{c}}] [3_{\dot{c}} 1_{\dot{a}}]}{s_{34}} + \text{cyclic}, \\ \mathcal{D}_{a\dot{a}b\dot{b}c\dot{c}d\dot{d}} &= - \left(\sum_{i=1}^4 \frac{1}{s_{ii+1}} \right) (\langle 1_a 2_b \rangle \langle 2_b 3_c \rangle \langle 3_c 4_d \rangle \langle 4_d 1_a \rangle + [1_{\dot{a}} 2_{\dot{b}}] [2_{\dot{b}} 3_{\dot{c}}] [3_{\dot{c}} 4_{\dot{d}}] [4_{\dot{d}} 1_{\dot{a}}]) \end{aligned} \quad (4.52)$$

- the non-minimal tree-level form factor of \mathcal{O}_3 with two external scalars

$$F_{\mathcal{O}_3}^{(0)}(1, 2, 3_{c\dot{c}}, 4_{d\dot{d}}; q) = \frac{1}{s_{12}} \left(\langle 3_c 4_d \rangle \langle 4_d | \not{p}_1 \not{p}_2 | 3_c \rangle - \langle 4_d 3_c \rangle \langle 3_c | \not{p}_1 \not{p}_2 | 4_d \rangle \right) \quad (4.53)$$

- the non-minimal tree-level form factor of $\mathcal{O}_{3,s}$ with two external scalars

$$\begin{aligned} F_{\mathcal{O}_{3,s}}^{(0)}(1, 2, 3_{c\dot{c}}, 4_{d\dot{d}}; q) &= \frac{\langle 3_c | \not{p}_4 \not{p}_2 | 3_c \rangle \langle 4_d | \not{p}_1 \not{p}_2 | 4_d \rangle}{s_{23}s_{34}} + \frac{\langle 4_d | \not{p}_1 \not{p}_3 | 4_d \rangle \langle 3_c | \not{p}_1 \not{p}_2 | 3_c \rangle}{s_{34}s_{41}} \\ &+ \langle 3_c | \not{p}_2 \not{p}_1 | 4_d \rangle \langle 4_d 3_c \rangle \left(\frac{1}{s_{34}} + \frac{1}{s_{23}} + \frac{1}{s_{41}} \right) \\ &- \langle 4_d | \not{p}_2 \not{p}_1 | 3_c \rangle \langle 3_c 4_d \rangle \frac{1}{s_{34}} + \langle 3_c | \not{p}_2 | 4_d \rangle [3_c | \not{p}_1 | 4_d] \left(\frac{1}{s_{23}} + \frac{1}{s_{41}} \right). \end{aligned} \quad (4.54)$$

These formulas have been obtained generating an ansatz similar to the one presented in (3.20) and by requiring the six-dimensional form factor to match, upon taking the four-dimensional limit, the known four-dimensional expressions in different helicity configurations [266, 273, 297, 298]. The resulting ansatz was then numerically compared with the results from Feynman diagrams and a complete match was found.

A rather surprising fact is that the result obtained from the six-dimensional generalisation of the BCFW recursion relations precisely matches this expression as well. This is quite remarkable because the two-line shift does not reproduce the correct result for $\text{Tr } F^3$ amplitudes with generic helicity configurations in four-dimensions [25, 298]. In particular, the all-plus (and all-minus) configuration cannot be obtained correctly with a two-line shift. While it exists a specific BCFW-shift which reproduces the single-minus (and single-plus) helicity configuration. The origin of this might be the *helicity-averaging* introduced by the tensor $X^{a\dot{a}}$ in equation (C.15), which “select” the best large- z behaviour, cancelling any pole at infinity. Such observation deserves a more detailed analysis.

4.2.3 $\text{Tr } F^4$ and Higher Dimensional Form Factors

The fourth power in the field strength can be considered as a turning point in the general behaviour of the operators, for reasons which will become clear in a moment. The renormalisation properties of gluonic operators of dimension up to eight was carried out in [299], and more recently in [104, 300]. It turns out that we can have four possible independent (single-trace) operators involving different contractions of four field strengths in d -dimensions:

$$\begin{aligned} \text{Tr } F^\mu{}_\nu F^\nu{}_\rho F^\rho{}_\sigma F^\sigma{}_\mu, & \quad \text{Tr } F^{\mu\nu} F_{\mu\nu} F^{\rho\sigma} F_{\rho\sigma}, \\ \text{Tr } F^\mu{}_\nu F^\rho{}_\sigma F^\nu{}_\rho F^\sigma{}_\mu, & \quad \text{Tr } F^{\mu\nu} F^{\rho\sigma} F_{\mu\nu} F_{\rho\sigma}. \end{aligned} \quad (4.55)$$

In pure gauge theories, which we are considering in this work, all these operators can appear with independent coefficients, while they are no more independent in the low energy effective action from the superstring theory [301–303]. In this section we will focus only on the first operator, which we will refer to as $\text{Tr } F^4$:

$$\mathcal{O}_4 := \text{Tr } F^4 := \text{Tr } F^\mu{}_\nu F^\nu{}_\rho F^\rho{}_\sigma F^\sigma{}_\mu. \quad (4.56)$$

This encloses all the main features of the operators with higher powers in the field strength, and at the end of this section we will be able to generalise some results to a peculiar operator involving a consecutive chain of n field strengths.

In four dimensions the main difference between $\text{Tr } F^4$ and the lower-power cases is that the structure of this operator allows the mixing of the self- and anti-self-dual components, *i.e.* schematically

$$\text{Tr } F^4 \simeq \text{Tr } F_{\text{SD}}^4 + \text{Tr} (F_{\text{SD}}^2 F_{\text{ASD}}^2) + \text{Tr } F_{\text{ASD}}^4. \quad (4.57)$$

Thus the usual all-plus (all-minus) minimal form factors appear along with MHV-like quantities:

$$\begin{aligned} F_{\mathcal{O}_4}^{(0)}(1^+, 2^+, 3^+, 4^+; q) &= 2[12][23][34][41], \\ F_{\mathcal{O}_4}^{(0)}(1^+, 2^+, 3^-, 4^-; q) &= [12]^2 \langle 34 \rangle^2, \\ F_{\mathcal{O}_4}^{(0)}(1^+, 2^-, 3^+, 4^-; q) &= [13]^2 \langle 24 \rangle^2, \end{aligned} \quad (4.58)$$

and all the other configurations can be obtained by symmetry and parity arguments.

In six dimensions the minimal form factor is

$$\begin{aligned}
F_{\mathcal{O}_4}^{(0)}(1_{a\dot{a}}, 2_{b\dot{b}}, 3_{c\dot{c}}, 4_{d\dot{d}}; q) &= F_{1a\dot{a}}^{AB} F_{2b\dot{b}}^{CD} F_{3c\dot{c}}^{EF} F_{4d\dot{d}}^{GH} F_{AB} \\
&= \langle 1_a 2_{\dot{b}} \rangle \langle 2_b 3_{\dot{c}} \rangle \langle 3_c 4_{\dot{d}} \rangle \langle 4_d 1_{\dot{a}} \rangle + [1_{\dot{a}} 2_b] [2_{\dot{b}} 3_c] [3_{\dot{c}} 4_d] [4_{\dot{d}} 1_a] \\
&\quad + \langle 1_a 2_b 3_c 4_d \rangle [1_{\dot{a}} 2_{\dot{b}} 3_{\dot{c}} 4_{\dot{d}}] ,
\end{aligned} \tag{4.59}$$

where we notice that at this power of the field strength the new structure $\langle \dots \rangle [\dots]$ involving four-spinor invariants appears, which is very reminiscent of the four-point amplitude, in (C.1). This new structure gives us the MHV-like components in (4.58) when we consider the appropriate little-group configurations in the four-dimensional limit (see Appendix C.1).

We have already identified the scalar operator associated to $\text{Tr } F^4$ in (4.12) and we define

$$\mathcal{O}_{4,s} \propto \text{Tr } D_\mu \phi D_\nu \phi F^\nu{}_\rho F^{\rho\mu} \tag{4.60}$$

such that its minimal form factor is

$$\begin{aligned}
F_{\mathcal{O}_{4,s}}(1, 2, 3_{c\dot{c}}, 4_{d\dot{d}}; q) &= \frac{1}{2} p_1^{AB} p_{2CD} F_{3c\dot{c}}^{CD} F_{4d\dot{d}}^{EF} F_{AB} \\
&= -\langle 3_c | \not{p}_2 \not{p}_1 | 4_{\dot{d}} \rangle \langle 4_d 3_{\dot{c}} \rangle + \frac{1}{4} \langle 2^a 2_a 3_c 4_d \rangle [1_{\dot{a}} 1^{\dot{a}} 3_{\dot{c}} 4_{\dot{d}}] .
\end{aligned} \tag{4.61}$$

The expression of $\text{Tr } F^4$ gives us some insight about the operators involving the n^{th} power of the field strength, where the Lorentz indices are contracted between adjacent field strengths, which we will refer to as $\text{Tr } F^n$:

$$\mathcal{O}_n := \text{Tr } F^n = \text{Tr } F_{\mu_1}{}^{\mu_2} F_{\mu_2}{}^{\mu_3} \dots F_{\mu_{n-1}}{}^{\mu_n} F_{\mu_n}{}^{\mu_1} . \tag{4.62}$$

It is easy to show that this operator can be decomposed in a sum of double traces (in the Lorentz indices) on the self-dual and anti-self-dual parts, schematically¹³:

$$\text{Tr } F^n \simeq \sum_{i=0}^n \text{Tr} (F_{\text{SD}}^{n-i} F_{\text{ASD}}^i) . \tag{4.63}$$

Take two disjoint and ordered subsets of labels $S_+ = \{p_k\}_{k=1\dots i}$ and $S_- = \{q_k\}_{k=1\dots n-i}$, with $S_+ \cup S_- = \{1, \dots, n\}$. Then all tree-level minimal form factors, for any helicity configuration, can be written in a very compact way:

$$F_{\mathcal{O}_n}^{(0)}(1^{h_1}, \dots, n^{h_n}; q) = c_{n,i} \prod_{k=1}^i [p_k p_{k+1}] \prod_{k=i+1}^n \langle q_k q_{k+1} \rangle , \tag{4.64}$$

where the overall coefficient is

$$c_{n,i} = \begin{cases} 2 & i = 0 \\ (-1)^{n-i} & i \neq 0, n . \\ (-)^{n2} & i = n \end{cases} \tag{4.65}$$

¹³We stress that this general structure was hidden by lower power-operators because the field strength is traceless: $\text{Tr } F_{\text{SD}}^{n-1} F_{\text{ASD}} = \text{Tr } F_{\text{SD}} F_{\text{ASD}}^{n-1} = 0$.

An explicit example of this general formula is given by

$$F_{\mathcal{O}_5}^{(0)}(1^-, 2^+, 3^-, 4^-, 5^+; q) = -\langle 13 \rangle \langle 34 \rangle \langle 41 \rangle [25] [52] . \quad (4.66)$$

The structure of $\text{Tr } F^n$ form factors in six dimensions is much more complicated than the four-dimensional one, the number of terms grows very fast, but nonetheless some general pattern can be observed. In particular if we restrict to a kinematic configuration for which only some of the legs are truly six dimensional and the others are defined on the embedded four-dimensional subspace, the formulae are much easier and compact. In principle, this is all we need in order to calculate rational terms with the dimensional reconstruction technique, since we need to consider only the limited number of internal loop legs as six dimensional. As an example, consider the minimal form factor of $\text{Tr } F^n$ with two six-dimensional legs and $n - 2$ four-dimensional legs in the all-plus helicity configuration. The general expression is given by

$$\begin{aligned} \text{Tr } F^n(1_{a\dot{a}}, 2_{b\dot{b}}, 3^+, \dots, n^+) = & (\langle 1_a 2_{\dot{b}} \rangle \langle 2_b 3_{\dot{1}} \rangle [34] \langle n_1 1_{\dot{a}} \rangle + [1_{\dot{a}} 2_b] \langle 2_{\dot{b}} 3_1 \rangle [34] [n_1 1_a] + \\ & + \langle 1_a 2_b n_1 3_1 \rangle [1_{\dot{a}} 2_{\dot{b}} 3_{\dot{1}} 4_{\dot{1}}]) \prod_{i=4}^{n-1} [ii + 1] . \end{aligned} \quad (4.67)$$

This result can be found by observing that the combination $\lambda_{i\dot{a}}^A \tilde{\lambda}_{iB\dot{a}}$ appears only once for each six-dimensional leg, which allows to write an ansatz comprising every possible combination with arbitrary coefficients to be fixed. The coefficients can then be determined by taking the four-dimensional limit of the six-dimensional gluons and requiring the form factor to match (4.64).

4.3 One-Loop Form Factors

In this section we will consider a number of one-loop applications of the dimensional reconstruction procedure discussed in Section 4.1. The results obtained for the minimal form factors of $\text{Tr } F^2$ and $\text{Tr } F^3$ were already known in the literature. We show that the latter has no rational terms, as it has also been argued by [266]. These calculations will be useful to set the stage and give an example of the procedure before dealing with more involved operators and kinematic configurations. In particular, we reproduce the known non-minimal form factor of $\text{Tr } F^2$ with three positive-helicity external gluons. Finally, we compute the complete minimal form factor of $\text{Tr } F^n$ with $n = 4$ at one loop and generalise some of the results to arbitrary n .

4.3.1 The Minimal $\text{Tr } F^2$ Form Factors

As a first proof of concept of the method we will confirm the well known statement that the minimal form factor of the operator $\text{Tr } F^2$ in pure Yang-Mills does not have any rational terms. In particular, we will consider the all-plus helicity configuration.

The quantity we want to compute can be written as

$$\begin{aligned} F_{\mathcal{O}_2}^{(1)}(1^+, 2^+; q) & := F_{\mathcal{O}_2}^{(0)}(1^+, 2^+; q) \cdot f^{(2)}(s_{12}) \\ & = 2[12][21] \cdot f^{(2)}(s_{12}) , \end{aligned} \quad (4.68)$$

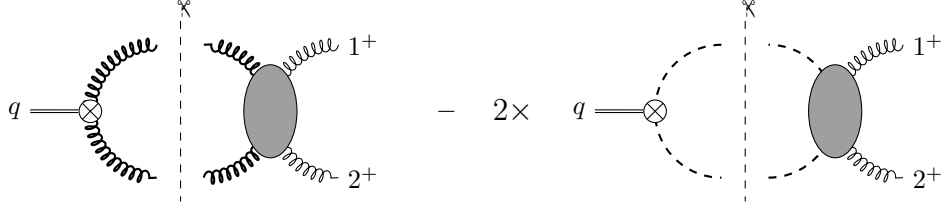


Figure 4.3: Two-particle cut of the one-loop form factor $\text{Tr } F^2$ in six dimensions.

where we factored out all the helicity dependence in the tree-level prefactor, and $f^{(2)}(s_{12})$ is a function only of the Mandelstam variable s_{12} . As explained in Section 4.1 this quantity can be computed using (4.9):

$$f^{(2)}(s_{12}) = f_{6\text{D}}^{(2)}(s_{12}) - 2f_{\phi}^{(2)}(s_{12}) , \quad (4.69)$$

where $f_{6\text{D}}^{(2)}(s_{12})$ and $f_{\phi}^{(2)}(s_{12})$ are the form factors with six-dimensional internal gluons or scalars respectively, normalised by the corresponding tree-level quantity.

At one loop, the two-particle cut represented in Figure 4.3 is¹⁴

$$f_{6\text{D}}^{(2)}(s_{12}) \Big|_{2\text{-cut}} = \frac{1}{2[12][21]} \int \text{dLIPS } F_{\mathcal{O}_2}^{(0)}(-l_1^{a\dot{a}}, -l_2^{b\dot{b}}) \mathcal{A}_g^{(0)}(l_2^{b\dot{b}}, l_1^{a\dot{a}}, 1_{1i}, 2_{2\dot{j}}) . \quad (4.70)$$

In order to simplify this expression we decompose the six-dimensional quantities in terms of four-dimensional ones, as explained in detail in Appendix A.2. These calculations are rather lengthy and we have devised a `MATHEMATICA` package to deal with them. Imposing that the external legs are defined in four dimensions is equivalent to setting $m_j = 0$ and $\tilde{m}_j = 0$ for $j = 1, 2$, which automatically removes any dependence of $f^{(2)}$ on $\mu_{j\alpha}$ and $\tilde{\mu}_{j\dot{\alpha}}$. From (A.39), momentum conservation implies

$$\sum_i m_i = 0 , \quad \sum_i \tilde{m}_i = 0 . \quad (4.71)$$

Only the two internal legs l_1 and l_2 have to be kept in six dimensions, in other words $p_i^5, p_i^6 \neq 0$ for $i = l_1, l_2$, which implies

$$m_{l_2} = -m_{l_1} := -m , \quad \tilde{m}_{l_2} = -\tilde{m}_{l_1} := -\tilde{m} , \quad (4.72)$$

where

$$\mu^2 = m\tilde{m} , \quad (4.73)$$

with μ^2 defined in (4.4). We immediately arrive at

$$f_{6\text{D}}^{(2)}(s_{12}) \Big|_{2\text{-cut}} = \int \text{dLIPS} \left(-i \frac{s_{12}}{s_{2l_2}} + 2i \frac{\mu^2}{s_{2l_2}} \right) . \quad (4.74)$$

Next we repeat a similar computation for the two-particle cut with internal gluons replaced by scalars:

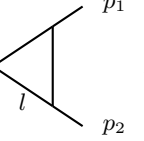
$$\begin{aligned} f_{\phi}^{(2)}(s_{12}) \Big|_{2\text{-cut}} &= \frac{1}{2[12][21]} \int \text{dLIPS } F_{\mathcal{O}_{2,s}}^{(0)}(-l_1, -l_2) \mathcal{A}^{(0)}(l_2, l_1, 1_{a\dot{a}}, 2_{b\dot{b}}) \\ &= \int \text{dLIPS } i \frac{\mu^2}{s_{2l_2}} . \end{aligned} \quad (4.75)$$

¹⁴The explicit expression of \mathcal{A}_g can be found in Appendix C.1.

Taking the difference between (4.74) and twice (4.75) leads to the desired four-dimensional result

$$f^{(2)}(s_{12})|_{2\text{-cut}} = -is_{12} \int \text{dLIPS} \frac{1}{s_{2l_2}}. \quad (4.76)$$

We can directly read off the one-loop result from (4.76):

$$f^{(2)}(s_{12}) = -is_{12} \cdot q \text{ (triangle diagram)} . \quad (4.77)$$


In this section we are only interested in showing that our method correctly computes those terms which are not captured by four-dimensional unitarity techniques. Then, we will always show the result in terms of the integral basis, rather than the integrated result. The triangle integral with outgoing momenta (p_1, p_2, q) is defined in Appendix D.

As anticipated, our result (4.77) does not contain any μ^2 term *i.e.* any rational term, and is thus in agreement with the very well known result. An equivalent result holds for the all-minus helicity configuration. As expected, there are no bubbles in the result, because both $\text{Tr } F_{\text{SD}}^2$ and $\text{Tr } F_{\text{ASD}}^2$ are protected operators in $\mathcal{N} = 4$ super-Yang-Mills and the form factor does not depend on the extra particle content of the theory.

4.3.2 The Non-Minimal $\text{Tr } F^2$ Form Factor

In this section we address the computation of the one-loop non-minimal form factor of the operator $\text{Tr } F^2$. As usual we begin by defining the normalised quantity $f^{(2;3)}$ as

$$F_{\mathcal{O}_2}^{(1)}(1^+, 2^+, 3^+; q) := 2[12][23][31] \cdot f^{(2;3)}(s_{12}, s_{23}, s_{13}), \quad (4.78)$$

with

$$f^{(2;3)}(s_{12}, s_{23}, s_{13}) = f_{6\text{D}}^{(2;3)}(s_{12}, s_{23}, s_{13}) - 2f_{\phi}^{(2;3)}(s_{12}, s_{23}, s_{13}), \quad (4.79)$$

Notice that we decided not to normalise by the corresponding tree-level form-factor, which carries additional non-trivial dependence on the Mandelstam variables, but simply by a factor $[12][23][31]$ which only captures the complete helicity dependence of the operator. Computing the discontinuity in the s_{12} -channel we have

$$f_{6\text{D}}^{(3)}(\{s_{ij}\})|_{s_{12}\text{-cut}} = \frac{1}{2[12][23][31]} \int \text{dLIPS} F_{\mathcal{O}_2}^{(0)}(l_1^{a\dot{a}}, l_2^{b\dot{b}}, 3_{11}) \mathcal{A}^{(0)}(-l_2^{a\dot{a}}, -l_1^{b\dot{b}}, 1_{11}, 2_{22}), \quad (4.80)$$

which, upon algebraic manipulations, becomes

$$f_{6\text{D}}^{(2;3)}(s_{12}, s_{23}, s_{13})|_{s_{12}\text{-cut}} = i \frac{[12]}{[23][31]} \int \text{dLIPS} [3] l_1^{(4)} l_2^{(4)} [3] \mathcal{I}_{6\text{D}}^{(2;3)}, \quad (4.81)$$

with

$$\mathcal{I}_{6\text{D}}^{(2;3)} = \frac{q^4 s_{12} - 2\mu^2 q^2 s_{12} - 4\mu^2 s_{3l_1} s_{3l_2}}{s_{12}^2 s_{2,-l_2} s_{3l_1} s_{3l_2}}. \quad (4.82)$$

Performing the appropriate scalar subtraction for the non-minimal configuration of the operator $\text{Tr } F^2$ is more subtle than in the minimal case. The double cut one needs to compute is represented in Figure 4.4. There are two different tree-level form factors

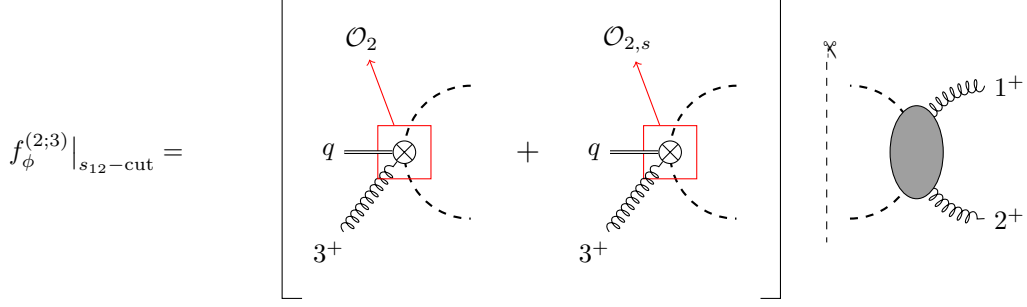


Figure 4.4: A double cut of the scalar contribution to $\text{Tr } F^2$ non-minimal. The red boxes highlight the two different operator insertions.

to be inserted into the cut: the non-minimal form factors with two external scalars and one gluon of the operators $\text{Tr } F^2$ and $(D\phi)^2$. The tree-level expression for these form factors are given in (4.41) and (4.42) respectively. Computing the complete result for the double-cut of the scalar contribution leads to

$$f_\phi^{(2;3)}(s_{12}, s_{23}, s_{13})|_{s_{12}\text{-cut}} = i \frac{[12]}{[23][31]} \int \text{dLIPS} [3|l_1^{(4)} l_2^{(4)}|3] \mathcal{I}_\phi^{(2;3)}, \quad (4.83)$$

with

$$\mathcal{I}_\phi^{(2;3)} = -\mu^2 \frac{q^2 s_{12} + s_{3l_1} s_{3l_2}}{s_{12}^2 s_{2,-l_2} s_{3l_1} s_{3l_2}}. \quad (4.84)$$

Upon subtracting twice (4.83) from (4.81), uplifting the cut and performing some algebraic manipulations on the numerator, one ends up with the final expression:

$$\begin{aligned} f^{(2,3)}(s_{12}, s_{23}, s_{13})|_{s_{12}\text{-disc}} = & - \frac{iq^4}{2s_{31}} \begin{array}{c} q \quad p_1 \\ \diagup \quad \diagdown \\ p_3 \quad p_2 \end{array} - \frac{iq^4}{2s_{23}} \begin{array}{c} q \quad p_3 \\ \diagup \quad \diagdown \\ p_2 \quad p_1 \end{array} \\ & - \frac{iq^4(s_{31}+s_{23})}{s_{12}s_{23}s_{31}} \cdot \left(q \begin{array}{c} p_1 \\ \diagup \quad \diagdown \\ p_2 \quad p_3 \end{array} + q \begin{array}{c} p_3 \\ \diagup \quad \diagdown \\ p_1 \quad p_2 \end{array} \right) \\ & + \frac{4i}{s_{12}^2} \cdot q \begin{array}{c} p_1 \\ \diagup \quad \diagdown \\ \mu^2 \quad p_2 \end{array} + \frac{2i}{s_{12}} \cdot q \begin{array}{c} p_1 \\ \diagup \quad \diagdown \\ \mu^2 \quad p_2 \end{array} \end{aligned} \quad (4.85)$$

where all integrals can be found in Appendix D.

Clearly the double cuts in the channels s_{23} and s_{13} can be derived from (4.85) by symmetry arguments, thus the only invariant channel left to compute would be s_{123} , see Figure 4.5. This double-cut involves the use of the five-point amplitudes in six dimensions with five gluons as well as with three gluons and two scalars¹⁵, combined

¹⁵Their analytic expression is given in Appendix C.1.

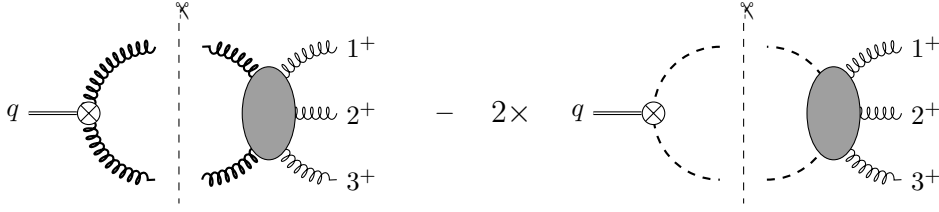


Figure 4.5: Two-particle cut of the one-loop form factor $\text{Tr } F^2$ in the s_{123} channel in six dimensions.

with the minimal form factor of \mathcal{O}_2 and $\mathcal{O}_{2,s}$ respectively. The only topology probed by this cut, which is not probed by any of the previous cuts, is the bubble with the form factor in one of the two vertices and all the momenta in the other. Performing the calculation, the associated coefficient turns out to be zero. Thus (4.85) and its permutations give the complete result, which matches the one given in [254, 304].

4.3.3 The Minimal $\text{Tr } F^3$ Form Factors

We now consider the $\text{Tr } F^3$ form factor in the all-plus helicity configuration. The procedure we follow is exactly the same as in the $\text{Tr } F^2$ case. First we factor out the helicity dependence as an overall tree-level prefactor:

$$\begin{aligned} F_{\mathcal{O}_3}^{(1)}(1^+, 2^+, 3^+; q) &:= F_{\mathcal{O}_3}^{(0)}(1^+, 2^+, 3^+; q) \cdot f^{(3)}(s_{12}, s_{23}, s_{13}) \\ &= -2[12][23][31] \cdot f^{(3)}(s_{12}, s_{23}, s_{13}), \end{aligned} \quad (4.86)$$

then we compute $f^{(3)}$ as the difference $f_{6D}^{(3)} - 2f_\phi^{(3)}$. We start with the two-particle cut in the s_{12} channel represented in Figure 4.6, which reads

$$\begin{aligned} f_{6D}^{(3)}(s_{12}) \Big|_{s_{12}\text{-cut}} &= -\frac{1}{2[12][23][31]} \int \text{dLIPS } F_{\mathcal{O}_3}^{(0)}(-l_1^{a\dot{a}}, -l_2^{b\dot{b}}, 3_{1i}) \mathcal{A}^{(0)}(l_2 a\dot{a}, l_1 b\dot{b}, 1_{1i}, 2_{2\dot{2}}) \\ &= i \int \text{dLIPS} \left(\frac{[12][3] \not{l}_1^{(4)} \not{l}_2^{(4)} |3\rangle}{s_{2l_2} [23][31]} + \mu^2 \frac{[3] \not{l}_1^{(4)} \not{l}_2^{(4)} |3\rangle}{[3] \not{p}_1 \not{p}_2 |3\rangle} \right). \end{aligned} \quad (4.87)$$

Computing the scalar contribution in a similar fashion leads to

$$f_\phi^{(3)}(s_{12}, s_{23}, s_{13}) \Big|_{s_{12}\text{-cut}} = \frac{i}{2} \int \text{dLIPS } \mu^2 \frac{[3] \not{l}_1^{(4)} \not{l}_2^{(4)} |3\rangle}{[3] \not{p}_1 \not{p}_2 |3\rangle}, \quad (4.88)$$

and finally

$$f^{(3)}(s_{12}, s_{23}, s_{13}) \Big|_{s_{12}\text{-cut}} = i \frac{[12]}{[23][31]} \int \text{dLIPS} \frac{[3] \not{l}_1^{(4)} \not{l}_2^{(4)} |3\rangle}{s_{2l_2}}. \quad (4.89)$$

Then, it is possible to write $f^{(3)}$ in terms of Mandelstam invariants:

$$f^{(3)}(s_{12}, s_{23}, s_{13}) \Big|_{s_{12}\text{-cut}} = -i \int \text{dLIPS} \left(\frac{s_{12}}{s_{2l_2}} + 2 \right) \quad (4.90)$$

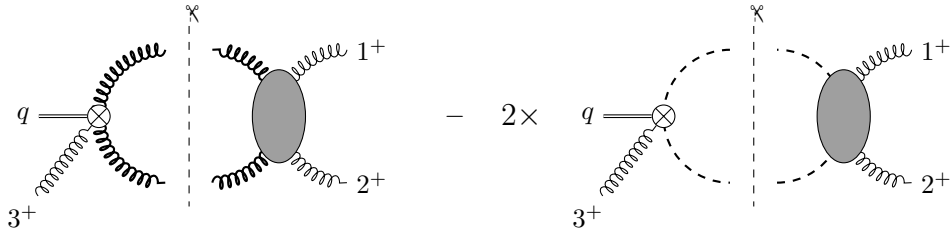


Figure 4.6: Two-particle cut of the one-loop form factor $\text{Tr } F^3$ in the s_{12} channel in six dimensions.

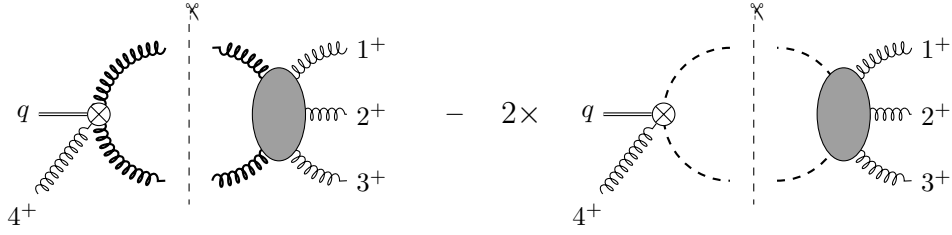


Figure 4.7: Two-particle cut of the one-loop non-minimal form factor $\text{Tr } F^3$ in the s_{123} channel.

modulo terms which integrate to zero, and uplifting this result leads to:

$$f^{(3)}(s_{12}, s_{23}, s_{13})|_{s_{12}\text{-disc}} = -i s_{12} \cdot \begin{array}{c} p_1 \\ \diagup \quad \diagdown \\ q \\ \diagdown \quad \diagup \\ p_3 \quad l \quad p_2 \end{array} - 2i \cdot \begin{array}{c} p_1 \\ \diagup \quad \diagdown \\ q \\ \diagdown \quad \diagup \\ p_3 \quad l \quad p_2 \end{array} . \quad (4.91)$$

Combining the discontinuities in the three channels s_{12} , s_{23} and s_{31} we arrive at the complete one-loop form factor

$$f^{(3)}(\{s_{ij}\}) = \sum_{k=1}^n f^{(3)}(\{s_{ij}\})|_{s_{k,k+1}\text{-disc}} , \quad (4.92)$$

where every term in the sum can be obtained from (4.91) by relabelling the external legs.

4.3.4 The Non-Minimal $\text{Tr } F^3$ Form Factor

In the previous sections we reproduced known results for form factors through the generalisation of the dimensional reconstruction technique. In this section we derive for the first time the complete form factor of the operator $\text{Tr } F^3$ with four gluons in the all-plus helicity configuration.

The procedure we follow has been described in detail earlier, hence we now only sketch the relevant derivations and provide the main results. There are two independent unitarity cuts to be computed, say in the s_{12} -channel and s_{123} -channel, up to cyclic permutation. Starting from the s_{123} -cut, one needs to evaluate the difference shown in 4.7. The tree-level form factor in the scalar subtraction term (second term in the figure) is the minimal form factor of the operator $\text{Tr } (D_\mu \phi D_\nu \phi F^{\mu\nu})$. The Passarino-Veltman

reductions of the resulting tensor integrals have been performed using the `Mathematica` package `FeynCalc` [305, 306]. From the two-particle cuts in the s_{123} -channel we obtain the following functions:

$$\begin{aligned}
 F_{\mathcal{O}_3}^{(1)}(1^+, 2^+, 3^+, 4^+; q) \Big|_{s_{123}\text{-disc}} = & D_0^{[0]} \text{ (box diagram) } + C_0^{[0]} \text{ (triangle diagram) } \\
 & + C_1^{[0]} \text{ (triangle diagram) } + B_0^{[0]} \text{ (bubble diagram) } ,
 \end{aligned} \tag{4.93}$$

with the coefficients

$$\begin{aligned}
 D_0^{[0]} &= -i F(1, 2, 3; 4) , \\
 C_0^{[0]} &= -i \frac{s_{12} + s_{31}}{s_{12}s_{23}} F(1, 2, 3; 4) , \\
 C_1^{[0]} &= -i \frac{s_{23} + s_{31}}{s_{12}s_{23}} F(1, 2, 3; 4) ,
 \end{aligned} \tag{4.94}$$

where

$$F(1, 2, 3; 4) := \frac{s_{123}}{s_{31}^2} (s_{12}[13][24] + s_{31}[12][34]) (s_{23}[13][24] + s_{31}[23][14]) . \tag{4.95}$$

Finally the coefficient of the bubble can be written as

$$B_0^{[0]} = 2i[12][23][34][41] b_0^{[0]} , \tag{4.96}$$

where the helicity-invariant function $b_0^{[0]}$ is defined as

$$b_0^{[0]} = \frac{s_{123}^2}{s_{12}s_{23}} \left(\frac{1}{s_{12} + s_{31}} + \frac{1}{s_{23} + s_{31}} \right) + \frac{[13][24]}{[12][34]} \frac{s_{123}^2}{s_{23}s_{31}} \cdot \frac{1}{s_{12} + s_{31}} + \frac{[13][24]}{[14][23]} \frac{s_{123}^2}{s_{12}s_{31}} \cdot \frac{1}{s_{23} + s_{31}} . \tag{4.97}$$

The result also contains a box integral with a μ^2 in the numerator, which after integration is of $\mathcal{O}(\epsilon)$. For completeness we quote its coefficient:

$$D_0^{[2]} = -2i s_{123} \left(\frac{[12]^2[34]^2}{s_{12}} + \frac{[23]^2[41]^2}{s_{23}} + \frac{[13]^2[24]^2}{s_{31}} \right) . \tag{4.98}$$

Next we consider the two-particle cut in the s_{12} -channel and, as discussed in earlier sections, the discontinuity of the complete form factor is determined from the difference

$$F_{6D}^{(1)}(1^+, 2^+, 3^+, 4^+; q) \Big|_{s_{12}\text{-cut}} - 2F_\phi^{(1)}(1^+, 2^+, 3^+, 4^+; q) \Big|_{s_{12}\text{-cut}} , \tag{4.99}$$

where the second term is the scalar subtraction. As in the case of the non-minimal form factor of $\text{Tr } F^2$, there are two contributions to the scalar quantity $F_\phi^{(1)}(1^+, 2^+, 3^+, 4^+; q)$, which are represented in Figure 4.8. The first contribution comes from the operator

$$F_\phi^{(1)}(1^+, 2^+, 3^+, 4^+; q)|_{s_{12}\text{-cut}} = \left[\begin{array}{c} \mathcal{O}_3 \\ \text{Diagram 1} \end{array} + \begin{array}{c} \mathcal{O}_{3,s} \\ \text{Diagram 2} \end{array} \right] \times \begin{array}{c} \text{Diagram 3} \\ \text{Diagram 4} \end{array}$$

Figure 4.8: A two-particle cut of the scalar contribution to the non-minimal $\text{Tr } F^3$ form factor. The red boxes highlight the two different operator insertions.

$\text{Tr } F^3$ with two scalars and two gluons, whereas the second one comes from the scalar operator $\text{Tr } D_\mu \phi D_\nu \phi F^{\mu\nu}$.

After tensor reductions, we find

$$F_{\mathcal{O}_3}^{(1)}(1^+, 2^+, 3^+, 4^+; q)|_{s_{12}\text{-disc}} = D_0^{[0]} \begin{array}{c} q \\ \text{Square 1} \\ p_4, p_3, p_2, p_1 \end{array} + D_1^{[0]} \begin{array}{c} q \\ \text{Square 2} \\ p_3, p_2, p_1, p_4 \end{array} \\ + C_1^{[0]} \begin{array}{c} q \\ \text{Triangle 1} \\ p_4, p_3, p_2, p_1 \end{array} + C_2^{[0]} \begin{array}{c} q \\ \text{Triangle 2} \\ p_3, p_2, p_1, p_4 \end{array} \\ + C_3^{[0]} \begin{array}{c} q \\ \text{Triangle 3} \\ p_4, p_3, p_2, p_1 \end{array} + C_3^{[2]} \begin{array}{c} q \\ \text{Triangle 4} \\ p_4, p_3, p_2, p_1, \mu^2 \end{array} \\ + B_1^{[0]} \begin{array}{c} q \\ \text{Circle 1} \\ p_4, p_3, p_2, p_1 \end{array} + B_1^{[2]} \begin{array}{c} q \\ \text{Circle 2} \\ p_4, p_3, p_2, p_1, \mu^2 \end{array}, \quad (4.100)$$

where we checked that the coefficients $D_0^{[p]}$, $D_1^{[p]}$, $C_0^{[p]}$ and $C_2^{[p]}$ match the ones found in the previous calculation, up to relabelling. The other coefficients for the triangles are

$$C_3^{[0]} = i[12][23][34][41]c_3^{[0]}, \\ C_3^{[2]} = \frac{4i}{s_{12}}[12][34][13][24], \quad (4.101)$$

where

$$\begin{aligned} c_3^{[0]} &= \frac{s_{12} + s_{31}}{s_{23}} + \frac{s_{12}}{s_{34}} \left(1 + \frac{s_{13}}{s_{14}} + \frac{s_{24}}{s_{23}} \right) - \frac{[13][24]}{[14][23]} \left[\frac{s_{123}(s_{12} + s_{31}) - s_{13}^2}{s_{13}^2} - \frac{s_{12}}{s_{34}} \right] \\ &\quad - \frac{[13][24]}{[12][34]} \frac{s_{12}}{s_{13}^2 s_{23}} \left[s_{123}(s_{23} + s_{31}) - 2s_{31}^2 \right] + (1, 4) \longleftrightarrow (2, 3) , \end{aligned} \quad (4.102)$$

while for the bubbles

$$\begin{aligned} B_1^{[0]} &= 2i[13]^2[24]^2 \left(\frac{1}{s_{31}} - \frac{1}{s_{23}} + \frac{s_{12}}{s_{23}s_{31}} \right) + 2i[12]^2[34]^2 \left(\frac{2}{s_{23}} - \frac{2s_{12}}{s_{23}(s_{13} + s_{23})} \right) \\ &\quad + 2i[12][34][13][24] \left(\frac{1}{s_{12}} + \frac{4}{s_{23}} - \frac{2}{s_{34}} - \frac{4s_{24}}{s_{23}s_{34}} \right) + (1, 4) \longleftrightarrow (2, 3) , \end{aligned} \quad (4.103)$$

and

$$B_1^{[2]} = \frac{4i}{s_{12}^2} [12][34] ([13][24] + [23][14]) . \quad (4.104)$$

We have checked that our result satisfies the expected infrared consistency conditions. In particular, using the results for the coefficients D_0 , C_0 and C_1 , one immediately finds that the coefficient of $\frac{(-s_{123})^{-\epsilon}}{\epsilon^2}$ vanishes, as required. We have also confirmed that the coefficient of $\frac{(-s_{12})^{-\epsilon}}{\epsilon^2}$ is proportional to the corresponding tree-level non-minimal form factor derived in [273],

$$F_{\mathcal{O}_3}^{(0)}(1^+, 2^+, 3^+, 4^+; q) = -2 \frac{[12][23][34][41]}{s_{12}} \left(1 + \frac{[13][24]}{[23][41]} - \frac{s_{24}}{s_{41}} \right) + \text{cyclic} . \quad (4.105)$$

4.3.5 The Minimal $\text{Tr } F^4$ Form Factors

In this section we consider the form factors of $\text{Tr } F^4$ in all possible helicity configurations. The case where all particles have the same helicity is interesting since it admits an immediate generalisation to the minimal form factors of operators of the form $\text{Tr } F^n$ defined in (4.62). In this family, $\text{Tr } F^4$ is the first operator whose minimal form factor contains rational terms. We are going to consider the quantities in the planar limit of the theory, *i.e.* at one loop we will probe only the discontinuities in the Mandelstam invariants of adjacent momenta in the colour-ordered form factor. At this point it is important to stress that non-planar contributions would need an additional consideration: as one can see from (4.12) there is no “non-planar” scalar operator, *i.e.* the scalars can only appear next to each other in the colour-ordered form factor, and then the complete four-dimensional contribution coincides with the diagrams with purely six-dimensional internal gluons.

All-Plus Helicity Configuration

We begin by defining

$$F_{\mathcal{O}_4}^{(1)}(1^+, 2^+, 3^+, 4^+; q) := 2[12][23][34][41] \cdot f^{(4)}(\{s_{ij}\}) . \quad (4.106)$$

At one loop, we can make the following observations:

- The cut-constructible part, coming from the form factor involving only gluons, has the same structure as $F_{\mathcal{O}_3}^{(1)}(1^+, 2^+, 3^+; q)$, with both UV and IR divergences.
- Terms proportional to μ^2 and μ^4 now appear. As already mentioned, these could not arise for $n < 4$ because of the limited kinematic, as we will show below. The new integrals are two triangles with μ^2 and μ^4 numerators¹⁶ and when expanded in powers of the dimensional regulator ϵ give a finite contribution in the $\epsilon \rightarrow 0$ limit. They are exactly the rational terms that cannot be seen by the completely four-dimensional cut construction, where clearly $\mu^2 = 0$.

Following the procedure outlined in the previous sections, we find

$$\begin{aligned}
f^4(\{s_{ij}\})|_{s_{12}\text{-disc}} = & -i \left(1 + \frac{[13][24]}{[14][23]}\right) \cdot \begin{array}{c} q \\ \parallel \\ p_4 \\ \parallel \\ p_3 \end{array} \begin{array}{c} p_1 \\ \diagup \\ \text{---} \\ \diagdown \\ p_2 \end{array} \begin{array}{c} \text{---} \\ \text{---} \\ \text{---} \\ \text{---} \\ l \end{array} - i s_{12} \cdot \begin{array}{c} q \\ \parallel \\ p_4 \\ \parallel \\ p_3 \end{array} \begin{array}{c} p_1 \\ \diagup \\ \text{---} \\ \diagdown \\ p_2 \end{array} \begin{array}{c} \text{---} \\ \text{---} \\ \text{---} \\ \text{---} \\ l \end{array} \\
& + i \frac{[12][34]}{[23][41]} \cdot \begin{array}{c} q \\ \parallel \\ p_4 \\ \parallel \\ p_3 \end{array} \begin{array}{c} p_1 \\ \diagup \\ \text{---} \\ \diagdown \\ p_2 \end{array} \begin{array}{c} \text{---} \\ \text{---} \\ \text{---} \\ \text{---} \\ l \end{array} \mu^2 - i \frac{[34]}{[3|p_2 p_1|4]} \cdot \begin{array}{c} q \\ \parallel \\ p_4 \\ \parallel \\ p_3 \end{array} \begin{array}{c} p_1 \\ \diagup \\ \text{---} \\ \diagdown \\ p_2 \end{array} \begin{array}{c} \text{---} \\ \text{---} \\ \text{---} \\ \text{---} \\ l \end{array} \mu^4
\end{aligned} \tag{4.107}$$

Notice that in the final result the integral $I_3^4[\mu^4]$ appears. In general, in a renormalisable gauge theory one would expect triangle integrals to appear with at most a third power of the loop momentum in the numerator, which allows for at most a μ^2 triangle contribution. However we are considering an effective field theory with an operator of mass-dimension eight, hence the possibility of having also an $I_3^4[\mu^4]$ term. The last step of the calculation is the sum over all the possible channel discontinuities, as we did in (4.92) for $\text{Tr } F^3$.

The above result can be immediately generalized to $\text{Tr } F^n$ for arbitrary n in the all-plus helicity configurations, where we define

$$\text{Tr } F^n(1^+, \dots, n^+; q)|_{1\text{-loop}} := (-)^n 2 \prod_{k=1}^n [kk+1] \cdot f^{(n)}(\{s_{ij}\}) , \tag{4.108}$$

and

$$\begin{aligned}
f^{(n)}(\{s_{ij}\})|_{s_{12}\text{-disc}} = & -i \left(1 + \frac{[13][2n]}{[1n][23]}\right) \cdot \begin{array}{c} q \\ \parallel \\ p_4 \\ \parallel \\ p_3 \end{array} \begin{array}{c} p_1 \\ \diagup \\ \text{---} \\ \diagdown \\ p_2 \end{array} \begin{array}{c} \text{---} \\ \text{---} \\ \text{---} \\ \text{---} \\ l \end{array} - i s_{12} \cdot \begin{array}{c} q \\ \parallel \\ p_4 \\ \parallel \\ p_3 \end{array} \begin{array}{c} p_1 \\ \diagup \\ \text{---} \\ \diagdown \\ p_2 \end{array} \begin{array}{c} \text{---} \\ \text{---} \\ \text{---} \\ \text{---} \\ l \end{array} \\
& + i \frac{[12][3n]}{[23][n1]} \cdot \begin{array}{c} q \\ \parallel \\ p_4 \\ \parallel \\ p_3 \end{array} \begin{array}{c} p_1 \\ \diagup \\ \text{---} \\ \diagdown \\ p_2 \end{array} \begin{array}{c} \text{---} \\ \text{---} \\ \text{---} \\ \text{---} \\ l \end{array} \mu^2 - i \frac{[3n]}{[3|p_2 p_1|n]} \cdot \begin{array}{c} q \\ \parallel \\ p_4 \\ \parallel \\ p_3 \end{array} \begin{array}{c} p_1 \\ \diagup \\ \text{---} \\ \diagdown \\ p_2 \end{array} \begin{array}{c} \text{---} \\ \text{---} \\ \text{---} \\ \text{---} \\ l \end{array} \mu^4
\end{aligned} \tag{4.109}$$

This simple generalisation is due to the fact that, upon properly normalising with the corresponding four-dimensional quantities, the six-dimensional minimal tree-level form

¹⁶For analytic expressions of such integrals see for example Appendix D.

factor of $\text{Tr } F^n$ is identical to that of $\text{Tr } F^4$ up to the replacement $4 \mapsto n$, as can be seen from (4.67). As a final remark, notice that we can a posteriori explain the absence of rational terms for $\text{Tr } F^3$: indeed we can recover (4.91) by simply replacing $n \mapsto 3$ in (4.109). Then, rational terms vanish since they are proportional to $[3n]$.

MHV Configuration: the Alternate and Split-Helicity Form Factors

We define the MHV colour-ordered form factor with alternate-helicity gluons as follows:

$$F_{\mathcal{O}_4}^{(1)}(1^+, 2^-, 3^+, 4^-; q) := \langle 24 \rangle^2 [13]^2 \cdot f_a^{(4)}(\{s_{ij}\}) . \quad (4.110)$$

Since this case presents some peculiarities in the calculations, we will give more details about it. In particular, the cut of the form factor with six-dimensional internal gluons in the s_{12} -channel is given by

$$\begin{aligned} f_{a,6D}^{(4)}(\{s_{ij}\}) \Big|_{s_{12}\text{-cut}} &= - \int \text{dLIPS} \frac{i}{s_{12}s_{2l_2}} \frac{\mathcal{I}_{6D}^2}{\langle 24 \rangle^2 [13]^2} \\ &= - \int \text{dLIPS} \frac{i}{s_{12}s_{2l_2}} (2k \cdot l_2)^2 , \end{aligned} \quad (4.111)$$

where

$$\mathcal{I}_{6D} = 2\mu^2 \langle 24 \rangle [13] + \langle 2 | l_1^{(4)} | 3 \rangle \langle 4 | l_2^{(4)} | 1 \rangle + \langle 2 | l_2^{(4)} | 3 \rangle \langle 4 | l_1^{(4)} | 1 \rangle \quad (4.112)$$

and in the last step we removed terms proportional to $\langle 2 | l_2^{(4)} | 1 \rangle$ that vanish upon integration. Also k_μ is a massive momentum defined by

$$k_{\alpha\dot{\alpha}} = \frac{[12]}{[13]} \lambda_{2\alpha} \tilde{\lambda}_{3\dot{\alpha}} - \frac{\langle 12 \rangle}{\langle 24 \rangle} \lambda_{4\alpha} \tilde{\lambda}_{1\dot{\alpha}} , \quad (4.113)$$

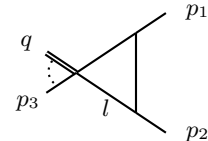
and it is easy to prove that it satisfies the following relations:

$$k^2 = 2p_1 \cdot k = 2p_2 \cdot k = s_{12} . \quad (4.114)$$

Surprisingly, the scalar contribution is identically zero after integration:

$$f_{a,\phi}^{(4)}(\{s_{ij}\}) \Big|_{s_{12}\text{-cut}} = \int \text{dLIPS} \frac{i}{s_{12}s_{2l_2}} \frac{\langle 4 | l_1^{(4)} | 3 \rangle \langle 4 | l_2^{(4)} | 3 \rangle \langle 2 | l_2^{(4)} | 1 \rangle^2}{\langle 24 \rangle^2 [13]^2} = 0 , \quad (4.115)$$

because of the presence of the term $\langle 2 | l_2^{(4)} | 1 \rangle^2$. Thus the discontinuity in the s_{12} -channel is completely given by the pure six-dimensional contribution (4.111), which after the integral reduction can be written as

$$f_a^{(4)}(\{s_{ij}\}) \Big|_{s_{12}\text{-disc}} = -i s_{12} \cdot \text{Diagram} . \quad (4.116)$$


It is worth stressing that all the other planar contributions can be obtained from the previous one easily by symmetry arguments.

As usual, for the split-helicity configuration we factorise the tree-level form factor:

$$F_{\mathcal{O}_4}^{(1)}(1^+, 3^+, 2^-, 4^-; q) := [13]^2 \langle 24 \rangle^2 \cdot f_s^{(4)}(\{s_{ij}\}) . \quad (4.117)$$

Unlike the previous case, in the planar limit we have two different cuts which cannot be related by symmetry: in particular, we can perform the cut in channels with same or opposite helicity gluons. The discontinuity in the s_{12} -channel, after the scalar subtraction, is given by

$$f_s^{(4)}(\{s_{ij}\})|_{s_{13}\text{-disc}} = -is_{13} \cdot \begin{array}{c} \text{---} p_1 \\ \diagup \quad \diagdown \\ q \quad \quad \quad l \\ \diagdown \quad \diagup \\ p_2 \quad \quad \quad p_3 \end{array} . \quad (4.118)$$

The cut in the s_{23} -channel is reminiscent of the alternate-helicity case, with vanishing scalar contribution up to integration:

$$f_s^{(4)}(\{s_{ij}\})|_{s_{23}\text{-cut}} \simeq - \int \text{dLIPS} \frac{i}{s_{13}s_{3l_2}} (2k \cdot l_2)^2 , \quad (4.119)$$

where the momentum k_μ is defined by

$$k_{\alpha\dot{\alpha}} = \frac{[23]}{[13]} \lambda_{2\alpha} \tilde{\lambda}_{1\dot{\alpha}} + \frac{\langle 23 \rangle}{\langle 24 \rangle} \lambda_{4\alpha} \tilde{\lambda}_{3\dot{\alpha}} , \quad (4.120)$$

and it satisfies the following relations:

$$k^2 = 2p_2 \cdot k = 2p_3 \cdot k = s_{23} . \quad (4.121)$$

The cut in the s_{23} channel is

$$f_s^{(4)}(\{s_{ij}\})|_{s_{23}\text{-disc}} = -is_{23} \cdot \begin{array}{c} \text{---} p_2 \\ \diagup \quad \diagdown \\ q \quad \quad \quad l \\ \diagdown \quad \diagup \\ p_4 \quad \quad \quad p_3 \end{array} . \quad (4.122)$$

Let us emphasise some relevant features of the result:

- The final result is free of rational terms. Thus we would have found the same, complete, quantity even with four-dimensional unitarity-cuts.
- The only operator that contributes in four dimensions is $\text{Tr}(F_{\text{SD}}^2 F_{\text{ASD}}^2)$, which is a descendant of $\text{Tr} \phi^4$ in $\mathcal{N} = 4$ SYM¹⁷.
- We note the absence of bubbles in the final result for this (unrenormalised) form factor. This may be related to the independence of the bare quantity on the matter content of the theory. One could then regard the computation as if it was performed in $\mathcal{N} = 4$ SYM, where the operator under consideration belongs to a protected multiplet.
- An unrelated observation is that the colour-ordered form factors with alternate and split-helicity configurations are the same:

$$F_{\mathcal{O}_4}^{(1)}(1^+, 2^-, 3^+, 4^-; q) = F_{\mathcal{O}_4}^{(1)}(1^+, 3^+, 2^-, 4^-; q) . \quad (4.123)$$

This is an accident due to the simple topology of the integral basis combined with the fact that bubbles do not appear. At first, the equality (4.123) could appear as a consequence of the photon decoupling identities which hold in Yang-Mills theory. However these identities are no longer valid when one considers interactions with higher powers of the field strength.

¹⁷See for example Table 7 in [307].

Chapter 5

One-Loop Anomalous Dimensions in the SMEFT

On-shell techniques provide powerful strategies to study the UV mixing in (non-supersymmetric) EFTs, as first pointed out in [98] using techniques developed for the study of the anomalous dimension of operators in $\mathcal{N} = 4$ super-Yang-Mills [308–311] (for a review, see [312] and references therein) from scattering amplitudes and form factors [287–290, 313–318] and recently applied to the SMEFT [99–107]. Furthermore, on-shell techniques also provided a good understanding of the mysterious pattern of zeros in the one-loop anomalous dimension matrix of the SMEFT [108–110]. At one-loop, such a calculation requires only two main ingredients: the tree-level (four-point) amplitudes in the SM and the identification of a complete (but not redundant) basis of EFT interactions/operators, which have been studied in the Chapters 2 and 3.

The first systematic and complete computation of the one-loop anomalous dimension matrix for dimension-six operators in the SMEFT has been carried out in [319–321]. So far, the study of the anomalous dimension of SMEFT interactions has been completed only partially in the literature for operators up to dimension 8 [104, 322–329]. In this chapter, we present the general on-shell set-up which will allowed us to fully compute the one-loop anomalous dimension matrix for all the operators in the SMEFT of mass dimension 8. As a proof of concept, we reproduce know results for the mixing matrix of operators of dimension 5, 6 and 7 and we present the mixing matrix of dimension 8 operators for the SMEFT considering a single flavour family $N_f = 1$. We compute the anomalous dimension matrix to linear order in the Wilson coefficients, *i.e.* we ignore the mixing between dimension-six and dimension-eight operators, which are however partially known in the literature (see Table 5 of [329]).

The present chapter is organised as follows. In Section 5.1, we review the computation of the one-loop anomalous dimension matrix from on-shell data through unitarity. We make use of the presented techniques to reproduce known results for dimension 5, 6, and 7 operators as well as to compute the mixing of dimension 8 operators at linear order in the Wilson coefficients and leading (quadratic) order in the renormalisable couplings. These general results are made available in separate ancillary files of the paper [104]. In Section 5.2 we present the explicit mixing coefficients for dimension 6 and 8 operators relevant for Higgs production with a W boson.

5.1 The UV anomalous mass dimension matrix at leading order

In Chapter 3 we argued that any tree-level amplitude in the Standard Model can be fully determined from its factorisation channels, and in Chapter 2 we gave a general algorithm to find all the SMEFT interactions. These are all the ingredients needed to compute the UV mixing matrix for the SMEFT interactions $\gamma_{d \rightarrow d}^{\text{UV}}$ ¹, where d is the mass dimension of the corresponding effective operators for $d = 5, 6, 7, 8$. In this chapter we restrict to the case of $N_f = 1$ and we leave the treatment of full flavour dependence for future work. The results for $\gamma_{d \rightarrow d}^{\text{UV}}$ were provided in the ancillary files of the work [104], and at the end of this chapter we show as an example the mixing coefficients of the dimension 6 and 8 operators relevant for Higgs plus W production from pp -scattering.

Sticking to the notation introduced in Section 3.1, we write the amplitudes with a single insertion of an irrelevant interaction as $\mathcal{F}_{n,d,i}(p_1^{a_1,h_1}, \dots, p_n^{a_n,h_n})$, where d is the dimension of the irrelevant operator and i is its corresponding label (for example, in the case of $N_f = 1$ and $d = 6$, $i = 1, \dots, 84$), in order to distinguish it from amplitudes \mathcal{A} with only relevant and marginal couplings. The central formula for our computations has been presented in [98] and gives the action of the *dilatation operator* $D = \frac{\partial}{\partial \log \mu}$ on the amplitude in terms of its discontinuity²:

$$e^{-i\pi D} \mathcal{F}^* = S \otimes \mathcal{F}^* , \quad (5.1)$$

where S is the full S-matrix and on the RHS the product has to be interpreted as a matrix product weighted over a proper Lorentz phase space integral which, via the Optical Theorem, correspond to a specific discontinuity of the effective amplitude.

The dilatation operator is linked to the UV mixing matrix $\gamma_{i \rightarrow j}^{\text{UV}}$ by the Callan-Symanzik equation [330–332]:

$$D\mathcal{F}_i = \left(\gamma_{j \rightarrow i}^{\text{UV}} - \gamma_i^{\text{IR}} \delta_{ij} + \beta(g_k^2) \frac{\partial}{\partial g_k^2} \delta_{ij} \right) \mathcal{F}_j , \quad (5.2)$$

where $\beta(g_k^2)$ is the beta-function for the coupling g_k and γ_i^{IR} is the IR contribution to the anomalous dimension of the amplitude \mathcal{F}_i which depends only on its external states.

Combining (5.1) and (5.2), expanding to leading order in the coupling and at linear

¹In principle, we could consider $\gamma_{d_1 \rightarrow d_2}^{\text{UV}}$, with $d_1 \neq d_2$, which involves amplitudes which are non-linear in the effective couplings. In this work we are not considering such contributions, but it is worth stressing that conceptually their treatment is very much the same.

²This formula has been first presented in [98] for \mathcal{F} being a form factor, but it trivially holds for (effective) amplitudes as well, by setting $q^\mu = 0$ in the form factor.

order in the effective interactions, we find³

$$\begin{aligned}
 \gamma_{j \rightarrow i}^{\text{UV}} \mathcal{F}_j(p_1^{h_1} \dots p_n^{h_n}) &= \frac{1}{\pi} \sum_{\substack{l=1 \\ l < m}}^n \sum_{\{l_1, l_2\}} \int \frac{d\Omega_2}{32\pi^2} \left[i \mathcal{A}_4(p_{l_1}^{h_{l_1}} p_{l_2}^{h_{l_2}} \rightarrow p_l^{h_l} p_m^{h_m}) \right. \\
 &\quad \left. + \sum_{k=1}^3 \frac{g_k^2 T_{k,l_1} \cdot T_{k,l_2}}{\cos^2 \theta \sin^2 \theta} \right] \cdot \mathcal{F}_i(\dots p_{l_1}^{h_{l_1}} \dots p_{l_2}^{h_{l_2}} \dots) \\
 &\quad + \mathcal{F}_i(p_1^{h_1} \dots p_n^{h_n}) \cdot \sum_{l=1}^n \frac{\gamma_{\text{coll}}^{(l)}}{16\pi^2},
 \end{aligned} \tag{5.3}$$

where

$$\int \frac{d\Omega_2}{4\pi} = \int_0^{2\pi} \frac{d\phi}{2\pi} \int_0^{\frac{\pi}{2}} d\theta 2 \cos \theta \sin \theta \tag{5.4}$$

is the two-particles Lorentz invariant phase space integral, the sum over $\{l_1, l_2\}$ is over the species and the helicity configurations of the internal particles, $\gamma_{\text{coll}}^{(l)}$ is the IR collinear anomalous dimension associated to the l^{th} -particle and the term with $T_{k,l_1} \cdot T_{k,l_2}$ takes care of the subtraction of the (divergent) IR cusp anomalous dimension (the label k runs over the three factors of the gauge group $U(1) \times SU(2) \times SU(3)$). In particular, the latter is non-zero if the in- and out-states of the four-point amplitude are the same and, if this is the case, it is a proper contraction of the Lie algebra generators (or the product of the hypercharges in the case of $U(1)$) associated to the outgoing (or equivalently incoming) particles. For example, if the four-point amplitude is $\mathcal{A}_4(\bar{Q}_{l_1} Q_{l_2} \rightarrow \bar{Q}_l Q_m)$, then

$$\sum_{k=1}^3 g_k^2 T_{k,l} \cdot T_{k,m} = \left(-\frac{1}{6} \right) \cdot \frac{1}{6} g_1^2 + g_2^2 \sigma^I_j{}^{i_m} \sigma^I_i{}^j + g_3^2 \tau^A_b{}^{a_m} \tau^A_a{}^b. \tag{5.5}$$

The helicity variables associated to the internal momenta, on the cut configuration, can be written in terms of the phase space angles θ and ϕ and the external momenta p_l and p_m , as first shown in [313]:

$$\begin{pmatrix} \lambda_{l_1} \\ \lambda_{l_2} \end{pmatrix} = \begin{pmatrix} \cos \theta & -\sin \theta e^{i\phi} \\ \sin \theta e^{-i\phi} & \cos \theta \end{pmatrix} \begin{pmatrix} \lambda_l \\ \lambda_m \end{pmatrix}, \tag{5.6}$$

together with the complex conjugate rotation for the spinors $\tilde{\lambda}_{l_1}$ and $\tilde{\lambda}_{l_2}$.

5.1.1 Infrared collinear anomalous dimensions in the Standard Model

The collinear anomalous dimensions for the particles in the Standard Model can be obtained by studying the anomalous dimension of UV protected operators, such as the stress-tensor as emphasised in [98]:

$$\begin{aligned}
 \langle p_1^{h_1} p_2^{h_2} | T^{\mu\nu} | 0 \rangle \cdot \sum_{l=1}^2 \frac{\gamma_{\text{coll}}^{(l)}}{16\pi^2} &= -\frac{1}{\pi} \sum_{\{l_1, l_2\}} \int \frac{d\Omega_2}{32\pi^2} \left[i \mathcal{A}_4(p_{l_1}^{h_{l_1}} p_{l_2}^{h_{l_2}} \rightarrow p_1^{h_1} p_2^{h_2}) \right. \\
 &\quad \left. + \sum_{k=1}^3 \frac{g_k^2 T_{k,l_1} \cdot T_{k,l_2}}{\cos^2 \theta \sin^2 \theta} \right] \cdot \langle p_{l_1}^{h_{l_1}} p_{l_2}^{h_{l_2}} | T^{\mu\nu} | 0 \rangle,
 \end{aligned} \tag{5.7}$$

³The results in the ancillary files of the paper [104] are given in terms of the matrix $\gamma_{ij}^{\text{UV}} \equiv 16\pi^2 \gamma_{j \rightarrow i}^{\text{UV}}$, where we factored out the usual loop factor $\frac{1}{16\pi^2}$.

We are going to show an example of the computation of the collinear anomalous dimension for the W bosons in the Standard Model and we will give the result for all the states of the theory.

We start by giving the stress-tensor form factor [18] following the normalisation procedure given in [98] for generic complex scalars, fermions and vectors respectively⁴:

$$\begin{aligned} \langle \bar{\phi}^{\mathbb{A}} \phi^{\mathbb{B}} | T^{\alpha\dot{\alpha}\beta\dot{\beta}} | 0 \rangle &= \frac{1}{3} \delta_{\mathbb{A}}^{\mathbb{B}} \left(\lambda_1^\alpha \lambda_1^\beta \tilde{\lambda}_1^{\dot{\alpha}} \tilde{\lambda}_1^{\dot{\beta}} - \lambda_1^\alpha \lambda_2^\beta \tilde{\lambda}_1^{\dot{\alpha}} \tilde{\lambda}_2^{\dot{\beta}} - \lambda_1^\alpha \lambda_2^\beta \tilde{\lambda}_2^{\dot{\alpha}} \tilde{\lambda}_1^{\dot{\beta}} - \lambda_2^\alpha \lambda_1^\beta \tilde{\lambda}_1^{\dot{\alpha}} \tilde{\lambda}_2^{\dot{\beta}} \right. \\ &\quad \left. - \lambda_2^\alpha \lambda_1^\beta \tilde{\lambda}_2^{\dot{\alpha}} \tilde{\lambda}_1^{\dot{\beta}} + \lambda_2^\alpha \lambda_2^\beta \tilde{\lambda}_2^{\dot{\alpha}} \tilde{\lambda}_2^{\dot{\beta}} \right) \\ \langle \bar{\psi}^{\mathbb{A}} \psi^{\mathbb{B}} | T^{\alpha\dot{\alpha}\beta\dot{\beta}} | 0 \rangle &= \frac{1}{2} \delta_{\mathbb{A}}^{\mathbb{B}} \left(\lambda_1^\alpha \lambda_1^\beta \tilde{\lambda}_2^{\dot{\alpha}} \tilde{\lambda}_1^{\dot{\beta}} + \lambda_1^\alpha \lambda_1^\beta \tilde{\lambda}_1^{\dot{\alpha}} \tilde{\lambda}_2^{\dot{\beta}} - \lambda_1^\alpha \lambda_2^\beta \tilde{\lambda}_2^{\dot{\alpha}} \tilde{\lambda}_2^{\dot{\beta}} - \lambda_2^\alpha \lambda_1^\beta \tilde{\lambda}_2^{\dot{\alpha}} \tilde{\lambda}_2^{\dot{\beta}} \right) \\ \langle v_-^{\mathbb{I}} v_+^{\mathbb{J}} | T^{\alpha\dot{\alpha}\beta\dot{\beta}} | 0 \rangle &= -2 \delta^{\mathbb{I}\mathbb{J}} \lambda_1^\alpha \lambda_1^\beta \tilde{\lambda}_2^{\dot{\alpha}} \tilde{\lambda}_2^{\dot{\beta}}, \end{aligned} \quad (5.8)$$

where $\mathbb{A}, \mathbb{B}, \mathbb{I}, \mathbb{J}$ are generic colour indices. Once we fix the minimal form factor for the stress tensor, we can apply the formula (5.7):

$$\begin{aligned} \langle W_-^I W_+^J | T^{\mu\nu} | 0 \rangle \cdot \sum_{l=1}^2 \frac{\gamma_{\text{coll}}^{(l)}}{16\pi^2} &= -\frac{1}{\pi} \sum_{\{l_1, l_2\}} \int \frac{d\Omega_2}{32\pi^2} \left[i \mathcal{A}_4(p_{l_1}^{h_{l_1}} p_{l_2}^{h_{l_2}} \rightarrow W_-^I W_+^J) \right. \\ &\quad \left. + \sum_{k=1}^3 \frac{g_k^2 T_{k,l_1} \cdot T_{k,l_2}}{\cos^2 \theta \sin^2 \theta} \right] \cdot \langle p_{l_1}^{h_{l_1}} p_{l_2}^{h_{l_2}} | T^{\mu\nu} | 0 \rangle, \end{aligned} \quad (5.9)$$

where the sum over $\{l_1, l_2\}$ runs over the pairs

$$\{ \{W_-, W_+\}, \{W_+, W_-\}, \{ \bar{Q}, Q \}, \{Q, \bar{Q}\}, \{ \bar{L}, L \}, \{L, \bar{L}\}, \{ \bar{H}, H \}, \{H, \bar{H}\} \}. \quad (5.10)$$

Considering that $\gamma_{\text{coll}}^{W_-} = \gamma_{\text{coll}}^{W_+} := \gamma_{\text{coll}}^W$, we can rewrite (5.9) as

$$\begin{aligned} \gamma_{\text{coll}}^W &= -8\pi \sum_{\{l_1, l_2\}} \int \frac{d\Omega_2}{32\pi^2} \left[i \mathcal{A}_4(p_{l_1}^{h_{l_1}} p_{l_2}^{h_{l_2}} \rightarrow W_-^I W_+^J) \right. \\ &\quad \left. + \sum_{k=1}^3 \frac{g_k^2 T_{k,l_1} \cdot T_{k,l_2}}{\cos^2 \theta \sin^2 \theta} \right] \cdot \frac{\langle p_{l_1}^{h_{l_1}} p_{l_2}^{h_{l_2}} | T^{\mu\nu} | 0 \rangle}{\langle W_-^I W_+^J | T^{\mu\nu} | 0 \rangle}, \end{aligned} \quad (5.11)$$

We will list now the different contributions from the W bosons (which need the infrared divergence subtraction), the quarks, the leptons and the Higgs doublet, respectively:

$$\gamma_{\text{coll}}^W = -g_2^2 \left(\frac{11}{3} \times 2 - \frac{N_f}{3} \times 3 - \frac{N_f}{3} - \frac{1}{6} \right), \quad (5.12)$$

where the factor of $\times 2$ in the first term is the Casimir of the adjoint representation of $SU(2)$, while the factor of $\times 3$ in the second term comes from the sum on different colour of the quarks. This is the usual result for the $SU(2)$ beta function with N_f Weyl fermions and 1 scalar, both transforming in the fundamental of the gauge group.

⁴The different overall minus sign with respect to [98] comes from our different convention choice for $\lambda_{-k}^\alpha = i\lambda_k^\alpha$ and $\tilde{\lambda}_{-k}^{\dot{\alpha}} = i\tilde{\lambda}_k^{\dot{\alpha}}$, while the authors in [98] chose $\lambda_{-k}^\alpha = \lambda_k^\alpha$ and $\tilde{\lambda}_{-k}^{\dot{\alpha}} = -\tilde{\lambda}_k^{\dot{\alpha}}$.

Finally, we give the explicit results for the other states in the Standard Model. We start from the vector bosons

$$\gamma_{\text{coll}}^B = \frac{2}{3} g_1^2 [(Y_Q^2 \times 2 + Y_u^2 + Y_d^2) \times 3 + (Y_L^2 \times 2 + Y_e^2) + Y_H^2] , \quad (5.13)$$

$$\gamma_{\text{coll}}^G = -g_3^2 \left(\frac{11}{3} \times 3 - \frac{N_f}{3} \times 2 \times 2 \right) , \quad (5.14)$$

where the first $\times 2$ in the second term of γ_{coll}^G comes from the sum over $SU(2)$ indices (or equivalently over d and u) and the second $\times 2$ factor comes from the fact that $SU(3)$ is not a chiral theory and the quarks behave as a doublet of Dirac fermions. Then we have the collinear anomalous dimensions for the fermions

$$\left(\gamma_{\text{coll}}^Q \right)_{mn} = -3 \left(g_1^2 Y_Q^2 + \frac{3}{4} g_2^2 + \frac{8}{6} g_3^2 \right) \delta_{mn} + \mathcal{Y}_{mp}^{(1)} \bar{\mathcal{Y}}_{pn}^{(1)} + \mathcal{Y}_{mp}^{(2)} \bar{\mathcal{Y}}_{pn}^{(2)} , \quad (5.15)$$

$$\left(\gamma_{\text{coll}}^u \right)_{mn} = -3 \left(g_1^2 Y_u^2 + \frac{8}{6} g_3^2 \right) \delta_{mn} + 2 \bar{\mathcal{Y}}_{np}^{(1)} \mathcal{Y}_{pm}^{(1)} , \quad (5.16)$$

$$\left(\gamma_{\text{coll}}^d \right)_{mn} = -3 \left(g_1^2 Y_d^2 + \frac{8}{6} g_3^2 \right) \delta_{mn} + 2 \bar{\mathcal{Y}}_{np}^{(2)} \mathcal{Y}_{pm}^{(2)} , \quad (5.17)$$

$$\left(\gamma_{\text{coll}}^L \right)_{mn} = -3 \left(g_1^2 Y_L^2 + \frac{3}{4} g_2^2 \right) \delta_{mn} + \mathcal{Y}_{mp}^{(3)} \bar{\mathcal{Y}}_{pn}^{(3)} , \quad (5.18)$$

$$\left(\gamma_{\text{coll}}^e \right)_{mn} = -3 g_1^2 Y_e^2 \delta_{mn} + 2 \bar{\mathcal{Y}}_{np}^{(3)} \mathcal{Y}_{pm}^{(3)} , \quad (5.19)$$

and, finally, the Higgs

$$\gamma_{\text{coll}}^H = -4 g_1^2 Y_H^2 - 4 g_2^2 \times \frac{3}{4} + 2 \text{Tr} \mathcal{Y}^{(1)} \cdot \bar{\mathcal{Y}}^{(1)} \times 3 + 2 \text{Tr} \mathcal{Y}^{(2)} \cdot \bar{\mathcal{Y}}^{(2)} \times 3 + 2 \text{Tr} \mathcal{Y}^{(3)} \cdot \bar{\mathcal{Y}}^{(3)} , \quad (5.20)$$

where $\frac{3}{4}$ and $\frac{8}{6}$ are the Casimir of the fundamental representation of $SU(2)$ and $SU(3)$, respectively.

5.2 The Higgs production in association with a W boson

As an illustrative application of the techniques discussed so far, we consider a subset of dimension-six and dimension-eight operators relevant for the Higgs production in association with a W boson via proton scattering, *i.e.* the operators contributing to the scattering $pp \rightarrow hW$ as considered in [84], with a technical difference due to the fact that in the mixing problem considered in this work we look at $N_f = 1$. In this section, we will compute the mixing among dimension-six and dimension-eight effective interactions separately. First, we present the relevant minimal amplitudes found using the algorithm presented in Section 2.3.1, which are in one-to-one correspondence with the independent operators considered in [84]. Then, using the techniques just reviewed we compute the two UV mixing matrices, comparing the mixing matrix for dimension-six operators with known results in the literature [99, 100, 319–321, 333]. The full mixing matrix for all the operators in the SMEFT up to dimension 8 can be found in the ancillary files of [104].

There are thirteen dimension-six operators (five of which are self-hermitian) contributing to the scattering $pp \rightarrow hW$ and such counting can be performed using Hilbert series method. In Table 5.1 and Table 5.2 we show the content of the various operators and their multiplicities as shown in reference [210] and the corresponding independent

#	Hilbert series	Minimal amplitude
1	$\bar{H}^3 H^3$	$\mathcal{Y}_{\langle 123 \rangle} \circ \delta_{j_1}^{i_4} \delta_{j_2}^{i_5} \delta_{j_3}^{i_6}$
2	$2D^2 \bar{H}^2 H^2$	$\mathcal{Y}_{\langle 12 \rangle} \circ \mathcal{Y}_{\langle 34 \rangle} \circ \langle 13 \rangle [13] \delta_{j_1}^{i_3} \delta_{j_2}^{i_4}$
3		$\mathcal{Y}_{\langle 12 \rangle} \circ \langle 12 \rangle [12] \delta_{j_1}^{i_3} \delta_{j_2}^{i_4}$
4	$2D\bar{Q}Q\bar{H}H$	$\langle 13 \rangle [23] \delta_{j_1}^{i_2} \delta_{j_3}^{i_4} \delta_{b_1}^{a_2}$
5		$\langle 13 \rangle [23] \delta_{j_3}^{i_2} \delta_{j_1}^{i_4} \delta_{b_1}^{a_2}$
6	$B_- B_- \bar{H} H$	$\langle 12 \rangle^2 \delta_{j_3}^{i_4}$
7	$B_+ B_+ \bar{H} H$	$[12]^2 \delta_{j_3}^{i_4}$
8	$W_- W_- \bar{H} H$	$\langle 12 \rangle^2 \delta^{I_1 I_2} \delta_{j_3}^{i_4}$
9	$W_+ W_+ \bar{H} H$	$[12]^2 \delta^{I_1 I_2} \delta_{j_3}^{i_4}$
10	$G_- G_- \bar{H} H$	$\langle 12 \rangle^2 \delta^{A_1 A_2} \delta_{j_3}^{i_4}$
11	$G_+ G_+ \bar{H} H$	$[12]^2 \delta^{A_1 A_2} \delta_{j_3}^{i_4}$
12	$B_- W_- \bar{H} H$	$\langle 12 \rangle^2 \sigma^{I_2 i_4} \delta_{j_3}^{i_4}$
13	$B_+ W_+ \bar{H} H$	$[12]^2 \sigma^{I_2 i_4} \delta_{j_3}^{i_4}$

Table 5.1: The table shows the thirteen dimension-six operators and their multiplicity as a result of the Hilbert series method. To each independent operator we associate and enumerate a set of independent minimal amplitudes.

minimal amplitudes, respectively for the dimension-six and the dimension-eight irrelevant operators.

The running of the Wilson coefficients

$$\dot{c}_i = 16\pi^2 \mu \frac{\partial}{\partial \mu} c_i, \quad (5.21)$$

of the thirteen dimension-six operators is

$$\begin{aligned} \dot{c}_1^{(6)} &= c_1^{(6)} \left(6g_1^2 Y_H^2 + \frac{9g_2^2}{2} + 108\lambda \right) + 6c_1^{(6)} \gamma_{\text{coll}}^H, \\ \dot{c}_2^{(6)} &= c_5^{(6)} (8g_1^2 Y_H Y_Q - 6g_2^2 + 48\mathcal{Y}_1 \bar{\mathcal{Y}}_1 + 24\mathcal{Y}_2 \bar{\mathcal{Y}}_2) + c_2^{(6)} \left(-\frac{8g_1^2 Y_H^2}{3} + 8g_2^2 + 24\lambda \right) + \\ &\quad + c_3^{(6)} \left(2g_1^2 Y_H^2 + \frac{17g_2^2}{2} - 12\lambda \right) + c_4^{(6)} (16g_1^2 Y_H Y_Q + 24\mathcal{Y}_1 \bar{\mathcal{Y}}_1 - 24\mathcal{Y}_2 \bar{\mathcal{Y}}_2) + 4c_2^{(6)} \gamma_{\text{coll}}^H + \dots, \\ \dot{c}_3^{(6)} &= c_3^{(6)} \left(26g_1^2 Y_H^2 + \frac{33g_2^2}{2} + 12\lambda \right) + c_4^{(6)} (32g_1^2 Y_H Y_Q + 48\mathcal{Y}_1 \bar{\mathcal{Y}}_1 - 48\mathcal{Y}_2 \bar{\mathcal{Y}}_2) \\ &\quad + c_5^{(6)} (16g_1^2 Y_H Y_Q + 24\mathcal{Y}_1 \bar{\mathcal{Y}}_1 - 24\mathcal{Y}_2 \bar{\mathcal{Y}}_2) - \frac{40}{3} c_2^{(6)} g_1^2 Y_H^2 + 4c_3^{(6)} \gamma_{\text{coll}}^H + \dots, \\ \dot{c}_4^{(6)} &= c_4^{(6)} \left(\frac{28g_1^2 Y_H^2}{3} + 14g_1^2 Y_Q^2 + \frac{21g_2^2}{2} + 8g_3^2 + 12\mathcal{Y}_1 \bar{\mathcal{Y}}_1 \right) + c_4^{(6)} (2\gamma_{\text{coll}}^H + 2\gamma_{\text{coll}}^Q) \\ &\quad + c_5^{(6)} \left(\frac{2g_1^2 Y_H^2}{3} + 4g_1^2 Y_Q^2 + \frac{11g_2^2}{6} - 4\mathcal{Y}_1 \bar{\mathcal{Y}}_1 + 8\mathcal{Y}_2 \bar{\mathcal{Y}}_2 \right) \\ &\quad + c_3^{(6)} \left(g_1^2 Y_H Y_Q - \frac{g_2^2}{12} + 2\mathcal{Y}_1 \bar{\mathcal{Y}}_1 - \mathcal{Y}_2 \bar{\mathcal{Y}}_2 \right) + c_2^{(6)} \left(-\frac{1}{3} g_1^2 Y_H Y_Q + \frac{g_2^2}{12} - \mathcal{Y}_1 \bar{\mathcal{Y}}_1 \right) + \dots, \end{aligned}$$

#	Hilbert series	Minimal amplitude	#	Hilbert series	Minimal amplitude
1	$\bar{H}^4 H^4$	$\mathcal{Y}_{[1234]} \circ \delta_{j_1}^{i_4} \delta_{j_2}^{i_5} \delta_{j_3}^{i_6} \delta_{j_4}^{i_8}$	34	$2D^2 B_- W_- \bar{H} H$	$(12)^3 [12] \sigma_{j_3}^{i_2 i_4}$
2	$B^2 \bar{H}^2 H^2$	$\mathcal{Y}_{[34]} \circ \langle 12 \rangle^2 \delta_{j_4}^{i_5} \delta_{j_3}^{i_6}$	35		$(12)^2 \langle 23 \rangle [23] \sigma_{j_3}^{i_2 i_4}$
3	$B_+^2 \bar{H}^2 H^2$	$\mathcal{Y}_{[34]} \circ [12]^2 \delta_{j_4}^{i_5} \delta_{j_3}^{i_6}$	36	$2D^2 B_+ W_+ \bar{H} H$	$[12]^3 \langle 12 \rangle \sigma_{j_3}^{i_2 i_4}$
4	$B_- W_- \bar{H}^2 H^2$	$\mathcal{Y}_{[34]} \circ \mathcal{Y}_{[56]} \circ \langle 12 \rangle^2 \delta_{j_4}^{i_6} \sigma_{j_3}^{i_2 i_5}$	37		$[12]^2 \langle 23 \rangle [23] \sigma_{j_3}^{i_2 i_4}$
5	$B_+ W_+ \bar{H}^2 H^2$	$\mathcal{Y}_{[34]} \circ \mathcal{Y}_{[56]} \circ [12]^2 \delta_{j_4}^{i_6} \sigma_{j_3}^{i_2 i_5}$	38	$D^2 B_- W_+ \bar{H} H$	$\langle 13 \rangle^2 [23]^2 \sigma_{j_3}^{i_2 i_4}$
6	$2W_- \bar{H}^2 H^2$	$\mathcal{Y}_{[34]} \circ \langle 12 \rangle^2 \delta_{j_4}^{i_5} \delta_{j_3}^{i_6}$	39	$D^2 W_- B_+ \bar{H} H$	$(13)^2 [23]^2 \sigma_{j_3}^{i_1 i_4}$
7		$\mathcal{Y}_{[12]} \circ \langle 12 \rangle^2 \sigma_{j_4}^{i_2 i_5 i_6} \sigma_{j_3}^{i_1}$	40	$2D^2 W_- \bar{H}^2 H^2$	$\mathcal{Y}_{[23]} \circ \mathcal{Y}_{[45]} \circ \langle 12 \rangle \langle 14 \rangle [24] \epsilon^{i_4 i_5} \sigma_{j_1}^{i_1}$
8	$2W_+^2 \bar{H}^2 H^2$	$\mathcal{Y}_{[34]} \circ [12]^2 \delta_{j_4}^{i_1} \delta_{j_3}^{i_5} \delta_{j_3}^{i_6}$	41		$\mathcal{Y}_{[23]} \circ \mathcal{Y}_{[45]} \circ \langle 12 \rangle \langle 13 \rangle [23] \delta_{j_3}^{i_5} \sigma_{j_3}^{i_1 i_4}$
9		$\mathcal{Y}_{[12]} \circ [12]^2 \sigma_{j_4}^{i_2 i_5 i_6} \sigma_{j_3}^{i_1}$	42	$2D^2 W_+ \bar{H}^2 H^2$	$\mathcal{Y}_{[23]} \circ \mathcal{Y}_{[45]} \circ [12] [14] \langle 24 \rangle \epsilon^{i_4 i_5} \sigma_{j_1}^{i_1}$
10	$G_-^2 \bar{H}^2 H^2$	$\mathcal{Y}_{[34]} \circ \langle 12 \rangle^2 \delta_{j_4}^{A_1 A_2} \delta_{j_3}^{i_5} \delta_{j_3}^{i_6}$	43		$\mathcal{Y}_{[23]} \circ \mathcal{Y}_{[45]} \circ [12] [13] \langle 23 \rangle \delta_{j_3}^{i_5} \sigma_{j_3}^{i_1 i_4}$
11	$G_+^2 \bar{H}^2 H^2$	$\mathcal{Y}_{[34]} \circ [12]^2 \delta_{j_4}^{A_1 A_2} \delta_{j_3}^{i_5} \delta_{j_3}^{i_6}$	44		$\mathcal{Y}_{[12]} \circ \langle 12 \rangle^2 [12]^2 \delta_{j_3}^{i_5} \delta_{j_3}^{i_4}$
12	$B_- W_-^2 \bar{H} H$	$\langle 12 \rangle \langle 23 \rangle \langle 13 \rangle \epsilon^{i_2 i_3} X_6 \sigma_{j_4}^{X_6 i_5}$	45	$3D^4 \bar{H}^2 H^2$	$\mathcal{Y}_{[12]} \circ \mathcal{Y}_{[34]} \circ \langle 13 \rangle^2 [13]^2 \delta_{j_1}^{i_2} \delta_{j_2}^{i_4}$
13	$B_+ W_+^2 \bar{H} H$	$[12] [23] [13] \epsilon^{i_2 i_3} X_6 \sigma_{j_4}^{X_6 i_5}$	46		$\mathcal{Y}_{[12]} \circ \mathcal{Y}_{[34]} \circ \langle 12 \rangle \langle 13 \rangle [12] [13] \delta_{j_1}^{i_2} \delta_{j_2}^{i_4}$
14	$W_-^3 \bar{H} H$	$\langle 12 \rangle \langle 23 \rangle \langle 13 \rangle \epsilon^{i_1 i_2 i_3} \delta_{j_4}^{i_5}$	47		$\mathcal{Y}_{[34]} \circ \mathcal{Y}_{[56]} \circ \langle 13 \rangle [23] \epsilon_{j_3 j_4}^{i_2 i_3} \delta_{j_1}^{i_5} \delta_{b_1}^{a_2}$
15	$W_+^3 \bar{H} H$	$[12] [23] [13] \epsilon^{i_1 i_2 i_3} \delta_{j_4}^{i_5}$	48	$4D \bar{Q} \bar{Q} \bar{H}^2 H^2$	$\mathcal{Y}_{[34]} \circ \mathcal{Y}_{[56]} \circ \langle 13 \rangle [23] \delta_{j_3}^{i_2} \delta_{j_3}^{i_5} \delta_{j_4}^{i_6} \delta_{b_1}^{a_2}$
16	$G_-^3 \bar{H} H$	$\langle 12 \rangle \langle 23 \rangle \langle 13 \rangle f^{A_1 A_2 A_3} \delta_{j_4}^{i_5}$	49		$\mathcal{Y}_{[34]} \circ \mathcal{Y}_{[56]} \circ \langle 15 \rangle [25] \delta_{j_3}^{i_2} \delta_{j_3}^{i_5} \delta_{j_4}^{i_6} \delta_{b_1}^{a_2}$
17	$G_+^3 \bar{H} H$	$[12] [23] [13] f^{A_1 A_2 A_3} \delta_{j_4}^{i_5}$	50		$\mathcal{Y}_{[34]} \circ \mathcal{Y}_{[56]} \circ \langle 13 \rangle [23] \delta_{j_1}^{i_2} \delta_{j_3}^{i_5} \delta_{j_3}^{i_6} \delta_{b_1}^{a_2}$
18	$2D^2 \bar{H}^3 H^3$	$\mathcal{Y}_{[123]} \circ \mathcal{Y}_{[456]} \circ \langle 12 \rangle [12] \delta_{j_1}^{i_4} \delta_{j_2}^{i_5} \delta_{j_3}^{i_6}$	51		$\langle 12 \rangle^2 [23] \delta_{j_4}^{i_5} \delta_{b_2}^{a_3} \sigma_{j_2}^{i_1 i_3}$
19		$\mathcal{Y}_{[123]} \circ \mathcal{Y}_{[456]} \circ \langle 14 \rangle [14] \delta_{j_1}^{i_4} \delta_{j_2}^{i_5} \delta_{j_3}^{i_6}$	52		$\langle 12 \rangle \langle 14 \rangle [34] \delta_{j_4}^{i_5} \delta_{b_2}^{a_3} \sigma_{j_2}^{i_1 i_3}$
20	$D^2 B_- B_+ \bar{H} H$	$\langle 13 \rangle^2 [23]^2 \delta_{j_3}^{i_4}$	53	$6DW_- \bar{Q} \bar{Q} \bar{H} H$	$\langle 12 \rangle^2 [23] \delta_{j_4}^{i_3} \delta_{b_2}^{a_3} \sigma_{j_2}^{i_1 i_5}$
21		$\langle 13 \rangle^2 [23]^2 \delta_{j_3}^{i_1} \delta_{j_3}^{i_4}$	54		$\langle 12 \rangle \langle 14 \rangle [34] \delta_{j_4}^{i_3} \delta_{b_2}^{a_3} \sigma_{j_2}^{i_1 i_5}$
22	$2D^2 W_- W_+ \bar{H} H$	$\langle 13 \rangle^2 [23]^2 \epsilon^{i_1 i_2} X_6 \sigma_{j_3}^{X_6 i_4}$	55		$\langle 12 \rangle^2 [23] \delta_{j_2}^{i_3} \delta_{b_2}^{a_3} \sigma_{j_4}^{i_1 i_5}$
23	$D^2 G_- G_+ \bar{H} H$	$\langle 13 \rangle^2 [23]^2 \delta_{j_3}^{A_1 A_2} \delta_{j_3}^{i_4}$	56		$\langle 12 \rangle \langle 14 \rangle [34] \delta_{j_2}^{i_3} \delta_{b_2}^{a_3} \sigma_{j_4}^{i_1 i_5}$
24	$D^2 B_- \bar{H}^2 H^2$	$\mathcal{Y}_{[23]} \circ \mathcal{Y}_{[45]} \circ \langle 12 \rangle \langle 14 \rangle [24] \delta_{j_3}^{i_4} \delta_{j_2}^{i_5}$	57		$[13]^2 \langle 23 \rangle \delta_{j_4}^{i_5} \delta_{b_2}^{a_3} \sigma_{j_2}^{i_1 i_3}$
25	$D^2 B_+ \bar{H}^2 H^2$	$\mathcal{Y}_{[23]} \circ \mathcal{Y}_{[45]} \circ [12] [14] \langle 24 \rangle \delta_{j_3}^{i_4} \delta_{j_2}^{i_5}$	58		$[13] [14] \langle 24 \rangle \delta_{j_4}^{i_3} \delta_{b_2}^{a_3} \sigma_{j_2}^{i_1 i_3}$
26	$D^2 B_-^2 \bar{H} H$	$\langle 12 \rangle^3 [12] \delta_{j_3}^{i_4}$	59	$6DW_+ \bar{Q} \bar{Q} \bar{H} H$	$[13]^2 \langle 23 \rangle \delta_{j_4}^{i_3} \delta_{b_2}^{a_3} \sigma_{j_2}^{i_1 i_5}$
27	$D^2 B_+^2 \bar{H} H$	$[12]^3 \langle 12 \rangle \delta_{j_3}^{i_4}$	60		$[13] [14] \langle 24 \rangle \delta_{j_4}^{i_3} \delta_{b_2}^{a_3} \sigma_{j_2}^{i_1 i_5}$
28		$\langle 12 \rangle^3 [12] \delta_{j_3}^{i_1} \delta_{j_3}^{i_4}$	61		$[13]^2 \langle 23 \rangle \delta_{j_2}^{i_3} \delta_{b_2}^{a_3} \sigma_{j_4}^{i_1 i_5}$
29	$2D^2 W_-^2 \bar{H} H$	$\mathcal{Y}_{[12]} \circ \langle 12 \rangle^2 \langle 23 \rangle [23] \epsilon^{i_1 i_2} X_6 \sigma_{j_3}^{X_6 i_4}$	62		$[13] [14] \langle 24 \rangle \delta_{j_2}^{i_3} \delta_{b_2}^{a_3} \sigma_{j_4}^{i_1 i_5}$
30		$[12]^3 \langle 12 \rangle \delta_{j_3}^{i_1} \delta_{j_3}^{i_4}$	63		$\langle 13 \rangle \langle 23 \rangle [23]^2 \delta_{j_3}^{i_2} \delta_{j_3}^{i_4} \delta_{b_1}^{a_2}$
31	$2D^2 W_+^2 \bar{H} H$	$\mathcal{Y}_{[12]} \circ [12]^2 \langle 23 \rangle [23] \epsilon^{i_1 i_2} X_6 \sigma_{j_3}^{X_6 i_4}$	64	$4D^3 \bar{Q} \bar{Q} \bar{H} H$	$\langle 12 \rangle \langle 13 \rangle [12] [23] \delta_{j_3}^{i_2} \delta_{j_3}^{i_4} \delta_{b_1}^{a_2}$
32		$\langle 12 \rangle^3 [12] \delta_{j_3}^{A_1 A_2} \delta_{j_3}^{i_4}$	65		$\langle 13 \rangle \langle 23 \rangle [23]^2 \delta_{j_1}^{i_2} \delta_{j_3}^{i_4} \delta_{b_1}^{a_2}$
33	$D^2 G_+^2 \bar{H} H$	$[12]^3 \langle 12 \rangle \delta_{j_3}^{A_1 A_2} \delta_{j_3}^{i_4}$	66		$\langle 12 \rangle \langle 13 \rangle [12] [23] \delta_{j_1}^{i_2} \delta_{j_3}^{i_4} \delta_{b_1}^{a_2}$

Table 5.2: The table shows all the dimension-eight operators, their multiplicity and a set of independent minimal amplitudes.

$$\begin{aligned}
\dot{c}_5^{(6)} &= c_5^{(6)} \left(8g_1^2 Y_H^2 + 6g_1^2 Y_Q^2 + \frac{41g_2^2}{6} + 8g_3^2 - 4\mathcal{Y}_1 \bar{\mathcal{Y}}_1 + 8\mathcal{Y}_2 \bar{\mathcal{Y}}_2 \right) + c_5^{(6)} \left(2\gamma_{\text{coll}}^H + 2\gamma_{\text{coll}}^Q \right) \\
&+ c_2^{(6)} \left(-\frac{g_2^2}{6} + \mathcal{Y}_1 \bar{\mathcal{Y}}_1 + \mathcal{Y}_2 \bar{\mathcal{Y}}_2 \right) + c_3^{(6)} \left(\frac{g_2^2}{6} - \mathcal{Y}_1 \bar{\mathcal{Y}}_1 - \mathcal{Y}_2 \bar{\mathcal{Y}}_2 \right) \\
&+ c_4^{(6)} (12\mathcal{Y}_2 \bar{\mathcal{Y}}_2 - 12\mathcal{Y}_1 \bar{\mathcal{Y}}_1) + \dots, \\
\dot{c}_6^{(6)} &= c_6^{(6)} \left(10g_1^2 Y_H^2 + \frac{3g_2^2}{2} + 12\lambda \right) + 6c_{12}^{(6)} g_1 g_2 Y_H + c_6^{(6)} (2\gamma_{\text{coll}}^H + 2\gamma_{\text{coll}}^B) + \dots, \\
\dot{c}_7^{(6)} &= c_7^{(6)} \left(10g_1^2 Y_H^2 + \frac{3g_2^2}{2} + 12\lambda \right) + 6c_{13}^{(6)} g_1 g_2 Y_H + c_7^{(6)} (2\gamma_{\text{coll}}^H + 2\gamma_{\text{coll}}^B) + \dots, \\
\dot{c}_8^{(6)} &= c_8^{(6)} \left(2g_1^2 Y_H^2 + \frac{7g_2^2}{2} + 12\lambda \right) + 2c_{12}^{(6)} g_1 g_2 Y_H + c_8^{(6)} (2\gamma_{\text{coll}}^H + 2\gamma_{\text{coll}}^W) + \dots, \\
\dot{c}_9^{(6)} &= c_9^{(6)} \left(2g_1^2 Y_H^2 + \frac{7g_2^2}{2} + 12\lambda \right) + 2c_{13}^{(6)} g_1 g_2 Y_H + c_9^{(6)} (2\gamma_{\text{coll}}^H + 2\gamma_{\text{coll}}^W) + \dots, \\
\dot{c}_{10}^{(6)} &= c_{10}^{(6)} \left(2g_1^2 Y_H^2 + \frac{3g_2^2}{2} + 12\lambda \right) + c_{10}^{(6)} (2\gamma_{\text{coll}}^H + 2\gamma_{\text{coll}}^G) + \dots, \\
\dot{c}_{11}^{(6)} &= c_{11}^{(6)} \left(2g_1^2 Y_H^2 + \frac{3g_2^2}{2} + 12\lambda \right) + c_{11}^{(6)} (2\gamma_{\text{coll}}^H + 2\gamma_{\text{coll}}^G) + \dots,
\end{aligned}$$

$$\begin{aligned}
\dot{c}_{12}^{(6)} &= c_{12}^{(6)} \left(6g_1^2 Y_H^2 + \frac{g_2^2}{2} + 4\lambda \right) + 4c_6^{(6)} g_1 g_2 Y_H + 4c_8^{(6)} g_1 g_2 Y_H \\
&\quad + c_{12}^{(6)} (2\gamma_{\text{coll}}^H + \gamma_{\text{coll}}^W + \gamma_{\text{coll}}^B) + \dots, \\
\dot{c}_{13}^{(6)} &= c_{13}^{(6)} \left(6g_1^2 Y_H^2 + \frac{g_2^2}{2} + 4\lambda \right) + 4c_7^{(6)} g_1 g_2 Y_H + 4c_9^{(6)} g_1 g_2 Y_H \\
&\quad + c_{13}^{(6)} (2\gamma_{\text{coll}}^H + \gamma_{\text{coll}}^W + \gamma_{\text{coll}}^B) + \dots,
\end{aligned}$$

where the dots indicate that the operator mixes with other operators which we are not considering, *i.e.* already at leading order in the couplings the sector we are looking at is not closed. The last term in the RG evolution of each coefficient is needed to isolate the UV contributions from the diagonal IR anomalous dimension. These results fully match with previous calculations in the literature, after a proper change of basis, and we take this as a cross-check for the on-shell methods techniques in this thesis.

Then we present the result for the running of the Wilson coefficients of the dimension-eight operators associated to the minimal amplitudes. Since most of the operators mix with operators outside the sector we are investigating, we are going to omit the dots, as well as the IR subtraction, *i.e.* we show $\dot{c}_i^{(8)} = \dot{c}_i^{(8),\text{UV}} - \dot{c}_i^{(8),\text{IR}}$.

$$\begin{aligned}
\dot{c}_1^{(8)} &= (6g_2^2 + 8g_1^2 Y_H^2 + 192\lambda) c_1^{(8)}, \\
\dot{c}_2^{(8)} &= (3g_2^2 + 20g_1^2 Y_H^2 + 48\lambda) c_2^{(8)} + 8g_1 g_2 Y_H c_4^{(8)}, \\
\dot{c}_3^{(8)} &= (3g_2^2 + 20g_1^2 Y_H^2 + 48\lambda) c_3^{(8)} + 8g_1 g_2 Y_H c_5^{(8)}, \\
\dot{c}_4^{(8)} &= 8g_1 g_2 Y_H c_2^{(8)} + (13g_2^2 + 12g_1^2 Y_H^2 + 40\lambda) c_4^{(8)} + 8g_1 g_2 Y_H c_6^{(8)} + 2g_1 g_2 Y_H c_7^{(8)}, \\
\dot{c}_5^{(8)} &= 8g_1 g_2 Y_H c_3^{(8)} + (13g_2^2 + 12g_1^2 Y_H^2 + 40\lambda) c_5^{(8)} + 8g_1 g_2 Y_H c_8^{(8)} + 2g_1 g_2 Y_H c_9^{(8)}, \\
\dot{c}_6^{(8)} &= 4g_1 g_2 Y_H c_4^{(8)} + (7g_2^2 + 4g_1^2 Y_H^2 + 48\lambda) c_6^{(8)} + (4g_2^2 - 4\lambda) c_7^{(8)}, \\
\dot{c}_7^{(8)} &= (31g_2^2 + 4g_1^2 Y_H^2 + 24\lambda) c_7^{(8)} + 8g_1 g_2 Y_H c_4^{(8)}, \\
\dot{c}_8^{(8)} &= 4g_1 g_2 Y_H c_5^{(8)} + (7g_2^2 + 4g_1^2 Y_H^2 + 48\lambda) c_8^{(8)} + (4g_2^2 - 4\lambda) c_9^{(8)}, \\
\dot{c}_9^{(8)} &= (31g_2^2 + 4g_1^2 Y_H^2 + 24\lambda) c_9^{(8)} + 8g_1 g_2 Y_H c_5^{(8)}, \\
\dot{c}_{10}^{(8)} &= (3g_2^2 + 4g_1^2 Y_H^2 + 48\lambda) c_{10}^{(8)}, \\
\dot{c}_{11}^{(8)} &= (3g_2^2 + 4g_1^2 Y_H^2 + 48\lambda) c_{11}^{(8)}, \\
\dot{c}_{12}^{(8)} &= \left(\frac{39g_2^2}{2} + 6g_1^2 Y_H^2 + 4\lambda \right) c_{12}^{(8)} + 4g_1 g_2 Y_H c_{14}^{(8)}, \\
\dot{c}_{13}^{(8)} &= \left(\frac{39g_2^2}{2} + 6g_1^2 Y_H^2 + 4\lambda \right) c_{13}^{(8)} + 4g_1 g_2 Y_H c_{15}^{(8)}, \\
\dot{c}_{14}^{(8)} &= \left(\frac{57g_2^2}{2} + 2g_1^2 Y_H^2 + 12\lambda \right) c_{14}^{(8)} + 3g_1 g_2 Y_H c_{12}^{(8)}, \\
\dot{c}_{15}^{(8)} &= \left(\frac{57g_2^2}{2} + 2g_1^2 Y_H^2 + 12\lambda \right) c_{15}^{(8)} + 3g_1 g_2 Y_H c_{13}^{(8)}, \\
\dot{c}_{16}^{(8)} &= \left(\frac{3g_2^2}{2} + 36g_3^2 + 2g_1^2 Y_H^2 + 12\lambda \right) c_{16}^{(8)}, \\
\dot{c}_{17}^{(8)} &= \left(\frac{3g_2^2}{2} + 36g_3^2 + 2g_1^2 Y_H^2 + 12\lambda \right) c_{17}^{(8)},
\end{aligned}$$

$$\begin{aligned}
\dot{c}'_{18} &= \left(10g_2^2 + \frac{116g_1^2 Y_H^2}{3} + 72\lambda \right) c_{18}^{(8)} + \left(\frac{17g_2^2}{6} - 26g_1^2 Y_H^2 - 4\lambda \right) c_{19}^{(8)} \\
&\quad + \left(-18g_2^2 + 108\mathcal{Y}_1 \bar{\mathcal{Y}}_1 + 108\mathcal{Y}_2 \bar{\mathcal{Y}}_2 \right) c_{47}^{(8)} + \left(18Y_H Y_Q g_1^2 + \frac{45g_2^2}{2} - 108\mathcal{Y}_1 \bar{\mathcal{Y}}_1 - 162\mathcal{Y}_2 \bar{\mathcal{Y}}_2 \right) c_{48}^{(8)} \\
&\quad + \left(-18Y_H Y_Q g_1^2 - \frac{9g_2^2}{2} + 54\mathcal{Y}_2 \bar{\mathcal{Y}}_2 \right) c_{49}^{(8)} + \left(36Y_H Y_Q g_1^2 + 54\mathcal{Y}_1 \bar{\mathcal{Y}}_1 - 54\mathcal{Y}_2 \bar{\mathcal{Y}}_2 \right) c_{50}^{(8)} , \\
\dot{c}'_{20} &= g_1^2 c_{44}^{(8)} Y_H^2 + \frac{1}{3} g_1^2 c_{45}^{(8)} Y_H^2 - \frac{1}{3} g_1^2 c_{46}^{(8)} Y_H^2 + 3g_1 g_2 c_{38}^{(8)} Y_H + 3g_1 g_2 c_{39}^{(8)} Y_H \\
&\quad + \left(9g_2^2 + 20g_1^2 Y_H^2 \right) c_{20}^{(8)} - 4g_1^2 Y_Q^2 c_{63}^{(8)} - 8g_1^2 Y_Q^2 c_{65}^{(8)} , \\
\dot{c}'_{19} &= \left(-\frac{34g_2^2}{3} - \frac{8g_1^2 Y_H^2}{3} + 16\lambda \right) c_{18}^{(8)} + \left(\frac{145g_2^2}{6} + 2g_1^2 Y_H^2 + 52\lambda \right) c_{19}^{(8)} \\
&\quad + \left(-27g_2^2 + 162\mathcal{Y}_1 \bar{\mathcal{Y}}_1 + 162\mathcal{Y}_2 \bar{\mathcal{Y}}_2 \right) c_{47}^{(8)} + \left(-18Y_H Y_Q g_1^2 + \frac{45g_2^2}{2} - 162\mathcal{Y}_1 \bar{\mathcal{Y}}_1 - 108\mathcal{Y}_2 \bar{\mathcal{Y}}_2 \right) c_{48}^{(8)} \\
&\quad + \left(18Y_H Y_Q g_1^2 + \frac{9g_2^2}{2} - 54\mathcal{Y}_2 \bar{\mathcal{Y}}_2 \right) c_{49}^{(8)} + \left(-36Y_H Y_Q g_1^2 - 54\mathcal{Y}_1 \bar{\mathcal{Y}}_1 + 54\mathcal{Y}_2 \bar{\mathcal{Y}}_2 \right) c_{50}^{(8)} , \\
\dot{c}'_{21} &= \frac{1}{4} c_{44}^{(8)} g_2^2 + \frac{1}{12} c_{45}^{(8)} g_2^2 - \frac{1}{12} c_{46}^{(8)} g_2^2 - c_{63}^{(8)} g_2^2 - 2c_{65}^{(8)} g_2^2 + g_1 Y_H c_{38}^{(8)} g_2 + g_1 Y_H c_{39}^{(8)} g_2 \\
&\quad + \left(\frac{77g_2^2}{3} + 12g_1^2 Y_H^2 \right) c_{21}^{(8)} , \\
\dot{c}'_{22} &= \left(\frac{25g_2^2}{3} + 12g_1^2 Y_H^2 \right) c_{22}^{(8)} - ig_2^2 c_{63}^{(8)} , \\
\dot{c}'_{23} &= -\frac{2}{3} c_{63}^{(8)} g_3^2 - \frac{4}{3} c_{65}^{(8)} g_3^2 + \left(9g_2^2 + 22g_3^2 + 12g_1^2 Y_H^2 \right) c_{23}^{(8)} , \\
\dot{c}'_{24} &= \left(\frac{25g_2^2}{2} + \frac{38g_1^2 Y_H^2}{3} + 12\lambda \right) c_{24}^{(8)} , \\
\dot{c}'_{25} &= \left(\frac{25g_2^2}{2} + \frac{38g_1^2 Y_H^2}{3} + 12\lambda \right) c_{25}^{(8)} , \\
\dot{c}'_{26} &= \left(\frac{3g_2^2}{2} + \frac{10g_1^2 Y_H^2}{3} + 12\lambda \right) c_{26}^{(8)} + g_1 g_2 Y_H c_{34}^{(8)} - \frac{1}{2} g_1 g_2 Y_H c_{35}^{(8)} , \\
\dot{c}'_{27} &= \left(\frac{3g_2^2}{2} + \frac{10g_1^2 Y_H^2}{3} + 12\lambda \right) c_{27}^{(8)} + g_1 g_2 Y_H c_{36}^{(8)} - \frac{1}{2} g_1 g_2 Y_H c_{37}^{(8)} , \\
\dot{c}'_{28} &= -\frac{25}{6} ic_{29}^{(8)} g_2^2 + \frac{1}{3} g_1 Y_H c_{34}^{(8)} g_2 - \frac{1}{6} g_1 Y_H c_{35}^{(8)} g_2 + \left(\frac{11g_2^2}{6} + 2g_1^2 Y_H^2 + 12\lambda \right) c_{28}^{(8)} , \\
\dot{c}'_{29} &= 20ic_{28}^{(8)} g_2^2 - 4ig_1 Y_H c_{34}^{(8)} g_2 + 2ig_1 Y_H c_{35}^{(8)} g_2 + \left(\frac{22g_2^2}{3} + 8g_1^2 Y_H^2 \right) c_{29}^{(8)} , \\
\dot{c}'_{30} &= -\frac{25}{6} ic_{31}^{(8)} g_2^2 - \frac{1}{3} g_1 Y_H c_{36}^{(8)} g_2 + \frac{1}{6} g_1 Y_H c_{37}^{(8)} g_2 + \left(\frac{11g_2^2}{6} + 2g_1^2 Y_H^2 + 12\lambda \right) c_{30}^{(8)} , \\
\dot{c}'_{31} &= 20ic_{30}^{(8)} g_2^2 + 4ig_1 Y_H c_{36}^{(8)} g_2 - 2ig_1 Y_H c_{37}^{(8)} g_2 + \left(\frac{22g_2^2}{3} + 8g_1^2 Y_H^2 \right) c_{31}^{(8)} , \\
\dot{c}'_{32} &= \left(\frac{3g_2^2}{2} + 2g_1^2 Y_H^2 + 12\lambda \right) c_{32}^{(8)} , \\
\dot{c}'_{33} &= \left(\frac{3g_2^2}{2} + 2g_1^2 Y_H^2 + 12\lambda \right) c_{33}^{(8)} ,
\end{aligned}$$

$$\begin{aligned}
\dot{c}_{34}^{(8)} &= \frac{2}{3}g_1g_2Y_Hc_{26}^{(8)} + \frac{2}{3}g_1g_2Y_Hc_{28}^{(8)} + \frac{5}{3}ig_1g_2Y_Hc_{29}^{(8)} + \left(-\frac{g_2^2}{3} + \frac{8g_1^2Y_H^2}{3} + 4\lambda\right)c_{34}^{(8)} \\
&\quad + \left(-\frac{5g_2^2}{12} + \frac{11g_1^2Y_H^2}{3} - 2\lambda\right)c_{35}^{(8)}, \\
\dot{c}_{35}^{(8)} &= \left(10g_1^2Y_H^2 - \frac{7g_2^2}{6}\right)c_{35}^{(8)}, \\
\dot{c}_{36}^{(8)} &= \frac{2}{3}g_1g_2Y_Hc_{27}^{(8)} + \frac{2}{3}g_1g_2Y_Hc_{30}^{(8)} + \frac{5}{3}ig_1g_2Y_Hc_{31}^{(8)} + \left(-\frac{g_2^2}{3} + \frac{8g_1^2Y_H^2}{3} + 4\lambda\right)c_{36}^{(8)} \\
&\quad + \left(-\frac{5g_2^2}{12} + \frac{11g_1^2Y_H^2}{3} - 2\lambda\right)c_{37}^{(8)}, \\
\dot{c}_{37}^{(8)} &= \left(10g_1^2Y_H^2 - \frac{7g_2^2}{6}\right)c_{37}^{(8)}, \\
\dot{c}_{38}^{(8)} &= 4g_1g_2Y_Hc_{20}^{(8)} + 4g_1g_2Y_Hc_{21}^{(8)} + (16g_1^2Y_H^2 - 2g_2^2)c_{38}^{(8)} + \frac{1}{3}g_1g_2Y_Hc_{44}^{(8)} + \frac{1}{3}g_1g_2Y_Hc_{45}^{(8)} \\
&\quad - \frac{1}{3}g_1g_2Y_Hc_{46}^{(8)} - 4g_1g_2Y_Qc_{63}^{(8)}, \\
\dot{c}_{39}^{(8)} &= 4g_1g_2Y_Hc_{20}^{(8)} + 4g_1g_2Y_Hc_{21}^{(8)} + (16g_1^2Y_H^2 - 2g_2^2)c_{39}^{(8)} + \frac{1}{3}g_1g_2Y_Hc_{44}^{(8)} + \frac{1}{3}g_1g_2Y_Hc_{45}^{(8)} \\
&\quad - \frac{1}{3}g_1g_2Y_Hc_{46}^{(8)} - 4g_1g_2Y_Qc_{63}^{(8)}, \\
\dot{c}_{40}^{(8)} &= \left(\frac{73g_2^2}{4} + 17g_1^2Y_H^2 + 10\lambda\right)c_{40}^{(8)} + \left(\frac{17g_2^2}{12} + \frac{g_1^2Y_H^2}{3} - 2\lambda\right)c_{41}^{(8)} \\
&\quad + (-4g_2^2 + 24\mathcal{Y}_1\bar{\mathcal{Y}}_1 + 24\mathcal{Y}_2\bar{\mathcal{Y}}_2)c_{51}^{(8)} + (2g_2^2 - 12\mathcal{Y}_1\bar{\mathcal{Y}}_1 - 12\mathcal{Y}_2\bar{\mathcal{Y}}_2)c_{52}^{(8)} \\
&\quad + (8Y_HY_Qg_1^2 + 2g_2^2 - 24\mathcal{Y}_2\bar{\mathcal{Y}}_2)c_{53}^{(8)} + (-4Y_HY_Qg_1^2 - g_2^2 + 12\mathcal{Y}_2\bar{\mathcal{Y}}_2)c_{54}^{(8)} \\
&\quad + (16Y_HY_Qg_1^2 + 24\mathcal{Y}_1\bar{\mathcal{Y}}_1 - 24\mathcal{Y}_2\bar{\mathcal{Y}}_2)c_{55}^{(8)} + (-8Y_HY_Qg_1^2 - 12\mathcal{Y}_1\bar{\mathcal{Y}}_1 + 12\mathcal{Y}_2\bar{\mathcal{Y}}_2)c_{56}^{(8)}, \\
\dot{c}_{41}^{(8)} &= \left(\frac{17g_2^2}{12} + \frac{g_1^2Y_H^2}{3} - 2\lambda\right)c_{40}^{(8)} + \left(\frac{73g_2^2}{4} + 17g_1^2Y_H^2 + 10\lambda\right)c_{41}^{(8)} \\
&\quad + (4g_2^2 - 24\mathcal{Y}_1\bar{\mathcal{Y}}_1 - 24\mathcal{Y}_2\bar{\mathcal{Y}}_2)c_{51}^{(8)} + (6g_2^2 - 36\mathcal{Y}_1\bar{\mathcal{Y}}_1 - 36\mathcal{Y}_2\bar{\mathcal{Y}}_2)c_{52}^{(8)} \\
&\quad + (-8Y_HY_Qg_1^2 + 6g_2^2 - 48\mathcal{Y}_1\bar{\mathcal{Y}}_1 - 24\mathcal{Y}_2\bar{\mathcal{Y}}_2)c_{53}^{(8)} + (-12Y_HY_Qg_1^2 + 9g_2^2 - 72\mathcal{Y}_1\bar{\mathcal{Y}}_1 - 36\mathcal{Y}_2\bar{\mathcal{Y}}_2)c_{54}^{(8)} \\
&\quad + (-16Y_HY_Qg_1^2 - 24\mathcal{Y}_1\bar{\mathcal{Y}}_1 + 24\mathcal{Y}_2\bar{\mathcal{Y}}_2)c_{55}^{(8)} + (-24Y_HY_Qg_1^2 - 36\mathcal{Y}_1\bar{\mathcal{Y}}_1 + 36\mathcal{Y}_2\bar{\mathcal{Y}}_2)c_{56}^{(8)}, \\
\dot{c}_{42}^{(8)} &= \left(\frac{73g_2^2}{4} + 17g_1^2Y_H^2 + 10\lambda\right)c_{42}^{(8)} + \left(\frac{17g_2^2}{12} + \frac{g_1^2Y_H^2}{3} - 2\lambda\right)c_{43}^{(8)} \\
&\quad + (4g_2^2 - 24\mathcal{Y}_1\bar{\mathcal{Y}}_1 - 24\mathcal{Y}_2\bar{\mathcal{Y}}_2)c_{57}^{(8)} + (2g_2^2 - 12\mathcal{Y}_1\bar{\mathcal{Y}}_1 - 12\mathcal{Y}_2\bar{\mathcal{Y}}_2)c_{58}^{(8)} \\
&\quad + (-8Y_HY_Qg_1^2 - 2g_2^2 + 24\mathcal{Y}_2\bar{\mathcal{Y}}_2)c_{59}^{(8)} + (-4Y_HY_Qg_1^2 - g_2^2 + 12\mathcal{Y}_2\bar{\mathcal{Y}}_2)c_{60}^{(8)} \\
&\quad + (-16Y_HY_Qg_1^2 - 24\mathcal{Y}_1\bar{\mathcal{Y}}_1 + 24\mathcal{Y}_2\bar{\mathcal{Y}}_2)c_{61}^{(8)} + (-8Y_HY_Qg_1^2 - 12\mathcal{Y}_1\bar{\mathcal{Y}}_1 + 12\mathcal{Y}_2\bar{\mathcal{Y}}_2)c_{62}^{(8)}, \\
\dot{c}_{43}^{(8)} &= \left(\frac{17g_2^2}{12} + \frac{g_1^2Y_H^2}{3} - 2\lambda\right)c_{42}^{(8)} + \left(\frac{73g_2^2}{4} + 17g_1^2Y_H^2 + 10\lambda\right)c_{43}^{(8)} \\
&\quad + (-4g_2^2 + 24\mathcal{Y}_1\bar{\mathcal{Y}}_1 + 24\mathcal{Y}_2\bar{\mathcal{Y}}_2)c_{57}^{(8)} + (6g_2^2 - 36\mathcal{Y}_1\bar{\mathcal{Y}}_1 - 36\mathcal{Y}_2\bar{\mathcal{Y}}_2)c_{58}^{(8)} \\
&\quad + (8Y_HY_Qg_1^2 - 6g_2^2 + 48\mathcal{Y}_1\bar{\mathcal{Y}}_1 + 24\mathcal{Y}_2\bar{\mathcal{Y}}_2)c_{59}^{(8)} + (-12Y_HY_Qg_1^2 + 9g_2^2 - 72\mathcal{Y}_1\bar{\mathcal{Y}}_1 - 36\mathcal{Y}_2\bar{\mathcal{Y}}_2)c_{60}^{(8)} \\
&\quad + (16Y_HY_Qg_1^2 + 24\mathcal{Y}_1\bar{\mathcal{Y}}_1 - 24\mathcal{Y}_2\bar{\mathcal{Y}}_2)c_{61}^{(8)} + (-24Y_HY_Qg_1^2 - 36\mathcal{Y}_1\bar{\mathcal{Y}}_1 + 36\mathcal{Y}_2\bar{\mathcal{Y}}_2)c_{62}^{(8)},
\end{aligned}$$

$$\begin{aligned}
\dot{c}_{44}^{(8)} &= 12c_{21}^{(8)}g_2^2 - \frac{8}{3}g_1Y_Hc_{38}^{(8)}g_2 - \frac{8}{3}g_1Y_Hc_{39}^{(8)}g_2 + 16g_1^2Y_H^2c_{20}^{(8)} + \left(26g_2^2 + \frac{100g_1^2Y_H^2}{3} + \frac{32\lambda}{3}\right)c_{44}^{(8)} \\
&+ \left(5g_2^2 + \frac{16\lambda}{3}\right)c_{45}^{(8)} + \left(-\frac{14g_2^2}{3} - \frac{28g_1^2Y_H^2}{3} - \frac{8\lambda}{3}\right)c_{46}^{(8)} + (2g_2^2 + 8\mathcal{Y}_1\bar{\mathcal{Y}}_1 - 8\mathcal{Y}_2\bar{\mathcal{Y}}_2)c_{63}^{(8)} \\
&+ (-4g_2^2 + 24\mathcal{Y}_1\bar{\mathcal{Y}}_1 + 24\mathcal{Y}_2\bar{\mathcal{Y}}_2)c_{64}^{(8)} + (24\mathcal{Y}_1\bar{\mathcal{Y}}_1 + 24\mathcal{Y}_2\bar{\mathcal{Y}}_2)c_{65}^{(8)}, \\
\dot{c}_{45}^{(8)} &= 2c_{21}^{(8)}g_2^2 + \frac{2}{3}g_1Y_Hc_{38}^{(8)}g_2 + \frac{2}{3}g_1Y_Hc_{39}^{(8)}g_2 + \frac{8}{3}g_1^2Y_H^2c_{20}^{(8)} + \left(-\frac{17g_2^2}{6} - \frac{22g_1^2Y_H^2}{3} + \frac{40\lambda}{3}\right)c_{44}^{(8)} \\
&+ \left(\frac{g_2^2}{2} - 6g_1^2Y_H^2 + \frac{88\lambda}{3}\right)c_{45}^{(8)} + \left(\frac{11g_2^2}{3} + 4g_1^2Y_H^2 - \frac{28\lambda}{3}\right)c_{46}^{(8)} \\
&+ (-4Y_HY_Qg_1^2 - g_2^2 + 16\mathcal{Y}_2\bar{\mathcal{Y}}_2)c_{63}^{(8)} + (8Y_HY_Qg_1^2 + 2g_2^2 - 24\mathcal{Y}_2\bar{\mathcal{Y}}_2)c_{64}^{(8)} \\
&+ (-8Y_HY_Qg_1^2 - 8\mathcal{Y}_1\bar{\mathcal{Y}}_1 + 16\mathcal{Y}_2\bar{\mathcal{Y}}_2)c_{65}^{(8)} + (16Y_HY_Qg_1^2 + 24\mathcal{Y}_1\bar{\mathcal{Y}}_1 - 24\mathcal{Y}_2\bar{\mathcal{Y}}_2)c_{66}^{(8)}, \\
\dot{c}_{46}^{(8)} &= 12c_{21}^{(8)}g_2^2 - \frac{28}{3}g_1Y_Hc_{38}^{(8)}g_2 - \frac{28}{3}g_1Y_Hc_{39}^{(8)}g_2 + 16g_1^2Y_H^2c_{20}^{(8)} + \left(\frac{41g_2^2}{3} - \frac{28g_1^2Y_H^2}{3} + \frac{16\lambda}{3}\right)c_{44}^{(8)} \\
&+ \left(5g_2^2 - 20g_1^2Y_H^2 + \frac{16\lambda}{3}\right)c_{45}^{(8)} + \left(\frac{23g_2^2}{3} + 20g_1^2Y_H^2 + \frac{8\lambda}{3}\right)c_{46}^{(8)} \\
&+ (-8Y_HY_Qg_1^2 + 2g_2^2 + 16\mathcal{Y}_1\bar{\mathcal{Y}}_1 - 16\mathcal{Y}_2\bar{\mathcal{Y}}_2)c_{63}^{(8)} + (16Y_HY_Qg_1^2 - 4g_2^2 + 48\mathcal{Y}_1\bar{\mathcal{Y}}_1)c_{64}^{(8)} \\
&+ (-16Y_HY_Qg_1^2 + 48\mathcal{Y}_2\bar{\mathcal{Y}}_2)c_{65}^{(8)} + (32Y_HY_Qg_1^2 + 48\mathcal{Y}_1\bar{\mathcal{Y}}_1 - 48\mathcal{Y}_2\bar{\mathcal{Y}}_2)c_{66}^{(8)}, \\
\dot{c}_{47}^{(8)} &= \left(\frac{2g_2^2}{27} - \frac{4\mathcal{Y}_1\bar{\mathcal{Y}}_1}{9} - \frac{4\mathcal{Y}_2\bar{\mathcal{Y}}_2}{9}\right)c_{18}^{(8)} + \left(-\frac{g_2^2}{27} + \frac{2\mathcal{Y}_1\bar{\mathcal{Y}}_1}{9} + \frac{2\mathcal{Y}_2\bar{\mathcal{Y}}_2}{9}\right)c_{19}^{(8)} \\
&+ \left(\frac{47g_2^2}{3} + 8g_3^2 + \frac{14g_1^2Y_H^2}{3} + 6g_1^2Y_Q^2 + 8\mathcal{Y}_1\bar{\mathcal{Y}}_1 + 8\mathcal{Y}_2\bar{\mathcal{Y}}_2 + 20\lambda\right)c_{47}^{(8)} \\
&+ \left(-\frac{17g_2^2}{12} + \frac{19g_1^2Y_H^2}{3} - 6\mathcal{Y}_1\bar{\mathcal{Y}}_1 + 6\mathcal{Y}_2\bar{\mathcal{Y}}_2 + 2\lambda\right)c_{48}^{(8)} \\
&+ \left(-\frac{17g_2^2}{12} - 7g_1^2Y_H^2 + 6\mathcal{Y}_1\bar{\mathcal{Y}}_1 - 6\mathcal{Y}_2\bar{\mathcal{Y}}_2 + 2\lambda\right)c_{49}^{(8)} + (12\mathcal{Y}_2\bar{\mathcal{Y}}_2 - 12\mathcal{Y}_1\bar{\mathcal{Y}}_1)c_{50}^{(8)}, \\
\dot{c}_{48}^{(8)} &= \left(\frac{4g_2^2}{27} - \frac{8\mathcal{Y}_1\bar{\mathcal{Y}}_1}{9} - \frac{8\mathcal{Y}_2\bar{\mathcal{Y}}_2}{9}\right)c_{18}^{(8)} + \left(-\frac{g_2^2}{27} + \frac{2\mathcal{Y}_1\bar{\mathcal{Y}}_1}{9} + \frac{2\mathcal{Y}_2\bar{\mathcal{Y}}_2}{9}\right)c_{19}^{(8)} \\
&+ \left(\frac{103g_2^2}{12} + 8g_3^2 + \frac{49g_1^2Y_H^2}{3} + 6g_1^2Y_Q^2 - 4\mathcal{Y}_1\bar{\mathcal{Y}}_1 + 20\mathcal{Y}_2\bar{\mathcal{Y}}_2 + 30\lambda\right)c_{48}^{(8)} \\
&+ \left(\frac{17g_2^2}{6} + \frac{2g_1^2Y_H^2}{3} - 4\lambda\right)c_{47}^{(8)} + \left(\frac{17g_2^2}{12} - 13g_1^2Y_H^2 + 12\mathcal{Y}_1\bar{\mathcal{Y}}_1 - 12\mathcal{Y}_2\bar{\mathcal{Y}}_2 - 2\lambda\right)c_{49}^{(8)} \\
&+ (24\mathcal{Y}_2\bar{\mathcal{Y}}_2 - 24\mathcal{Y}_1\bar{\mathcal{Y}}_1)c_{50}^{(8)}, \\
\dot{c}_{49}^{(8)} &= \left(\frac{g_2^2}{27} - \frac{2\mathcal{Y}_1\bar{\mathcal{Y}}_1}{9} - \frac{2\mathcal{Y}_2\bar{\mathcal{Y}}_2}{9}\right)c_{19}^{(8)} + \left(-\frac{17g_2^2}{6} - \frac{2g_1^2Y_H^2}{3} + 4\lambda\right)c_{47}^{(8)} \\
&+ \left(\frac{205g_2^2}{12} + 8g_3^2 + 5g_1^2Y_H^2 + 6g_1^2Y_Q^2 + 8\mathcal{Y}_1\bar{\mathcal{Y}}_1 + 8\mathcal{Y}_2\bar{\mathcal{Y}}_2 + 18\lambda\right)c_{49}^{(8)} \\
&+ \left(-\frac{17g_2^2}{12} - \frac{g_1^2Y_H^2}{3} + 2\lambda\right)c_{48}^{(8)},
\end{aligned}$$

$$\begin{aligned}
\dot{c}_{50}^{(8)} &= \left(\frac{16}{27} Y_H Y_Q g_1^2 - \frac{2g_2^2}{27} + \frac{4\mathcal{Y}_1 \bar{\mathcal{Y}}_1}{3} - \frac{4\mathcal{Y}_2 \bar{\mathcal{Y}}_2}{9} \right) c_{18}^{(8)} \\
&+ \left(-\frac{4}{9} Y_H Y_Q g_1^2 + \frac{g_2^2}{27} - \frac{8\mathcal{Y}_1 \bar{\mathcal{Y}}_1}{9} + \frac{4\mathcal{Y}_2 \bar{\mathcal{Y}}_2}{9} \right) c_{19}^{(8)} + \left(-\frac{17g_2^2}{6} - \frac{2g_1^2 Y_H^2}{3} + 4\lambda \right) c_{47}^{(8)} \\
&+ \left(\frac{11g_2^2}{6} + \frac{2g_1^2 Y_H^2}{3} + 4g_1^2 Y_Q^2 - 4\mathcal{Y}_1 \bar{\mathcal{Y}}_1 + 8\mathcal{Y}_2 \bar{\mathcal{Y}}_2 \right) c_{48}^{(8)} \\
&+ (g_2^2 - 4g_1^2 Y_Q^2 + 4\mathcal{Y}_1 \bar{\mathcal{Y}}_1 - 8\mathcal{Y}_2 \bar{\mathcal{Y}}_2 - 4\lambda) c_{49}^{(8)} \\
&+ \left(\frac{41g_2^2}{3} + 8g_3^2 + 18g_1^2 Y_H^2 + 14g_1^2 Y_Q^2 + 24\mathcal{Y}_1 \bar{\mathcal{Y}}_1 + 28\lambda \right) c_{50}^{(8)}, \\
\dot{c}_{51}^{(8)} &= \left(-\frac{g_2^2}{6} + \mathcal{Y}_1 \bar{\mathcal{Y}}_1 + \mathcal{Y}_2 \bar{\mathcal{Y}}_2 \right) c_{40}^{(8)} \\
&+ (2Y_H^2 g_1^2 + 6Y_Q^2 g_1^2 + 4Y_H Y_Q g_1^2 + 14g_2^2 + 8g_3^2 + 6\mathcal{Y}_1 \bar{\mathcal{Y}}_1 + 2\mathcal{Y}_2 \bar{\mathcal{Y}}_2 + 12\lambda) c_{51}^{(8)} \\
&+ \left(-\frac{11}{3} Y_H^2 g_1^2 - 2Y_H Y_Q g_1^2 - \frac{11g_2^2}{4} - 2\mathcal{Y}_2 \bar{\mathcal{Y}}_2 + 6\lambda \right) c_{52}^{(8)} \\
&+ \left(-\frac{g_2^2}{6} - 2\mathcal{Y}_1 \bar{\mathcal{Y}}_1 + 4\mathcal{Y}_2 \bar{\mathcal{Y}}_2 + 4\lambda \right) c_{53}^{(8)} + \left(-\frac{17g_2^2}{12} - \frac{g_1^2 Y_H^2}{3} + 2\lambda \right) c_{54}^{(8)} \\
&+ \left(\frac{16g_2^2}{3} + 4\mathcal{Y}_2 \bar{\mathcal{Y}}_2 \right) c_{55}^{(8)}, \\
\dot{c}_{52}^{(8)} &= \left(\frac{g_2^2}{6} - \mathcal{Y}_1 \bar{\mathcal{Y}}_1 - \mathcal{Y}_2 \bar{\mathcal{Y}}_2 \right) c_{40}^{(8)} + \left(-8Y_H Y_Q g_1^2 - 2g_2^2 - \frac{8\mathcal{Y}_2 \bar{\mathcal{Y}}_2}{3} \right) c_{51}^{(8)} \\
&+ \left(\frac{28Y_H^2 g_1^2}{3} + 6Y_Q^2 g_1^2 - 4Y_H Y_Q g_1^2 + \frac{33g_2^2}{2} + 8g_3^2 + 6\mathcal{Y}_1 \bar{\mathcal{Y}}_1 + 2\mathcal{Y}_2 \bar{\mathcal{Y}}_2 \right) c_{52}^{(8)} \\
&+ \left(\frac{8g_2^2}{3} + \frac{2g_1^2 Y_H^2}{3} - 2\mathcal{Y}_1 \bar{\mathcal{Y}}_1 + 4\mathcal{Y}_2 \bar{\mathcal{Y}}_2 \right) c_{54}^{(8)} + \left(-2g_2^2 - 4\mathcal{Y}_1 \bar{\mathcal{Y}}_1 + \frac{4\mathcal{Y}_2 \bar{\mathcal{Y}}_2}{3} \right) c_{55}^{(8)} \\
&+ \left(\frac{7g_2^2}{3} - 6\mathcal{Y}_1 \bar{\mathcal{Y}}_1 + 6\mathcal{Y}_2 \bar{\mathcal{Y}}_2 \right) c_{56}^{(8)}, \\
\dot{c}_{53}^{(8)} &= \left(\frac{g_2^2}{6} - \mathcal{Y}_1 \bar{\mathcal{Y}}_1 - \mathcal{Y}_2 \bar{\mathcal{Y}}_2 \right) c_{40}^{(8)} + \left(-2g_2^2 - \frac{20\mathcal{Y}_1 \bar{\mathcal{Y}}_1}{3} + 4\mathcal{Y}_2 \bar{\mathcal{Y}}_2 \right) c_{51}^{(8)} \\
&+ \left(2Y_H^2 g_1^2 + 6Y_Q^2 g_1^2 + 4Y_H Y_Q g_1^2 + \frac{37g_2^2}{3} + 8g_3^2 - \frac{8\mathcal{Y}_1 \bar{\mathcal{Y}}_1}{3} + 4\mathcal{Y}_2 \bar{\mathcal{Y}}_2 + 4\lambda \right) c_{53}^{(8)} \\
&+ \left(g_2^2 - \frac{2\mathcal{Y}_1 \bar{\mathcal{Y}}_1}{3} + 2\mathcal{Y}_2 \bar{\mathcal{Y}}_2 \right) c_{52}^{(8)} + \left(-3Y_H^2 g_1^2 - 2Y_H Y_Q g_1^2 + \frac{13g_2^2}{12} - \frac{2\mathcal{Y}_1 \bar{\mathcal{Y}}_1}{3} + 2\lambda \right) c_{54}^{(8)} \\
&+ \left(-\frac{26g_2^2}{3} - \frac{16\mathcal{Y}_1 \bar{\mathcal{Y}}_1}{3} \right) c_{55}^{(8)} + \left(-g_2^2 + \frac{2\mathcal{Y}_1 \bar{\mathcal{Y}}_1}{3} - 2\mathcal{Y}_2 \bar{\mathcal{Y}}_2 \right) c_{56}^{(8)}, \\
\dot{c}_{54}^{(8)} &= \left(-\frac{g_2^2}{6} + \mathcal{Y}_1 \bar{\mathcal{Y}}_1 + \mathcal{Y}_2 \bar{\mathcal{Y}}_2 \right) c_{40}^{(8)} + \left(\frac{g_2^2}{6} - \mathcal{Y}_1 \bar{\mathcal{Y}}_1 - \mathcal{Y}_2 \bar{\mathcal{Y}}_2 \right) c_{41}^{(8)} \\
&+ \left(4g_2^2 + \frac{8\mathcal{Y}_1 \bar{\mathcal{Y}}_1}{3} + \frac{8\mathcal{Y}_2 \bar{\mathcal{Y}}_2}{3} \right) c_{51}^{(8)} + \left(2g_2^2 - \frac{4\mathcal{Y}_1 \bar{\mathcal{Y}}_1}{3} + 4\mathcal{Y}_2 \bar{\mathcal{Y}}_2 \right) c_{52}^{(8)} \\
&+ \left(8Y_H^2 g_1^2 + 6Y_Q^2 g_1^2 - 4Y_H Y_Q g_1^2 + \frac{79g_2^2}{6} + 8g_3^2 + \frac{8\mathcal{Y}_1 \bar{\mathcal{Y}}_1}{3} + 4\mathcal{Y}_2 \bar{\mathcal{Y}}_2 \right) c_{54}^{(8)} \\
&+ \left(-8Y_H Y_Q g_1^2 + 2g_2^2 + \frac{8\mathcal{Y}_1 \bar{\mathcal{Y}}_1}{3} \right) c_{53}^{(8)} + \left(\frac{16\mathcal{Y}_1 \bar{\mathcal{Y}}_1}{3} - \frac{16\mathcal{Y}_2 \bar{\mathcal{Y}}_2}{3} \right) c_{55}^{(8)} \\
&+ \left(-\frac{20g_2^2}{3} + \frac{4\mathcal{Y}_1 \bar{\mathcal{Y}}_1}{3} - 4\mathcal{Y}_2 \bar{\mathcal{Y}}_2 \right) c_{56}^{(8)},
\end{aligned}$$

$$\begin{aligned}
c_{55}^{\prime(8)} &= \left(\frac{1}{3} Y_H Y_Q g_1^2 - \frac{g_2^2}{12} + \mathcal{Y}_1 \bar{\mathcal{Y}}_1 \right) c_{40}^{(8)} + \left(2g_2^2 + \frac{2\mathcal{Y}_1 \bar{\mathcal{Y}}_1}{3} + 2\mathcal{Y}_2 \bar{\mathcal{Y}}_2 \right) c_{51}^{(8)} \\
&+ \left(-g_2^2 + \frac{2\mathcal{Y}_1 \bar{\mathcal{Y}}_1}{3} - 2\mathcal{Y}_2 \bar{\mathcal{Y}}_2 \right) c_{52}^{(8)} + \left(-\frac{11g_2^2}{6} + 4g_1^2 Y_Q^2 - \frac{4\mathcal{Y}_1 \bar{\mathcal{Y}}_1}{3} + 2\mathcal{Y}_2 \bar{\mathcal{Y}}_2 \right) c_{53}^{(8)} \\
&+ \left(2Y_H^2 g_1^2 + 14Y_Q^2 g_1^2 + 4Y_H Y_Q g_1^2 + \frac{62g_2^2}{3} + 8g_3^2 + \frac{16\mathcal{Y}_1 \bar{\mathcal{Y}}_1}{3} + 4\mathcal{Y}_2 \bar{\mathcal{Y}}_2 + 4\lambda \right) c_{55}^{(8)} \\
&+ \left(-g_2^2 + \frac{2\mathcal{Y}_1 \bar{\mathcal{Y}}_1}{3} - 2\mathcal{Y}_2 \bar{\mathcal{Y}}_2 \right) c_{54}^{(8)} + \left(-3Y_H^2 g_1^2 - 2Y_H Y_Q g_1^2 + \frac{13g_2^2}{12} - \frac{2\mathcal{Y}_1 \bar{\mathcal{Y}}_1}{3} + 2\lambda \right) c_{56}^{(8)}, \\
c_{56}^{\prime(8)} &= \left(-\frac{1}{3} Y_H Y_Q g_1^2 + \frac{g_2^2}{12} - \mathcal{Y}_1 \bar{\mathcal{Y}}_1 \right) c_{40}^{(8)} + \left(-\frac{1}{3} Y_H Y_Q g_1^2 - \frac{g_2^2}{12} + \mathcal{Y}_2 \bar{\mathcal{Y}}_2 \right) c_{41}^{(8)} \\
&+ \left(-4g_2^2 - \frac{8\mathcal{Y}_1 \bar{\mathcal{Y}}_1}{3} - \frac{8\mathcal{Y}_2 \bar{\mathcal{Y}}_2}{3} \right) c_{51}^{(8)} + \left(-2g_2^2 - \frac{14\mathcal{Y}_1 \bar{\mathcal{Y}}_1}{3} + 2\mathcal{Y}_2 \bar{\mathcal{Y}}_2 \right) c_{52}^{(8)} \\
&+ \left(-2g_2^2 + \frac{4\mathcal{Y}_1 \bar{\mathcal{Y}}_1}{3} - 4\mathcal{Y}_2 \bar{\mathcal{Y}}_2 \right) c_{53}^{(8)} + \left(-\frac{17g_2^2}{6} + 4g_1^2 Y_Q^2 - \frac{2\mathcal{Y}_1 \bar{\mathcal{Y}}_1}{3} \right) c_{54}^{(8)} \\
&+ \left(8Y_H^2 g_1^2 + 14Y_Q^2 g_1^2 - 4Y_H Y_Q g_1^2 + \frac{37g_2^2}{2} + 8g_3^2 + \frac{14\mathcal{Y}_1 \bar{\mathcal{Y}}_1}{3} + 6\mathcal{Y}_2 \bar{\mathcal{Y}}_2 \right) c_{56}^{(8)} \\
&+ \left(-8Y_H Y_Q g_1^2 - \frac{4\mathcal{Y}_1 \bar{\mathcal{Y}}_1}{3} + \frac{4\mathcal{Y}_2 \bar{\mathcal{Y}}_2}{3} \right) c_{55}^{(8)}, \\
c_{57}^{\prime(8)} &= (2Y_H^2 g_1^2 + 6Y_Q^2 g_1^2 - 4Y_H Y_Q g_1^2 + 14g_2^2 + 8g_3^2 + 2\mathcal{Y}_1 \bar{\mathcal{Y}}_1 + 6\mathcal{Y}_2 \bar{\mathcal{Y}}_2 + 12\lambda) c_{57}^{(8)} \\
&+ \left(\frac{g_2^2}{6} - \mathcal{Y}_1 \bar{\mathcal{Y}}_1 - \mathcal{Y}_2 \bar{\mathcal{Y}}_2 \right) c_{42}^{(8)} + \left(\frac{11Y_H^2 g_1^2}{3} - 2Y_H Y_Q g_1^2 + \frac{11g_2^2}{4} + 2\mathcal{Y}_1 \bar{\mathcal{Y}}_1 - 6\lambda \right) c_{58}^{(8)} \\
&+ \left(-\frac{11g_2^2}{2} - 2\mathcal{Y}_2 \bar{\mathcal{Y}}_2 + 4\lambda \right) c_{59}^{(8)} + \left(\frac{17g_2^2}{12} + \frac{g_1^2 Y_H^2}{3} - 2\lambda \right) c_{60}^{(8)} \\
&+ \left(-\frac{16g_2^2}{3} - 4\mathcal{Y}_1 \bar{\mathcal{Y}}_1 \right) c_{61}^{(8)}, \\
c_{58}^{\prime(8)} &= \left(\frac{g_2^2}{6} - \mathcal{Y}_1 \bar{\mathcal{Y}}_1 - \mathcal{Y}_2 \bar{\mathcal{Y}}_2 \right) c_{42}^{(8)} + \left(-8Y_H Y_Q g_1^2 + 2g_2^2 + \frac{8\mathcal{Y}_1 \bar{\mathcal{Y}}_1}{3} \right) c_{57}^{(8)} \\
&+ \left(\frac{28Y_H^2 g_1^2}{3} + 6Y_Q^2 g_1^2 + 4Y_H Y_Q g_1^2 + \frac{33g_2^2}{2} + 8g_3^2 + 2\mathcal{Y}_1 \bar{\mathcal{Y}}_1 + 6\mathcal{Y}_2 \bar{\mathcal{Y}}_2 \right) c_{58}^{(8)} \\
&+ \left(-2g_2^2 + \frac{4\mathcal{Y}_1 \bar{\mathcal{Y}}_1}{3} - 4\mathcal{Y}_2 \bar{\mathcal{Y}}_2 \right) c_{59}^{(8)} + \left(\frac{g_2^2}{3} + \frac{2g_1^2 Y_H^2}{3} - 2\mathcal{Y}_1 \bar{\mathcal{Y}}_1 + 4\mathcal{Y}_2 \bar{\mathcal{Y}}_2 \right) c_{60}^{(8)} \\
&+ \left(-2g_2^2 + \frac{4\mathcal{Y}_1 \bar{\mathcal{Y}}_1}{3} - 4\mathcal{Y}_2 \bar{\mathcal{Y}}_2 \right) c_{61}^{(8)} + \left(-\frac{7g_2^2}{3} - 6\mathcal{Y}_1 \bar{\mathcal{Y}}_1 + 6\mathcal{Y}_2 \bar{\mathcal{Y}}_2 \right) c_{62}^{(8)}, \\
c_{59}^{\prime(8)} &= \left(-\frac{g_2^2}{6} + \mathcal{Y}_1 \bar{\mathcal{Y}}_1 + \mathcal{Y}_2 \bar{\mathcal{Y}}_2 \right) c_{42}^{(8)} + \left(-2g_2^2 + 4\mathcal{Y}_1 \bar{\mathcal{Y}}_1 - \frac{20\mathcal{Y}_2 \bar{\mathcal{Y}}_2}{3} \right) c_{57}^{(8)} \\
&+ \left(2Y_H^2 g_1^2 + 6Y_Q^2 g_1^2 - 4Y_H Y_Q g_1^2 + 21g_2^2 + 8g_3^2 + 4\mathcal{Y}_1 \bar{\mathcal{Y}}_1 + \frac{8\mathcal{Y}_2 \bar{\mathcal{Y}}_2}{3} + 4\lambda \right) c_{59}^{(8)} \\
&+ \left(3Y_H^2 g_1^2 - 2Y_H Y_Q g_1^2 - \frac{25g_2^2}{12} - 2\mathcal{Y}_1 \bar{\mathcal{Y}}_1 + \frac{4\mathcal{Y}_2 \bar{\mathcal{Y}}_2}{3} - 2\lambda \right) c_{60}^{(8)} \\
&+ \left(-g_2^2 - 2\mathcal{Y}_1 \bar{\mathcal{Y}}_1 + \frac{2\mathcal{Y}_2 \bar{\mathcal{Y}}_2}{3} \right) c_{58}^{(8)} + \left(\frac{26g_2^2}{3} + \frac{16\mathcal{Y}_2 \bar{\mathcal{Y}}_2}{3} \right) c_{61}^{(8)} \\
&+ \left(-g_2^2 - 2\mathcal{Y}_1 \bar{\mathcal{Y}}_1 + \frac{2\mathcal{Y}_2 \bar{\mathcal{Y}}_2}{3} \right) c_{62}^{(8)},
\end{aligned}$$

$$\begin{aligned}
\dot{c}'_{60} &= \left(-\frac{g_2^2}{6} + \mathcal{Y}_1 \bar{\mathcal{Y}}_1 + \mathcal{Y}_2 \bar{\mathcal{Y}}_2 \right) c_{42}^{(8)} + \left(\frac{g_2^2}{6} - \mathcal{Y}_1 \bar{\mathcal{Y}}_1 - \mathcal{Y}_2 \bar{\mathcal{Y}}_2 \right) c_{43}^{(8)} \\
&+ \left(-4g_2^2 - \frac{8\mathcal{Y}_1 \bar{\mathcal{Y}}_1}{3} - \frac{8\mathcal{Y}_2 \bar{\mathcal{Y}}_2}{3} \right) c_{57}^{(8)} + \left(2g_2^2 + 4\mathcal{Y}_1 \bar{\mathcal{Y}}_1 - \frac{4\mathcal{Y}_2 \bar{\mathcal{Y}}_2}{3} \right) c_{58}^{(8)} \\
&+ \left(-8Y_H Y_Q g_1^2 - 2g_2^2 - \frac{16\mathcal{Y}_1 \bar{\mathcal{Y}}_1}{3} + \frac{8\mathcal{Y}_2 \bar{\mathcal{Y}}_2}{3} \right) c_{59}^{(8)} \\
&+ \left(8Y_H^2 g_1^2 + 6Y_Q^2 g_1^2 + 4Y_H Y_Q g_1^2 + \frac{119g_2^2}{6} + 8g_3^2 + 8\mathcal{Y}_1 \bar{\mathcal{Y}}_1 + \frac{4\mathcal{Y}_2 \bar{\mathcal{Y}}_2}{3} \right) c_{60}^{(8)} \\
&+ \left(\frac{16\mathcal{Y}_2 \bar{\mathcal{Y}}_2}{3} - \frac{16\mathcal{Y}_1 \bar{\mathcal{Y}}_1}{3} \right) c_{61}^{(8)} + \left(\frac{20g_2^2}{3} + 4\mathcal{Y}_1 \bar{\mathcal{Y}}_1 - \frac{4\mathcal{Y}_2 \bar{\mathcal{Y}}_2}{3} \right) c_{62}^{(8)} , \\
\dot{c}'_{61} &= \left(-\frac{1}{3} Y_H Y_Q g_1^2 + \frac{g_2^2}{12} - \mathcal{Y}_1 \bar{\mathcal{Y}}_1 \right) c_{42}^{(8)} + (6\mathcal{Y}_2 \bar{\mathcal{Y}}_2 - 6\mathcal{Y}_1 \bar{\mathcal{Y}}_1) c_{57}^{(8)} \\
&+ \left(\frac{3g_2^2}{2} + 4g_1^2 Y_Q^2 - 2\mathcal{Y}_1 \bar{\mathcal{Y}}_1 + 4\mathcal{Y}_2 \bar{\mathcal{Y}}_2 \right) c_{59}^{(8)} + \left(3Y_H^2 g_1^2 - 2Y_H Y_Q g_1^2 - \frac{g_2^2}{12} + 2\mathcal{Y}_1 \bar{\mathcal{Y}}_1 - 2\lambda \right) c_{62}^{(8)} \\
&+ (2Y_H^2 g_1^2 + 14Y_Q^2 g_1^2 - 4Y_H Y_Q g_1^2 + 12g_2^2 + 8g_3^2 + 4\mathcal{Y}_1 \bar{\mathcal{Y}}_1 + 4\lambda) c_{61}^{(8)} , \\
\dot{c}'_{62} &= \left(-\frac{1}{3} Y_H Y_Q g_1^2 + \frac{g_2^2}{12} - \mathcal{Y}_1 \bar{\mathcal{Y}}_1 \right) c_{42}^{(8)} + \left(-\frac{1}{3} Y_H Y_Q g_1^2 - \frac{g_2^2}{12} + \mathcal{Y}_2 \bar{\mathcal{Y}}_2 \right) c_{43}^{(8)} \\
&+ (6\mathcal{Y}_2 \bar{\mathcal{Y}}_2 - 6\mathcal{Y}_1 \bar{\mathcal{Y}}_1) c_{58}^{(8)} + \left(\frac{3g_2^2}{2} + 4g_1^2 Y_Q^2 - 2\mathcal{Y}_1 \bar{\mathcal{Y}}_1 + 4\mathcal{Y}_2 \bar{\mathcal{Y}}_2 \right) c_{60}^{(8)} \\
&+ \left(8Y_H^2 g_1^2 + 14Y_Q^2 g_1^2 + 4Y_H Y_Q g_1^2 + \frac{71g_2^2}{6} + 8g_3^2 + 2\mathcal{Y}_1 \bar{\mathcal{Y}}_1 + 6\mathcal{Y}_2 \bar{\mathcal{Y}}_2 \right) c_{62}^{(8)} \\
&+ (-8Y_H Y_Q g_1^2 + 4\mathcal{Y}_1 \bar{\mathcal{Y}}_1 - 4\mathcal{Y}_2 \bar{\mathcal{Y}}_2) c_{61}^{(8)} , \\
\dot{c}'_{63} &= \frac{4}{3} i c_{22}^{(8)} g_2^2 - \frac{8}{3} g_1 Y_Q c_{38}^{(8)} g_2 - \frac{8}{3} g_1 Y_Q c_{39}^{(8)} g_2 + \left(\frac{2\mathcal{Y}_2 \bar{\mathcal{Y}}_2}{3} - \frac{2\mathcal{Y}_1 \bar{\mathcal{Y}}_1}{3} \right) c_{44}^{(8)} \\
&+ \left(\frac{2\mathcal{Y}_2 \bar{\mathcal{Y}}_2}{3} - \frac{2\mathcal{Y}_1 \bar{\mathcal{Y}}_1}{3} \right) c_{45}^{(8)} + \left(\frac{2\mathcal{Y}_1 \bar{\mathcal{Y}}_1}{3} - \frac{2\mathcal{Y}_2 \bar{\mathcal{Y}}_2}{3} \right) c_{46}^{(8)} \\
&+ \left(12Y_H^2 g_1^2 + \frac{34Y_Q^2 g_1^2}{3} - 4Y_H Y_Q g_1^2 + \frac{19g_2^2}{6} + \frac{136g_3^2}{9} - \frac{16\mathcal{Y}_1 \bar{\mathcal{Y}}_1}{3} + 8\mathcal{Y}_2 \bar{\mathcal{Y}}_2 \right) c_{63}^{(8)} \\
&+ \left(8Y_H Y_Q g_1^2 + 2g_2^2 + \frac{16\mathcal{Y}_1 \bar{\mathcal{Y}}_1}{3} - \frac{8\mathcal{Y}_2 \bar{\mathcal{Y}}_2}{3} \right) c_{64}^{(8)} + \left(-2g_2^2 - \frac{32\mathcal{Y}_1 \bar{\mathcal{Y}}_1}{3} + 8\mathcal{Y}_2 \bar{\mathcal{Y}}_2 \right) c_{65}^{(8)} \\
&+ \left(4g_2^2 + \frac{8\mathcal{Y}_1 \bar{\mathcal{Y}}_1}{3} + \frac{8\mathcal{Y}_2 \bar{\mathcal{Y}}_2}{3} \right) c_{66}^{(8)} , \\
\dot{c}'_{64} &= \frac{2}{3} i c_{22}^{(8)} g_2^2 - \frac{4}{3} g_1 Y_Q c_{38}^{(8)} g_2 - \frac{4}{3} g_1 Y_Q c_{39}^{(8)} g_2 + \left(-\frac{g_2^2}{6} + \frac{2\mathcal{Y}_1 \bar{\mathcal{Y}}_1}{3} + \frac{4\mathcal{Y}_2 \bar{\mathcal{Y}}_2}{3} \right) c_{44}^{(8)} \\
&+ \left(\frac{g_2^2}{6} - \frac{4\mathcal{Y}_1 \bar{\mathcal{Y}}_1}{3} - \frac{2\mathcal{Y}_2 \bar{\mathcal{Y}}_2}{3} \right) c_{45}^{(8)} + \left(\frac{\mathcal{Y}_1 \bar{\mathcal{Y}}_1}{3} - \frac{\mathcal{Y}_2 \bar{\mathcal{Y}}_2}{3} \right) c_{46}^{(8)} \\
&+ \left(2Y_H^2 g_1^2 + \frac{8Y_Q^2 g_1^2}{3} + 8Y_H Y_Q g_1^2 - \frac{13g_2^2}{3} + \frac{32g_3^2}{9} + \frac{8\mathcal{Y}_1 \bar{\mathcal{Y}}_1}{3} \right) c_{63}^{(8)} \\
&+ \left(8Y_H^2 g_1^2 + 6Y_Q^2 g_1^2 + 4Y_H Y_Q g_1^2 + \frac{107g_2^2}{6} + 8g_3^2 + \frac{16\mathcal{Y}_1 \bar{\mathcal{Y}}_1}{3} \right) c_{64}^{(8)} \\
&+ \left(4g_2^2 - \frac{8\mathcal{Y}_1 \bar{\mathcal{Y}}_1}{3} + 8\mathcal{Y}_2 \bar{\mathcal{Y}}_2 \right) c_{65}^{(8)} + \left(2g_2^2 + \frac{8\mathcal{Y}_1 \bar{\mathcal{Y}}_1}{3} \right) c_{66}^{(8)} ,
\end{aligned}$$

$$\begin{aligned}
\dot{c}_{65}^{(8)} &= -4c_{21}^{(8)}g_2^2 - \frac{2}{3}ic_{22}^{(8)}g_2^2 + \frac{4}{3}g_1Y_Qc_{38}^{(8)}g_2 + \frac{4}{3}g_1Y_Qc_{39}^{(8)}g_2 - \frac{16}{3}g_1^2Y_Q^2c_{20}^{(8)} \\
&\quad - \frac{64}{9}g_3^2c_{23}^{(8)} + \left(\frac{4\mathcal{Y}_1\bar{\mathcal{Y}}_1}{3} + \frac{2\mathcal{Y}_2\bar{\mathcal{Y}}_2}{3}\right)c_{44}^{(8)} + \frac{2}{3}\mathcal{Y}_1\bar{\mathcal{Y}}_1c_{45}^{(8)} - \frac{2}{3}\mathcal{Y}_1\bar{\mathcal{Y}}_1c_{46}^{(8)} \\
&\quad + \left(\frac{17g_2^2}{3} - \frac{8\mathcal{Y}_1\bar{\mathcal{Y}}_1}{3} + 4\mathcal{Y}_2\bar{\mathcal{Y}}_2\right)c_{63}^{(8)} + \left(2g_2^2 - \frac{4\mathcal{Y}_1\bar{\mathcal{Y}}_1}{3} + 4\mathcal{Y}_2\bar{\mathcal{Y}}_2\right)c_{64}^{(8)} \\
&\quad + \left(12Y_H^2g_1^2 + \frac{34Y_Q^2g_1^2}{3} - 4Y_HY_Qg_1^2 + \frac{37g_2^2}{2} + \frac{136g_3^2}{9} + \frac{32\mathcal{Y}_1\bar{\mathcal{Y}}_1}{3}\right)c_{65}^{(8)} \\
&\quad + \left(8Y_HY_Qg_1^2 - 2g_2^2 - \frac{8\mathcal{Y}_1\bar{\mathcal{Y}}_1}{3}\right)c_{66}^{(8)}, \\
\dot{c}_{66}^{(8)} &= -2c_{21}^{(8)}g_2^2 - \frac{1}{3}ic_{22}^{(8)}g_2^2 + \frac{2}{3}g_1Y_Qc_{38}^{(8)}g_2 + \frac{2}{3}g_1Y_Qc_{39}^{(8)}g_2 - \frac{8}{3}g_1^2Y_Q^2c_{20}^{(8)} \\
&\quad - \frac{32}{9}g_3^2c_{23}^{(8)} + \left(-Y_HY_Qg_1^2 + \frac{g_2^2}{12} - \frac{4\mathcal{Y}_1\bar{\mathcal{Y}}_1}{3} + \frac{4\mathcal{Y}_2\bar{\mathcal{Y}}_2}{3}\right)c_{44}^{(8)} \\
&\quad + \left(\frac{1}{3}Y_HY_Qg_1^2 - \frac{g_2^2}{12} + \frac{4\mathcal{Y}_1\bar{\mathcal{Y}}_1}{3}\right)c_{45}^{(8)} + \left(\frac{2}{3}Y_HY_Qg_1^2 + \frac{2\mathcal{Y}_1\bar{\mathcal{Y}}_1}{3} - \mathcal{Y}_2\bar{\mathcal{Y}}_2\right)c_{46}^{(8)} \\
&\quad + \left(\frac{83g_2^2}{12} - \frac{g_1^2Y_H^2}{3} - 2g_1^2Y_Q^2 - \frac{8\mathcal{Y}_1\bar{\mathcal{Y}}_1}{3} + 8\mathcal{Y}_2\bar{\mathcal{Y}}_2\right)c_{63}^{(8)} \\
&\quad + \left(-\frac{13g_2^2}{6} + \frac{2g_1^2Y_H^2}{3} + 4g_1^2Y_Q^2 - \frac{4\mathcal{Y}_1\bar{\mathcal{Y}}_1}{3}\right)c_{64}^{(8)} \\
&\quad + \left(\frac{4Y_H^2g_1^2}{3} - \frac{4Y_Q^2g_1^2}{3} + 8Y_HY_Qg_1^2 + \frac{3g_2^2}{2} + \frac{32g_3^2}{9} + \frac{8\mathcal{Y}_1\bar{\mathcal{Y}}_1}{3}\right)c_{65}^{(8)} \\
&\quad + \left(\frac{28Y_H^2g_1^2}{3} + 14Y_Q^2g_1^2 + 4Y_HY_Qg_1^2 + \frac{19g_2^2}{2} + 8g_3^2 - \frac{8\mathcal{Y}_1\bar{\mathcal{Y}}_1}{3}\right)c_{66}^{(8)}.
\end{aligned}$$

Chapter 6

Gravitational EFTs and the Eikonal Limit

One of the exciting applications of scattering amplitudes focuses on the computation of classical observables in gauge theory and gravity [140], such as deflection angles and time delay/advance, or effective Hamiltonians describing the dynamics of binary systems. Early results in this direction date back to [125], where it was already noted that loop amplitudes contribute to classical processes. The intimate connection between loops and classical physics was sharpened in [129], and had already been applied in [128] to obtain the classical and quantum $\mathcal{O}(G^2)$ corrections to Newton's potential, where G is Newton's constant. In this approach, gravity is treated as an effective theory [127], where one can make predictions at low energy despite the non-renormalisability of the theory.

More recently, a systematic approach employing scattering amplitudes in conjunction with unitarity was developed to compute classical quantities in gauge theory and gravity. Classical [131] and quantum [130, 131] corrections to Newton's potential can be obtained from a two-to-two scattering amplitude of two massive scalars, in particular narrowing down to terms that have discontinuities in the channel corresponding to the momentum transfer \vec{q} of the process [129]. An additional simplification stems from the fact that in the unitarity-based calculation the cuts can be kept in four dimensions, as discrepancies with d -dimensional results only give rise to analytic terms, at least up to two loops [334] (but not beyond [335]). Unitarity has also been applied in [132, 134, 135, 141, 336, 337] to compute the deflection angle for light or for gravitons passing by a heavy mass, a quantity that has the advantage of being gauge invariant.

In this chapter, we compute the graviton deflection angle and time delay/advance for the three interactions R^3 , R^4 and FFR , and in addition the photon deflection and time delay induced by the FFR interaction. The single most important qualitative difference with the EH theory is that the propagation and speed of the massless particle acquire a dependence on its polarisation. This generically leads to a time advance at small impact parameter b in the classical theory. Interestingly, in the case of graviton scattering due to R^4 and FFR , causality violation can be avoided if the coefficients of the interactions obey certain positivity constraints which, for R^4 , are in precise agreement with those of [338, 339]. For the R^3 interaction our results are fully consistent with the tree-level findings of [340], extending them to one loop. Note that while we used a massive scalar, [340] used a coherent state to set up the background in which the graviton is deflected.

Similarly, the FFR interaction induces superluminal propagation of photons.

The chapter is organised as follows. In Section 6.1, we present the action of the system under consideration, classifying all the independent effective interactions beyond Hilbert-Einstein. In Section 6.2, we review the basics of the eikonal approximation of scattering amplitudes and how to compute observables from it. We discuss our kinematic set-up and provide explicit expressions for the spinor helicity variables associated to each massless particle in the eikonal limit. We then discuss some general aspects of the eikonal approximation, in particular the extraction of the phases δ_L from the loop scattering amplitudes. Section 6.3 contains the computations of all tree-level and one-loop amplitudes relevant for our analysis. As a warm up we consider the EH theory, where we re-discuss the graviton deflection computation of [141]. We then move on to present the relevant four-point two-scalar two-graviton amplitudes with and without helicity flip in the case of R^3 , R^4 and FFR , as well as the two-scalar two-photon amplitudes for the FFR case, all at tree and one-loop level. While at tree level we present exact expressions, at one loop we work in the eikonal approximation and we only consider cuts in the q^2 -channel which produce non-analytic terms arising from the long-range propagation of two massless particles. Section 6.4 is dedicated to the computation of the leading and subleading eikonal matrices δ_0 and δ_1 , from which we will then obtain the $\mathcal{O}(G)$ and $\mathcal{O}(G^2)$ corrections to the deflection angle and time advance/delay for the four cases considered – scattering of gravitons in the presence of R^3 , R^4 and FFR terms, and scattering of photons induced by the FFR interaction.

6.1 Gravity with higher-derivative couplings

Much attention has been devoted to the study of effective theories of gravity obtained by adding higher-derivative interactions to the Einstein-Hilbert (EH) action. In particular, efforts have been made in [341–343] to confront such modifications with gravitational wave observations. It was also noted that for these effects to be measurable by experiments such as LIGO the cutoff of the effective theory must not be much larger than $\mathcal{O}(\text{km}^{-1})$. A study of the effects that these higher-derivative terms have on the Hamiltonian and deflection angle was initiated in [173]. In this chapter, based on the work [174], we sharpen this study by rooting it in the eikonal approximation – specifically, applying it to three types of terms, denoted schematically as R^3 , R^4 and FFR , for which we compute the corresponding corrections to the deflection angle and time delay/advance. More in detail, the particular action we consider for the graviton, photon and a massive scalar has the form:

$$S = \int d^4x \sqrt{-g} \left[-\frac{2}{\kappa^2} R - \frac{1}{4} F^{\mu\nu} F_{\mu\nu} + \frac{1}{2} (D_\mu \phi)(D^\mu \phi) - \frac{1}{2} m^2 \phi^2 - \frac{2}{\kappa^2} \left(\frac{\alpha'^2}{48} I_1 + \frac{\alpha'^2}{24} G_3 \right) + \frac{2}{\kappa^2} \mathcal{L}_8 - \frac{\alpha_\gamma}{8} F^{\mu\nu} F^{\rho\sigma} R_{\mu\nu\rho\sigma} \right], \quad (6.1)$$

where

$$I_1 := R^{\alpha\beta}{}_{\mu\nu} R^{\mu\nu}{}_{\rho\sigma} R^{\rho\sigma}{}_{\alpha\beta}, \quad G_3 := I_1 - 2R^{\mu\nu\alpha}{}_{\beta} R^{\beta\gamma}{}_{\nu\sigma} R^{\sigma}{}_{\mu\gamma\alpha}, \quad (6.2)$$

while

$$\mathcal{L}_8 = \beta_1 \mathcal{C}^2 + \beta_2 \mathcal{C} \tilde{\mathcal{C}} + \beta_3 \tilde{\mathcal{C}}^2, \quad (6.3)$$

where

$$\mathcal{C} := R_{\mu\nu\rho\sigma} R^{\mu\nu\rho\sigma}, \quad \tilde{\mathcal{C}} := \frac{1}{2} R_{\mu\nu\alpha\beta} \epsilon^{\alpha\beta}{}_{\gamma\delta} R^{\gamma\delta\mu\nu}. \quad (6.4)$$

A few comments on the various couplings in (6.1) are in order here. First, there are two types of R^3 terms, denoted as I_1 and G_3 above. Such terms arise naturally in the low-energy effective description of bosonic string theory. Their effects on gravitational scattering of different matter fields have been discussed recently in [173, 344]; specifically for the scattering of two massive scalars, both independent structures I_1 and G_3 were found to contribute. On the other hand, for the helicity-preserving deflection of massless particles of spin 0, 1 and 2, it was shown in [173] that the G_3 interaction has no effect. Additional interesting features about the I_1 and G_3 couplings are that I_1 is the only coupling that contributes to pure graviton scattering in $d \leq 6$ [298, 345] and is the two-loop counterterm in pure gravity [346]. G_3 is a topological term in six dimensions: as such, for $d \leq 6$, we can always perform a field redefinition at the amplitude level of the action such that such term is not present (in the case of pure gravity) or re-written in terms of tidal effects. For example, if we consider a theory of gravity with matter, *e.g.* massive scalars (mimicking black holes or neutron stars), the presence of a G_3 coupling alters their dynamics. In particular the four-point amplitude with two gravitons and two scalars becomes [173, 344]

$$\mathcal{M}_{\text{EH}+G_3}^{(0)}(\phi_1, \phi_2, h_3^{++}, h_4^{++}) = \mathcal{M}_{\text{EH}}^{(0)}(\phi_1, \phi_2, h_3^{++}, h_4^{++}) + i \frac{\alpha_2}{32} \left(\frac{\kappa}{2}\right)^2 [34]^4 (2m^2 + s). \quad (6.5)$$

The non-trivial contribution to the scattering amplitude of two massive scalars and two gravitons from the G_3 interactions modifies the classical potential in the two-body system, as shown in [173, 344]. It is easy to show that the contact term proportional to $[34]^4 (2m^2 + s)$ in the amplitude (6.5) is (up to a numerical coefficient) the amplitude arising from a particular tidal interactions of the form $R^{\mu\nu\rho\sigma} R_{\mu\nu\rho\sigma} m^2 \phi^2 - \nabla^\alpha R^{\mu\nu\rho\sigma} \nabla_\alpha R_{\mu\nu\rho\sigma} \phi^2$, see for example [347]. But, in the following we will be concerned with (helicity-preserving and flipping) scattering of massless gravitons in the background produced by a massive scalar, in which case only the I_1 structure contributes, hence we will refer to it simply as the R^3 term, since no confusion can arise.

The second interaction we study is of the type R^4 . In principle there are 26 independent parity-even quartic contractions of the Riemann tensor [348], but only the seven which do not contain the Ricci scalar or tensor survive on shell in arbitrary dimensions, as can also be seen using field redefinitions [349, 350]. In four dimensions these reduce to two independent parity-even structures [341, 351], plus one parity-odd structure [342], as shown in (6.3). In agreement with [351] we find that these interactions induce the following four-point graviton amplitudes: those with all-equal helicities, and the amplitude with two positive- and two negative-helicity gravitons (the MHV configuration). If β_2 in (6.3) is non-vanishing, then the all-plus and all-minus graviton amplitudes are independent. We also note that a particular contraction of four Riemann tensors appears in type-II superstring theories where it is the first higher-derivative curvature correction to the EH theory, and can be determined from four-graviton scattering [352].

The third interaction we consider is an FFR term, where F is the electromagnetic field strength. It is known to arise in string theory as well as from integrating out massive, charged electrons in the case of electrodynamics coupled to gravity, as discussed in [353, 354], and considered more recently in [355, 356].

As we have already mentioned, we have also introduced in the action a minimally coupled massive scalar to represent a black hole¹.

¹In order to describe charged black holes the real scalar in (6.1) should be replaced by an electrically charged complex scalar.

Note that in (6.1) we have excluded terms quadratic in the curvatures since from an effective field theory/on-shell point of view they have no effect to any order in four dimensions (for example, see [357] for a recent review).

6.2 Physical observables from the eikonal phase matrix

The physical observables of interest are the classical deflection angle and the time delay/advance [358] experienced by massless gravitons and photons when they scatter off a (possibly charged) massive scalar. A method ideally suited for obtaining classical observables directly from amplitudes, without passing through intermediate, unphysical quantities, is the eikonal [359–364]². In this approach the relevant amplitudes are evaluated in an approximation where the momentum transfer $|\vec{q}|$ is taken to be much smaller than both the mass m of the heavy scalar and the energy ω of the massless particle, or more precisely taking $m \gg \omega \gg |\vec{q}|$. Crucial for this is a convenient parameterisation of spinor helicity variables for the massless particles in the eikonal limit. The amplitudes thus obtained are then transformed to impact parameter space via a two-dimensional Fourier transform. In this space the amplitudes are expected to exponentiate into an eikonal phase, from which one can extract directly the classical deflection angle and time advance/delay. Recent applications of this method to this type of problem include [367] for the deflection angle of massless scalars up to 2PM, [134] for photons and fermions up to 2PM order, and up to 3PM order in [147, 162, 368].

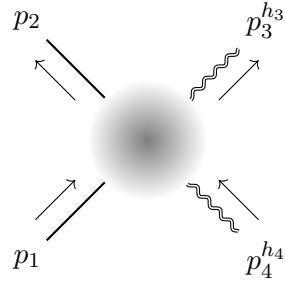
An important point we wish to make is that in our case, because helicity-preserving as well as helicity-violating processes contribute, the eikonal *phase* is promoted to an eikonal *phase matrix* in the space of helicities of the external massless particles, with $(+-)$ and $(-+)$ being the diagonal entries associated to no-flip scattering (in a convention where all particles' momenta are outgoing), while $(++)$ and $(--)$ are the off-diagonal entries, with helicity flip. The associated mixing problem has to be resolved in order to obtain the physical quantities of interest. Whenever the two eigenvalues of the eikonal phase matrix are distinct, a possible violation of causality at small impact parameter arises, as noticed already at tree level in [340]. See also [355, 356, 369–374] for further discussions and resolutions of this issue in UV-complete theories and [353, 354] for related discussions involving helicity flip and no-flip amplitudes.

In this section we first give a precise definition of the eikonal limit providing an explicit parametrisation for all the momenta and spinor-helicity variables we need. We then briefly review the connection between amplitudes in the eikonal limit (Fourier-transformed to impact parameter space) and the eikonal phase matrix, the deflection angle and the time delay.

6.2.1 Kinematics of the scattering

We begin by describing the kinematics of the scattering processes we consider. We denote by p_1 and p_2 the four-momenta of the incoming and outgoing scalars, respectively, with m being their common mass, while the momenta of the incoming and outgoing massless particles (gravitons or photons) are p_4 and p_3 . We will work in the centre of mass frame, with the following parameterisation:

²This eikonal was intensively studied in the context of gravity and string theory in the nineties [363, 364]. For related recent work see also [142, 365, 366] and references therein.



$$\begin{aligned}
 p_4^\mu &= -(E_4, -\vec{p} + \vec{q}/2), \\
 p_1^\mu &= -(E_1, \vec{p} - \vec{q}/2), \\
 p_2^\mu &= (E_2, \vec{p} + \vec{q}/2), \\
 p_3^\mu &= (E_3, -\vec{p} - \vec{q}/2).
 \end{aligned} \tag{6.6}$$

In our conventions we take all momenta to be outgoing, hence the minus signs in the expressions of p_1 and p_4 since particles 1 and 4 are incoming. We also have

$$\begin{aligned}
 E_1 &= E_2 = \sqrt{m^2 + \vec{p}^2 + \vec{q}^2/4}, \\
 E_3 &= E_4 = \sqrt{\vec{p}^2 + \vec{q}^2/4} := \omega,
 \end{aligned} \tag{6.7}$$

where $\vec{p} \cdot \vec{q} = 0$ due to momentum conservation. Hence \vec{q} lives in a two-dimensional space orthogonal to \vec{p} . In this thesis we define the Mandelstam variables as

$$s := (p_1 + p_2)^2 = -\vec{q}^2, \quad t := (p_1 + p_4)^2 = (E_1 + E_4)^2, \quad u := (p_1 + p_3)^2, \tag{6.8}$$

with $s + t + u = 2m^2$. In this notation the spacelike momentum transfer squared is given by s , while t denotes the centre of mass energy squared, and ω is the energy of the scattered massless particle.

In the above parameterisation, the kinematic limit we are interested is

$$m \gg \omega \gg |\vec{q}|, \tag{6.9}$$

which implies for the Mandelstam variables

$$t \simeq m^2 + 2m\omega, \quad ut - m^4 \simeq -(2m\omega)^2, \tag{6.10}$$

and for the energies of the massless particles

$$E_3 = E_4 := \omega \simeq |\vec{p}| \left(1 + \frac{\vec{q}^2}{8\vec{p}^2} \right). \tag{6.11}$$

For definiteness we choose $\vec{p} = |\vec{p}| \hat{z}$ with $|\vec{p}| \gg |\vec{q}|$, as implied by (6.9). In this approximation we can write the four-momentum p_3 of the massless particle in spinor notation as

$$p_3 = \begin{pmatrix} \frac{\vec{q}^2}{8|\vec{p}|} & -\frac{\bar{q}}{2} \\ -\frac{q}{2} & 2|\vec{p}| \end{pmatrix}, \tag{6.12}$$

with $q := q_1 + iq_2$ and $\bar{q} := q_1 - iq_2$. One can then find an explicit parameterisation for the spinors associated to the null momenta $p_i = \lambda_i \tilde{\lambda}_i$, $i = 3, 4$, with the result

$$\begin{aligned}
 \lambda_3 &= \sqrt{2|\vec{p}|} \begin{pmatrix} -\frac{\bar{q}}{4|\vec{p}|} \\ 1 \end{pmatrix}, & \tilde{\lambda}_3 &= \sqrt{2|\vec{p}|} \begin{pmatrix} -\frac{q}{4|\vec{p}|} & 1 \end{pmatrix}, \\
 \lambda_4 &= i\sqrt{2|\vec{p}|} \begin{pmatrix} \frac{\bar{q}}{4|\vec{p}|} \\ 1 \end{pmatrix}, & \tilde{\lambda}_4 &= i\sqrt{2|\vec{p}|} \begin{pmatrix} \frac{q}{4|\vec{p}|} & 1 \end{pmatrix}.
 \end{aligned} \tag{6.13}$$

Note the extra factors of i due to the negative energy-component of p_4 corresponding to an incoming particle.

6.2.2 Eikonal phase, deflection angle and time delay

In this section we briefly review relevant aspects of the eikonal approximation and the eikonal phase matrix which allows for an efficient extraction of the deflection angle and time delay/advance from scattering amplitudes.

First, we introduce the amplitude in impact parameter space $\tilde{\mathcal{A}}$. This is defined as a Fourier transform of the amplitude \mathcal{A} with respect to the momentum transfer \vec{q} ,

$$\tilde{\mathcal{A}}(\vec{b}) := \frac{1}{4m\omega} \int \frac{d^{d-2}q}{(2\pi)^{d-2}} e^{i\vec{q}\cdot\vec{b}} \mathcal{A}(\vec{q}) , \quad (6.14)$$

where \vec{b} is the impact parameter, and the number of dimensions will eventually be set to $d = 4 - 2\epsilon$.

In the eikonal approximation the gravitational S -matrix is conjectured to be of the form [363, 367]

$$S_{\text{eik}} = e^{i(\delta_0 + \delta_1 + \dots)} , \quad (6.15)$$

where δ_0 is the leading eikonal phase, which is $\mathcal{O}(G)$, δ_1 the first subleading correction, of $\mathcal{O}(G^2)$, and the dots represent subsubleading contributions. Alternatively, one can write the S -matrix in impact parameter space as

$$S_{\text{eik}} = 1 + \tilde{\mathcal{A}}_\omega^{(0)} + \tilde{\mathcal{A}}_{\omega^2}^{(1)} + \tilde{\mathcal{A}}_\omega^{(1)} + \tilde{\mathcal{A}}_{\omega^3}^{(2)} + \tilde{\mathcal{A}}_{\omega^2}^{(2)} + \tilde{\mathcal{A}}_\omega^{(2)} + \dots , \quad (6.16)$$

where the superscript indicates the loop order L and the subscript the power in the energy ω of the massless particle. That the maximal power of ω at a given loop order is $L + 1$ is a well-established fact in (super)gravity and we will see below that the R^3 corrections do not alter this expectation. However, we also find that the R^4 corrections lead to higher powers of ω starting at one loop, which is not surprising since higher-derivative corrections worsen the high-energy behaviour. In the effective field theory approach we adopt, we are not really interested in high-energy physics (or high-energy completions of the theory) – we use the eikonal approximation as an efficient and elegant tool to extract deflection angles and time delay/advances without passing through the computation of non gauge-invariant intermediate quantities such as effective potentials or Hamiltonians.

Equating (6.15) with (6.16) one gets

$$\delta_0 = -i \tilde{\mathcal{A}}_\omega^{(0)} , \quad (6.17)$$

$$\delta_1 = -i \tilde{\mathcal{A}}_\omega^{(1)} , \quad (6.18)$$

as well as the condition

$$-\frac{(\delta_0)^2}{2} = \tilde{\mathcal{A}}_{\omega^2}^{(1)} , \quad (6.19)$$

which implies the consistency condition

$$\tilde{\mathcal{A}}_{\omega^2}^{(1)} = \frac{1}{2} (\tilde{\mathcal{A}}_\omega^{(0)})^2 . \quad (6.20)$$

Thus, the contribution to the one-loop amplitude that is leading in ω , $\tilde{\mathcal{A}}_{\omega^2}^{(1)}$, does not provide any new information about the S -matrix. In general, it is only the term in

$\tilde{\mathcal{A}}^{(L)}$ that is linear in ω , $\tilde{\mathcal{A}}_\omega^{(L)}$, that provides new information entering δ_L . Also, (6.17)–(6.20) are conjectured to be valid as matrix equations in the linear space of helicity configurations of external states.

Note that a priori these statements are known to hold for EH gravity. The results in this thesis show that (6.20) also holds for the higher-derivative interactions discussed here at least up to one loop.

Finally, the particle deflection angle can be obtained from the eigenvalues $\delta^{(i)}$ of the eikonal phase matrix δ . Using a saddle-point approximation [134, 137, 363] one finds, for small θ ,

$$\theta^{(i)} = \frac{1}{\omega} \frac{\partial}{\partial b} \delta^{(i)}, \quad (6.21)$$

where i runs over all eigenvalues of δ and $b = |\vec{b}|$. For the time delay, we will use instead [375–377]

$$t^{(i)} = \frac{\partial \delta^{(i)}}{\partial \omega}. \quad (6.22)$$

6.3 The relevant scattering amplitudes

In this section we compute the relevant amplitudes needed to extract the deflection angle and time delay/advance induced by the various interactions in (6.1). At tree level we will present exact expressions, while at one loop we only need to compute the part of the amplitude with a discontinuity in the s -channel³ and we will write the relevant expressions after expanding them in the eikonal approximation (6.9) – this will be denoted in the following by the \simeq symbol. A direct extraction of the classical part of the deflection angle and time delay can be performed using triple cuts, and in an even more refined way using the holomorphic classical limit [158]. We chose instead to compute the one-loop amplitudes through two-particle cuts, which also determine the quantum part of the amplitude. The reason for doing this is twofold: at the practical level, computing the relevant terms in the amplitude from generalised unitarity does not improve the computation significantly, and the additional terms, despite not being used in the present thesis, could become relevant when considering the exponentiation in the eikonal limit at higher orders (see, for example, the discussion about the eikonal exponentiation of $\mathcal{N} = 8$ four-point amplitude in [366]).

We will begin our discussion with the simple case of EH gravity, quoting from [141] the relevant two-scalar two-graviton amplitude without helicity flip. We also compute the amplitude with helicity flip, and show that it does not contribute in the eikonal approximation, as correctly assumed in previous treatments. We will then move on to compute the relevant tree and one-loop amplitudes that are necessary to compute the corrections induced by the R^3 , R^4 and FFR terms in (6.1). The two-particle cut diagrams relevant for the R^3 and R^4 cases are shown in Figure 6.1. The corrections induced by the FFR interaction need a separate analysis and we show the corresponding diagrams in Figures 6.2 and 6.3. Indeed, for the R^3 and R^4 interactions both internal and external particles are gravitons, while in the case of FFR we either have external gravitons and internal photons, or viceversa.

³We recall that $s = -|\vec{q}|^2$ where \vec{q} is the momentum exchange between the classical source and the graviton.

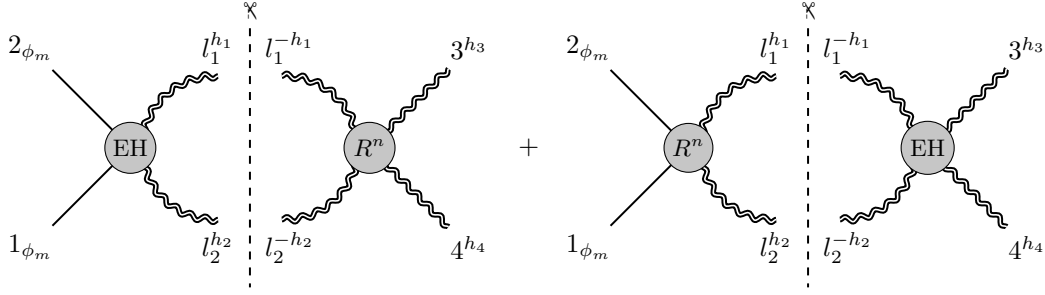


Figure 6.1: The two-particle cut diagrams for the R^n ($n = 3, 4$) interaction in the $s = -\vec{q}^2$ -channel. In our conventions external momenta are all outgoing and internal loop momenta flow from left to right in the diagram.

A comment is in order here. Focusing on the cuts relevant for R^n depicted in Figure 6.1, the case $h_3 = h_4$ corresponds to the massless particle flipping helicity upon interacting with the scalar, whereas $h_3 = -h_4$ corresponds to the helicity-preserving process, since in our conventions all external particles are outgoing. A simple way to take into account particle statistics is to sum over all values of the internal helicities h_1 and h_2 and divide the result by 2, which correspond to the Bose symmetry factor for the internal gravitons.

6.3.1 Four-point scalar/graviton scattering in EH gravity

The relevant tree-level amplitudes in the EH case are the two-scalar/two-graviton amplitudes in the two helicity configurations for the gravitons⁴:

$$\begin{aligned} \mathcal{A}_{\text{EH}}^{(0)}(1^\phi, 2^\phi, 3^{--}, 4^{++}) &= -\left(\frac{\kappa}{2}\right)^2 \frac{\langle 3|1|4 \rangle^4}{s^2} \left[\frac{i}{t-m^2} + \frac{i}{u-m^2} \right], \\ \mathcal{A}_{\text{EH}}^{(0)}(1^\phi, 2^\phi, 3^{++}, 4^{++}) &= -\left(\frac{\kappa}{2}\right)^2 m^4 \frac{[34]^2}{\langle 34 \rangle^2} \left[\frac{i}{t-m^2} + \frac{i}{u-m^2} \right], \end{aligned} \quad (6.23)$$

The computation of the four-point one-loop amplitude without helicity flip in the eikonal approximation (6.9) was performed in [141], with the result

$$\begin{aligned} \mathcal{A}_{\text{EH}}^{(1)}(1^\phi, 2^\phi, 3^{--}, 4^{++}) &\simeq \mathcal{N}_h \left(\frac{\kappa}{2}\right)^4 \left[(2m\omega)^4 (I_4(s, t; m) + I_4(s, u; m)) - 15(m^2\omega)^2 I_3(s; m) \right. \\ &\quad \left. + (4m\omega)^2 s I_3(s) - \frac{29}{2} (m\omega)^2 I_2(s) \right], \end{aligned} \quad (6.24)$$

where

$$\mathcal{N}_h := \left(\frac{\langle 3|2|4 \rangle}{2m\omega} \right)^4 \quad (6.25)$$

is a pure phase and $\mathcal{N}_h \rightarrow 1$ in the eikonal approximation. We have also computed the new amplitude with helicity flip in the same approximation, with the result

$$\mathcal{A}_{\text{EH}}^{(1)}(1^\phi, 2^\phi, 3^{++}, 4^{++}) \simeq \left(\frac{\kappa}{2}\right)^4 \frac{[34]^2}{\langle 34 \rangle^2} (m^2 s)^2 \left[I_4(s, t; m) + I_4(s, u; m) \right]. \quad (6.26)$$

⁴See for instance [173, 378].

6.3.2 Four-point scalar/graviton scattering in EH + R^3

We now consider the amplitudes with addition of the R^3 interaction in (6.1): the helicity-preserving amplitude at tree-level is vanishing

$$\mathcal{A}_{R^3}^{(0)}(1^\phi, 2^\phi, 3^{--}, 4^{++}) = 0, \quad (6.27)$$

while the helicity-flip amplitude is

$$\mathcal{A}_{R^3}^{(0)}(1^\phi, 2^\phi, 3^{++}, 4^{++}) = i \left(\frac{\kappa}{2}\right)^2 \left(\frac{\alpha'}{4}\right)^2 [34]^4 \frac{(t-m^2)(u-m^2)}{s}. \quad (6.28)$$

At one loop, the result of [173] for the no-flip amplitude gives:

$$\begin{aligned} \mathcal{A}_{R^3}^{(1)}(1^\phi, 2^\phi, 3^{--}, 4^{++}) \simeq & \left(\frac{\kappa}{2}\right)^4 \left(\frac{\alpha'}{4}\right)^2 \mathcal{N}_h \left[(ms)^4 (I_4(s, t; m) + I_4(s, u; m)) + (m^2 s \omega)^2 I_3(s; m) \right. \\ & \left. + \frac{3}{2} (ms \omega)^2 I_2(s) \right]. \end{aligned} \quad (6.29)$$

The one-loop amplitude with helicity flip requires a new computation and the result in the eikonal approximation is

$$\begin{aligned} \mathcal{A}_{R^3}^{(1)}(1^\phi, 2^\phi, 3^{++}, 4^{++}) \simeq & \left(\frac{\kappa}{2}\right)^4 \left(\frac{\alpha'}{4}\right)^2 [34]^4 \left[(2m\omega)^4 (I_4(s, t; m) + I_4(s, u; m)) \right. \\ & \left. - 13(m^2 \omega)^2 I_3(s; m) + 16(m\omega)^2 s I_3(s) + \frac{153}{10} (m\omega)^2 I_2(s) \right]. \end{aligned} \quad (6.30)$$

6.3.3 Four-point scalar/graviton scattering in EH + R^4

In this section we consider the addition of an R^4 interaction to the EH action. Such interaction affects the two-scalar two-graviton amplitude at one loop and thus contributes to graviton deflection and time delay at order G^2 . In order to build this amplitude using the unitarity-based method we first need to find out the expression for the four-graviton tree-level amplitudes in the R^4 theory. We do so here starting from the Lagrangian in (6.3) in order to make contact with the notation of [341]. We also present an alternative derivation only relying on the algorithm presented in Chapter 2, which does not require writing down any Lagrangian.

Deriving the four-graviton amplitudes from (6.3) is straightforward – we simply have to replace the four Riemann tensors in each term by their linearised form corresponding to the four on-shell gravitons. For particle i the well-known expression in momentum space is

$$R(i)_{\mu\nu\rho\sigma} = \frac{1}{2} F(i)_{\mu\nu} F(i)_{\rho\sigma} \quad (6.31)$$

where

$$F(i)_{\mu\nu} = p_{i\mu} \varepsilon_{i\nu} - p_{i\nu} \varepsilon_{i\mu}. \quad (6.32)$$

Since we are interested in helicity amplitudes, we choose the field strengths $F(i)$ to be selfdual (negative helicity) or anti-selfdual (positive helicity), hence in spinor-helicity formalism their form is

$$F(i)_{\text{SD } \alpha\dot{\alpha}\beta\dot{\beta}} = -\sqrt{2} \lambda_{i\alpha} \lambda_{i\beta} \epsilon_{\dot{\alpha}\dot{\beta}} \quad \text{and} \quad F(i)_{\text{ASD } \alpha\dot{\alpha}\beta\dot{\beta}} = -\sqrt{2} \tilde{\lambda}_{i\dot{\alpha}} \tilde{\lambda}_{i\dot{\beta}} \epsilon_{\alpha\beta}. \quad (6.33)$$

The building blocks in (6.4) are bilinear in Riemann tensors, and take the form

$$\mathcal{C} \simeq (F(i)_{(A)SD} \cdot F(j)_{(A)SD})^2, \quad (6.34)$$

and

$$\tilde{\mathcal{C}} \simeq (F(i)_{(A)SD} \cdot F(j)_{(A)SD}) \left(F(i)_{(A)SD} \cdot \frac{1}{i} * F(j)_{(A)SD} \right), \quad (6.35)$$

where \cdot denotes Lorentz contractions and $*$ denotes the usual Hodge dual which acts on the (anti-)selfdual field strengths as $*F_{SD} = F_{SD}$ and $*F_{ASD} = -F_{ASD}$. Furthermore, given the form (6.33) these expressions are only non-vanishing if both particles i and j have the same helicity. In summary, if both gravitons have negative helicity (SD field strength) we have

$$\mathcal{C} = i\tilde{\mathcal{C}} = \frac{1}{2} \langle ij \rangle^4, \quad (6.36)$$

while if both gravitons have positive helicity (ASD field strength) we have

$$\mathcal{C} = -i\tilde{\mathcal{C}} = \frac{1}{2} [ij]^4. \quad (6.37)$$

With these results one easily arrives at

$$\begin{aligned} \mathcal{A}_{R^4}^{(0)}(1^{++}, 2^{++}, 3^{++}, 4^{++}) &= i\beta^+ \left(\frac{\kappa}{2}\right)^2 ([12]^4[34]^4 + [13]^4[24]^4 + [14]^4[23]^4), \\ \mathcal{A}_{R^4}^{(0)}(1^{--}, 2^{--}, 3^{--}, 4^{--}) &= i\beta^- \left(\frac{\kappa}{2}\right)^2 (\langle 12 \rangle^4 \langle 34 \rangle^4 + \langle 13 \rangle^4 \langle 24 \rangle^4 + \langle 14 \rangle^4 \langle 23 \rangle^4), \\ \mathcal{A}_{R^4}^{(0)}(1^{++}, 2^{++}, 3^{--}, 4^{--}) &= i\tilde{\beta} \left(\frac{\kappa}{2}\right)^2 [12]^4 \langle 34 \rangle^4, \end{aligned} \quad (6.38)$$

with

$$\beta^+ = 4 \left(\beta_1 + \frac{i}{2} \beta_2 - \beta_3 \right), \quad (6.39)$$

$$\beta^- = 4 \left(\beta_1 - \frac{i}{2} \beta_2 - \beta_3 \right), \quad (6.40)$$

$$\tilde{\beta} = 4 \left(\beta_1 + \beta_3 \right). \quad (6.41)$$

Note that if we do not allow the parity-odd coupling ($\beta_2 = 0$), then the coefficient of the all-plus and all-minus amplitudes are the same $\beta^+ = \beta^- := \beta$.

The next step is to carry out one-loop amplitude calculations in the eikonal approximation, as done in previous sections. The result for the relevant amplitudes is:

$$\begin{aligned} \mathcal{A}_{R^4}^{(1)}(1^\phi, 2^\phi, 3^{--}, 4^{++}) &\simeq -\mathcal{N}_h \tilde{\beta} \left(\frac{\kappa}{2}\right)^4 s^2 \left[\frac{35}{4} (m\omega)^4 I_3(s; m) + \frac{93}{8} (m\omega^2)^2 I_2(s) \right], \\ \mathcal{A}_{R^4}^{(1)}(1^\phi, 2^\phi, 3^{++}, 4^{++}) &\simeq -\beta^+ \left(\frac{\kappa}{2}\right)^4 [34]^4 \left[\frac{3}{4} (m\omega)^4 I_3(s; m) + \frac{55}{24} (m\omega^2)^2 I_2(s) \right], \\ \mathcal{A}_{R^4}^{(1)}(1^\phi, 2^\phi, 3^{--}, 4^{--}) &\simeq -\beta^- \left(\frac{\kappa}{2}\right)^4 \langle 34 \rangle^4 \left[\frac{3}{4} (m\omega)^4 I_3(s; m) + \frac{55}{24} (m\omega^2)^2 I_2(s) \right]. \end{aligned} \quad (6.42)$$

R^4 contact terms from the graph-based method

Here we show an alternative and simpler way to compute four-graviton contact terms induced by R^4 -type interactions, based on the algorithm presented in Chapter 2. Despite being simpler, such method does not provide a normalisation of the amplitude in terms of the couplings appearing at the level of the action (6.1).

The first observation is that the terms we are after are polynomial in the spinor variables for which the degree of homogeneity are either $(+2, +2, +2, +2)$ (and its complex conjugate) or $(+2, +2, -2, -2)$. Then, we are looking for the structures with the minimal mass dimension, *i.e.* with the minimum number of momentum insertions, which in this case turn out to be zero. This means that all the planar graphs give a basis of kinematically independent monomials. The MHV configuration $(+2, +2, -2, -2)$ is trivial because there is only one monomial: which also respect the correct permutation

$$\mathcal{A}_{R^4}^{(0)}(1^{++}, 2^{++}, 3^{--}, 4^{--}) \propto \mathbb{M} \circ \begin{array}{c} \begin{array}{c} 1 \begin{array}{c} \leftarrow \quad \rightarrow \\ \leftarrow \quad \rightarrow \end{array} 2 \\ \\ 4 \begin{array}{c} \leftarrow \quad \rightarrow \\ \leftarrow \quad \rightarrow \end{array} 3 \end{array} \end{array} = [12]^4 [34]^4 ,$$

symmetries.

For the all-plus configuration we have five kinematically independent monomials:

$$\begin{array}{c} \mathbb{M} \circ \begin{array}{c} 1 \begin{array}{c} \leftarrow \quad \rightarrow \\ \leftarrow \quad \rightarrow \end{array} 2 \\ \\ 4 \begin{array}{c} \leftarrow \quad \rightarrow \\ \leftarrow \quad \rightarrow \end{array} 3 \end{array} = [12]^4 [34]^4 , \quad \mathbb{M} \circ \begin{array}{c} 1 \quad 2 \\ \leftarrow \quad \rightarrow \\ 4 \quad 3 \end{array} = [14]^4 [23]^4 , \\ \\ \mathbb{M} \circ \begin{array}{c} 1 \begin{array}{c} \leftarrow \quad \rightarrow \\ \leftarrow \quad \rightarrow \end{array} 2 \\ \leftarrow \quad \rightarrow \\ 4 \begin{array}{c} \leftarrow \quad \rightarrow \\ \leftarrow \quad \rightarrow \end{array} 3 \end{array} = [12]^3 [14] [23] [34]^3 , \quad \mathbb{M} \circ \begin{array}{c} 1 \quad 2 \\ \leftarrow \quad \rightarrow \\ \leftarrow \quad \rightarrow \\ 4 \quad 3 \end{array} = [12] [14]^3 [23]^3 [34] , \\ \\ \mathbb{M} \circ \begin{array}{c} 1 \begin{array}{c} \leftarrow \quad \rightarrow \\ \leftarrow \quad \rightarrow \end{array} 2 \\ \leftarrow \quad \rightarrow \\ 4 \begin{array}{c} \leftarrow \quad \rightarrow \\ \leftarrow \quad \rightarrow \end{array} 3 \end{array} = [12]^2 [14]^2 [23]^2 [34]^2 . \end{array}$$

Upon imposing permutation symmetry to such terms, we find that the first and the second couple of terms give the same contact terms. Moreover, after symmetrising such structures, we find that the polynomials are written in terms of non planar monomials. For example, for the first we find:

$$\frac{1}{3} [14]^4 [23]^4 + \frac{1}{3} [13]^4 [24]^4 + \frac{1}{3} [12]^4 [34]^4 ,$$

where the first term correspond to

$$\mathbb{M}^{-1}([14]^4[23]^4) = \begin{array}{c} \begin{array}{cc} 1 & 2 \\ \text{---} & \text{---} \\ \text{---} & \text{---} \\ \text{---} & \text{---} \\ \text{---} & \text{---} \\ \text{---} & \text{---} \\ 4 & 3 \end{array} \\ \cdot \end{array}$$

We can recursively untie the crossing of such graphs to write them as a linear combination of the planar monomials, using recursively the graph identity shown in Figure 2.2. Once we perform this decomposing we find that the three remaining terms are all proportional to each other. Then there is a unique kinematically independent contact term for the all-plus configuration

$$\mathcal{A}_{R^4}^{(0)}(1^{++}, 2^{++}, 3^{++}, 4^{++}) \propto \mathcal{Y}_{\overline{1234}} \circ \mathbb{M} \circ \begin{array}{c} \begin{array}{cc} 1 & 2 \\ \text{---} & \text{---} \\ \text{---} & \text{---} \\ \text{---} & \text{---} \\ \text{---} & \text{---} \\ \text{---} & \text{---} \\ 4 & 3 \end{array} \end{array} = \frac{1}{3} ([14]^4[23]^4 + [13]^4[24]^4 + [12]^4[34]^4) .$$

6.3.4 Scattering with the FFR interaction

The last interaction we wish to consider is the *FFR* term in (6.1). From an on-shell point of view this is the simplest non-minimal modification of the coupling of photons to gravity. As we will show below this leads to new corrections to the bending and time delay/advance of light and graviton propagation in the background of a very massive scalar particle.

This new interaction modifies the three-point two-photon/one-graviton amplitude:

$$\mathcal{A}_{\text{FFR}}^{(0)}(1^+, 2^+, 3^{++}) = i \left(\frac{\kappa}{2} \right) \left(\frac{\alpha_\gamma}{4} \right) [13]^2 [23]^2 , \quad (6.43)$$

which we will now use to construct the relevant amplitudes at tree level and one loop to compute deflection angles and time delay in the presence of this interaction. Note that this amplitude is determined by its helicity structure and dimensional analysis up to a normalisation which we fixed from the our action (6.1).

Graviton deflection

Using their factorisation properties or Feynman diagrams, we have computed the four-point amplitudes relevant for graviton deflection from a massive *charged* source (such as a charged black hole). The new *FFR* interaction involves two photons and one graviton, hence one cannot generate a tree-level correction to the amplitude with two scalars and two gravitons. The first corrections arise at one loop, from the cut diagrams in Figure 6.2.

For the cut diagram on the left-hand side of the figure, we need the tree-level scalar QED amplitude with two photons and two massive scalars [130]

$$\mathcal{A}_{\text{SQED}}^{(0)}(1^\phi, 2^\phi, 3^+, 4^+) = Q^2 m^2 \frac{[34]^2}{s} \left(\frac{i}{t - m^2} + \frac{i}{u - m^2} \right) , \quad (6.44)$$

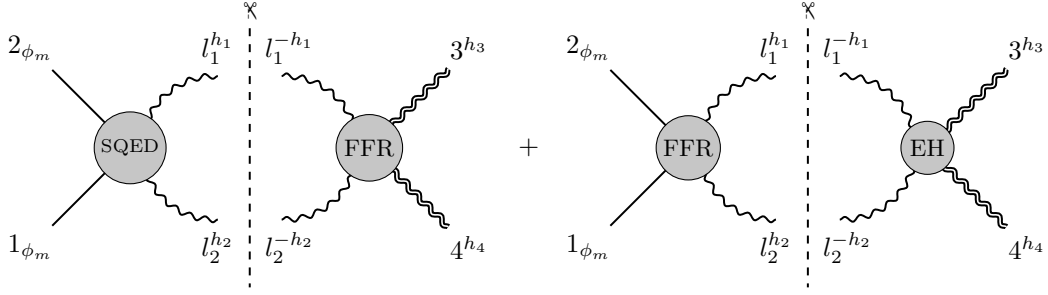


Figure 6.2: The two-particle cut diagrams in the $s = -\vec{q}^2$ -channel of the graviton deflection angle in the presence of an FFR interaction. The internal lines are photons. The first diagram is proportional to $\kappa^2 e^2$ and is only non-vanishing for $h_1 = h_2$ for the internal photons. The second diagram is proportional to κ^4 , it is non-vanishing when $h_4 = -h_3$ and $h_2 = -h_1$ thus it contributes solely to the helicity-preserving configuration. Also, it only produces quantum corrections (bubble integrals) with coefficients that vanish in the case of four-dimensional external kinematics.

along with the modification to the two-graviton/two-photon amplitudes arising from the FFR coupling for both helicity configurations of the graviton: no flip,

$$\mathcal{A}_{FFR}^{(0)}(1^+, 2^+, 3^{--}, 4^{++}) = -i \left(\frac{\kappa}{2}\right)^2 \left(\frac{\alpha_\gamma}{4}\right) [12]^2 \frac{\langle 3|1|4 \rangle^4}{stu}, \quad (6.45)$$

or flipped,

$$\mathcal{A}_{FFR}^{(0)}(1^+, 2^+, 3^{++}, 4^{++}) = i \left(\frac{\kappa}{2}\right)^2 \left(\frac{\alpha_\gamma}{4}\right) \left(\frac{[13]^2 [34]^2 [42]^2}{s_{13}} + \frac{[23]^2 [34]^2 [41]^2}{s_{23}} \right). \quad (6.46)$$

Both amplitudes can be computed with on-shell techniques. Specifically, (6.45) can be constructed using BCFW recursion relations [22] by shifting appropriately the graviton momenta, while it is easy to verify [25] that (6.46) can be derived via an (holomorphic) all-line shift. Note that the two-particle cut is non-vanishing only in the singlet configuration (internal photons with the same helicities). This is because the four-point amplitude with two photons and two gravitons induced by the FFR interaction is non-vanishing only for same-helicity photons.

We now move to the cut diagram on the right-hand side of Figure 6.2. The two-photon/two-graviton EH amplitude only exists in the configuration where the gravitons and the photons have opposite helicity (see for instance [134]),

$$\mathcal{A}_{EH}^{(0)}(1^+, 2^-, 3^{++}, 4^{--}) = -i \left(\frac{\kappa}{2}\right)^2 [13]^2 \langle 24 \rangle^2 \frac{\langle 4|1|3 \rangle^2}{stu}, \quad (6.47)$$

and thus it contributes only in the helicity-preserving process. Hence, in order to compute the cut we will only need the following two-scalar/two-photon amplitude involving an FFR interaction:

$$\mathcal{A}_{FFR}^{(0)}(1^\phi, 2^\phi, 3^-, 4^+) = -i \left(\frac{\kappa}{2}\right)^2 \left(\frac{\alpha_\gamma}{4}\right) \langle 3|1|4 \rangle^2. \quad (6.48)$$

Such amplitude is a contact term and can be only computed consistently with the action (6.1) using the corresponding Feynman rules.

Following the above considerations, the one-loop amplitudes in the eikonal limit can be computed entirely from the LHS of Figure 6.2, and are found to be

$$\begin{aligned} \mathcal{A}_{\text{FFR}}^{(1)}(1^\phi, 2^\phi, 3^{--}, 4^{++}) &\simeq -\mathcal{N}_h Q^2 \left(\frac{\kappa}{2}\right)^2 \left(\frac{\alpha_\gamma}{4}\right) s \left[(ms)^2 (I_4(s, t; m) + I_4(s, u; m)) \right. \\ &\quad \left. + (m\omega)^2 I_3(s; m) + \frac{3}{4} \frac{s^3}{\omega^2} I_3(s) + \frac{3}{2} \omega^2 I_2(s) \right], \\ \mathcal{A}_{\text{FFR}}^{(1)}(1^\phi, 2^\phi, 3^{++}, 4^{++}) &= Q^2 \left(\frac{\kappa}{2}\right)^2 \left(\frac{\alpha_\gamma}{4}\right) m^2 [34]^4 I_3(s; m), \end{aligned} \quad (6.49)$$

where again \mathcal{N}_h is the phase defined in (6.25), and Q denotes the charge of the classical source (the black hole).

Photon deflection

It is interesting to study how this new *FFR* interaction affects the bending and time delay/advance of light. In order to do so, we now review the known two-scalar/two-photon amplitudes for minimally coupled photons [134], and present the new corresponding amplitudes induced by the *FFR* interaction, both at tree and one-loop level.

In the following we consider processes where the internal legs are gravitons. In the EH theory, for the two-photon two-scalar process, only the helicity-preserving amplitude is non vanishing, both at tree level

$$\mathcal{A}_{\text{EH}}^{(0)}(1^\phi, 2^\phi, 3^-, 4^+) = i \left(\frac{\kappa}{2}\right)^2 \frac{\langle 3|1|4 \rangle^2}{s}, \quad (6.50)$$

and at one loop [134],

$$\begin{aligned} \mathcal{A}_{\text{EH}}^{(1)}(1^\phi, 2^\phi, 3^-, 4^+) &\simeq -\mathcal{N}_\gamma \left(\frac{\kappa}{2}\right)^4 \left[(2m\omega)^4 (I_4(s, t; m) + I_4(s, u; m)) - 15(m^2\omega)^2 I_3(s; m) \right. \\ &\quad \left. + 3s(2m\omega)^2 I_3(s) - \frac{161}{30} (m\omega)^2 I_2(s) \right], \end{aligned} \quad (6.51)$$

where the phase factor \mathcal{N}_γ is

$$\mathcal{N}_\gamma = \left(\frac{\langle 3|1|4 \rangle}{2m\omega}\right)^2 \simeq -1. \quad (6.52)$$

We now discuss the corrections to the two-scalar two-photon amplitudes arising from one insertion of the *FFR* interaction. These come from a single graviton exchange between a minimally coupled scalar and the *FFR* three-point vertex. At tree level, only the helicity-flip amplitude

$$\mathcal{A}_{\text{FFR}}^{(0)}(1^\phi, 2^\phi, 3^+, 4^+) = -i \left(\frac{\kappa}{2}\right)^2 \left(\frac{\alpha_\gamma}{4}\right) [34]^2 \left[\frac{(t-m^2)(u-m^2)}{s} + m^2 \right], \quad (6.53)$$

contributes in the eikonal approximation, while the no-flip amplitude, already quoted in (6.48), is a contact term that is subleading in the eikonal limit (it does not have a pole

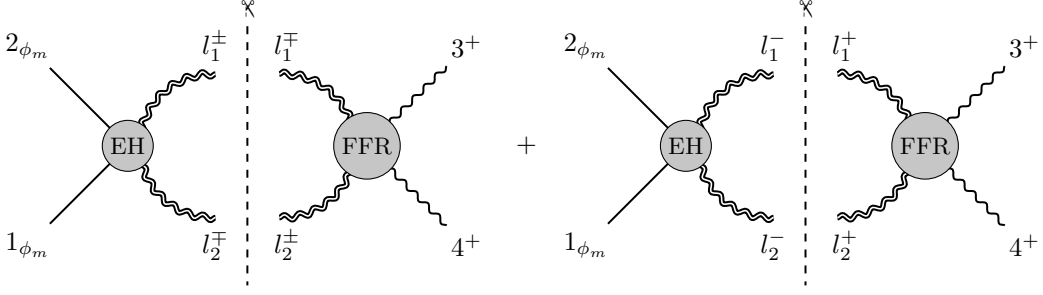


Figure 6.3: The two-particle cut diagrams in the $s = -|\vec{q}|^2$ -channel contributing to photon deflection to first order in the FFR interaction. We only show the helicity-flip configuration since the helicity-preserving cuts vanish. The cut diagram on the RHS of the figure only contributes terms which are subleading in the eikonal limit.

in $s = -|\vec{q}|^2$). We also notice that this amplitude can not be completely fixed using on-shell arguments, in a consistent way with (6.1), then we needed the corresponding Feynman rules.

Moving to one loop, the relevant two-particle cuts for the $(++)$ configuration are shown in Figure 6.3. We find that the amplitude with photons in the $(++)$ helicity configuration in the eikonal approximation is

$$\begin{aligned} \mathcal{A}_{\text{FFR}}^{(1)}(1^\phi, 2^\phi, 3^+, 4^+) \simeq - \left(\frac{\kappa}{2}\right)^4 \left(\frac{\alpha_\gamma}{4}\right) [34]^2 \Big[& (2m\omega)^4 (I_4(s, t; m) + I_4(s, u; m)) \\ & - 15(m^2\omega)^2 I_3(s; m) + 3s (2m\omega)^2 I_3(s) \\ & + \frac{3}{10}(m\omega)^2 I_2(s) \Big], \end{aligned} \quad (6.54)$$

while the amplitude with photons in the $(+-)$ helicity configuration vanishes:

$$\mathcal{A}_{\text{FFR}}^{(1)}(1^\phi, 2^\phi, 3^-, 4^+) = 0. \quad (6.55)$$

6.4 Eikonal phase matrix, deflection angle and time delay

In the previous section we have derived the relevant tree and one-loop amplitudes which we will now use to extract the deflection angle and time delay up to 2PM order (or $\mathcal{O}(G^2)$) generated by the addition of the various couplings in (6.1). The key quantity is the eikonal phase matrix δ , to be introduced below, of which we will compute the leading, δ_0 , and subleading contributions, δ_1 . As an important consistency check we will confirm that the leading-energy contribution of the one-loop amplitudes captures the required exponentiation of the leading-order eikonal phase matrix δ_0 .

In the following we focus on the classical contribution to δ . We stress that for the cases we consider, δ will be a 2×2 matrix: the diagonal entries correspond to the two amplitudes $\mathcal{A}(1^\phi, 2^\phi, 3^{h_1}, 4^{h_2})$ where the helicity of the massless particle is not flipped (which in our all-outgoing convention corresponds to $h_1 = -h_2$), while the off-diagonal ones correspond to the two helicity-flip processes (with $h_1 = h_2$).

As a final comment, we note that the combined effect of the interactions in (6.1) is simply the sum of the contributions of each interaction treated independently; hence

we will study them separately, and begin our discussion by reviewing the computation in EH gravity.

6.4.1 Graviton deflection angle and time delay in Einstein-Hilbert gravity

Leading eikonal

The relevant tree-level amplitudes in EH gravity are given in (6.23). In the eikonal approximation (6.9) they become

$$\begin{aligned}\mathcal{A}_{\text{EH}}^{(0)}(1^\phi, 2^\phi, 3^{--}, 4^{++}) &\simeq i \left(\frac{\kappa}{2}\right)^2 \frac{(2m\omega)^2}{\vec{q}^2}, \\ \mathcal{A}_{\text{EH}}^{(0)}(1^\phi, 2^\phi, 3^{++}, 4^{++}) &\simeq i \left(\frac{\kappa}{2}\right)^2 \frac{m^2}{(2\omega)^2} \frac{q^4}{\vec{q}^2} \simeq 0,\end{aligned}\tag{6.56}$$

where the second amplitude is subleading compared to the first.

The amplitudes in impact parameter space are obtained from those in momentum space using (6.14). To compute them, we will use repeatedly the result

$$f(p, d) := \int \frac{d^d q}{(2\pi)^d} e^{i\vec{q}\cdot\vec{b}} |\vec{q}|^p = \frac{2^p \pi^{-d/2} \Gamma\left(\frac{d+p}{2}\right)}{\Gamma\left(-\frac{p}{2}\right)} \frac{1}{b^{d+p}},\tag{6.57}$$

where $b := |\vec{b}|$. We then have

$$\begin{aligned}\tilde{\mathcal{A}}_{\text{EH}}^{(0)}(1^\phi, 2^\phi, 3^{--}, 4^{++})\Big|_\omega &= i \left(\frac{\kappa}{2}\right)^2 \frac{m\omega}{4\pi^{\frac{d-2}{2}}} \Gamma\left(\frac{d}{2} - 2\right) \frac{1}{b^{d-4}}, \\ \tilde{\mathcal{A}}_{\text{EH}}^{(0)}(1^\phi, 2^\phi, 3^{++}, 4^{++})\Big|_\omega &= 0,\end{aligned}\tag{6.58}$$

therefore the leading eikonal phase matrix is

$$\delta_{0,\text{EH}} = \left(\frac{\kappa}{2}\right)^2 (m\omega) f(-2, d-2) \mathbb{1}_2 \simeq -\left(\frac{\kappa}{2}\right)^2 \frac{m\omega}{2\pi} \left[\frac{1}{4-d} + \log b \right] \mathbb{1}_2 + \dots,\tag{6.59}$$

where we omitted terms of $\mathcal{O}(d-4)$ and finite terms which do not depend on \vec{b} .

Next we consider the one-loop amplitudes (6.24) and (6.26). In order to check exponentiation (6.20) we only keep terms that are leading in energy in the eikonal approximation, *i.e.* $\mathcal{O}(\omega^3)$ in momentum space (or $\mathcal{O}(\omega^2)$ in impact parameter space). These are

$$\begin{aligned}\mathcal{A}_{\text{EH}}^{(1)}(1^\phi, 2^\phi, 3^{--}, 4^{++})\Big|_{\omega^3} &= \left(\frac{\kappa}{2}\right)^4 (2m\omega)^4 \left[I_4(s, t; m) + I_4(s, u; m) \right], \\ \mathcal{A}_{\text{EH}}^{(1)}(1^\phi, 2^\phi, 3^{++}, 4^{++})\Big|_{\omega^3} &= 0,\end{aligned}\tag{6.60}$$

where the sum of the box integrals $I_4(s, t; m) + I_4(s, u; m)$ was evaluated in d dimensions in [142] and is given in (D.12). Transforming to impact parameter space, we have

$$\tilde{\mathcal{A}}_{\text{EH}}^{(1)}(1^\phi, 2^\phi, 3^{--}, 4^{++})\Big|_{\omega^2} = -\left(\frac{\kappa}{2}\right)^4 (m\omega)^2 \frac{2^{d-7} \Gamma(d-4)}{\pi^{\frac{d}{2}} (d-4) \Gamma(3-d/2)} \frac{1}{b^{2d-8}}.\tag{6.61}$$

As expected from (6.20), we find that

$$\tilde{\mathcal{A}}_{\text{EH}}^{(1)}(1^\phi, 2^\phi, 3^{--}, 4^{++})\Big|_{\omega^2} = \frac{1}{2} \left[\tilde{\mathcal{A}}_{\text{EH}}^{(0)}(1^\phi, 2^\phi, 3^{--}, 4^{++})\Big|_\omega \right]^2 + \mathcal{O}(d-4).\tag{6.62}$$

Subleading eikonal

In momentum space, the subleading contribution to the eikonal phase matrix is extracted from the $\mathcal{O}(\omega^2)$ contribution to the amplitude in (6.24):⁵

$$\mathcal{A}_{\text{EH}}^{(1)}(1^\phi, 2^\phi, 3^{--}, 4^{++}) \Big|_{\omega^2} = \left(\frac{\kappa}{2}\right)^4 (-15 m^4 \omega^2) I_3(s; m), \quad (6.63)$$

where $I_3(s; m)$ is given in (D.11), and as usual $s = -|\vec{q}|^2$. In the following we focus on the first term on the right-hand side of (D.11), since the log term only contributes quantum corrections. Using

$$\int \frac{d^{d-2}q}{(2\pi)^{d-2}} e^{i\vec{q}\cdot\vec{b}} |\vec{q}|^{-1} = \frac{1}{2\pi} \frac{1}{b} + \mathcal{O}(d-4), \quad (6.64)$$

we obtain the subleading part of the amplitude in impact parameter space:

$$\tilde{\mathcal{A}}_{\text{EH}}^{(1)}(1^\phi, 2^\phi, 3^{--}, 4^{++}) \Big|_{\omega} = i \left(\frac{\kappa}{2}\right)^4 \frac{15}{256\pi} \frac{m^2 \omega}{b}, \quad (6.65)$$

and finally, using (6.18), δ_1 :

$$\delta_{1,\text{EH}} = \left(\frac{\kappa}{2}\right)^4 \frac{15}{256\pi} \frac{m^2 \omega}{b} \mathbb{1}_2. \quad (6.66)$$

The eikonal phase matrix up to one loop in EH is then given by

$$\delta_{\text{EH}} = \delta_{0,\text{EH}} + \delta_{1,\text{EH}} + \dots = - \left(\frac{\kappa}{2}\right)^2 \frac{m\omega}{2\pi} \left[\frac{1}{4-d} + \log b - \left(\frac{\kappa}{2}\right)^2 \frac{15}{256\pi} \frac{m}{b} \right] \mathbb{1}_2 + \dots \quad (6.67)$$

Note that this matrix is proportional to the identity, since the polarisation of the gravitons scattered by the classical source is unchanged. The deflection angle can now be extracted using (6.21). While the eigenvalues of δ are divergent in $d = 4$, the corresponding deflection angle is finite:

$$\theta_{\text{EH}} = -\frac{1}{2\pi} \left(\frac{\kappa}{2}\right)^2 \frac{m}{b} \left[1 + \left(\frac{\kappa}{2}\right)^2 \frac{15}{128} \frac{m}{b} \right] = -\frac{4 G m}{b} \left(1 + G \frac{15\pi m}{16 b} \right). \quad (6.68)$$

This result agrees with the derivation of [141], and as expected matches the photon deflection angle [132, 134], first computed by Einstein.⁶

Another quantity of interest which can be extracted from the eigenvalues of the eikonal matrix is the time delay. Using (6.22) applied to the leading eikonal phase (6.59), we get

$$t_{\text{EH}} = - \left(\frac{\kappa}{2}\right)^2 \frac{m}{2\pi} \left(\frac{1}{4-d} + \log b \right). \quad (6.69)$$

As is well known, in order to define the time delay in four dimensions we need to take the difference of two time delays as measured by an observer at b and one at a much larger distance $b_0 \gg b$ [340]. Doing so the pole in (6.69) drops out, and neglecting power-suppressed terms in b_0 one gets

$$t_{\text{EH}} = \left(\frac{\kappa}{2}\right)^2 \frac{m}{2\pi} \log \frac{b_0}{b} = 4 G m \log \frac{b_0}{b}, \quad (6.70)$$

⁵Note that such a contribution is absent in (6.26).

⁶Initially up to a factor of two [379].

in agreement with [380]. Including now also the contribution from δ_1 , we arrive at the result

$$t_{\text{EH}} = \left(\frac{\kappa}{2}\right)^2 \frac{m}{2\pi} \left[\log \frac{b_0}{b} + \left(\frac{\kappa}{2}\right)^2 \frac{15}{128} \frac{m}{b} \right] = 4Gm \left[\log \frac{b_0}{b} + G \frac{15\pi m}{16b} \right]. \quad (6.71)$$

In the next sections we compute the corrections $\Delta\theta_X$ and Δt_X to the deflection angle (6.68) and time delay (6.70) in EH due to the inclusion of an interactions X in (6.1). The complete deflection angle and time delay will then be $\theta_{\text{EH}} + \Delta\theta_X$ and $t_{\text{EH}} + \Delta t_X$.

6.4.2 Graviton deflection angle and time delay in EH + R^3

Leading eikonal

The relevant new amplitudes are obtained by evaluating (6.27) and (6.28) in the eikonal limit (6.9), with the result

$$\begin{aligned} \mathcal{A}_{R^3}^{(0)}(1^\phi, 2^\phi, 3^{--}, 4^{++}) &= 0, \\ \mathcal{A}_{R^3}^{(0)}(1^\phi, 2^\phi, 3^{++}, 4^{++}) &\simeq i \left(\frac{\kappa}{2}\right)^2 \left(\frac{\alpha'}{4}\right)^2 (2m\omega)^2 \frac{q^4}{\vec{q}^2}, \end{aligned} \quad (6.72)$$

where from (6.12) we have $[34]^4 = q^4$. In order to transform to impact parameter space we rewrite

$$\vec{b} \cdot \vec{q} = \mathfrak{b}\bar{q} + \bar{\mathfrak{b}}q, \quad (6.73)$$

with $\mathfrak{b} := (b_1 + ib_2)/2$, and $\bar{\mathfrak{b}} := (b_1 - ib_2)/2$ (and we recall our previous definitions $q = q_1 + iq_2$, $\bar{q} = q_1 - iq_2$), from which $\mathfrak{b}\bar{\mathfrak{b}} = b^2/4$. Then in \vec{b} -space we have

$$\begin{aligned} \tilde{\mathcal{A}}_{R^3}^{(0)}(1^\phi, 2^\phi, 3^{++}, 4^{++}) \Big|_\omega &= i \left(\frac{\kappa}{2}\right)^2 \left(\frac{\alpha'}{4}\right)^2 (m\omega) \left(\frac{\partial}{\partial \bar{\mathfrak{b}}}\right)^4 f(-2, d-2) \\ &= i \left(\frac{\kappa}{2}\right)^2 \left(\frac{\alpha'}{4}\right)^2 \frac{(m\omega)}{\bar{\mathfrak{b}}^4} \xi f(-2, d-2), \end{aligned} \quad (6.74)$$

where

$$\xi := \left(\frac{d}{2} - 2\right) \left(\frac{d}{2} - 1\right) \left(\frac{d}{2}\right) \left(\frac{d}{2} + 1\right). \quad (6.75)$$

Hence the leading eikonal phase matrix δ_0 , including the first contribution from the R^3 interaction, has the form

$$\delta_0 = \delta_{0,\text{EH}} + \delta_{0,R^3}, \quad (6.76)$$

where $\delta_{0,\text{EH}}$ is given in (6.59), and

$$\delta_{0,R^3} = \left(\frac{\kappa}{2}\right)^2 \left(\frac{\alpha'}{4}\right)^2 (m\omega) \left[\xi f(-2, d-2) \right] \begin{pmatrix} 0 & \bar{\mathfrak{b}}^{-4} \\ \mathfrak{b}^{-4} & 0 \end{pmatrix}, \quad (6.77)$$

where we have used (6.17).

Moving on to one loop, from (6.29) and (6.30) we obtain

$$\begin{aligned} \mathcal{A}_{R^3}^{(1)}(1^\phi, 2^\phi, 3^{--}, 4^{++}) \Big|_{\omega^3} &= 0, \\ \mathcal{A}_{R^3}^{(1)}(1^\phi, 2^\phi, 3^{++}, 4^{++}) \Big|_{\omega^3} &= \left(\frac{\kappa}{2}\right)^4 \left(\frac{\alpha'}{4}\right)^2 [34]^4 (2m\omega)^4 \left[I_4(s, t) + I_4(s, u) \right]. \end{aligned} \quad (6.78)$$

Transforming to impact parameter space, and using (D.12), we arrive at

$$\begin{aligned}\tilde{\mathcal{A}}_{R^3}^{(1)}(1^\phi, 2^\phi, 3^{++}, 4^{++})\Big|_{\omega^2} &= -\left(\frac{\kappa}{2}\right)^4 \left(\frac{\alpha'}{4}\right)^2 \frac{(m\omega)^2}{2\pi} \frac{1}{d-4} \left(\frac{\partial}{\partial \bar{\mathbf{b}}}\right)^4 f(d-6, d-2) \\ &= -\left(\frac{\kappa}{2}\right)^4 \left(\frac{\alpha'}{4}\right)^2 \frac{(m\omega)^2}{2\pi \bar{\mathbf{b}}^4} \frac{\xi'}{d-4} f(d-6, d-2),\end{aligned}\tag{6.79}$$

where

$$\xi' := (d-4)(d-3)(d-2)(d-1).\tag{6.80}$$

The leading one-loop amplitude matrix in the eikonal approximation is then found to be

$$\tilde{\mathcal{A}}_{\omega^2}^{(1)} = -\left(\frac{\kappa}{2}\right)^4 (m\omega)^2 \frac{f(d-6, d-2)}{2\pi(d-4)} \begin{pmatrix} 1 & \left(\frac{\alpha'}{4}\right)^2 \frac{\xi'}{\bar{\mathbf{b}}^4} \\ \left(\frac{\alpha'}{4}\right)^2 \frac{\xi'}{\bar{\mathbf{b}}^4} & 1 \end{pmatrix}.\tag{6.81}$$

One can then check the matrix relation

$$\mathcal{A}_{\omega^2}^{(1)} = -\frac{1}{2}(\delta_0)^2 + \mathcal{O}(d-4),\tag{6.82}$$

in agreement with (6.20). In writing (6.82) we have used that,

$$(\delta_0)^2 = \left(\frac{\kappa}{2}\right)^4 (m\omega)^2 [f(-2, d-2)]^2 \begin{pmatrix} 1 & \left(\frac{\alpha'}{4}\right)^2 \frac{2\xi}{\bar{\mathbf{b}}^4} \\ \left(\frac{\alpha'}{4}\right)^2 \frac{2\xi}{\bar{\mathbf{b}}^4} & 1 \end{pmatrix},\tag{6.83}$$

up to and including $\mathcal{O}((\alpha'/4)^2)$.

Finally we compute the eigenvalues of the matrix δ_0 in (6.76). Using

$$\xi f(-2, d-2) = \frac{3}{2\pi} + \mathcal{O}(d-4),\tag{6.84}$$

we can rewrite it as

$$\delta_0 = \left(\frac{\kappa}{2}\right)^2 \frac{m\omega}{2\pi} \begin{pmatrix} -\frac{1}{2\epsilon} - \log b & \left(\frac{\alpha'}{4}\right)^2 \frac{3}{\bar{\mathbf{b}}^4} \\ \left(\frac{\alpha'}{4}\right)^2 \frac{3}{\bar{\mathbf{b}}^4} & -\frac{1}{2\epsilon} - \log b \end{pmatrix},\tag{6.85}$$

whose eigenvalues are

$$\delta_0^{(1,2)} = \left(\frac{\kappa}{2}\right)^2 \frac{m\omega}{2\pi} \left[-\frac{1}{2\epsilon} - \log b \pm \left(\frac{\alpha'}{4}\right)^2 \frac{48}{\bar{\mathbf{b}}^4} \right].\tag{6.86}$$

Following identical steps to those leading from (6.67) to (6.71), one obtains for the time delay at $\mathcal{O}(G)$

$$t_{\text{EH}+R^3} = 4Gm \left[\log \frac{b_0}{b} \pm \left(\frac{\alpha'}{4}\right)^2 \frac{48}{\bar{\mathbf{b}}^4} \right],\tag{6.87}$$

where $G = \kappa^2/(32\pi)$. For sufficiently small b the eigenvalue with the choice of negative sign may become negative, leading to a time advance.

Comparison to the work of [340]

The time advance due to R^3 terms was first discovered in [340], from which it was argued that the only way to avoid causality violations is to embed the R^3 theory into an appropriate ultraviolet completion – in other words a consistent ultraviolet completion of gravitational theories with an R^3 interaction requires the addition of an infinite tower of massive particles with higher spins. Here we wish to briefly compare our results to theirs.

The authors of [340] considered the interaction of a graviton with the background produced by a coherent state of massless particles, and computed the eikonal phase in order to obtain the Shapiro time delay. The coherent state simulates a large number of successive interactions of the graviton with a single weakly-coupled particle, each instance being considered as independent and contributing with a small amount to the total phase shift. It is then observed that the presence of the R^3 coupling, which modifies the three-point graviton amplitude, leads to non-degenerate eigenvalues of the eikonal phase matrix. This set-up avoids a subtlety which is present when we consider the graviton scattered off a black hole. Indeed, such causality violation can be observed only for very small impact parameter. On the other hand, such classical scattering is meaningful only if the impact parameter is larger than the Schwarzschild radius of the black hole, $b \gg 2Gm$. In the shockwave scattering considered in [340] such constrain is lifted and this is an example of causality violation of the classical theory. On the other hand, the quantum (effective) theory is well-defined up to a UV scale Λ ($b \gg \frac{1}{\Lambda}$), with $\alpha' = \frac{c_{\alpha'}}{\Lambda^2}$ and $c_{\alpha'}$ a order unit coefficient. Indeed, it is easy to check that such causality violation appear at length scales $b \sim \frac{1}{\Lambda}$, where the predictivity of the theory breaks down.

Concretely, it is interesting to compare the eigenvalues (6.86) of the leading eikonal phase matrix (6.76). Pleasingly, these eigenvalues turn out to be identical⁷ to the eigenvalues (3.22) of [340], upon replacing $m\omega \rightarrow \omega^2$. This is due to the fact that we consider a different set-up, with massless gravitons moving in the background produced by massive scalar objects of mass m . In both cases the time advance is induced by the novel three-graviton coupling generated by the R^3 interaction.

Subleading eikonal

We now go back to the one-loop amplitudes (6.29) and (6.30) and extract the triangle contributions which are the relevant terms contributing to the subleading eikonal matrix:

$$\begin{aligned} \mathcal{A}_{R^3}^{(1)}(1^\phi, 2^\phi, 3^{--}, 4^{++}) \Big|_{\omega^2} &= \left(\frac{\kappa}{2}\right)^4 \left(\frac{\alpha'}{4}\right)^2 |\vec{q}|^4 m^4 \omega^2 I_3(s; m), \\ \mathcal{A}_{R^3}^{(1)}(1^\phi, 2^\phi, 3^{++}, 4^{++}) \Big|_{\omega^2} &= -13 \left(\frac{\kappa}{2}\right)^4 \left(\frac{\alpha'}{4}\right)^2 q^4 m^4 \omega^2 I_3(s; m). \end{aligned} \tag{6.88}$$

⁷Note that in (3.22) of [340] the $1/\epsilon$ pole was not written explicitly. This pole does not affect either the time delay (6.87) or the particle bending angle. Our $1/\epsilon$ pole corresponds to the $\log L$ term in [340], where L is an infrared cutoff.

We can now transform to impact parameter space, using

$$\int \frac{d^{d-2}q}{(2\pi)^{d-2}} e^{i\vec{q}\cdot\vec{b}} |\vec{q}|^3 = \frac{9}{2\pi} \frac{1}{b^5} + \mathcal{O}(d-4), \quad (6.89)$$

$$\left(\frac{\partial}{\partial \vec{b}}\right)^4 \int \frac{d^{d-2}q}{(2\pi)^{d-2}} e^{i\vec{q}\cdot\vec{b}} |\vec{q}|^{-1} = \frac{105}{32\pi} \frac{1}{b} \frac{1}{b^4} + \mathcal{O}(d-4). \quad (6.90)$$

The amplitudes in impact parameter space then become

$$\begin{aligned} \tilde{\mathcal{A}}_{R^3}^{(1)}(1^\phi, 2^\phi, 3^{--}, 4^{++}) \Big|_\omega &= -i \left(\frac{\kappa}{2}\right)^4 \left(\frac{\alpha'}{4}\right)^2 \frac{9}{256\pi} \frac{m^2\omega}{b^5}, \\ \tilde{\mathcal{A}}_{R^3}^{(1)}(1^\phi, 2^\phi, 3^{++}, 4^{++}) \Big|_\omega &= i \left(\frac{\kappa}{2}\right)^4 \left(\frac{\alpha'}{4}\right)^2 \frac{1365}{4096\pi} \frac{m^2\omega}{b} \frac{1}{b^4}. \end{aligned} \quad (6.91)$$

Using (6.17), we can extract the contribution of the R^3 interaction to the subleading eikonal matrix δ_1 :

$$\delta_{1,R^3} = \left(\frac{\kappa}{2}\right)^4 \left(\frac{\alpha'}{4}\right)^2 \frac{1}{256\pi} \frac{m^2\omega}{b} \begin{pmatrix} -\frac{9}{b^4} & \frac{1365}{16} \frac{1}{b^4} \\ \frac{1365}{16} \frac{1}{b^4} & -\frac{9}{b^4} \end{pmatrix}. \quad (6.92)$$

Then the correction to the graviton deflection angle is

$$\Delta\theta_{R^3}^{(1,2)} = -\frac{4Gm}{b} \left(\frac{\alpha'}{4}\right)^2 \left[\pm \frac{192}{b^4} + \frac{5\pi}{16} (-9 \pm 1365) \frac{Gm}{b^5} \right]. \quad (6.93)$$

The deflection involving a graviton whose helicity is preserved in the scattering process has already been studied in [173], instead the flipped helicity case is presented here for the first time.

Finally, for the time delay we arrive at

$$\Delta t_{R^3}^{(1,2)} = 4Gm \left(\frac{\alpha'}{4}\right)^2 \left[\pm 48 \frac{1}{b^4} + \frac{\pi}{16} (-9 \pm 1365) \frac{Gm}{b^5} \right]. \quad (6.94)$$

6.4.3 Graviton deflection angle and time delay in $\text{EH} + R^4$

In this section we consider the deflection of gravitons induced by eight-derivative couplings in the Lagrangian, which we collectively denote as R^4 . We will only consider the parity-even interactions in (6.3) in order to present more compact formulae, therefore we set $\beta_2 = 0$, and hence $\beta^+ = \beta^- = \beta$ in (6.38) and (6.42). Furthermore, since these interactions do not produce a three-graviton vertex, it is impossible to build any tree-level two-scalar two-graviton amplitude involving R^4 . Thus there is no tree-level (1PM) bending associated to the new term in the Lagrangian, and one has

$$\delta_{0,R^4} = 0, \quad (6.95)$$

and the leading contribution arises at 2PM order. Furthermore, since the R^4 term only produces a contact term four-graviton interaction, the resulting one-loop amplitudes does not contain any box integral. This is consistent with the absence of a tree-level

contribution in (6.95) which, in the eikonal approximation, is expected to exponentiate, and would result at one loop in the appearance of box integrals. The same situation occurs for the graviton deflection due to *FFR* couplings discussed in Section 6.4.4.

The relevant one-loop amplitudes are given in (6.42), and from the massive triangle contributions we extract the following results in the eikonal approximation:

$$\begin{aligned}\mathcal{A}_{R^4}^{(1)}(1^\phi, 2^\phi, 3^{--}, 4^{++})\Big|_{\omega^4} &= i\tilde{\beta} \left(\frac{\kappa}{2}\right)^4 \frac{35}{128} m^3 \omega^4 |\vec{q}|^3, \\ \mathcal{A}_{R^4}^{(1)}(1^\phi, 2^\phi, 3^{++}, 4^{++})\Big|_{\omega^4} &= i\beta \left(\frac{\kappa}{2}\right)^4 \frac{3}{128} m^3 \omega^4 \frac{q^4}{|\vec{q}|},\end{aligned}\tag{6.96}$$

which then translate in impact parameter space into

$$\begin{aligned}\tilde{\mathcal{A}}_{R^4}^{(1)}(1^\phi, 2^\phi, 3^{--}, 4^{++})\Big|_{\omega^3} &= i\tilde{\beta} \left(\frac{\kappa}{2}\right)^4 \frac{315}{512} \frac{m^2 \omega^3}{2\pi b^5}, \\ \tilde{\mathcal{A}}_{R^4}^{(1)}(1^\phi, 2^\phi, 3^{++}, 4^{++})\Big|_{\omega^3} &= i\beta \left(\frac{\kappa}{2}\right)^4 \frac{315}{512} \frac{m^2 \omega^3}{32\pi b} \frac{1}{b^4}.\end{aligned}\tag{6.97}$$

The subleading eikonal phase matrix resulting from the previous amplitudes is given by

$$\delta_{1,R^4} = \left(\frac{\kappa}{2}\right)^4 \frac{315}{512} \frac{m^2 \omega^3}{2\pi} \frac{1}{b} \begin{pmatrix} \tilde{\beta} \frac{1}{b^4} & \beta \frac{1}{16 b^4} \\ \beta \frac{1}{16 b^4} & \tilde{\beta} \frac{1}{b^4} \end{pmatrix}.\tag{6.98}$$

Upon extracting the eigenvalues and using (6.21), we can compute the deflection angle

$$\Delta\theta_{R^4}^{(1,2)} = -\left(\tilde{\beta} \pm \beta\right) (Gm)^2 \frac{1575\pi \omega^2}{16 b^6},\tag{6.99}$$

and the time delay

$$\Delta t_{R^4}^{(1,2)} = \left(\tilde{\beta} \pm \beta\right) \left(\frac{\kappa}{2}\right)^4 \frac{945}{512} \frac{m^2 \omega^2}{2\pi} \frac{1}{b^5} = \left(\tilde{\beta} \pm \beta\right) (Gm)^2 \frac{945\pi \omega^2}{16 b^5}.\tag{6.100}$$

We can express (6.99) and (6.100) in terms of the couplings introduced in (6.3). In the parity-even theory ($\beta_2 = 0$) we get $\beta + \tilde{\beta} = 8\beta_1$, and $\tilde{\beta} - \beta = 8\beta_3$. In order to avoid a potential time-advance and associated causality violation in the classical theory, we need to require

$$\beta_1 > 0 \quad \text{and} \quad \beta_3 > 0.\tag{6.101}$$

Interestingly this positivity constraint is the same as derived from causality considerations in [338] and general *S*-matrix analyticity properties in [339]. On the other hand, the computation of the time delay is not completely well-posed as the eikonal phase $\delta \propto \omega^3$ is expected to break causality and unitarity (as discussed for the signal model in Appendix D of [340]).

6.4.4 Graviton deflection angle and time delay in EH + *FFR*

Next we focus our attention on graviton deflection in EH theory with the addition of an *FFR* coupling. As discussed in Section 6.3.4, at tree level there is no new two-scalar two-graviton amplitude generated by this interaction, hence

$$\delta_{0,\text{FFR}} = 0.\tag{6.102}$$

In order to compute the subleading eikonal phase matrix, we look at the massive triangle contribution to the one-loop amplitudes in (6.49),

$$\begin{aligned}\mathcal{A}_{\text{FFR}}^{(1)}(1^\phi, 2^\phi, 3^{--}, 4^{++})\Big|_{\omega^2} &= -i Q^2 \left(\frac{\kappa}{2}\right)^2 \left(\frac{\alpha_\gamma}{4}\right) \frac{m\omega^2}{32} |\vec{q}|, \\ \mathcal{A}_{\text{FFR}}^{(1)}(1^\phi, 2^\phi, 3^{++}, 4^{++})\Big|_{\omega^2} &= 0.\end{aligned}\tag{6.103}$$

Using

$$\int \frac{d^{d-2}q}{(2\pi)^{d-2}} e^{i\vec{q}\cdot\vec{b}} |\vec{q}| = -\frac{1}{2\pi} \frac{1}{b^3} + \mathcal{O}(d-4),\tag{6.104}$$

we obtain

$$\begin{aligned}\tilde{\mathcal{A}}_{\text{FFR}}^{(1)}(1^\phi, 2^\phi, 3^{--}, 4^{++})\Big|_{\omega} &= i Q^2 \left(\frac{\kappa}{2}\right)^2 \left(\frac{\alpha_\gamma}{4}\right) \frac{\omega}{256\pi} \frac{1}{b^3}, \\ \tilde{\mathcal{A}}_{\text{FFR}}^{(1)}(1^\phi, 2^\phi, 3^{++}, 4^{++})\Big|_{\omega} &= 0,\end{aligned}\tag{6.105}$$

In this case the eikonal phase matrix is diagonal and the subleading contribution $\delta_{1,\text{FFR}}$ is immediately seen to be

$$\delta_{1,\text{FFR}} = Q^2 \left(\frac{\kappa}{2}\right)^2 \left(\frac{\alpha_\gamma}{4}\right) \frac{\omega}{256\pi} \frac{1}{b^3} \mathbb{1}_2.\tag{6.106}$$

The new contribution to the graviton deflection angle due to the *FFR* interaction is

$$\Delta\theta_{\text{FFR}} = -Q^2 \left(\frac{\kappa}{2}\right)^2 \left(\frac{\alpha_\gamma}{4}\right) \frac{3}{256\pi} \frac{1}{b^4} = -Q^2 G \left(\frac{\alpha_\gamma}{4}\right) \frac{3}{32} \frac{1}{b^4}.\tag{6.107}$$

and the time delay is

$$\Delta t_{\text{FFR}} = Q^2 \left(\frac{\kappa}{2}\right)^2 \left(\frac{\alpha_\gamma}{4}\right) \frac{1}{256\pi} \frac{1}{b^3} = Q^2 G \left(\frac{\alpha_\gamma}{4}\right) \frac{1}{32} \frac{1}{b^3}.\tag{6.108}$$

The bending in this case is due to the electric charge Q of the black hole, not to its mass, which does not appear in either (6.107) or (6.108). We conclude that in order to avoid possible causality violation due to time advance the coefficient of the *FFR* interaction must obey the positivity constraint

$$\alpha_\gamma > 0.\tag{6.109}$$

6.4.5 Photon deflection angle and time delay in EH + *FFR*

In this section we consider the photon deflection angle and the time delay/advance arising from the *FFR* interaction. Compared to the case of graviton bending considered in the previous section, there is a non-vanishing tree-level contribution to the deflection, thus we consider the leading and subleading eikonal cases separately.

Leading eikonal

The first contribution we consider arises from the EH tree-level amplitude (6.50), which in the eikonal approximation becomes⁸

$$\mathcal{A}_{\text{EH}}^{(0)}(1^\phi, 2^\phi, 3^-, 4^+) \simeq i \left(\frac{\kappa}{2}\right)^2 \frac{(2m\omega)^2}{\vec{q}^2},\tag{6.110}$$

⁸We recall from Section 6.3.4 that $\mathcal{A}_{\text{EH}}^{(0)}(1^\phi, 2^\phi, 3^+, 4^+) = \mathcal{A}_{\text{EH}}^{(0)}(1^\phi, 2^\phi, 3^-, 4^-) = 0$.

or, upon transforming to impact parameter,

$$\tilde{\mathcal{A}}_{\text{EH}}^{(0)}(1^\phi, 2^\phi, 3^-, 4^+) \simeq i \left(\frac{\kappa}{2}\right)^2 m \omega f(-2, d-2). \quad (6.111)$$

Note that (6.110) has the same form as the two-scalar two-graviton amplitude in the eikonal approximation, first equation in (6.56), as consequence of the equivalence principle.

At tree-level the helicity-preserving *FFR* amplitude (6.48) is purely a contact term, while the helicity-flip amplitude is given in (6.53). The leading contribution in the eikonal limit is then

$$\begin{aligned} \mathcal{A}_{\text{FFR}}^{(0)}(1^\phi, 2^\phi, 3^-, 4^+) &\simeq 0, \\ \mathcal{A}_{\text{FFR}}^{(0)}(1^\phi, 2^\phi, 3^+, 4^+) &\simeq i \left(\frac{\kappa}{2}\right)^2 \left(\frac{\alpha_\gamma}{4}\right) (2m\omega)^2 \frac{q^2}{|\vec{q}|^2}, \end{aligned} \quad (6.112)$$

where we used $[34]^2 = -q^2$. Transforming the non-vanishing helicity-flip amplitude to impact parameter space we obtain

$$\tilde{\mathcal{A}}_{\text{FFR}}^{(0)}(1^\phi, 2^\phi, 3^+, 4^+) \simeq i \left(\frac{\kappa}{2}\right)^2 \left(\frac{\alpha_\gamma}{4}\right) \frac{m\omega}{\mathfrak{b}^2} \xi'' f(-2, d-2), \quad (6.113)$$

where

$$\xi'' = \left(\frac{d}{2} - 2\right) \left(\frac{d}{2} - 1\right). \quad (6.114)$$

Defining

$$\delta_0^\gamma = \delta_{0,\text{EH}}^\gamma + \delta_{0,\text{FFR}}^\gamma, \quad (6.115)$$

we can combine (6.111) and (6.113) into a single leading eikonal phase matrix

$$\delta_{0,\text{FFR}}^\gamma = - \left(\frac{\kappa}{2}\right)^2 \frac{m\omega}{2\pi} \begin{pmatrix} \frac{1}{4-d} + \log b & - \left(\frac{\alpha_\gamma}{4}\right) \frac{1}{2\mathfrak{b}^2} \\ - \left(\frac{\alpha_\gamma}{4}\right) \frac{1}{2\mathfrak{b}^2} & \frac{1}{4-d} + \log b \end{pmatrix}. \quad (6.116)$$

Next, in order to test the expected exponentiation property of the leading eikonal phase matrix, we consider the terms of $\mathcal{O}(\omega^2)$ in the one-loop amplitudes. These are given in impact parameter space by

$$\begin{aligned} \tilde{\mathcal{A}}_{\text{EH}}^{(1)}(1^\phi, 2^\phi, 3^-, 4^+) \Big|_{\omega^2} &= - \left(\frac{\kappa}{2}\right)^4 (m\omega)^2 \frac{f(d-6, d-2)}{2\pi(d-4)}, \\ \tilde{\mathcal{A}}_{\text{FFR}}^{(1)}(1^\phi, 2^\phi, 3^+, 4^+) \Big|_{\omega^2} &= - \left(\frac{\kappa}{2}\right)^4 \left(\frac{\alpha_\gamma}{4}\right) \frac{(m\omega)^2}{\mathfrak{b}^2} (d-3) \frac{f(d-6, d-2)}{2\pi}, \end{aligned} \quad (6.117)$$

which are obtained from (6.51) and (6.54). Expanding around $d=4$ we find that $\tilde{\mathcal{A}}_{\omega^2}^{(1)}$ satisfies the matrix equation

$$\tilde{\mathcal{A}}_{\omega^2}^{(1)} = -\frac{1}{2}(\delta_0)^2 + \mathcal{O}(d-4), \quad (6.118)$$

as expected.

Subleading eikonal

Next we consider the subleading eikonal phase. The only non-vanishing EH contribution comes from the one-loop massive triangles in the helicity-preserving amplitude (6.51), and reads

$$\tilde{\mathcal{A}}_{\text{EH}}^{(1)}(1^\phi, 2^\phi, 3^-, 4^+) \Big|_\omega = i \left(\frac{\kappa}{2}\right)^4 \frac{15}{256\pi} \frac{m^2\omega}{b}. \quad (6.119)$$

Just as in the case of the leading eikonal phase, the bending angle of photons in pure EH is the same as the graviton bending (6.66) thanks to the equivalence principle.

The contributions coming from the *FFR* interaction are obtained from (6.55) and (6.54), and in impact parameter space are

$$\begin{aligned} \tilde{\mathcal{A}}_{\text{FFR}}^{(1)}(1^\phi, 2^\phi, 3^-, 4^+) \Big|_\omega &= 0, \\ \tilde{\mathcal{A}}_{\text{FFR}}^{(1)}(1^\phi, 2^\phi, 3^+, 4^+) \Big|_\omega &= i \left(\frac{\kappa}{2}\right)^4 \left(\frac{\alpha_\gamma}{4}\right) \frac{45}{1024\pi} \frac{m^2\omega}{b} \frac{1}{\mathfrak{b}^2}. \end{aligned} \quad (6.120)$$

Combining these results into a subleading eikonal phase matrix we get

$$\delta_{1,\text{FFR}}^\gamma = \left(\frac{\kappa}{2}\right)^4 \frac{15}{256\pi} \frac{m^2\omega}{b} \begin{pmatrix} 1 & \left(\frac{\alpha_\gamma}{4}\right) \frac{3}{4\mathfrak{b}^2} \\ \left(\frac{\alpha_\gamma}{4}\right) \frac{3}{4\mathfrak{b}^2} & 1 \end{pmatrix}. \quad (6.121)$$

Deflection angle and time delay

Having computed the eikonal phase matrix at leading and subleading order, we can now extract the light bending angle and time advance/delay. First we compute the eigenvalues of the eikonal phase matrix (6.116), which at leading order match qualitatively the result of photon deflection in a shockwave background (see [370], and [356] for related work). We find the light bending angle up to $\mathcal{O}(G^2)$:

$$\begin{aligned} \Delta\theta_{\text{FFR}}^{\gamma(1,2)} &= -\left(\frac{\kappa}{2}\right)^2 \frac{1}{2\pi} \frac{m}{b} \left\{ 1 \pm \left(\frac{\alpha_\gamma}{4}\right) \frac{4}{b^2} + \left(\frac{\kappa}{2}\right)^2 \frac{15}{128} \frac{m}{b} \left[1 \pm \left(\frac{\alpha_\gamma}{4}\right) \frac{9}{b^2} \right] \right\} \\ &= -\frac{4Gm}{b} \left\{ 1 \pm \left(\frac{\alpha_\gamma}{4}\right) \frac{4}{b^2} + \frac{15\pi}{16} \frac{Gm}{b} \left[1 \pm \left(\frac{\alpha_\gamma}{4}\right) \frac{9}{b^2} \right] \right\}, \end{aligned} \quad (6.122)$$

and the time delay up to $\mathcal{O}(G^2)$:

$$\begin{aligned} \Delta t_{\text{FFR}}^{\gamma(1,2)} &= \left(\frac{\kappa}{2}\right)^2 \frac{m}{2\pi} \left\{ \log \frac{b_0}{b} \pm \left(\frac{\alpha_\gamma}{4}\right) \frac{2}{b^2} + \left(\frac{\kappa}{2}\right)^2 \frac{15}{128} \frac{m}{b} \left[1 \pm \left(\frac{\alpha_\gamma}{4}\right) \frac{3}{b^2} \right] \right\} \\ &= 4Gm \left\{ \log \frac{b_0}{b} \pm \left(\frac{\alpha_\gamma}{4}\right) \frac{2}{b^2} + \frac{15\pi}{16} \frac{Gm}{b} \left[1 \pm \left(\frac{\alpha_\gamma}{4}\right) \frac{3}{b^2} \right] \right\}. \end{aligned} \quad (6.123)$$

We note that the $\mathcal{O}(G\alpha_\gamma)$ part of our result (6.122) is in precise agreement with [354] while it disagrees with [353]⁹. Note that (6.123) generically leads to a potential time advance and causality violation independent of the sign of the coupling α_γ . This parallels the situation for the R^3 interaction which requires an appropriate UV completion to restore causality [340].

⁹The result of [353] for $\Delta\theta_{\text{FFR}}^\gamma$ was already identified as incorrect in [354] due to an inappropriate definition of the deflection angle.

Chapter 7

Conclusions and outlook

In this thesis, we applied modern on-shell techniques to study different aspects of effective field theories.

In Chapter 2, we introduced a novel method to construct bases of polynomial terms in any EFT, which are in one-to-one correspondence with operators in the usual Lagrangian formulation of perturbative QFTs. The method works for particles with any mass and spin in four dimensions and we showed applications to the SMEFT and to the classification of spin-tidal effects relevant to the study of the binary problem in classical GR.

Knowing such polynomial terms allows to bootstrap tree-level amplitudes in generic EFTs. In Chapter 3, we proposed an alternative to BCFW-like recursion relations, to compute tree-level n -point amplitudes, which extends beyond the regime of applicability of the latter. Indeed, the method is valid for any EFT with only massless states, even with irrelevant interactions involving explicit derivatives. A natural future direction is the extension of this method to theories with massive states and to d -dimensional amplitudes, which are the necessary building blocks for loop integrands in dimensional regularisation. We also showed how rational terms in loop amplitudes (which are not seen using four-dimensional unitarity cuts) determine anomaly cancellation conditions in the Standard Model for non-abelian groups. There are still questions to be answered in this context: it is not clear how to extend the method to fully abelian anomaly cancellation conditions, like (3.65) and (3.66). It would also be interesting to prove the Adler-Bardeen theorem [381], *i.e.* the non-renormalisation of anomaly cancellation conditions beyond one loop, from a purely on-shell point of view.

Tree-level amplitudes are used to determine integrands for loop amplitudes. In Chapter 4, we showed how d -dimensional generalised unitarity is enough to fully determine loop-level form factors. In particular, we used the power of six-dimensional spinor helicity formalism and dimensional reconstruction techniques to construct the full integrands for a class of operators relevant to Higgs physics and QCD.

In Chapter 5, we used (5.1) and the tools developed in Chapter 2 and 3 to compute the one-loop UV mixing of all the operators of mass dimension eight within the SMEFT, between themselves and at leading order in the couplings. In particular, we showed explicitly the anomalous dimension of all the operators relevant to the Higgs production in association with a W boson. The results in [104] can be extended in many different directions. In the following, we will mention a few (computational and conceptual) problems that we have encountered.

1. The first and most trivial problem to take into account is the extension to a generic number of flavours, or simply $N_f = 3$. This does not represent either a computational or a conceptual problem as we only need to code the flavour structures and a systematic algorithm to take into account their symmetries.
2. Automatising the computation of the anomalous dimension matrix beyond leading order (*i.e.* beyond quadratic order in the gauge and Yukawa couplings and linear order in the Higgs self-coupling) at one loop requires a deeper understanding of the different contributions in the computation of the Lorentz-invariant phase space integral. Indeed, as already noticed in [98], beyond leading order the computation requires tree-level amplitude with more than four points and non-minimal form factors. When considering separately each combination with the proper configuration of the external states, such contributions give rise to intermediate logarithms which cancel out at the very end. While in the automatization this might not be strictly a problem, we notice that in more complicated theories, like the SMEFT, the result of this computation is contaminated by terms which are already computed at lower order. For example, consider three operators with the same mass dimension, two of length L (with different field insertions, for simplicity), labelled as \mathcal{O}_1 and \mathcal{O}_2 , and another of length $L+1$, \mathcal{O}_3 . At leading order, only \mathcal{O}_1 and \mathcal{O}_2 mix, like shown in Chapter 5. In general, at the next to leading order, gluing for example \mathcal{O}_1 with the proper five-point amplitudes and integrating over the Lorentz-invariant phase space give the contribution of the anomalous dimension of \mathcal{O}_3 from \mathcal{O}_1 , but the result may be contaminated by the contribution of the anomalous dimension of \mathcal{O}_2 from \mathcal{O}_1 computed through a non-minimal form factor. The problem of disentangling these contributions is strictly related to the final cancellation of intermediate logarithms. A possible solution of such problem may be found using generalised unitarity, trying to disentangle the different contributions using the proper unitarity cuts.
3. There is an additional direction in which the result of [104] can be extended: we could consider the contributions to the anomalous dimensions from operators with different mass dimensions (*i.e.* beyond linear order). In fact, multiple insertions of lower-dimensional operators in the (non-minimal) form factor or in the scattering amplitude could contribute to the anomalous dimension of higher-dimensional operators. This step is straightforward. On the other hand, if the theory under consideration has a relevant coupling, like a mass term for example (for example, in the Standard Model lagrangian we have $-\mu^2 \bar{H}H$, with $\mu^2 < 0$), then higher-dimensional operators can also contribute to the anomalous dimension of lower-dimensional one. For example, in [319] it was shown how dimension-six operators contribute to the anomalous dimension of the marginal couplings. It is not clear how the central formula (5.1) has to be modified in massive EFTs.
4. It is worth mentioning that extending the formalism and the computations to two loops, following the work presented in [102, 107], is a valid direction.

In Chapter 6, we studied correction to the bending angle and time delay for a massless particle scattered off a celestial object. In particular, we focused on the corrections induced by higher derivative interactions and we used the eikonal representation of the amplitude to extract such quantities. In the context of studying the classical two-body problem in GR, it would be interesting to study, using scattering amplitudes techniques, other observables which might be relevant also to GW experiments in the near future.

In this direction, one direction might be the direct extraction of waveforms from on-shell quantities. On the line of previous works in the literature [179, 180, 382–385], it is interesting to study scattering amplitudes of two massive heavy particles scattering and emitting a number of gravitons. In particular, the (classical part of the) one-loop five-point scattering amplitude is not known in the literature and it would be interesting to compute it using the recently developed heavy-mass Effective Field Theory (HEFT) and its corresponding gauge-invariant double copy [150, 232]. We hope to come back to some of these questions in the near future.

Appendix A

Spinor Helicity Formalism

A.1 Four-Dimensional Spinor Helicity Formalism

In this section we briefly review the four-dimensional Spinor Helicity Formalism (SHF) [18, 214–217, 386], having as a main goal to present our notation and conventions.

Most of the work in this thesis has been done working in $(+ - - -)$ signature, where usual four-momenta can be converted to bi-spinors using Pauli matrices as a realisation of the isomorphism $so(1, 3) \sim sl(2, \mathbb{C})$: $p_{\alpha\dot{\alpha}} = p_\mu \sigma_{\alpha\dot{\alpha}}^\mu$, $p^{\dot{\alpha}\alpha} = p_\mu \bar{\sigma}^{\mu\dot{\alpha}\alpha}$, where the Pauli matrices are $\sigma_{\alpha\dot{\alpha}}^\mu = (\mathbf{1}, \vec{\sigma})$ and $\bar{\sigma}^{\mu\dot{\alpha}\alpha} = (\mathbf{1}, -\vec{\sigma})$. The undotted and dotted indices transform in the fundamental and anti-fundamental representation of the $SL(2, \mathbb{C})$ group. These spinor indices are raised and lowered by the two-dimensional ϵ -tensors, such that:

$$\epsilon_{\alpha\beta}\epsilon^{\beta\gamma} = \delta_\alpha^\gamma, \quad \epsilon_{\dot{\alpha}\dot{\beta}}\epsilon^{\dot{\beta}\dot{\gamma}} = \delta_{\dot{\alpha}}^{\dot{\gamma}}. \quad (\text{A.1})$$

For massless and massive momenta we have

$$\begin{aligned} \det p_{i\alpha\dot{\alpha}} = 0 &\quad \Rightarrow \quad p_{i\alpha\dot{\alpha}} \equiv \lambda_{i\alpha} \tilde{\lambda}_{i\dot{\alpha}}, \\ \det p_{i\alpha\dot{\alpha}} = M_i^2 &\quad \Rightarrow \quad p_{i\alpha\dot{\alpha}} \equiv \lambda_{i\alpha}^I \tilde{\lambda}_{i\dot{\alpha}I}, \end{aligned} \quad (\text{A.2})$$

where I is an index in the fundamental of $SU(2)$ (massive little group)¹. Uniformly to (A.1), $SU(2)$ indices are raised and lower by ϵ -tensor defined such that

$$\epsilon_{IJ}\epsilon^{JK} = \delta_I^K. \quad (\text{A.4})$$

The two spinors are related by complex conjugation:

$$(\lambda_\alpha)^* = \text{sign}(p^0) \tilde{\lambda}_{\dot{\alpha}}, \quad (\lambda_\alpha^I)^* = \text{sign}(p^0) \tilde{\lambda}_{\dot{\alpha}I} \quad (\text{A.5})$$

The Lorentz invariants are defined as

$$\langle ij \rangle = \langle i||j \rangle \equiv \lambda_i^\alpha \lambda_{j\alpha}, \quad [ij] = [i||j] \equiv \tilde{\lambda}_{i\dot{\alpha}} \tilde{\lambda}_{j\dot{\alpha}}, \quad (\text{A.6})$$

¹The massless spinors as well are not completely determined by such definition. Indeed, the rescaling

$$\lambda_{i\alpha} \longrightarrow e^{-\frac{i\phi_i}{2}} \lambda_{i\alpha}, \quad \tilde{\lambda}_{i\dot{\alpha}} \longrightarrow e^{\frac{i\phi_i}{2}} \tilde{\lambda}_{i\dot{\alpha}}. \quad (\text{A.3})$$

leaves momentum invariant and correspond to a little group transformation for massless particle. The little group in four dimensions is the double covering of $SO(2) \simeq U(1)$ and we choose to assign helicity $-\frac{1}{2}$ to λ and $+\frac{1}{2}$ to $\tilde{\lambda}$. Thus it is now manifest how the new variables can carry information about both the momentum and the helicity of an associated particle.

where the spinors in this definition can be either massless or massive, in which case we omitted the spinor indices. Spinors satisfy the Dirac equation

$$\begin{aligned} p_i|i\rangle &= 0, & p_i|i] &= 0, \\ p_i|i^I\rangle &= m_i|i^I], & p_i|i^I] &= \tilde{m}_i|i^I\rangle, \end{aligned} \quad (\text{A.7})$$

where $m_i = e^{i\alpha}M_i$ and $\tilde{m}_i = -e^{-i\alpha}M_i$, with α being a constant real number. This distinction is immaterial and we will set $\alpha = 0$ at the very end of the calculations, but it is relevant when we evaluate these structures numerically, as explained in detail in Appendix A.3. This is guaranteed if we define m_i and \tilde{m}_i as

$$\langle i^I i^J \rangle = -m_i \epsilon^{IJ}, \quad [i^I i^J] = \tilde{m}_i \epsilon^{IJ}. \quad (\text{A.8})$$

Finally, when flipping the sign of the momentum p we adopt the symmetric convention on the associated spinors

$$\lambda_{-p\alpha} = i \lambda_{p\alpha}, \quad \tilde{\lambda}_{-p\dot{\alpha}} = i \tilde{\lambda}_{p\dot{\alpha}}, \quad (\text{A.9})$$

this convention enters also when performing the crossing of fermions from in to out state, leading to a factor $\frac{1}{i}$ for every crossed fermion.

The spinors satisfy some crucial identities. For example, it is simple to convince oneself that the so called *Schouten identity* holds:

$$\langle ij \rangle \lambda_{k\alpha} + \langle jk \rangle \lambda_{i\alpha} + \langle ki \rangle \lambda_{j\alpha} = 0. \quad (\text{A.10})$$

A similar identity can be written for the $\tilde{\lambda}$'s as well and for the massive spinors. Moreover, the sigma matrices satisfy the Clifford algebra

$$\{\sigma_\mu, \bar{\sigma}_\nu\} = 2\eta_{\mu\nu}, \quad (\text{A.11})$$

where $\bar{\sigma}^{\mu\dot{\alpha}\alpha} := \epsilon^{\alpha\beta} \epsilon^{\dot{\alpha}\dot{\beta}} \sigma_{\dot{\beta}\beta}^\mu$. Then we have that

$$p_i^{\dot{\alpha}\alpha} p_{j\alpha\dot{\alpha}} = 2p_i \cdot p_j. \quad (\text{A.12})$$

At this point, to connect the four- and six-dimensional helicity formalism presented later in the next section and the dimensional reduction procedure, we turn our attention to the spinor helicity description of massive momenta. One can always write a massive momentum L as [386]

$$L^\mu = l^\mu + \frac{L^2}{2l \cdot \eta} \eta^\mu, \quad (\text{A.13})$$

where both l and η are massless momenta and $L^2 = m^2$ is the mass associated to this momentum. The previous expression fixes l^μ in terms of the massive momentum L^μ completely once we have chosen the *arbitrary* η^μ vector:

$$l^\mu = L^\mu - \frac{L^2}{2L \cdot \eta} \eta^\mu. \quad (\text{A.14})$$

We can write (A.13) in terms of helicity spinors as

$$p_{i\alpha\dot{\alpha}} = \lambda_{i\alpha} \tilde{\lambda}_{i\dot{\alpha}} + \frac{m^2}{\langle \lambda_i \mu_i \rangle [\tilde{\mu}_i \tilde{\lambda}_i]} \mu_{i\alpha} \tilde{\mu}_{i\dot{\alpha}}. \quad (\text{A.15})$$

Focusing on the number of degrees of freedom, we expect to have 3 from the spinor variables, plus an additional one from the mass squared m^2 . The quantity $\lambda_\alpha \tilde{\lambda}_{\dot{\alpha}}$ already carries by itself 3 degrees of freedom, but μ_α and $\tilde{\mu}_{\dot{\alpha}}$ apparently carry two additional degrees, which coincide with their direction. Indeed, the momentum is invariant under the rescaling

$$\mu_\alpha \longrightarrow a \mu_\alpha, \quad \tilde{\mu}_{\dot{\alpha}} \longrightarrow b \tilde{\mu}_{\dot{\alpha}}, \quad (\text{A.16})$$

where $a, b \in \mathbb{C}$. The redundancy is taken into account by the four-dimensional massive little group $\text{SU}(2)$, which has two additional generators, with respect to the massless one. Indeed, we can write a massive momentum in terms of the irreducible $\text{SU}(2)$ helicity spinors [18]

$$\lambda_\alpha^I = \left(\lambda_\alpha \quad \frac{m}{\langle \lambda \mu \rangle} \mu_\alpha \right), \quad (\text{A.17})$$

and, in this form, it is obvious that any $\text{SU}(2)$ transformation

$$\lambda_\alpha^I \longrightarrow \lambda_\alpha^J U_J^I \quad (\text{A.18})$$

leaves the momentum invariant.

A.2 Six-Dimensional Spinor Helicity Formalism

In this section we give a concise overview of the six-dimensional spinor helicity formalism. In particular, we will show how it can be dimensional-reduced in terms of four-dimensional spinors. For a more detailed discussion see [30, 295].

In six-dimensional Minkowski spacetime, the Lorentz group is $\text{SO}(1, 5)$. As in the four-dimensional case, it is useful to exploit the isomorphism between the double-covering of this group with $\text{SL}(2, \mathbb{H})$, where \mathbb{H} are the quaternions. For simplicity, we will denote this group as $\text{SU}^*(4)$. Indeed, its representations are in one-to-one correspondence to those of $\text{SU}(4)$ (which is the universal covering of group of rotation in the euclidean six dimensions, $\text{SO}(6)$). The six-dimensional massless little group is $\widetilde{\text{SO}}(4) \simeq \text{SU}(2) \times \text{SU}(2)$.

Let us denote with \square^A and \square_A the objects transforming respectively in the fundamental and anti-fundamental representations of the Lorentz group $\text{SU}^*(4)$, and a and \dot{a}) the indices of the two inequivalent fundamental representations of the little group.

The Clifford algebra is defined by

$$\{\gamma^\mu, \tilde{\gamma}^\nu\}_A^B := \gamma_{AC}^\mu \tilde{\gamma}^{\nu CB} + \gamma_{AC}^\nu \tilde{\gamma}^{\mu CB} = 2\eta^{\mu\nu} \delta_A^B, \quad (\text{A.19})$$

where $\mu = 0, \dots, 6$, $\gamma_{AB}^\mu \equiv \gamma_{[AB]}^\mu$ and $\tilde{\gamma}^{\mu AB} \equiv \tilde{\gamma}^{\mu[AB]}$. These gamma matrices transform in the pseudo-real representation $\mathbf{6} = \mathbf{4} \wedge \mathbf{4}$ of $\text{SU}^*(4)$ and are related by

$$\tilde{\gamma}^{\mu AB} = (\gamma_{AB}^\mu)^* = \frac{1}{2} \epsilon^{ABCD} \gamma_{AB}^\mu. \quad (\text{A.20})$$

Six-dimensional momenta can be written as

$$p_{AB} := p_\mu \gamma_{AB}^\mu, \quad (\text{A.21})$$

and the massless condition becomes

$$p^2 \sim \epsilon^{ABCD} p_{AB} p_{CD} = 0, \quad (\text{A.22})$$

which can be solved by expressing the momentum as the bi-spinor product

$$p_{AB} = \epsilon^{\dot{a}\dot{b}} \tilde{\lambda}_{\dot{a}A} \tilde{\lambda}_{\dot{b}B} = \tilde{\lambda}_{\dot{a}A} \tilde{\lambda}_{\dot{a}B}^{\dot{a}} , \quad (\text{A.23})$$

where $\tilde{\lambda}_{\dot{a}A}$ is a pseudo-real spinor. Analogously, we can write

$$p^{AB} = \lambda^{aA} \lambda_a^B = -\epsilon^{ab} \lambda_a^A \lambda_b^B , \quad (\text{A.24})$$

which satisfies

$$p^{AB} = (p_{AB})^* = -\frac{1}{2} \epsilon^{ABCD} p_{CD} . \quad (\text{A.25})$$

Notice that, given the above definitions, the spinors λ_{aA} and $\tilde{\lambda}_{\dot{a}A}$ *automatically* satisfy the Dirac equation:

$$p_{AB} \lambda_a^B = -\frac{1}{2} \epsilon_{ABCD} \lambda_a^B \lambda^{bC} \lambda_b^D = -\epsilon_{ABCD} \lambda_a^B \lambda_1^C \lambda_2^D = 0 , \quad (\text{A.26})$$

and similarly for $\tilde{\lambda}_{\dot{a}A}$. The Dirac equation can be also written equivalently as a relation between λ and $\tilde{\lambda}$:

$$0 = \lambda^{aA} \lambda_a^B \tilde{\lambda}_{B\dot{a}} = -\lambda_1^A \lambda_2^B \tilde{\lambda}_{B\dot{a}} + \lambda_2^A \lambda_1^B \tilde{\lambda}_{B\dot{a}} , \quad (\text{A.27})$$

which implies

$$\lambda_a^A \tilde{\lambda}_{A\dot{a}} = 0 . \quad (\text{A.28})$$

SU*(4) Spinor Identities

In this subsection we present some useful identities for six-dimensional spinors. We focus on the SU*(4) structure of the spinors and keep the little group indices implicit. Of course little-group indices can be restored at any time because they are unambiguously related to each spinor.

Consider a certain number of spinors λ_i^A (and $\tilde{\lambda}_{iA}$), with labels $i = 1, \dots, n$. The Lorentz invariant objects which can be built out of these spinors are of three types:

- Bi-spinor invariant objects:

$$\lambda_i^A \tilde{\lambda}_{jA} := \langle ij \rangle \quad (\text{A.29})$$

- Two distinct four-spinors invariant objects:

$$\epsilon_{ABCD} \lambda_i^A \lambda_j^B \lambda_k^C \lambda_l^D := \langle ijkl \rangle , \quad \epsilon^{ABCD} \tilde{\lambda}_{iA} \tilde{\lambda}_{jB} \tilde{\lambda}_{kC} \tilde{\lambda}_{lD} := [ijkl] . \quad (\text{A.30})$$

The spinors transform in the fundamental representation of SU*(4), thus $A = 1, \dots, 4$. Two identities (and their two complex conjugate) follow immediately from this:

$$\lambda_1^{[A} \lambda_2^B \lambda_3^C \lambda_4^D \lambda_5^E] = 0 , \quad (\text{A.31})$$

and

$$\lambda_1^{[A} \lambda_2^B \lambda_3^C \lambda_4^D] = \frac{1}{4!} \epsilon^{ABCD} \langle 1234 \rangle , \quad (\text{A.32})$$

and analogous relations hold for $\tilde{\lambda}_{iA}$. These can be combined to give the six-dimensional generalisation of the Schouten identities:

$$\sum_{\text{cyclic}} \langle 1234 \rangle \lambda_5^A = 0 . \quad (\text{A.33})$$

From Six-Dimensional to Four-Dimensional Quantities

It is fundamental to our purposes to write six-dimensional spinors in terms of four-dimensional ones, to make the dimensional reconstruction unitarity technique more clean.

The first step is to write six-dimensional null vectors as four-dimensional massive ones, by defining the two complex mass parameters

$$m := p_4 + ip_5, \quad \tilde{m} := p_4 - ip_5, \quad (\text{A.34})$$

where p_4 and p_5 are the fifth and the sixth components of the six-dimensional momentum p_μ . Then, the massless condition becomes

$$p^2 = (p^{(4)})^2 - m\tilde{m} = 0. \quad (\text{A.35})$$

where $(p^{(4)})^2 = p_0^2 - p_1^2 - p_2^2 - p_3^2$ is the four-dimensional massive momentum associated to p_μ . We found it more efficient for our calculation to describe these momenta as a combination of two massless momenta, as in (A.15). This allows to decompose six-dimensional helicity spinors in terms of four-dimensional spinors as

$$\lambda_a^A = \begin{pmatrix} -\frac{m}{\langle\lambda\mu\rangle}\mu_\alpha & \lambda_\alpha \\ \tilde{\lambda}^{\dot{\alpha}} & \frac{\tilde{m}}{[\mu\lambda]}\tilde{\mu}^{\dot{\alpha}} \end{pmatrix}, \quad \tilde{\lambda}_{A\dot{a}} = \begin{pmatrix} \frac{\tilde{m}}{\langle\lambda\mu\rangle}\mu^\alpha & \lambda^\alpha \\ -\tilde{\lambda}_{\dot{\alpha}} & \frac{m}{[\mu\lambda]}\tilde{\mu}_{\dot{\alpha}} \end{pmatrix}, \quad (\text{A.36})$$

where the little group indices label the columns and the $\text{SU}^*(4)$ indices label the rows. The $\text{SU}^*(4)$ index structure can be broken down into two $\text{SL}(2, \mathbb{C})$ complex conjugated indices:

$$\square^A = \begin{pmatrix} \square_\alpha \\ \square_{\dot{\alpha}} \end{pmatrix}, \quad \square_A = \begin{pmatrix} \square^\alpha \\ \square^{\dot{\alpha}} \end{pmatrix}. \quad (\text{A.37})$$

This embedding is specific of a particular choice of gamma matrices: indeed, we can choose them such that, for $\mu = 0, \dots, 3$, they reduce to the familiar chiral representation in four dimensions².

p^{AB} and p_{AB} are invariant under the little group $\text{SU}(2) \times \text{SU}(2)$ transformations

$$\lambda_a^A = U_a{}^b \lambda_b^A, \quad \tilde{\lambda}_{A\dot{a}} = U_{\dot{a}}{}^b \tilde{\lambda}_{Ab}, \quad (U_a{}^b, U_{\dot{a}}{}^b) \in \text{SU}(2) \times \text{SU}(2). \quad (\text{A.38})$$

The six-dimensional momentum in four-dimensional components reads:

$$p^{AB} = \begin{pmatrix} -m\epsilon_{\alpha\beta} & \lambda_\alpha \tilde{\lambda}^{\dot{\beta}} + \rho \mu_\alpha \tilde{\mu}^{\dot{\beta}} \\ -\tilde{\lambda}^{\dot{\alpha}} \lambda_\beta - \rho \tilde{\mu}^{\dot{\alpha}} \mu_\beta & \tilde{m} \epsilon^{\dot{\alpha}\dot{\beta}} \end{pmatrix}, \quad (\text{A.39})$$

where $\rho = \frac{m\tilde{m}}{\langle\lambda\mu\rangle[\mu\lambda]}$. In our choice of gamma matrices, the off-diagonal components precisely coincide with the four-dimensional massive momentum:

$$p_{\alpha\dot{\alpha}}^{(4)} = \lambda_\alpha \tilde{\lambda}_{\dot{\alpha}} + \rho \mu_\alpha \tilde{\mu}_{\dot{\alpha}}, \quad (p^{(4)})^2 = m\tilde{m}. \quad (\text{A.40})$$

It is easy to see that the two copies of $\text{SU}(2)$ of the little group act in an identical way on $p^{(4)}$ and we recover the usual massive little group: indeed, they depend only on the combination $m\tilde{m}$ and we can obtain dotted transformations from the undotted by simply replacing

$$m \longrightarrow -\tilde{m}, \quad \tilde{m} \longrightarrow -m. \quad (\text{A.41})$$

²For the explicit basis of gamma matrices see Appendix A of [30].

The Lorentz invariant quantities $\langle i_a j_{\dot{a}} \rangle$, $\langle i_a j_b k_{\dot{c}} l_{\dot{d}} \rangle$, $[i_{\dot{a}} j_{\dot{b}} k_{\dot{c}} l_{\dot{d}}]$ can be written in terms of four-dimensional angle and square brackets, once the helicity indices are fixed ($a, b, c, d = 1, 2$ and $\dot{a}, \dot{b}, \dot{c}, \dot{d} = \dot{1}, \dot{2}$), by using the decomposition given in (A.37) and decomposing $\epsilon_{ABCD} \sim \sum \epsilon^{\alpha\beta} \epsilon_{\dot{\alpha}\dot{\beta}}$ and $\delta_B^A = \text{diag}(\delta_{\alpha}^{\beta}, \delta_{\dot{\beta}}^{\dot{\alpha}})$.

A.3 Momentum Twistors and Rational Kinematics

Rational (or finite field) kinematics in four dimensions has been fundamental in various steps of the computations presented in the bulk chapters:

1. Numerical checks on analytic expressions obtained throughout this work (for both tree-level amplitudes and loop integrands) have been checked using rational kinematics.
2. To verify that the structures in our basis are kinematically independent and to probe the independence of structures upon symmetrisation, we evaluate the polynomial structures found using the algorithm presented in Section 2.1 and 2.2 over rational kinematics.
3. The recursion algorithm for tree-level amplitude in generic EFTs presented in Section 3.2 relies heavily on the fact that we can fix the coefficient of the ansatz exactly, evaluating it over different factorisation channels using a on-shell kinematic finite over finite fields.

Indeed, the fundamental feature which make the kinematics over rational or finite field extremely useful is that it allows for numerical evaluations of rational functions without loss of precision, as discussed in detail in Section A.4.

It is widely known that it is possible to generate rational kinematics satisfying both on-shell and momentum conservation conditions [239, 255]. Such generation can be performed, for example, via the analytic continuation to $(++--)$ signature and generating the kinematics in terms of the *momentum twistors* variables, introduced in [238]. This construction was introduced for fully massless four-dimensional kinematics. The generalisation to the massive case is presented below.

The spinor helicity formalism in split signature is formally different from the one introduced in the previous section, but practically the same. The little group for massless and massive particles are \mathbb{R} and $\text{SL}(2, \mathbb{R})$, respectively. Besides m_i and \tilde{m}_i are two real numbers such that $m_i \tilde{m}_i = M_i^2$. The condition (A.5) is lifted and the dotted and undotted spinors are real and independent from each other.

Introducing spinor helicity variables automatically makes the momenta satisfy on-shell conditions, but the momentum conservation identity is a quadratic constraint on our kinematic variables. To make sure that the kinematic stays in the field of rational numbers, we need to rewrite this constrain in terms of linear equations. This is possible in four dimensions expressing the kinematic in terms of momentum twistor variables. Momenta can be rewritten in terms of *dual momentum variables* x_i :

$$p_i = x_i - x_{i+1} , \tag{A.42}$$

which make momentum conservation between n particles trivial:

$$x_{n+1} = x_1 . \tag{A.43}$$

Then, each massless momentum is associated with two null-separated points and momentum conservation tells us that the set of dual variables forms a polygon. The on-shell condition defines a new variable $[\mu_i]$, through the *incidence relation*

$$[\mu_i] = \langle i|x_i = \langle i|x_{i+1} . \quad (\text{A.44})$$

Given a (randomly generated) set of pair of spinors $Z_i^A = (\lambda_i^\alpha, \mu_{i\dot{\alpha}})$, named momentum twistor variables, such that $Z_{n+1} = Z_1$, and using the incidence relation, we can define the spinors $\tilde{\lambda}_i^{\dot{\alpha}}$ through the *dual twistor*

$$W_{iA} = (\tilde{\mu}_{i\alpha}, \tilde{\lambda}_i^{\dot{\alpha}}) = \frac{\epsilon_{ABCD} Z_{i-1}^B Z_i^C Z_{i+1}^D}{\langle (i-1)i \rangle \langle i(i+1) \rangle} . \quad (\text{A.45})$$

Planar Mandelstam invariants can be written in terms of twistor variables:

$$s_{i,i+1,\dots,j-1} = (x_i - x_j)^2 = \frac{\epsilon_{ABCD} Z_{i-1}^A Z_i^B Z_{j-1}^C Z_j^D}{\langle (i-1)i \rangle \langle (j-1)j \rangle} . \quad (\text{A.46})$$

This procedure was introduced to generate a fully massless kinematics over rational or finite fields. However, it can be generalised to the massive case once we decompose massive momenta into a couple of massless ones:

$$p_{i\alpha\dot{\alpha}} = \lambda_{i\alpha}^1 \tilde{\lambda}_{i\dot{\alpha}1} + \lambda_{i\alpha}^2 \tilde{\lambda}_{i\dot{\alpha}2} \equiv k_{i\alpha\dot{\alpha}} + q_{i\alpha\dot{\alpha}} , \quad (\text{A.47})$$

where k^μ and q^μ are two massless momenta such that $q_{i\alpha\dot{\alpha}} k_i^{\dot{\alpha}\alpha} = M_i^2$. Then if we are considering a scattering amplitude for n massless and m massive states, we need to randomly generate $n + 2m$ twistor variables

$$\{Z_i^{IA}, Z_j^A\} \quad (\text{A.48})$$

$i = 1, \dots, m, j = m + 1, \dots, n + m$ and $I = 1, 2$. By doing so, the masses are randomly generated as well

$$M_i^2 = \frac{\epsilon_{ABCD} Z_{i-1}^{2A} Z_i^{1B} Z_i^{2C} Z_{i+1}^{1D}}{\langle (i-1)^2 i^1 \rangle \langle i^2 j^1 \rangle} , \quad (\text{A.49})$$

where $Z_0^{2A} = Z_{n+m}^A$ and $Z_{n+1}^{1D} = Z_{n+1}^D$. However, we might be interested in cases where some states have the same mass, like the examples considered in Section 2.3.3 and 2.3.4. For example, we can consider l particles with the same mass. In such case, we can generate a bi-twistor associated with one of these particles fully randomly, while for the others we can leave, for example, the component μ_{i2}^2 undetermined. These are fully fixed by $l - 1$ *linear* equations requiring that the masses obtained from equation (A.49) must be equal to the one we generated randomly.

A.4 Finite Field Arithmetic

In this section we briefly describe the main features of finite field kinematics and the application to the recursive algorithm presented in Section 3.2. Our goal is to give just a taste of the method, motivating its usefulness in our particular context, highlighting at the same time the caveats which come along the benefits. For a more in depth mathematical primer we refer to [387] and references therein, whereas for a discussion of applications to modern theoretical physics problems to [237, 388].

Consider the integer numbers \mathbb{Z} endowed with the standard addition and multiplication and choose a natural number $p \in \mathbb{N}$. We define a set of p equivalence classes through the modulo operation mod : we say that a is equivalent to b or a equals b modulo p if

$$a = b \text{ mod } p \quad \iff \quad \exists n \in \mathbb{Z} \text{ s.t. } a - b = n \cdot p. \quad (\text{A.50})$$

The set of natural numbers

$$\mathbb{Z}_p \equiv \{0, 1, \dots, p - 1\} \quad (\text{A.51})$$

can be chosen as the most intuitive representatives of these equivalence classes, and it is easy to see that this set endowed with the standard addition ($\text{mod } p$) is a representation of the cyclic group of order p , hence the use of the symbol \mathbb{Z}_p . It can be shown that if p is a prime number then \mathbb{Z}_p endowed also with the usual multiplication ($\text{mod } p$) is a field, which is finite by construction and we thus call it *finite field*. The modulo operation provides clearly a simple map from \mathbb{Z} to \mathbb{Z}_p , what is less obvious, but still holds true as long as p is a prime, is that under some restriction there is also a unique and well defined map from the rationals \mathbb{Q} to \mathbb{Z}_p . This map is based on the possibility of defining a multiplicative inverse a^{-1} for every $a \in \mathbb{Z}_p$ such that $a a^{-1} = a^{-1} a = 1 \text{ mod } p$.

Now that we have given an operative definition of finite fields we can focus on why and how we use them. Performing some sort of analytic computation on a computer (especially on a laptop) can often prove challenging, in that the computational time required is too large for a result to be successfully obtained. In similar situations it might be a good idea to change the perspective on the problem and try to reformulate it using a numeric approach. In our case this amounts to switching from trying to directly obtain the amplitude from simplifying (1.23) analytically to building numeric systems to be solved as in Section 3.2.1. The advantage of numerics is that in principle it is clearly much faster, since potentially large intermediate expressions are replaced with numbers. This is certainly true when dealing for example with floating-point arithmetic. On the other hand, the use of numeric expressions requires carefully keeping track of possible precision loss and makes arbitrary precision arithmetic at times more appealing, which is however slower. Here is where finite fields enter the game, since we can map our problem from \mathbb{Q} to \mathbb{Z}_p , which avoids the precision loss of floating point numbers, and then perform the numeric computations on \mathbb{Z}_p . This is extremely fast because we can choose p to be a machine-size prime and the whole computation will only involve machine-size natural numbers. The obvious issue is that, once the problem at hand has been solved on \mathbb{Z}_p , we need to map the solution back to \mathbb{Q} , through a map which cannot by any means be a bijection.

Despite the fact that the map $\mathbb{Q} \rightarrow \mathbb{Z}_p$ is not injective, it is possible under certain circumstances to “invert it”, or rather to make an educated guess of which element $\frac{n}{d} \in \mathbb{Q}$ corresponds to a given $b \in \mathbb{Z}_p$. In particular it can be shown (see for example [389]) that given b there is only one pair of n and d such that $n^2, d^2 < \frac{p}{2}$. In other words, if the correct values of n and d which we are looking for are small enough compared to the prime p which we chose as the order of the field \mathbb{Z}_p , then we can uniquely obtain their value from $b \in \mathbb{Z}_p$. The size of p however has an upper bound being the machine-size primes, since the whole point of using finite fields is to deal with machine-size integers. Consequently, one cannot simply choose an arbitrarily large prime so to be confident that the inverted map yields the correct result. Instead, one uses the so called Chinese remainder theorem³, which allows to combine the outcome X of the same calculation

³See for example [237].

on multiple fields $\mathbb{Z}_{p_1}, \dots, \mathbb{Z}_{p_n}$ to obtain the value of $X \bmod P$ where $P = \prod_i p_i$. In other words, the Chinese remainder theorem defines a ring isomorphism⁴

$$\begin{aligned} \mathbb{Z}_{p_1} \times \cdots \times \mathbb{Z}_{p_n} &\rightarrow \mathbb{Z}_P \\ (X \bmod p_1, \dots, X \bmod p_n) &\mapsto X \bmod P \end{aligned} \tag{A.52}$$

which allows us to access the value $X \bmod P$ on \mathbb{Z}_P where P is large, through computations on fields with small values of p_i . Applying then the “inverse” mapping to the value found on \mathbb{Z}_P will very likely return the correct result. This procedure is iterated adding more fields $\mathbb{Z}_{p_{n+1}}$ until the inverse of $b \in \mathbb{Z}_P$ converges to a definite $\frac{n}{d} \in \mathbb{Q}$.

In our specific case it is usually enough to perform the calculation on a single field \mathbb{Z}_p : since we are using finite fields to do numeric evaluations aimed at solving the system (3.34), once a solution has been found we can simply test it through a single evaluation of (3.32) on \mathbb{Q} . As a final remark, we discuss one caveat of the method. Since everything relies on the possibility of mapping \mathbb{Q} to \mathbb{Z}_p , one can only apply the so far presented techniques in the case the problem at hand is entirely described by rational functions. This is indeed the scenario we are interested in: indeed, the tree-level scattering amplitudes present an entirely rational dependence on the spinor invariants and thus on the spinor components. Furthermore, one has to take special care of elements appearing in the calculations which do belong to more extended number fields than \mathbb{Q} , in particular for us this means square roots and imaginary units. How these are dealt with is often a matter of the specific problem, where our choices have been described in Section 3.2.1.

⁴Since P is not a prime \mathbb{Z}_P is not a field but a ring.

Appendix B

SMEFT Conventions and Notations

B.1 The Standard Model gauge group

In Table B.1 we write explicitly the representations under which each particle in the infrared spectrum of the Standard Model transforms, for the gauge group $U(1) \times SU(2) \times SU(3)$.

	$U(1)$	$SU(2)$	$SU(3)$
B_{\pm}	0	1	1
W_{\pm}	0	3	1
G_{\pm}	0	1	8
\bar{Q}	$-\frac{1}{6}$	2	3
\bar{u}	$+\frac{2}{3}$	1	3
\bar{d}	$-\frac{1}{3}$	1	3
\bar{L}	$+\frac{1}{2}$	2	1
\bar{e}	-1	1	1
Q	$+\frac{1}{6}$	2	3
u	$-\frac{2}{3}$	1	3
d	$+\frac{1}{3}$	1	3
L	$-\frac{1}{2}$	2	1
e	+1	1	1
\bar{H}	$-\frac{1}{2}$	2	1
H	$+\frac{1}{2}$	2	1

Table B.1: The spectrum of the Standard Model and the transformation properties of all the fields.

Our convention on the colour factor are completely specified by the decomposition of the contraction of two generators for both the $SU(N)$ and $SU(2)$ groups respectively:

$$\tau^{Aa}{}_c \tau^{Bc}{}_b = \frac{1}{2N} \delta^{AB} \delta_b^a + \frac{i}{2} f^{ABC} \tau^C{}_b^a + \frac{1}{2} d^{ABC} \tau^C{}_b^a, \quad (\text{B.1})$$

where f^{ABC} are the structure constants and d^{ABC} is the traceless completely symmetry d -tensor, and

$$\sigma^{Ii}{}_k \sigma^{Jk}{}_j = \frac{1}{4} \delta^{IJ} \delta_j^i + \frac{i}{2} \epsilon^{IJK} \sigma^K{}_j^i. \quad (\text{B.2})$$

For the $SU(2)$ group we also need to specify how indices in the fundamental are raised and lowered by the ϵ -tensor:

$$x_i = \epsilon_{ij} x^j = \epsilon_{ij} \epsilon^{jk} x_k . \quad (\text{B.3})$$

B.2 Three-point amplitudes in the Standard Model

In this section we present the complete set of non-vanishing three-point amplitudes in the Standard Model. As already mentioned in section 3.1, consistent factorisation of the four-point amplitudes imposes constraints which not only fix the colour structures but also relate the couplings of the various three-point amplitudes among each other. Once these constraints are taken into account a small set of the numerical coefficients in front of the amplitudes is still arbitrary and up to convention.

$$\begin{aligned}
\mathcal{A}(W_-^I, W_-^J, W_+^K) &= g_2 \epsilon^{IJK} \frac{\langle 12 \rangle^3}{\langle 23 \rangle \langle 31 \rangle} , & \mathcal{A}(W_-^I, W_+^J, W_+^K) &= -g_2 \epsilon^{IJK} \frac{[23]^3}{[12][31]} , \\
\mathcal{A}(G_-^A, G_-^B, G_+^C) &= g_3 f^{ABC} \frac{\langle 12 \rangle^3}{\langle 23 \rangle \langle 31 \rangle} , & \mathcal{A}(G_-^A, G_+^B, G_+^C) &= -g_3 f^{ABC} \frac{[23]^3}{[12][31]} , \\
\mathcal{A}(B_-, \bar{e}_m, e_n) &= i g_1 \delta_{nm} \frac{\langle 12 \rangle^2}{\langle 23 \rangle} , & \mathcal{A}(B_+, \bar{e}_m, e_n) &= i g_1 \delta_{nm} \frac{[13]^2}{[23]} , \\
\mathcal{A}(B_-, \bar{L}_m^i, L_n^j) &= -i \frac{g_1}{2} \delta_{mn} \delta_i^j \frac{\langle 12 \rangle^2}{\langle 23 \rangle} , & \mathcal{A}(B_+, \bar{L}_m^i, L_n^j) &= -i \frac{g_1}{2} \delta_{mn} \delta_i^j \frac{[13]^2}{[23]} , \\
\mathcal{A}(B_-, \bar{u}_m^a, u_n^b) &= -i \frac{2g_1}{3} \delta_{nm} \delta_b^a \frac{\langle 12 \rangle^2}{\langle 23 \rangle} , & \mathcal{A}(B_+, \bar{u}_m^a, u_n^b) &= -i \frac{2g_1}{3} \delta_{nm} \delta_b^a \frac{[13]^2}{[23]} , \\
\mathcal{A}(B_-, \bar{d}_m^a, d_n^b) &= i \frac{g_1}{3} \delta_{nm} \delta_b^a \frac{\langle 12 \rangle^2}{\langle 23 \rangle} , & \mathcal{A}(B_+, \bar{d}_m^a, d_n^b) &= i \frac{g_1}{3} \delta_{nm} \delta_b^a \frac{[13]^2}{[23]} , \\
\mathcal{A}(B_-, \bar{Q}_m^{a,i}, Q_n^{b,j}) &= i \frac{g_1}{6} \delta_{mn} \delta_i^j \delta_a^b \frac{\langle 12 \rangle^2}{\langle 23 \rangle} , & \mathcal{A}(B_+, \bar{Q}_m^{a,i}, Q_n^{b,j}) &= i \frac{g_1}{6} \delta_{mn} \delta_i^j \delta_a^b \frac{[13]^2}{[23]} , \\
\mathcal{A}(B_-, \bar{H}^i, H^j) &= i \frac{g_1}{2} \delta_i^j \frac{\langle 12 \rangle \langle 31 \rangle}{\langle 23 \rangle} , & \mathcal{A}(B_+, \bar{H}^i, H^j) &= -i \frac{g_1}{2} \delta_i^j \frac{[12][31]}{[23]} , \\
\mathcal{A}(W_-^I, \bar{L}_m^i, L_n^j) &= i g_2 \delta_{mn} \sigma^{Ij}_i \frac{\langle 12 \rangle^2}{\langle 23 \rangle} , & \mathcal{A}(W_+^I, \bar{L}_m^i, L_n^j) &= i g_2 \delta_{mn} \sigma^{Ij}_i \frac{[13]^2}{[23]} , \\
\mathcal{A}(W_-^I, \bar{Q}_m^{a,i}, Q_n^{b,j}) &= i g_2 \delta_{mn} \sigma^{Ij}_i \delta_a^b \frac{\langle 12 \rangle^2}{\langle 23 \rangle} , & \mathcal{A}(W_+^I, \bar{Q}_m^{a,i}, Q_n^{b,j}) &= i g_2 \delta_{mn} \sigma^{Ij}_i \delta_a^b \frac{[13]^2}{[23]} , \\
\mathcal{A}(W_-^I, \bar{H}^i, H^j) &= i g_2 \sigma^{Ij}_i \frac{\langle 12 \rangle \langle 31 \rangle}{\langle 23 \rangle} , & \mathcal{A}(W_+^I, \bar{H}^i, H^j) &= -i g_2 \sigma^{Ij}_i \frac{[12][31]}{[23]} , \\
\mathcal{A}(G_-^A, \bar{u}_m^a, u_n^b) &= -i g_3 \delta_{nm} \tau^{Aa}_b \frac{\langle 12 \rangle^2}{\langle 23 \rangle} , & \mathcal{A}(G_+^A, \bar{u}_m^a, u_n^b) &= -i g_3 \delta_{nm} \tau^{Aa}_b \frac{[13]^2}{[23]} ,
\end{aligned}$$

$$\begin{aligned} \mathcal{A}(G_-^A, \bar{d}_m^a, d_n^b) &= -i g_3 \delta_{nm} \tau^A{}_b \frac{\langle 12 \rangle^2}{\langle 23 \rangle}, & \mathcal{A}(G_+^A, \bar{d}_m^a, d_n^b) &= -i g_3 \delta_{nm} \delta_i^j \tau^A{}_b \frac{[13]^2}{[23]}, \\ \mathcal{A}(G_-^A, \bar{Q}_m^{a,i}, Q_n^{b,j}) &= i g_3 \delta_{mn} \tau^A{}_a \delta_i^j \frac{\langle 12 \rangle^2}{\langle 23 \rangle}, & \mathcal{A}(G_+^A, \bar{Q}_m^{a,i}, Q_n^{b,j}) &= i g_3 \delta_{mn} \delta_i^j \tau^A{}_a \frac{[13]^2}{[23]}, \end{aligned}$$

$$\begin{aligned} \mathcal{A}(\bar{Q}_m^{a,i}, \bar{u}_n^b, \bar{H}^j) &= i \mathcal{Y}_{mn}^{(1)} \epsilon_{ij} \delta_a^b \langle 12 \rangle, & \mathcal{A}(Q_m^{a,i}, u_n^b, H^j) &= -i \bar{\mathcal{Y}}_{nm}^{(1)} \epsilon^{ij} \delta_b^a [12], \\ \mathcal{A}(Q_m^{a,i}, d_n^b, \bar{H}^j) &= i \mathcal{Y}_{nm}^{(2)} \delta_j^i \delta_b^a [12], & \mathcal{A}(\bar{Q}_m^{a,i}, \bar{d}_n^b, H^j) &= i \bar{\mathcal{Y}}_{mn}^{(2)} \delta_i^j \delta_a^b \langle 12 \rangle, \\ \mathcal{A}(L_m^i, e_n, \bar{H}^j) &= i \mathcal{Y}_{nm}^{(3)} \delta_j^i [12], & \mathcal{A}(\bar{L}_m^i, \bar{e}_n, H^j) &= i \bar{\mathcal{Y}}_{mn}^{(3)} \delta_i^j \langle 12 \rangle. \end{aligned}$$

Appendix C

Tree-level Amplitudes in 6D

C.1 Six-Dimensional Scattering Amplitudes

Six-dimensional tree-level amplitudes are the basic ingredients of our unitarity-based recipe. In this section we give the analytic expressions needed for our calculations and comment on how to recover four-dimensional expressions in a specific limit.

As we already mentioned, in six dimensions the notion of four-dimensional helicity is encoded in a tensorial structure, which must be reflected by the amplitudes. The advantage of this tensorial nature of six-dimensional helicity is that a single expression of the amplitude contains all the possible four-dimensional helicity configurations, when dimensional reduced. The drawback however is that one loses some of the simplicity which was peculiar to specific helicity configurations. In particular there is no concept of MHV amplitudes.

Moreover, taking four-dimensional limit also represents a good consistency check for six-dimensional results. Indeed, for an appropriate limit these results must return their four-dimensional counterparts. More specifically, accordingly to our embedding, it turns out that states characterised by little-group indices $(1, \dot{1})$ and $(2, \dot{2})$ correspond to the positive and the negative helicity states in the four-dimensional limit $(m, \tilde{m} \rightarrow 0)$, because of representation we chose for the gamma matrices. On the other hand, the additional $(1, 2)$ and $(2, 1)$ components coincide with two 4D scalars.

The four-gluon amplitude, computed in [30], is

$$\mathcal{A}_g(1_{a\dot{a}}, 2_{b\dot{b}}, 3_{c\dot{c}}, 4_{d\dot{d}}) =
 \begin{array}{c}
 1_{a\dot{a}} \\
 \text{~~~~~} \\
 \text{~~~~~} \\
 \text{~~~~~} \\
 \text{~~~~~} \\
 \text{~~~~~} \\
 \text{~~~~~} \\
 4_{d\dot{d}}
 \end{array}
 \begin{array}{c}
 \text{tree} \\
 \text{~~~~~} \\
 \text{~~~~~} \\
 \text{~~~~~} \\
 \text{~~~~~} \\
 \text{~~~~~} \\
 \text{~~~~~} \\
 3_{c\dot{c}}
 \end{array}
 \begin{array}{c}
 2_{b\dot{b}} \\
 \text{~~~~~} \\
 \text{~~~~~} \\
 \text{~~~~~} \\
 \text{~~~~~} \\
 \text{~~~~~} \\
 \text{~~~~~} \\
 3_{c\dot{c}}
 \end{array}
 = -\frac{i}{s_{12}s_{23}} \langle 1_a 2_b 3_c 4_d \rangle [1_{\dot{a}}, 2_{\dot{b}}, 3_{\dot{c}}, 4_{\dot{d}}].
 \tag{C.1}$$

According to our embedding, we expect $\mathcal{A}_g(1_{22}, 2_{22}, 3_{11}, 4_{11})$ to reproduce the MHV amplitude $\mathcal{A}(1^-, 2^-, 3^+, 4^+)$ in the limit $m_i, \tilde{m}_i \rightarrow 0$ for $i = 1, \dots, 4$, which is indeed the case:

$$\mathcal{A}_g(1_{22}, 2_{22}, 3_{11}, 4_{11}) \Big|_{4D} = i \frac{\langle 12 \rangle^4}{\langle 12 \rangle \langle 23 \rangle \langle 34 \rangle \langle 41 \rangle}.
 \tag{C.2}$$

While $\mathcal{A}_g(1_{12}, 2_{21}, 3_{11}, 4_{22})$ reproduces the four-point amplitude with two scalars and two opposite-helicity gluons $\mathcal{A}(1_\phi, 2_{\bar{\phi}}, 3^+, 4^-)$:

$$\mathcal{A}_g(1_{12}, 2_{21}, 3_{11}, 4_{22}) = i \frac{\langle 14 \rangle^2 \langle 24 \rangle^2}{\langle 12 \rangle \langle 23 \rangle \langle 34 \rangle \langle 41 \rangle}. \quad (\text{C.3})$$

Another amplitude of which we make frequent use is the six-dimensional four-point amplitude with two gluons and two scalars [254]

$$\mathcal{A}_s(1_{a\dot{a}}, 2_{b\dot{b}}, 3, 4) = \begin{array}{c} 1_{a\dot{a}} \\ \text{wavy} \\ \text{tree} \\ \text{dashed} \\ 4 \end{array} \begin{array}{c} 2_{b\dot{b}} \\ \text{wavy} \\ \text{tree} \\ \text{dashed} \\ 3 \end{array} = -\frac{i}{4s_{12}s_{23}} \langle 1_a 2_b 3_c 3^c \rangle [1_{\dot{a}}, 2_{\dot{b}}, 4^d, 4_{\dot{d}}]. \quad (\text{C.4})$$

The massless scalars in six dimensions behave as massive scalars when reduced to four dimensions. Taking the limits $m_1, m_2, \tilde{m}_1, \tilde{m}_2 \rightarrow 0$ and choosing the helicity components we found the four-point amplitudes for gluons and massive scalars in four dimensions:

$$\begin{aligned} \mathcal{A}_s(1_{22}, 2_{11}, 3, 4) \Big|_{4D} &= -i \frac{\langle 1 | \not{p}_3^{(4)} | 2 \rangle}{s_{12}s_{23}}, \\ \mathcal{A}_s(1_{11}, 2_{11}, 3, 4) \Big|_{4D} &= i\mu^2 \frac{[12]^2}{s_{12}s_{23}}, \end{aligned} \quad (\text{C.5})$$

where μ^2 coincides in this case with the mass of the scalar squared.

Finally, the last amplitude one needs for our unitarity computations is the five-point tree-level amplitude. The amplitude with five-gluons has first been computed in [30]. In [60, 295] this result has been extended to the five-point superamplitude in the $\mathcal{N} = (1, 1)$ theory. This superamplitude also contains information about the amplitude with scalar fields which is needed for the scalar subtraction when doing dimensional reconstruction. The amplitude with five gluons is

$$\mathcal{A}_g(1_{a\dot{a}}, 2_{b\dot{b}}, 3_{c\dot{c}}, 4_{d\dot{d}}, 5_{e\dot{e}}) = \frac{i}{s_{12}s_{23}s_{34}s_{45}s_{51}} (-\mathcal{M}_{a\dot{a}b\dot{b}c\dot{c}d\dot{d}e\dot{e}} + \mathcal{D}_{a\dot{a}b\dot{b}c\dot{c}d\dot{d}e\dot{e}}) \quad (\text{C.6})$$

with

$$\mathcal{M}_{a\dot{a}b\dot{b}c\dot{c}d\dot{d}e\dot{e}} = \langle 1_a | \not{p}_2 \not{p}_3 \not{p}_4 \not{p}_5 | 1_{\dot{a}} \rangle \langle 2_b 3_c 4_d 5_e \rangle [2_{\dot{b}} 3_{\dot{c}} 4_{\dot{d}} 5_{\dot{e}}] + \text{cyclic}, \quad (\text{C.7})$$

and

$$\begin{aligned} 2\mathcal{D}_{a\dot{a}b\dot{b}c\dot{c}d\dot{d}e\dot{e}} &= \langle 1_a \tilde{\Sigma}_{2\dot{b}} \rangle \langle 2_b 3_c 4_d 5_e \rangle [1_{\dot{a}} 3_{\dot{c}} 4_{\dot{d}} 5_{\dot{e}}] + \langle 3_c \tilde{\Sigma}_{4\dot{d}} \rangle \langle 1_a 2_b 4_d 5_e \rangle [1_{\dot{a}} 2_{\dot{b}} 3_{\dot{c}} 5_{\dot{e}}] \\ &+ \langle 4_d \tilde{\Sigma}_{5\dot{e}} \rangle \langle 1_a 2_b 3_c 5_e \rangle [1_{\dot{a}} 2_{\dot{b}} 3_{\dot{c}} 4_{\dot{d}}] - \langle 3_c \tilde{\Sigma}_{5\dot{e}} \rangle \langle 1_a 2_b 4_d 5_e \rangle [1_{\dot{a}} 2_{\dot{b}} 3_{\dot{c}} 4_{\dot{d}}] \\ &- [1_{\dot{a}} \Sigma_{2b}] \langle 1_a 3_c 4_d 5_e \rangle [2_{\dot{b}} 3_{\dot{c}} 4_{\dot{d}} 5_{\dot{e}}] - [3_{\dot{c}} \Sigma_{4d}] \langle 1_a 2_b 3_c 5_e \rangle [1_{\dot{a}} 2_{\dot{b}} 4_{\dot{d}} 5_{\dot{e}}] \\ &- [4_{\dot{d}} \Sigma_{5e}] \langle 1_a 2_b 3_c 4_d \rangle [1_{\dot{a}} 2_{\dot{b}} 3_{\dot{c}} 5_{\dot{e}}] + [3_{\dot{c}} \tilde{\Sigma}_{5e}] \langle 1_a 2_b 3_c 4_d \rangle [1_{\dot{a}} 2_{\dot{b}} 4_{\dot{d}} 5_{\dot{e}}]. \end{aligned} \quad (\text{C.8})$$

The amplitude with two scalars and three gluons is

$$\mathcal{A}_g(1_\phi, 2_{\bar{\phi}}, 3_{c\dot{c}}, 4_{d\dot{d}}, 5_{e\dot{e}}) = -\frac{i}{s_{12}s_{23}s_{34}s_{45}s_{51}} (\mathcal{M}_{c\dot{c}d\dot{d}e\dot{e}}^s + \mathcal{D}_{c\dot{c}d\dot{d}e\dot{e}}^s), \quad (\text{C.9})$$

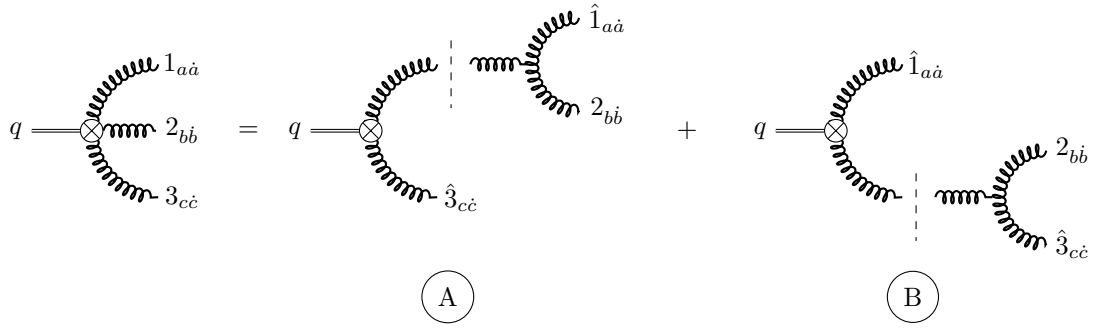


Figure C.1: BCFW construction of the tree-level non-minimal $\text{Tr } F^2$ form factor in six dimensions.

with

$$\begin{aligned} \mathcal{M}_{c\dot{c}d\dot{d}e\dot{e}}^s &= \langle 3_c | \not{p}_1 | 4_d \rangle [3_{\dot{c}} | \not{p}_2 | 4_{\dot{d}}] \langle 5_e | \not{p}_1 \not{p}_2 \not{p}_3 \not{p}_4 | 5_{\dot{e}} \rangle + \langle 4_d | \not{p}_1 | 5_e \rangle [4_{\dot{d}} | \not{p}_2 | 5_{\dot{e}}] \langle 3_c | \not{p}_4 \not{p}_5 \not{p}_1 \not{p}_2 | 3_{\dot{c}} \rangle \\ &+ \langle 3_c | \not{p}_1 | 5_e \rangle [3_{\dot{c}} | \not{p}_2 | 5_{\dot{e}}] \langle 4_d | \not{p}_5 \not{p}_1 \not{p}_2 \not{p}_3 | 4_{\dot{d}} \rangle + \frac{1}{2} \langle 3_c 4_d 5_e 1^a \rangle [3_{\dot{c}} 4_{\dot{d}} 5_{\dot{e}} 2_{\dot{b}}] \langle 1_a \tilde{\Sigma}_2^{\dot{b}} \rangle, \end{aligned} \quad (\text{C.10})$$

and

$$\begin{aligned} 2\mathcal{D}_{c\dot{c}d\dot{d}e\dot{e}}^s &= -\langle 4_d | \not{p}_1 | 5_e \rangle [3_{\dot{c}} | \not{p}_2 | 5_{\dot{e}}] \langle 3_c \tilde{\Sigma}_{4d} \rangle + \langle 4_d | \not{p}_1 | 5_e \rangle [3_{\dot{c}} | \not{p}_2 | 4_{\dot{d}}] \langle 3_c \tilde{\Sigma}_{5e} \rangle \\ &- \langle 3_c | \not{p}_1 | 5_e \rangle [3_{\dot{c}} | \not{p}_2 | 4_{\dot{d}}] \langle 4_d \tilde{\Sigma}_{5e} \rangle + \langle 3_c | \not{p}_1 | 5_e \rangle [4_{\dot{d}} | \not{p}_2 | 5_{\dot{e}}] \langle 3_c \Sigma_{4d} \rangle \\ &- \langle 3_c | \not{p}_1 | 4_d \rangle [4_{\dot{d}} | \not{p}_2 | 5_{\dot{e}}] \langle 3_c \Sigma_{5e} \rangle + \langle 3_c | \not{p}_1 | 4_d \rangle [3_{\dot{c}} | \not{p}_2 | 5_{\dot{e}}] \langle 4_{\dot{d}} \Sigma_{5e} \rangle. \end{aligned} \quad (\text{C.11})$$

The Σ and $\tilde{\Sigma}$ that appear in the previous formulae are defined as

$$\begin{aligned} |\Sigma_{ia}\rangle &= \left(\not{p}_i \not{p}_{i+1} \not{p}_{i+2} \not{p}_{i+3} - \not{p}_i \not{p}_{i+3} \not{p}_{i+2} \not{p}_{i+1} \right) |i_a\rangle \\ |\tilde{\Sigma}_{ia}\rangle &= \left(\not{p}_i \not{p}_{i+1} \not{p}_{i+2} \not{p}_{i+3} - \not{p}_i \not{p}_{i+3} \not{p}_{i+2} \not{p}_{i+1} \right) |i_a\rangle \end{aligned} \quad (\text{C.12})$$

where we define $\not{p}_6 \equiv \not{p}_1$.

C.1.1 Non-Minimal Form Factors

In this section we will address the computation of six-dimensional tree-level building blocks using BCFW recursion relations¹. In particular we briefly comment on the main steps of the calculation of $\text{Tr } F^2$ in the non-minimal configuration. Diagrammatically the terms we need to compute are represented in Figure C.1. In this computation one needs to make use of the three-point on-shell amplitudes in six-dimensions. These are most conveniently defined in terms of a set of auxiliary $\text{SU}(2)$ spinors which we denote by $u_a, \tilde{u}_{\dot{a}}, w_a$ and $\tilde{w}_{\dot{a}}$, following the conventions of [30]. These objects are not Lorentz invariants in six dimensions and thus are not allowed to appear in the final expression, however they enjoy useful properties which simplify the calculation. The on-shell three-point amplitude cleanly expressed in terms of the above mentioned spinors:

$$\mathcal{A}_3(1_{a\dot{a}}, 2_{b\dot{b}}, 3_{c\dot{c}}) = i \Gamma_{abc}(1, 2, 3) \tilde{\Gamma}_{\dot{a}\dot{b}\dot{c}}(1, 2, 3), \quad (\text{C.13})$$

¹For a more detailed account of six-dimensional BCFW see [30].

with

$$\begin{aligned}\Gamma_{abc}(1, 2, 3) &= u_{1a}u_{2b}w_{3c} + u_{1a}w_{2b}u_{3c} + w_{1a}u_{2b}u_{3c}, \\ \tilde{\Gamma}_{\dot{a}\dot{b}\dot{c}}(1, 2, 3) &= \tilde{u}_{1\dot{a}}\tilde{u}_{2\dot{b}}\tilde{w}_{3\dot{c}} + \tilde{u}_{1\dot{a}}\tilde{w}_{2\dot{b}}\tilde{u}_{3\dot{c}} + \tilde{w}_{1\dot{a}}\tilde{u}_{2\dot{b}}\tilde{u}_{3\dot{c}}.\end{aligned}\quad (\text{C.14})$$

Consider now applying six-dimensional BCFW as in Figure C.1. The hatted momenta are shifted by a quantity proportional to the complex parameter z as

$$\begin{aligned}\hat{p}_1 &= p_1 + z X^{a\dot{a}} \varepsilon_{1a\dot{a}}, \\ \hat{p}_3 &= p_3 - z X^{a\dot{a}} \varepsilon_{1a\dot{a}},\end{aligned}\quad (\text{C.15})$$

where $X^{a\dot{a}}$ is an arbitrary tensor needed to saturate the little group indices. This tensor, which also multiplies C.19, will be removed at the end of the calculation. The on-shell condition $\hat{p}_{1,2}^2 = 0$ implies $\det X = 0$, which allows to express X as

$$X^{a\dot{a}} = x^a \tilde{x}^{\dot{a}}. \quad (\text{C.16})$$

Furthermore we can define the quantities

$$y^b = \tilde{x}^{\dot{a}} \langle 3_b 1^{\dot{a}} \rangle^{-1}, \quad \tilde{y}_{\dot{b}} = x^a \langle 1^a 3^{\dot{b}} \rangle^{-1}, \quad (\text{C.17})$$

which allow us to rewrite the momentum shift C.15 in terms of the spinor shifts

$$\begin{aligned}|\hat{1}^a\rangle &= |1^a\rangle + z x^a y_b |3^b\rangle, \\ |\hat{3}^b\rangle &= |3^b\rangle + z y^b x_a |1^a\rangle, \\ |\hat{1}^{\dot{a}}] &= |1^{\dot{a}}] - z \tilde{x}^{\dot{a}} \tilde{y}_{\dot{b}} |3^{\dot{b}}], \\ |\hat{3}^{\dot{b}}] &= |3^{\dot{b}}] - z \tilde{y}^{\dot{b}} \tilde{x}_{\dot{a}} |1^{\dot{a}}].\end{aligned}\quad (\text{C.18})$$

Considering now for example term A in Figure C.1 one has

$$\begin{aligned}(\text{A}) &= X^{a\dot{a}} \mathcal{A}_3(\hat{1}_{a\dot{a}}, 2_{b\dot{b}}, \hat{k}_{d\dot{d}}) \frac{-i}{s_{12}} F_{\mathcal{O}_2}^{(0)}(-\hat{k}^{d\dot{d}}, \hat{3}_{c\dot{c}}; q) \\ &= \frac{i}{s_{12}} X^{a\dot{a}} \Gamma_{abd}(\hat{1}, 2, \hat{k}) \tilde{\Gamma}_{\dot{a}\dot{b}\dot{d}}(\hat{1}, 2, \hat{k}) \langle \hat{k}^d \hat{3}_{\dot{c}} \rangle \langle \hat{3}_{\dot{c}} \hat{k}^{\dot{d}} \rangle.\end{aligned}\quad (\text{C.19})$$

Before substituting the definitions (C.18) in (C.19), we make use of the properties of $u, \tilde{u}, w, \tilde{w}$ to simplify this expression. The most useful identities are

$$\begin{aligned}u_{ia}w_{ib} - u_{ib}w_{ia} &= \epsilon_{ab}, \quad \tilde{u}_{i\dot{a}}\tilde{w}_{i\dot{b}} - \tilde{u}_{i\dot{b}}\tilde{w}_{i\dot{a}} = \epsilon_{\dot{a}\dot{b}}, \\ |u_i \cdot i\rangle &= |u_j \cdot j\rangle, \quad |\tilde{u}_i \cdot i] = |\tilde{u}_j \cdot j] \quad \forall i, j = 1, 2, k, \\ |w_1 \cdot 1\rangle + |w_2 \cdot 2\rangle + |w_k \cdot k\rangle &= 0, \\ |\tilde{w}_1 \cdot 1] + |\tilde{w}_2 \cdot 2] + |\tilde{w}_k \cdot k] &= 0,\end{aligned}\quad (\text{C.20})$$

where we used the shorthand notation $u_{ia}|i^a\rangle = |u_i \cdot i\rangle$ and $\tilde{u}_{i\dot{a}}|\dot{i}^{\dot{a}}] = |\tilde{u}_i \cdot i]$. These identities allow us to rewrite

$$\begin{aligned}\Gamma_{abd}(\hat{1}, 2, \hat{k}) \langle \hat{k}^d \rangle &= \langle \hat{1}_a | u_{2b} + \langle 2_b | u_{\hat{1}_a}, \\ \tilde{\Gamma}_{\dot{a}\dot{b}\dot{d}}(\hat{1}, 2, \hat{k}) |\hat{k}^{\dot{d}}] &= |\hat{1}_{\dot{a}}] \tilde{u}_{2\dot{b}} + |2_{\dot{b}}] \tilde{u}_{\hat{1}_{\dot{a}}},\end{aligned}\quad (\text{C.21})$$

which in turn leads to

$$(A) = \frac{i}{s_{12}} X^{a\dot{a}} \left(\langle \hat{1}_a \hat{3}_{\dot{c}} \rangle \langle \hat{3}_c \hat{1}_{\dot{a}} \rangle u_{2b} \tilde{u}_{2\dot{b}} + \langle \hat{1}_a \hat{3}_{\dot{c}} \rangle \langle \hat{3}_c 2_{\dot{b}} \rangle u_{2b} \tilde{u}_{1\dot{a}} \right. \\ \left. + \langle 2_b \hat{3}_{\dot{c}} \rangle \langle \hat{3}_c \hat{1}_{\dot{a}} \rangle u_{1a} \tilde{u}_{2\dot{b}} + \langle 2_b \hat{3}_{\dot{c}} \rangle \langle \hat{3}_c 2_{\dot{b}} \rangle u_{1a} \tilde{u}_{1\dot{a}} \right). \quad (C.22)$$

To further simplify the result, and to eliminate the residual SU(2) spinors, we make the following observations:

- pairs of u_i, \tilde{u}_j with $i \neq j$ can be immediately rewritten in terms of six-dimensional invariants as

$$u_{1a} \tilde{u}_{2\dot{b}} = \langle 1_a 2_{\dot{b}} \rangle, \quad u_{2b} \tilde{u}_{1\dot{a}} = -\langle 2_b 1_{\dot{a}} \rangle, \\ u_{2b} \tilde{u}_{k\dot{c}} = \langle 2_b k_{\dot{c}} \rangle, \quad u_{kc} \tilde{u}_{2\dot{b}} = -\langle k_c 2_{\dot{b}} \rangle. \quad (C.23)$$

- pairs of u_i, \tilde{u}_j with $i = j$ can be rewritten using the identity [295]

$$u_{ia} \tilde{u}_{i\dot{a}} = \frac{(-1)^{\mathcal{P}_{ij}}}{s_{iP}} \langle i_a | p_j P | i_{\dot{a}} \rangle, \quad (C.24)$$

where p_j is any other momentum belonging to the same three-point amplitude as p_i , and $\mathcal{P}_{ij} = +1$ for clockwise ordering of the states (i, j) . Also P is any given arbitrary momentum.

Repeating a similar reasoning on term (B) one gets

$$(B) = \frac{i}{s_{23}} X^{a\dot{a}} \left(\langle \hat{1}_a \hat{3}_{\dot{c}} \rangle \langle \hat{3}_c \hat{1}_{\dot{a}} \rangle u_{2b} \tilde{u}_{2\dot{b}} + \langle \hat{1}_a \hat{3}_{\dot{c}} \rangle \langle 2_b \hat{1}_{\dot{a}} \rangle u_{3c} \tilde{u}_{2\dot{b}} \right. \\ \left. + \langle \hat{1}_a 2_{\dot{b}} \rangle \langle \hat{3}_c \hat{1}_{\dot{a}} \rangle u_{2b} \tilde{u}_{3\dot{c}} + \langle \hat{1}_a 2_{\dot{b}} \rangle \langle 2_b \hat{1}_{\dot{a}} \rangle u_{3c} \tilde{u}_{3\dot{c}} \right). \quad (C.25)$$

The on-shell condition for the intermediate propagators in (A) and (B) defines two different BCFW shift parameters, which we label z_A and z_B respectively. By computing z_A and z_B one can see that they are related by

$$z_B = -\frac{s_{23}}{s_{12}} z_A. \quad (C.26)$$

Thanks to this relation multiple cancellations happen between terms in (A) and terms in (B). With some further algebra and removing the $X^{a\dot{a}}$ tensor, one arrives at (4.40).

The analytic expression of the six-dimensional form factor $F_{\mathcal{O}_2}^{(0)}(1_{a\dot{a}}, 2_{b\dot{b}}, 3_{c\dot{c}}; q)$ could also be computed using Feynman diagrams, see for example [254]. Due to the low multiplicity of this form factor, there is just a small number of contributing Feynman diagrams. The diagrammatic approach may thus be considered as equivalently viable as BCFW in this case, the latter method however leads to a far more compact expression with all the symmetries manifest.

In a similar way but with much less involved calculation, we can find both the non-minimal form factors with two scalars and one gluon (4.41) and (4.42). In Figure C.2 and Figure C.3 we show the BCFW factorization channels for these calculations. The only missing ingredient is the three-point amplitude with two scalars and one gluon in six dimensions, which turns out to be very simple:

$$\mathcal{A}(1_{a\dot{a}}, 2, 3) = i u_{1a} \tilde{u}_{1\dot{a}}. \quad (C.27)$$

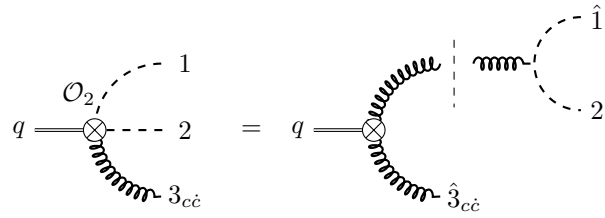


Figure C.2: BCFW construction of the tree-level non-minimal $\text{Tr } F^2$ form factor with two scalars.

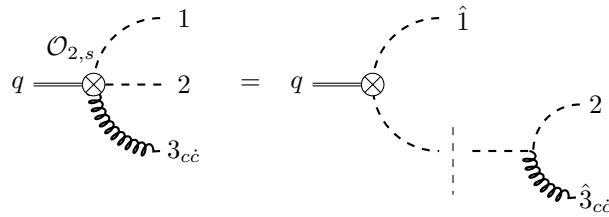


Figure C.3: BCFW construction of the tree-level non-minimal $D\phi^2$ form factor.

Appendix D

Feynman Integrals

The integrals needed in Chapter 4 and Section 3.3 (the latter are named I_2 , I_3 and I_4) are:

$$\begin{aligned}
 \text{Diagram 1} &= I_2(s_{12}) = \int \frac{d^{4-2\epsilon}l}{(2\pi)^{4-2\epsilon}} \frac{1}{l^2 (l+p_1+p_2)^2} = \frac{i c_\Gamma}{(4\pi)^{2-\epsilon}} \frac{(-s_{12})^{-\epsilon}}{\epsilon(1-2\epsilon)}, \\
 \text{Diagram 2} &= I_3(s_{12}) = \int \frac{d^{4-2\epsilon}l}{(2\pi)^{4-2\epsilon}} \frac{1}{l^2 (l+p_2)^2 (l+p_1+p_2)^2} = -\frac{i c_\Gamma}{(4\pi)^{2-\epsilon}} \frac{(-s_{12})^{-1-\epsilon}}{\epsilon^2}, \\
 \text{Diagram 3} &= -\frac{i c_\Gamma}{(4\pi)^{2-\epsilon}} \frac{1}{\epsilon^2} \left[\frac{(-q^2)^{-\epsilon} - (-p^2)^{-\epsilon}}{q^2 - p^2} \right],
 \end{aligned} \tag{D.1}$$

and

$$\begin{aligned}
 \text{Diagram 4} &= \int \frac{d^{4-2\epsilon}l}{(2\pi)^{4-2\epsilon}} \frac{1}{l^2 (l+p_1)^2 (l+p_1+p_2)^2 (l+p_1+p_2+p_3)^2} \\
 &= \frac{i c_\Gamma}{(4\pi)^{2-\epsilon}} \frac{1}{s_{12}s_{23}} \left[\frac{2}{\epsilon^2} \left((-s_{12})^{-\epsilon} + (-s_{23})^{-\epsilon} - (-q^2)^{-\epsilon} \right) + \right. \\
 &\quad \left. -2\text{Li}_2\left(1 - \frac{s_{12}}{q^2}\right) - 2\text{Li}_2\left(1 - \frac{s_{23}}{q^2}\right) - \log^2\left(\frac{s_{12}}{s_{23}}\right) - \frac{\pi^2}{3} \right] + \mathcal{O}(\epsilon),
 \end{aligned} \tag{D.2}$$

where

$$c_\Gamma = \frac{\Gamma[1+\epsilon] \Gamma[1-\epsilon]^2}{\Gamma[1-2\epsilon]} . \tag{D.3}$$

The result with $q^\mu = p_4^\mu$ ($q^2 = 0$), needed in Section 3.3, is

$$\begin{aligned} I_4(s_{12}, s_{14}) &= \int \frac{d^{4-2\epsilon}l}{(2\pi)^{4-2\epsilon}} \frac{1}{l^2 (l-p_3)^2 (l-p_3-p_4)^2 (l+p_2)^2} \\ &= \frac{i c_\Gamma}{(4\pi)^{2-\epsilon}} \frac{1}{s_{12}s_{14}} \left[\frac{2}{\epsilon^2} ((-s_{12})^{-\epsilon} + (-s_{14})^{-\epsilon}) - \log^2 \left(\frac{-s_{12}}{-s_{14}} \right) - \pi^2 \right] + \mathcal{O}(\epsilon). \end{aligned} \quad (\text{D.4})$$

These results are exact to all orders in ϵ , and the expression of the corresponding integral functions in a different number of dimensions can be obtained by simply replacing ϵ to the appropriate value, for instance $\epsilon \mapsto \epsilon - 1$ and $\epsilon \mapsto \epsilon - 2$ for $d = 6 - 2\epsilon$ and $d = 8 - 2\epsilon$, respectively. In particular it turns out that all the integrals which give the rational terms, *i.e.* those with a non-trivial numerator written in (4.5), can always be expressed as integrals in higher dimensions [55]. Indeed consider the general integral function

$$I_n^d[\mu^{2p}] = \int \frac{d^{4-2\epsilon}l}{(2\pi)^{4-2\epsilon}} (\mu^2)^p f_n(\{p_i\}, l) = \int \frac{d^4l^{(4)}}{(2\pi)^4} \int \frac{d^{-2\epsilon}\mu}{(2\pi)^{-2\epsilon}} (\mu^2)^p f_n(\{p_i\}, l), \quad (\text{D.5})$$

and the μ -measure can be rewritten as

$$\begin{aligned} \int d^{-2\epsilon}\mu (\mu^2)^p &= \frac{1}{2} \int d\Omega_{-1-2\epsilon} \int_0^{+\infty} d\mu^2 (\mu^2)^{-1-\epsilon+p} \\ &= \frac{\int \Omega_{-1-2\epsilon}}{\int d\Omega_{2p-1-2\epsilon}} \int d^{2p-2\epsilon}\mu. \end{aligned} \quad (\text{D.6})$$

Then (D.5) can be written as

$$\begin{aligned} I_n^d[\mu^{2p}] &= \frac{(2\pi)^{2p} \int d\Omega_{-1-2\epsilon}}{\int d\Omega_{2p-1-2\epsilon}} \int \frac{d^{4+2p-2\epsilon}l}{(2\pi)^{4+2p-2\epsilon}} f_n(\{p_i\}, l) \\ &= -\epsilon(1-\epsilon)(2-\epsilon) \cdots (p-1-\epsilon) (4\pi)^p I_n^{d+2p}[1], \end{aligned} \quad (\text{D.7})$$

where

$$\int d\Omega_x = \frac{2\pi^{\frac{x+1}{2}}}{\Gamma[\frac{x+1}{2}]}. \quad (\text{D.8})$$

Then to compute this integrals becomes just simple algebra:

$$\begin{aligned} \text{Bubble}(\mu^2) &= \frac{-i}{(4\pi)^2} \cdot \frac{s_{12}}{6} + \mathcal{O}(\epsilon), & \text{Square}(\mu^2) &= \mathcal{O}(\epsilon), \\ \text{Triangle}(\mu^2) &= \frac{i}{(4\pi)^2} \cdot \frac{1}{2} + \mathcal{O}(\epsilon), & \text{Square}(\mu^4) &= \frac{-i}{(4\pi)^2} \cdot \frac{1}{6} + \mathcal{O}(\epsilon), \\ \text{Triangle}(\mu^4) &= \frac{i}{(4\pi)^2} \cdot \frac{s_{12}}{24} + \mathcal{O}(\epsilon), & & \end{aligned}$$

Finally, we give the explicit expression for the integral functions appearing in Chapter 6. These expressions are expanded in ϵ up to the relevant orders, and only terms with an s -channel discontinuity are kept.

$$I_2(s) \simeq \frac{i}{16\pi^2} \left[\frac{1}{\epsilon} - \log(-s) \right], \quad (\text{D.9})$$

$$I_3(s) \simeq \frac{i}{16\pi^2 s} \left[\frac{1}{\epsilon^2} - \frac{\log(-s)}{\epsilon} + \frac{1}{2} \log^2(-s) \right], \quad (\text{D.10})$$

$$I_3(s; m) \simeq -\frac{i}{32} \left[\frac{1}{m\sqrt{-s}} + \frac{\log(-s/m^2)}{\pi^2 m^2} \right], \quad (\text{D.11})$$

$$\begin{aligned} I_4(s, t; m) + I_4(s, u; m) &\simeq -\frac{1}{8\pi} \frac{1}{m\omega} \frac{1}{d-4} (-s)^{\frac{d-6}{2}} \\ &\simeq -\frac{1}{16\pi s (m\omega)} \left[\frac{1}{\epsilon} - \log\left(-\frac{s}{m^2}\right) \right]. \end{aligned} \quad (\text{D.12})$$

Bibliography

- [1] L. J. Dixon, *Calculating scattering amplitudes efficiently*, in Theoretical Advanced Study Institute in Elementary Particle Physics (TASI 95): QCD and Beyond (Jan. 1996), pp. 539–584, [arXiv:hep-ph/9601359](#).
- [2] L. J. Dixon, *A brief introduction to modern amplitude methods*, in [Theoretical Advanced Study Institute in Elementary Particle Physics: Particle Physics: The Higgs Boson and Beyond](#) (2014), pp. 31–67, [arXiv:1310.5353 \[hep-ph\]](#).
- [3] H. Elvang and Y.-t. Huang, *Scattering Amplitudes*, (2013), [arXiv:1308.1697 \[hep-th\]](#).
- [4] J. M. Henn and J. C. Plefka, *Scattering Amplitudes in Gauge Theories*, Vol. 883 (Springer, Berlin, 2014).
- [5] C. Cheung, “TASI Lectures on Scattering Amplitudes”, in [Proceedings, Theoretical Advanced Study Institute in Elementary Particle Physics : Anticipating the Next Discoveries in Particle Physics \(TASI 2016\): Boulder, CO, USA, June 6–July 1, 2016](#), edited by R. Essig and I. Low (2018), pp. 571–623, [arXiv:1708.03872 \[hep-ph\]](#).
- [6] G. Travaglini et al., *The SAGEX Review on Scattering Amplitudes*, (2022), [arXiv:2203.13011 \[hep-th\]](#).
- [7] A. Brandhuber, J. Plefka, and G. Travaglini, *The SAGEX Review on Scattering Amplitudes, Chapter 1: Modern Fundamentals of Amplitudes*, (2022), [arXiv:2203.13012 \[hep-th\]](#).
- [8] S. Weinberg, *The Quantum theory of fields. Vol. 1: Foundations* (Cambridge University Press, June 2005).
- [9] J. A. Wheeler, *On the Mathematical Description of Light Nuclei by the Method of Resonating Group Structure*, [Phys. Rev.](#) **52**, 1107–1122 (1937).
- [10] W. Heisenberg, *Die “beobachtbaren größen” in der theorie der elementarteilchen*, [Zeitschrift für Physik](#) **120**, 513–538 (1943).
- [11] R. J. Eden, P. V. Landshoff, D. I. Olive, and J. C. Polkinghorne, *The analytic S-matrix* (Cambridge Univ. Press, Cambridge, 1966).
- [12] A. D. Martin and T. D. Spearman, *Elementary particle theory.*, (1970).
- [13] G. Sommer, *Present state of rigorous analytic properties of scattering amplitudes*, [Fortsch. Phys.](#) **18**, 577–688 (1970).
- [14] M. D. Schwartz, *Quantum Field Theory and the Standard Model* (Cambridge University Press, Mar. 2014).
- [15] Z. Bern and G. Chalmers, *Factorization in one loop gauge theory*, [Nucl. Phys. B](#) **447**, 465–518 (1995), [arXiv:hep-ph/9503236](#).

- [16] P. Benincasa and F. Cachazo, *Consistency Conditions on the S-Matrix of Massless Particles*, (2007), [arXiv:0705.4305 \[hep-th\]](#).
- [17] M. S. Costa, J. Penedones, D. Poland, and S. Rychkov, *Spinning Conformal Correlators*, *JHEP* **11**, 071 (2011), [arXiv:1107.3554 \[hep-th\]](#).
- [18] N. Arkani-Hamed, T.-C. Huang, and Y.-t. Huang, *Scattering amplitudes for all masses and spins*, *JHEP* **11**, 070 (2021), [arXiv:1709.04891 \[hep-th\]](#).
- [19] G. Durieux, T. Kitahara, Y. Shadmi, and Y. Weiss, *The electroweak effective field theory from on-shell amplitudes*, *JHEP* **01**, 119 (2020), [arXiv:1909.10551 \[hep-ph\]](#).
- [20] S. De Angelis, *Amplitude bases in generic EFTs*, (2022), [arXiv:2202.02681 \[hep-th\]](#).
- [21] R. Britto, F. Cachazo, and B. Feng, *Generalized unitarity and one-loop amplitudes in $N=4$ super-Yang-Mills*, *Nucl. Phys. B* **725**, 275–305 (2005), [arXiv:hep-th/0412103](#).
- [22] R. Britto, F. Cachazo, B. Feng, and E. Witten, *Direct proof of tree-level recursion relation in Yang-Mills theory*, *Phys. Rev. Lett.* **94**, 181602 (2005), [arXiv:hep-th/0501052](#).
- [23] N. Arkani-Hamed and J. Kaplan, *On Tree Amplitudes in Gauge Theory and Gravity*, *JHEP* **04**, 076 (2008), [arXiv:0801.2385 \[hep-th\]](#).
- [24] K. Risager, *A Direct proof of the CSW rules*, *JHEP* **12**, 003 (2005), [arXiv:hep-th/0508206](#).
- [25] T. Cohen, H. Elvang, and M. Kiermaier, *On-shell constructibility of tree amplitudes in general field theories*, *JHEP* **04**, 053 (2011), [arXiv:1010.0257 \[hep-th\]](#).
- [26] K. Kampf, J. Novotny, and J. Trnka, *Recursion relations for tree-level amplitudes in the $SU(N)$ nonlinear sigma model*, *Phys. Rev. D* **87**, 081701 (2013), [arXiv:1212.5224 \[hep-th\]](#).
- [27] C. Cheung, K. Kampf, J. Novotny, and J. Trnka, *Effective Field Theories from Soft Limits of Scattering Amplitudes*, *Phys. Rev. Lett.* **114**, 221602 (2015), [arXiv:1412.4095 \[hep-th\]](#).
- [28] C. Cheung, K. Kampf, J. Novotny, C.-H. Shen, and J. Trnka, *On-Shell Recursion Relations for Effective Field Theories*, *Phys. Rev. Lett.* **116**, 041601 (2016), [arXiv:1509.03309 \[hep-th\]](#).
- [29] C. Cheung, C.-H. Shen, and J. Trnka, *Simple Recursion Relations for General Field Theories*, *JHEP* **06**, 118 (2015), [arXiv:1502.05057 \[hep-th\]](#).
- [30] C. Cheung and D. O’Connell, *Amplitudes and Spinor-Helicity in Six Dimensions*, *JHEP* **07**, 075 (2009), [arXiv:0902.0981 \[hep-th\]](#).
- [31] J. C. Collins, *Renormalization: An Introduction to Renormalization, The Renormalization Group, and the Operator Product Expansion*, Vol. 26, Cambridge Monographs on Mathematical Physics (Cambridge University Press, Cambridge, 1986).
- [32] R. V. Harlander, D. R. T. Jones, P. Kant, L. Mihaila, and M. Steinhauser, *Four-loop beta function and mass anomalous dimension in dimensional reduction*, *JHEP* **12**, 024 (2006), [arXiv:hep-ph/0610206](#).

- [33] R. Harlander, P. Kant, L. Mihaila, and M. Steinhauser, *Dimensional Reduction applied to QCD at three loops*, *JHEP* **09**, 053 (2006), [arXiv:hep-ph/0607240](#).
- [34] L. D. Landau, *On analytic properties of vertex parts in quantum field theory*, *Nucl. Phys.* **13**, 181–192 (1959).
- [35] Z. Bern, L. J. Dixon, D. C. Dunbar, and D. A. Kosower, *One loop n point gauge theory amplitudes, unitarity and collinear limits*, *Nucl. Phys. B* **425**, 217–260 (1994), [arXiv:hep-ph/9403226](#).
- [36] Z. Bern, L. J. Dixon, D. C. Dunbar, and D. A. Kosower, *Fusing gauge theory tree amplitudes into loop amplitudes*, *Nucl. Phys. B* **435**, 59–101 (1995), [arXiv:hep-ph/9409265](#).
- [37] Z. Bern, L. J. Dixon, and D. A. Kosower, *One loop amplitudes for $e^+ e^-$ to four partons*, *Nucl. Phys. B* **513**, 3–86 (1998), [arXiv:hep-ph/9708239](#).
- [38] G. Ossola, C. G. Papadopoulos, and R. Pittau, *Reducing full one-loop amplitudes to scalar integrals at the integrand level*, *Nucl. Phys. B* **763**, 147–169 (2007), [arXiv:hep-ph/0609007](#).
- [39] R. Britto, B. Feng, and P. Mastrolia, *The Cut-constructible part of QCD amplitudes*, *Phys. Rev. D* **73**, 105004 (2006), [arXiv:hep-ph/0602178](#).
- [40] P. Mastrolia, *On Triple-cut of scattering amplitudes*, *Phys. Lett. B* **644**, 272–283 (2007), [arXiv:hep-th/0611091](#).
- [41] D. Forde, *Direct extraction of one-loop integral coefficients*, *Phys. Rev. D* **75**, 125019 (2007), [arXiv:0704.1835 \[hep-ph\]](#).
- [42] P. Mastrolia, G. Ossola, C. G. Papadopoulos, and R. Pittau, *Optimizing the Reduction of One-Loop Amplitudes*, *JHEP* **06**, 030 (2008), [arXiv:0803.3964 \[hep-ph\]](#).
- [43] P. Mastrolia, *Double-Cut of Scattering Amplitudes and Stokes' Theorem*, *Phys. Lett. B* **678**, 246–249 (2009), [arXiv:0905.2909 \[hep-ph\]](#).
- [44] Z. Bern, L. J. Dixon, and D. A. Kosower, *Two-loop $g \rightarrow gg$ splitting amplitudes in QCD*, *JHEP* **08**, 012 (2004), [arXiv:hep-ph/0404293](#).
- [45] R. Britto, *Loop Amplitudes in Gauge Theories: Modern Analytic Approaches*, *J. Phys. A* **44**, 454006 (2011), [arXiv:1012.4493 \[hep-th\]](#).
- [46] Z. Bern and Y.-t. Huang, *Basics of Generalized Unitarity*, *J. Phys. A* **44**, 454003 (2011), [arXiv:1103.1869 \[hep-th\]](#).
- [47] J. J. M. Carrasco and H. Johansson, *Generic multiloop methods and application to $N=4$ super-Yang-Mills*, *J. Phys. A* **44**, 454004 (2011), [arXiv:1103.3298 \[hep-th\]](#).
- [48] G. Passarino and M. J. G. Veltman, *One Loop Corrections for $e^+ e^-$ Annihilation Into $\mu^+ \mu^-$ in the Weinberg Model*, *Nucl. Phys. B* **160**, 151–207 (1979).
- [49] W. L. van Neerven and J. A. M. Vermaseren, *Large loop integrals*, *Phys. Lett. B* **137**, 241–244 (1984).
- [50] Y.-t. Huang and D. McGady, *Consistency Conditions for Gauge Theory S Matrices from Requirements of Generalized Unitarity*, *Phys. Rev. Lett.* **112**, 241601 (2014), [arXiv:1307.4065 \[hep-th\]](#).
- [51] W.-M. Chen, Y.-t. Huang, and D. A. McGady, *Anomalies without an action*, (2014), [arXiv:1402.7062 \[hep-th\]](#).

- [52] Z. Bern, L. J. Dixon, and D. A. Kosower, *On-shell recurrence relations for one-loop QCD amplitudes*, *Phys. Rev. D* **71**, 105013 (2005), [arXiv:hep-th/0501240](#).
- [53] Z. Bern, L. J. Dixon, and D. A. Kosower, *The last of the finite loop amplitudes in QCD*, *Phys. Rev. D* **72**, 125003 (2005), [arXiv:hep-ph/0505055](#).
- [54] Z. Bern, L. J. Dixon, and D. A. Kosower, *Bootstrapping multi-parton loop amplitudes in QCD*, *Phys. Rev. D* **73**, 065013 (2006), [arXiv:hep-ph/0507005](#).
- [55] Z. Bern and A. G. Morgan, *Massive loop amplitudes from unitarity*, *Nucl. Phys. B* **467**, 479–509 (1996), [arXiv:hep-ph/9511336](#).
- [56] A. Brandhuber, S. McNamara, B. J. Spence, and G. Travaglini, *Loop amplitudes in pure Yang-Mills from generalised unitarity*, *JHEP* **10**, 011 (2005), [arXiv:hep-th/0506068](#).
- [57] C. Anastasiou, R. Britto, B. Feng, Z. Kunszt, and P. Mastrolia, *D-dimensional unitarity cut method*, *Phys. Lett. B* **645**, 213–216 (2007), [arXiv:hep-ph/0609191](#).
- [58] C. Anastasiou, R. Britto, B. Feng, Z. Kunszt, and P. Mastrolia, *Unitarity cuts and Reduction to master integrals in d dimensions for one-loop amplitudes*, *JHEP* **03**, 111 (2007), [arXiv:hep-ph/0612277](#).
- [59] W. T. Giele, Z. Kunszt, and K. Melnikov, *Full one-loop amplitudes from tree amplitudes*, *JHEP* **04**, 049 (2008), [arXiv:0801.2237 \[hep-ph\]](#).
- [60] Z. Bern, J. J. Carrasco, T. Dennen, Y.-t. Huang, and H. Ita, *Generalized Unitarity and Six-Dimensional Helicity*, *Phys. Rev. D* **83**, 085022 (2011), [arXiv:1010.0494 \[hep-th\]](#).
- [61] A. Brandhuber, B. Spence, G. Travaglini, and G. Yang, *Form Factors in N=4 Super Yang-Mills and Periodic Wilson Loops*, *JHEP* **01**, 134 (2011), [arXiv:1011.1899 \[hep-th\]](#).
- [62] Y. Shadmi and Y. Weiss, *Effective Field Theory Amplitudes the On-Shell Way: Scalar and Vector Couplings to Gluons*, *JHEP* **02**, 165 (2019), [arXiv:1809.09644 \[hep-ph\]](#).
- [63] F. A. Berends and W. Giele, *The Six Gluon Process as an Example of Weyl-Van Der Waerden Spinor Calculus*, *Nucl. Phys. B* **294**, 700–732 (1987).
- [64] M. L. Mangano, *The Color Structure of Gluon Emission*, *Nucl. Phys. B* **309**, 461–475 (1988).
- [65] Z. Bern, J. J. Carrasco, M. Chiodaroli, H. Johansson, and R. Roiban, *The Duality Between Color and Kinematics and its Applications*, (2019), [arXiv:1909.01358 \[hep-th\]](#).
- [66] F. Cachazo, P. Svrcek, and E. Witten, *MHV vertices and tree amplitudes in gauge theory*, *JHEP* **09**, 006 (2004), [arXiv:hep-th/0403047](#).
- [67] A. Brandhuber, B. J. Spence, and G. Travaglini, *One-loop gauge theory amplitudes in N=4 super Yang-Mills from MHV vertices*, *Nucl. Phys. B* **706**, 150–180 (2005), [arXiv:hep-th/0407214](#).
- [68] I. Brivio and M. Trott, *The Standard Model as an Effective Field Theory*, *Phys. Rept.* **793**, 1–98 (2019), [arXiv:1706.08945 \[hep-ph\]](#).
- [69] G. W. Bennett et al. (Muon g-2), *Final Report of the Muon E821 Anomalous Magnetic Moment Measurement at BNL*, *Phys. Rev. D* **73**, 072003 (2006), [arXiv:hep-ex/0602035](#).

- [70] T. Aoyama et al., *The anomalous magnetic moment of the muon in the Standard Model*, *Phys. Rept.* **887**, 1–166 (2020), [arXiv:2006.04822 \[hep-ph\]](#).
- [71] B. Abi et al. (Muon g-2), *Measurement of the Positive Muon Anomalous Magnetic Moment to 0.46 ppm*, *Phys. Rev. Lett.* **126**, 141801 (2021), [arXiv:2104.03281 \[hep-ex\]](#).
- [72] S. Weinberg, *Baryon and Lepton Nonconserving Processes*, *Phys. Rev. Lett.* **43**, 1566–1570 (1979).
- [73] B. Henning, X. Lu, and H. Murayama, *How to use the Standard Model effective field theory*, *JHEP* **01**, 023 (2016), [arXiv:1412.1837 \[hep-ph\]](#).
- [74] I. Brivio, Y. Jiang, and M. Trott, *The SMEFTsim package, theory and tools*, *JHEP* **12**, 070 (2017), [arXiv:1709.06492 \[hep-ph\]](#).
- [75] I. Brivio, T. Corbett, and M. Trott, *The Higgs width in the SMEFT*, *JHEP* **10**, 056 (2019), [arXiv:1906.06949 \[hep-ph\]](#).
- [76] S. Dawson, S. Homiller, and S. D. Lane, *Putting standard model EFT fits to work*, *Phys. Rev. D* **102**, 055012 (2020), [arXiv:2007.01296 \[hep-ph\]](#).
- [77] A. David and G. Passarino, *Use and reuse of SMEFT*, (2020), [arXiv:2009.00127 \[hep-ph\]](#).
- [78] J. Ellis, M. Madigan, K. Mimasu, V. Sanz, and T. You, *Top, Higgs, Diboson and Electroweak Fit to the Standard Model Effective Field Theory*, *JHEP* **04**, 279 (2021), [arXiv:2012.02779 \[hep-ph\]](#).
- [79] M. Trott, *Methodology for theory uncertainties in the standard model effective field theory*, *Phys. Rev. D* **104**, 095023 (2021), [arXiv:2106.13794 \[hep-ph\]](#).
- [80] J. Ellis, N. E. Mavromatos, and T. You, *Light-by-Light Scattering Constraint on Born-Infeld Theory*, *Phys. Rev. Lett.* **118**, 261802 (2017), [arXiv:1703.08450 \[hep-ph\]](#).
- [81] J. Ellis and S.-F. Ge, *Constraining Gluonic Quartic Gauge Coupling Operators with $gg \rightarrow \gamma\gamma$* , *Phys. Rev. Lett.* **121**, 041801 (2018), [arXiv:1802.02416 \[hep-ph\]](#).
- [82] J. Ellis, H.-J. He, and R.-Q. Xiao, *Probing new physics in dimension-8 neutral gauge couplings at e^+e^- colliders*, *Sci. China Phys. Mech. Astron.* **64**, 221062 (2021), [arXiv:2008.04298 \[hep-ph\]](#).
- [83] N. Arkani-Hamed and K. Harigaya, *Naturalness and the muon magnetic moment*, *JHEP* **09**, 025 (2021), [arXiv:2106.01373 \[hep-ph\]](#).
- [84] C. Hays, A. Martin, V. Sanz, and J. Setford, *On the impact of dimension-eight SMEFT operators on Higgs measurements*, *JHEP* **02**, 123 (2019), [arXiv:1808.00442 \[hep-ph\]](#).
- [85] T. Corbett, A. Martin, and M. Trott, *Consistent higher order $\sigma(\mathcal{G}\mathcal{G} \rightarrow h)$, $\Gamma(h \rightarrow \mathcal{G}\mathcal{G})$ and $\Gamma(h \rightarrow \gamma\gamma)$ in geoSMEFT*, *JHEP* **12**, 147 (2021), [arXiv:2107.07470 \[hep-ph\]](#).
- [86] S. Alioli, R. Boughezal, E. Mereghetti, and F. Petriello, *Novel angular dependence in Drell-Yan lepton production via dimension-8 operators*, *Phys. Lett. B* **809**, 135703 (2020), [arXiv:2003.11615 \[hep-ph\]](#).
- [87] R. Boughezal, E. Mereghetti, and F. Petriello, *Dilepton production in the SMEFT at $O(1/\Lambda^4)$* , *Phys. Rev. D* **104**, 095022 (2021), [arXiv:2106.05337 \[hep-ph\]](#).
- [88] T. Corbett, A. Helset, A. Martin, and M. Trott, *EWPD in the SMEFT to dimension eight*, *JHEP* **06**, 076 (2021), [arXiv:2102.02819 \[hep-ph\]](#).

- [89] T. Corbett, *The one-loop tadpole in the geoSMEFT*, SciPost Phys. **11**, 097 (2021), [arXiv:2106.10284 \[hep-ph\]](#).
- [90] A. Martin and M. Trott, *The ggh variations*, (2021), [arXiv:2109.05595 \[hep-ph\]](#).
- [91] A. Azatov, R. Contino, C. S. Machado, and F. Riva, *Helicity selection rules and noninterference for BSM amplitudes*, Phys. Rev. D **95**, 065014 (2017), [arXiv:1607.05236 \[hep-ph\]](#).
- [92] A. Adams, N. Arkani-Hamed, S. Dubovsky, A. Nicolis, and R. Rattazzi, *Causality, analyticity and an IR obstruction to UV completion*, JHEP **10**, 014 (2006), [arXiv:hep-th/0602178](#).
- [93] B. Bellazzini, J. Elias Miró, R. Rattazzi, M. Riembau, and F. Riva, *Positive moments for scattering amplitudes*, Phys. Rev. D **104**, 036006 (2021), [arXiv:2011.00037 \[hep-th\]](#).
- [94] N. Arkani-Hamed, T.-C. Huang, and Y.-T. Huang, *The EFT-Hedron*, JHEP **05**, 259 (2021), [arXiv:2012.15849 \[hep-th\]](#).
- [95] G. N. Remmen and N. L. Rodd, *Flavor Constraints from Unitarity and Analyticity*, Phys. Rev. Lett. **125**, [Erratum: Phys.Rev.Lett. 127, 149901 (2021)], 081601 (2020), [arXiv:2004.02885 \[hep-ph\]](#).
- [96] C. Zhang, *SMEFTs living on the edge: determining the UV theories from positivity and extremality*, (2021), [arXiv:2112.11665 \[hep-ph\]](#).
- [97] L. D. Rose, B. von Harling, and A. Pomarol, *Wilson Coefficients and Natural Zeros from the On-Shell Viewpoint*, (2022), [arXiv:2201.10572 \[hep-ph\]](#).
- [98] S. Caron-Huot and M. Wilhelm, *Renormalization group coefficients and the S-matrix*, JHEP **12**, 010 (2016), [arXiv:1607.06448 \[hep-th\]](#).
- [99] J. Elias Miró, J. Ingoldby, and M. Riembau, *EFT anomalous dimensions from the S-matrix*, JHEP **09**, 163 (2020), [arXiv:2005.06983 \[hep-ph\]](#).
- [100] P. Baratella, C. Fernandez, and A. Pomarol, *Renormalization of Higher-Dimensional Operators from On-shell Amplitudes*, Nucl. Phys. B **959**, 115155 (2020), [arXiv:2005.07129 \[hep-ph\]](#).
- [101] M. Jiang, T. Ma, and J. Shu, *Renormalization Group Evolution from On-shell SMEFT*, JHEP **01**, 101 (2021), [arXiv:2005.10261 \[hep-ph\]](#).
- [102] Z. Bern, J. Parra-Martinez, and E. Sawyer, *Structure of two-loop SMEFT anomalous dimensions via on-shell methods*, JHEP **10**, 211 (2020), [arXiv:2005.12917 \[hep-ph\]](#).
- [103] P. Baratella, C. Fernandez, B. von Harling, and A. Pomarol, *Anomalous Dimensions of Effective Theories from Partial Waves*, JHEP **03**, 287 (2021), [arXiv:2010.13809 \[hep-ph\]](#).
- [104] M. Accettulli Huber and S. De Angelis, *Standard Model EFTs via on-shell methods*, JHEP **11**, 221 (2021), [arXiv:2108.03669 \[hep-th\]](#).
- [105] P. Baratella, D. Haslehner, M. Ruhdorfer, J. Serra, and A. Weiler, *RG of GR from On-shell Amplitudes*, (2021), [arXiv:2109.06191 \[hep-th\]](#).
- [106] J. Elias Miro, C. Fernandez, M. A. Gumus, and A. Pomarol, *Gearing up for the next generation of LFV experiments, via on-shell methods*, (2021), [arXiv:2112.12131 \[hep-ph\]](#).

- [107] P. Baratella, *Two-Loop Infrared Renormalization with On-shell Methods*, (2022), [arXiv:2207.08831 \[hep-th\]](#).
- [108] C. Cheung and C.-H. Shen, *Nonrenormalization Theorems without Supersymmetry*, *Phys. Rev. Lett.* **115**, 071601 (2015), [arXiv:1505.01844 \[hep-ph\]](#).
- [109] Z. Bern, J. Parra-Martinez, and E. Sawyer, *Nonrenormalization and Operator Mixing via On-Shell Methods*, *Phys. Rev. Lett.* **124**, 051601 (2020), [arXiv:1910.05831 \[hep-ph\]](#).
- [110] M. Jiang, J. Shu, M.-L. Xiao, and Y.-H. Zheng, *Partial Wave Amplitude Basis and Selection Rules in Effective Field Theories*, *Phys. Rev. Lett.* **126**, 011601 (2021), [arXiv:2001.04481 \[hep-ph\]](#).
- [111] T. Ma, J. Shu, and M.-L. Xiao, *Standard Model Effective Field Theory from On-shell Amplitudes*, (2019), [arXiv:1902.06752 \[hep-ph\]](#).
- [112] R. Aoude and C. S. Machado, *The Rise of SMEFT On-shell Amplitudes*, *JHEP* **12**, 058 (2019), [arXiv:1905.11433 \[hep-ph\]](#).
- [113] A. Falkowski, *Bases of massless EFTs via momentum twistors*, (2019), [arXiv:1912.07865 \[hep-ph\]](#).
- [114] G. Durieux and C. S. Machado, *Enumerating higher-dimensional operators with on-shell amplitudes*, *Phys. Rev. D* **101**, 095021 (2020), [arXiv:1912.08827 \[hep-ph\]](#).
- [115] A. Falkowski, G. Isabella, and C. S. Machado, *On-shell effective theory for higher-spin dark matter*, *SciPost Phys.* **10**, 101 (2021), [arXiv:2011.05339 \[hep-ph\]](#).
- [116] G. Durieux, T. Kitahara, C. S. Machado, Y. Shadmi, and Y. Weiss, *Constructing massive on-shell contact terms*, *JHEP* **12**, 175 (2020), [arXiv:2008.09652 \[hep-ph\]](#).
- [117] H.-L. Li, Z. Ren, J. Shu, M.-L. Xiao, J.-H. Yu, and Y.-H. Zheng, *Complete set of dimension-eight operators in the standard model effective field theory*, *Phys. Rev. D* **104**, 015026 (2021), [arXiv:2005.00008 \[hep-ph\]](#).
- [118] H.-L. Li, Z. Ren, M.-L. Xiao, J.-H. Yu, and Y.-H. Zheng, *Complete set of dimension-nine operators in the standard model effective field theory*, *Phys. Rev. D* **104**, 015025 (2021), [arXiv:2007.07899 \[hep-ph\]](#).
- [119] H.-L. Li, Z. Ren, M.-L. Xiao, J.-H. Yu, and Y.-H. Zheng, *Operators For Generic Effective Field Theory at any Dimension: On-shell Amplitude Basis Construction*, (2022), [arXiv:2201.04639 \[hep-ph\]](#).
- [120] R. Balkin, G. Durieux, T. Kitahara, Y. Shadmi, and Y. Weiss, *On-shell Higgsing for EFTs*, (2021), [arXiv:2112.09688 \[hep-ph\]](#).
- [121] Z.-Y. Dong, T. Ma, J. Shu, and Y.-H. Zheng, *Constructing Generic Effective Field Theory for All Masses and Spins*, (2022), [arXiv:2202.08350 \[hep-ph\]](#).
- [122] H.-L. Li, Y.-H. Ni, M.-L. Xiao, and J.-H. Yu, *The Bottom-Up EFT: Complete UV Resonances of the SMEFT Operators*, (2022), [arXiv:2204.03660 \[hep-ph\]](#).
- [123] B. P. Abbott et al. (LIGO Scientific, Virgo), *Observation of Gravitational Waves from a Binary Black Hole Merger*, *Phys. Rev. Lett.* **116**, 061102 (2016), [arXiv:1602.03837 \[gr-qc\]](#).
- [124] B. P. Abbott et al. (LIGO Scientific, Virgo), *GW170817: Observation of Gravitational Waves from a Binary Neutron Star Inspiral*, *Phys. Rev. Lett.* **119**, 161101 (2017), [arXiv:1710.05832 \[gr-qc\]](#).

- [125] Y. Iwasaki, *Fourth-order gravitational potential based on quantum field theory*, *Lett. Nuovo Cim.* **1S2**, 783–786 (1971).
- [126] Y. Iwasaki, *Quantum theory of gravitation vs. classical theory. - fourth-order potential*, *Prog. Theor. Phys.* **46**, 1587–1609 (1971).
- [127] J. F. Donoghue, *General relativity as an effective field theory: The leading quantum corrections*, *Phys. Rev. D* **50**, 3874–3888 (1994), [arXiv:gr-qc/9405057](#).
- [128] N. E. J. Bjerrum-Bohr, J. F. Donoghue, and B. R. Holstein, *Quantum gravitational corrections to the nonrelativistic scattering potential of two masses*, *Phys. Rev. D* **67**, [Erratum: *Phys.Rev.D* 71, 069903 (2005)], 084033 (2003), [arXiv:hep-th/0211072](#).
- [129] B. R. Holstein and J. F. Donoghue, *Classical physics and quantum loops*, *Phys. Rev. Lett.* **93**, 201602 (2004), [arXiv:hep-th/0405239](#).
- [130] N. E. J. Bjerrum-Bohr, J. F. Donoghue, and P. Vanhove, *On-shell Techniques and Universal Results in Quantum Gravity*, *JHEP* **02**, 111 (2014), [arXiv:1309.0804 \[hep-th\]](#).
- [131] D. Neill and I. Z. Rothstein, *Classical Space-Times from the S Matrix*, *Nucl. Phys. B* **877**, 177–189 (2013), [arXiv:1304.7263 \[hep-th\]](#).
- [132] N. E. J. Bjerrum-Bohr, J. F. Donoghue, B. R. Holstein, L. Planté, and P. Vanhove, *Bending of Light in Quantum Gravity*, *Phys. Rev. Lett.* **114**, 061301 (2015), [arXiv:1410.7590 \[hep-th\]](#).
- [133] I. Z. Rothstein, *Progress in effective field theory approach to the binary inspiral problem*, *Gen. Rel. Grav.* **46**, 1726 (2014).
- [134] N. E. J. Bjerrum-Bohr, J. F. Donoghue, B. R. Holstein, L. Plante, and P. Vanhove, *Light-like Scattering in Quantum Gravity*, *JHEP* **11**, 117 (2016), [arXiv:1609.07477 \[hep-th\]](#).
- [135] D. Bai and Y. Huang, *More on the Bending of Light in Quantum Gravity*, *Phys. Rev. D* **95**, 064045 (2017), [arXiv:1612.07629 \[hep-th\]](#).
- [136] F. Cachazo and A. Guevara, *Leading Singularities and Classical Gravitational Scattering*, *JHEP* **02**, 181 (2020), [arXiv:1705.10262 \[hep-th\]](#).
- [137] N. E. J. Bjerrum-Bohr, B. R. Holstein, J. F. Donoghue, L. Planté, and P. Vanhove, *Illuminating Light Bending*, *PoS CORFU2016*, 077 (2017), [arXiv:1704.01624 \[gr-qc\]](#).
- [138] C. Cheung, I. Z. Rothstein, and M. P. Solon, *From Scattering Amplitudes to Classical Potentials in the Post-Minkowskian Expansion*, *Phys. Rev. Lett.* **121**, 251101 (2018), [arXiv:1808.02489 \[hep-th\]](#).
- [139] N. E. J. Bjerrum-Bohr, P. H. Damgaard, G. Festuccia, L. Planté, and P. Vanhove, *General Relativity from Scattering Amplitudes*, *Phys. Rev. Lett.* **121**, 171601 (2018), [arXiv:1806.04920 \[hep-th\]](#).
- [140] D. A. Kosower, B. Maybee, and D. O’Connell, *Amplitudes, Observables, and Classical Scattering*, *JHEP* **02**, 137 (2019), [arXiv:1811.10950 \[hep-th\]](#).
- [141] H.-H. Chi, *Graviton Bending in Quantum Gravity from One-Loop Amplitudes*, *Phys. Rev. D* **99**, 126008 (2019), [arXiv:1903.07944 \[hep-th\]](#).
- [142] A. Koemans Collado, P. Di Vecchia, and R. Russo, *Revisiting the second post-Minkowskian eikonal and the dynamics of binary black holes*, *Phys. Rev. D* **100**, 066028 (2019), [arXiv:1904.02667 \[hep-th\]](#).

- [143] D. A. Kosower, R. Monteiro, and D. O’Connell, *The SAGEX Review on Scattering Amplitudes, Chapter 14: Classical Gravity from Scattering Amplitudes*, (2022), [arXiv:2203.13025 \[hep-th\]](#).
- [144] T. Damour, *High-energy gravitational scattering and the general relativistic two-body problem*, *Phys. Rev. D* **97**, 044038 (2018), [arXiv:1710.10599 \[gr-qc\]](#).
- [145] Z. Bern, C. Cheung, R. Roiban, C.-H. Shen, M. P. Solon, and M. Zeng, *Scattering Amplitudes and the Conservative Hamiltonian for Binary Systems at Third Post-Minkowskian Order*, *Phys. Rev. Lett.* **122**, 201603 (2019), [arXiv:1901.04424 \[hep-th\]](#).
- [146] C. Cheung and M. P. Solon, *Classical gravitational scattering at $\mathcal{O}(G^3)$ from Feynman diagrams*, *JHEP* **06**, 144 (2020), [arXiv:2003.08351 \[hep-th\]](#).
- [147] J. Parra-Martinez, M. S. Ruf, and M. Zeng, *Extremal black hole scattering at $\mathcal{O}(G^3)$: graviton dominance, eikonal exponentiation, and differential equations*, *JHEP* **11**, 023 (2020), [arXiv:2005.04236 \[hep-th\]](#).
- [148] P. Di Vecchia, C. Heissenberg, R. Russo, and G. Veneziano, *Universality of ultra-relativistic gravitational scattering*, *Phys. Lett. B* **811**, 135924 (2020), [arXiv:2008.12743 \[hep-th\]](#).
- [149] N. E. J. Bjerrum-Bohr, P. H. Damgaard, L. Planté, and P. Vanhove, *The amplitude for classical gravitational scattering at third Post-Minkowskian order*, *JHEP* **08**, 172 (2021), [arXiv:2105.05218 \[hep-th\]](#).
- [150] A. Brandhuber, G. Chen, G. Travaglini, and C. Wen, *Classical gravitational scattering from a gauge-invariant double copy*, *JHEP* **10**, 118 (2021), [arXiv:2108.04216 \[hep-th\]](#).
- [151] T. Damour, *Radiative contribution to classical gravitational scattering at the third order in G* , *Phys. Rev. D* **102**, 124008 (2020), [arXiv:2010.01641 \[gr-qc\]](#).
- [152] E. Herrmann, J. Parra-Martinez, M. S. Ruf, and M. Zeng, *Gravitational Bremsstrahlung from Reverse Unitarity*, *Phys. Rev. Lett.* **126**, 201602 (2021), [arXiv:2101.07255 \[hep-th\]](#).
- [153] E. Herrmann, J. Parra-Martinez, M. S. Ruf, and M. Zeng, *Radiative classical gravitational observables at $\mathcal{O}(G^3)$ from scattering amplitudes*, *JHEP* **10**, 148 (2021), [arXiv:2104.03957 \[hep-th\]](#).
- [154] P. Di Vecchia, C. Heissenberg, R. Russo, and G. Veneziano, *The eikonal approach to gravitational scattering and radiation at $\mathcal{O}(G^3)$* , *JHEP* **07**, 169 (2021), [arXiv:2104.03256 \[hep-th\]](#).
- [155] P. Di Vecchia, C. Heissenberg, R. Russo, and G. Veneziano, *Radiation Reaction from Soft Theorems*, *Phys. Lett. B* **818**, 136379 (2021), [arXiv:2101.05772 \[hep-th\]](#).
- [156] Z. Bern, J. Parra-Martinez, R. Roiban, M. S. Ruf, C.-H. Shen, M. P. Solon, and M. Zeng, *Scattering Amplitudes and Conservative Binary Dynamics at $\mathcal{O}(G^4)$* , *Phys. Rev. Lett.* **126**, 171601 (2021), [arXiv:2101.07254 \[hep-th\]](#).
- [157] Z. Bern, D. Kosmopoulos, and A. Zhiboedov, *Gravitational effective field theory islands, low-spin dominance, and the four-graviton amplitude*, *J. Phys. A* **54**, 344002 (2021), [arXiv:2103.12728 \[hep-th\]](#).
- [158] A. Guevara, *Holomorphic Classical Limit for Spin Effects in Gravitational and Electromagnetic Scattering*, *JHEP* **04**, 033 (2019), [arXiv:1706.02314 \[hep-th\]](#).

- [159] M.-Z. Chung, Y.-T. Huang, J.-W. Kim, and S. Lee, *The simplest massive S-matrix: from minimal coupling to Black Holes*, *JHEP* **04**, 156 (2019), [arXiv:1812.08752 \[hep-th\]](#).
- [160] B. Maybee, D. O’Connell, and J. Vines, *Observables and amplitudes for spinning particles and black holes*, *JHEP* **12**, 156 (2019), [arXiv:1906.09260 \[hep-th\]](#).
- [161] M.-Z. Chung, Y.-T. Huang, and J.-W. Kim, *Classical potential for general spinning bodies*, *JHEP* **09**, 074 (2020), [arXiv:1908.08463 \[hep-th\]](#).
- [162] Z. Bern, A. Luna, R. Roiban, C.-H. Shen, and M. Zeng, *Spinning black hole binary dynamics, scattering amplitudes, and effective field theory*, *Phys. Rev. D* **104**, 065014 (2021), [arXiv:2005.03071 \[hep-th\]](#).
- [163] D. Kosmopoulos and A. Luna, *Quadratic-in-spin Hamiltonian at $\mathcal{O}(G^2)$ from scattering amplitudes*, *JHEP* **07**, 037 (2021), [arXiv:2102.10137 \[hep-th\]](#).
- [164] M. Chiodaroli, H. Johansson, and P. Pichini, *Compton Black-Hole Scattering for $s \leq 5/2$* , (2021), [arXiv:2107.14779 \[hep-th\]](#).
- [165] R. Aoude and A. Ochirov, *Classical observables from coherent-spin amplitudes*, *JHEP* **10**, 008 (2021), [arXiv:2108.01649 \[hep-th\]](#).
- [166] K. Haddad, *Exponentiation of the leading eikonal phase with spin*, *Phys. Rev. D* **105**, 026004 (2022), [arXiv:2109.04427 \[hep-th\]](#).
- [167] Z. Bern, D. Kosmopoulos, A. Luna, R. Roiban, and F. Teng, *Binary Dynamics Through the Fifth Power of Spin at $\mathcal{O}(G^2)$* , (2022), [arXiv:2203.06202 \[hep-th\]](#).
- [168] C. Cheung and M. P. Solon, *Tidal Effects in the Post-Minkowskian Expansion*, *Phys. Rev. Lett.* **125**, 191601 (2020), [arXiv:2006.06665 \[hep-th\]](#).
- [169] K. Haddad and A. Helset, *Tidal effects in quantum field theory*, *JHEP* **12**, 024 (2020), [arXiv:2008.04920 \[hep-th\]](#).
- [170] Z. Bern, J. Parra-Martinez, R. Roiban, E. Sawyer, and C.-H. Shen, *Leading Non-linear Tidal Effects and Scattering Amplitudes*, *JHEP* **05**, 188 (2021), [arXiv:2010.08559 \[hep-th\]](#).
- [171] J.-W. Kim and M. Shim, *Quantum corrections to tidal Love number for Schwarzschild black holes*, *Phys. Rev. D* **104**, 046022 (2021), [arXiv:2011.03337 \[hep-th\]](#).
- [172] R. Aoude, K. Haddad, and A. Helset, *Tidal effects for spinning particles*, *JHEP* **03**, 097 (2021), [arXiv:2012.05256 \[hep-th\]](#).
- [173] A. Brandhuber and G. Travaglini, *On higher-derivative effects on the gravitational potential and particle bending*, *JHEP* **01**, 010 (2020), [arXiv:1905.05657 \[hep-th\]](#).
- [174] M. Accattulli Huber, A. Brandhuber, S. De Angelis, and G. Travaglini, *Eikonal phase matrix, deflection angle and time delay in effective field theories of gravity*, *Phys. Rev. D* **102**, 046014 (2020), [arXiv:2006.02375 \[hep-th\]](#).
- [175] W. D. Goldberger and I. Z. Rothstein, *An Effective field theory of gravity for extended objects*, *Phys. Rev. D* **73**, 104029 (2006), [arXiv:hep-th/0409156](#).
- [176] G. Kälin and R. A. Porto, *Post-Minkowskian Effective Field Theory for Conservative Binary Dynamics*, *JHEP* **11**, 106 (2020), [arXiv:2006.01184 \[hep-th\]](#).
- [177] G. Kälin, Z. Liu, and R. A. Porto, *Conservative Dynamics of Binary Systems to Third Post-Minkowskian Order from the Effective Field Theory Approach*, *Phys. Rev. Lett.* **125**, 261103 (2020), [arXiv:2007.04977 \[hep-th\]](#).

- [178] G. Mogull, J. Plefka, and J. Steinhoff, *Classical black hole scattering from a worldline quantum field theory*, *JHEP* **02**, 048 (2021), [arXiv:2010.02865 \[hep-th\]](#).
- [179] G. U. Jakobsen, G. Mogull, J. Plefka, and J. Steinhoff, *Classical Gravitational Bremsstrahlung from a Worldline Quantum Field Theory*, *Phys. Rev. Lett.* **126**, 201103 (2021), [arXiv:2101.12688 \[gr-qc\]](#).
- [180] S. Mougiakakos, M. M. Riva, and F. Vernizzi, *Gravitational Bremsstrahlung in the post-Minkowskian effective field theory*, *Phys. Rev. D* **104**, 024041 (2021), [arXiv:2102.08339 \[gr-qc\]](#).
- [181] C. Dlapa, G. Kälin, Z. Liu, and R. A. Porto, *Dynamics of binary systems to fourth Post-Minkowskian order from the effective field theory approach*, *Phys. Lett. B* **831**, 137203 (2022), [arXiv:2106.08276 \[hep-th\]](#).
- [182] G. U. Jakobsen, G. Mogull, J. Plefka, and J. Steinhoff, *Gravitational Bremsstrahlung and Hidden Supersymmetry of Spinning Bodies*, *Phys. Rev. Lett.* **128**, 011101 (2022), [arXiv:2106.10256 \[hep-th\]](#).
- [183] G. U. Jakobsen, G. Mogull, J. Plefka, and J. Steinhoff, *SUSY in the sky with gravitons*, *JHEP* **01**, 027 (2022), [arXiv:2109.04465 \[hep-th\]](#).
- [184] M. M. Riva and F. Vernizzi, *Radiated momentum in the post-Minkowskian worldline approach via reverse unitarity*, *JHEP* **11**, 228 (2021), [arXiv:2110.10140 \[hep-th\]](#).
- [185] G. U. Jakobsen and G. Mogull, *Conservative and Radiative Dynamics of Spinning Bodies at Third Post-Minkowskian Order Using Worldline Quantum Field Theory*, *Phys. Rev. Lett.* **128**, 141102 (2022), [arXiv:2201.07778 \[hep-th\]](#).
- [186] S. Mougiakakos, M. M. Riva, and F. Vernizzi, *Gravitational Bremsstrahlung with tidal effects in the post-Minkowskian expansion*, (2022), [arXiv:2204.06556 \[hep-th\]](#).
- [187] M. M. Riva, F. Vernizzi, and L. K. Wong, *Gravitational Bremsstrahlung from Spinning Binaries in the Post-Minkowskian Expansion*, (2022), [arXiv:2205.15295 \[hep-th\]](#).
- [188] G. U. Jakobsen, G. Mogull, J. Plefka, and B. Sauer, *All Things Retarded: Radiation-Reaction in Worldline Quantum Field Theory*, (2022), [arXiv:2207.00569 \[hep-th\]](#).
- [189] N. Arkani-Hamed and J. Trnka, *The Amplituhedron*, *JHEP* **10**, 030 (2014), [arXiv:1312.2007 \[hep-th\]](#).
- [190] L. Ferro and T. Lukowski, *Amplituhedra, and beyond*, *J. Phys. A* **54**, 033001 (2021), [arXiv:2007.04342 \[hep-th\]](#).
- [191] E. Herrmann and J. Trnka, *The SAGEX Review on Scattering Amplitudes, Chapter 7: Positive Geometry of Scattering Amplitudes*, (2022), [arXiv:2203.13018 \[hep-th\]](#).
- [192] Z. Bern, J. J. M. Carrasco, and H. Johansson, *New Relations for Gauge-Theory Amplitudes*, *Phys. Rev. D* **78**, 085011 (2008), [arXiv:0805.3993 \[hep-ph\]](#).
- [193] Z. Bern, J. J. M. Carrasco, and H. Johansson, *Perturbative Quantum Gravity as a Double Copy of Gauge Theory*, *Phys. Rev. Lett.* **105**, 061602 (2010), [arXiv:1004.0476 \[hep-th\]](#).
- [194] Z. Bern, J. J. Carrasco, M. Chiodaroli, H. Johansson, and R. Roiban, *The SAGEX Review on Scattering Amplitudes, Chapter 2: An Invitation to Color-Kinematics Duality and the Double Copy*, (2022), [arXiv:2203.13013 \[hep-th\]](#).

- [195] S. Weinzierl, *Feynman Integrals*, (2022), [arXiv:2201.03593 \[hep-th\]](#).
- [196] S. Abreu, R. Britto, and C. Duhr, *The SAGEX Review on Scattering Amplitudes, Chapter 3: Mathematical structures in Feynman integrals*, (2022), [arXiv:2203.13014 \[hep-th\]](#).
- [197] J. Blümlein and C. Schneider, *The SAGEX Review on Scattering Amplitudes, Chapter 4: Multi-loop Feynman Integrals*, (2022), [arXiv:2203.13015 \[hep-th\]](#).
- [198] N. Arkani-Hamed, D. Baumann, H. Lee, and G. L. Pimentel, *The Cosmological Bootstrap: Inflationary Correlators from Symmetries and Singularities*, *JHEP* **04**, 105 (2020), [arXiv:1811.00024 \[hep-th\]](#).
- [199] P. Benincasa, *Amplitudes meet Cosmology: A (Scalar) Primer*, (2022), [arXiv:2203.15330 \[hep-th\]](#).
- [200] Z. Bern, L. J. Dixon, and V. A. Smirnov, *Iteration of planar amplitudes in maximally supersymmetric Yang-Mills theory at three loops and beyond*, *Phys. Rev. D* **72**, 085001 (2005), [arXiv:hep-th/0505205](#).
- [201] L. J. Dixon, J. M. Drummond, M. von Hippel, and J. Pennington, *Hexagon functions and the three-loop remainder function*, *JHEP* **12**, 049 (2013), [arXiv:1308.2276 \[hep-th\]](#).
- [202] L. J. Dixon and M. von Hippel, *Bootstrapping an NMHV amplitude through three loops*, *JHEP* **10**, 065 (2014), [arXiv:1408.1505 \[hep-th\]](#).
- [203] L. J. Dixon, M. von Hippel, and A. J. McLeod, *The four-loop six-gluon NMHV ratio function*, *JHEP* **01**, 053 (2016), [arXiv:1509.08127 \[hep-th\]](#).
- [204] S. Caron-Huot, L. J. Dixon, A. McLeod, and M. von Hippel, *Bootstrapping a Five-Loop Amplitude Using Steinmann Relations*, *Phys. Rev. Lett.* **117**, 241601 (2016), [arXiv:1609.00669 \[hep-th\]](#).
- [205] S. Caron-Huot, L. J. Dixon, F. Dulat, M. von Hippel, A. J. McLeod, and G. Papathanasiou, *Six-Gluon amplitudes in planar $\mathcal{N} = 4$ super-Yang-Mills theory at six and seven loops*, *JHEP* **08**, 016 (2019), [arXiv:1903.10890 \[hep-th\]](#).
- [206] G. Papathanasiou, *The SAGEX Review on Scattering Amplitudes, Chapter 5: Analytic Bootstraps for Scattering Amplitudes and Beyond*, (2022), [arXiv:2203.13016 \[hep-th\]](#).
- [207] M. Accettulli Huber, A. Brandhuber, S. De Angelis, and G. Travaglini, *Complete Form Factors in Yang-Mills from Unitarity and Spinor Helicity in Six Dimensions*, *Phys. Rev. D* **101**, 026004 (2020), [arXiv:1910.04772 \[hep-th\]](#).
- [208] L. Lehman and A. Martin, *Hilbert Series for Constructing Lagrangians: expanding the phenomenologist's toolbox*, *Phys. Rev. D* **91**, 105014 (2015), [arXiv:1503.07537 \[hep-ph\]](#).
- [209] B. Henning, X. Lu, T. Melia, and H. Murayama, *Hilbert series and operator bases with derivatives in effective field theories*, *Commun. Math. Phys.* **347**, 363–388 (2016), [arXiv:1507.07240 \[hep-th\]](#).
- [210] B. Henning, X. Lu, T. Melia, and H. Murayama, *2, 84, 30, 993, 560, 15456, 11962, 261485, ...: Higher dimension operators in the SM EFT*, *JHEP* **08**, [Erratum: *JHEP* **09**, 019 (2019)], 016 (2017), [arXiv:1512.03433 \[hep-ph\]](#).
- [211] B. Grzadkowski, M. Iskrzynski, M. Misiak, and J. Rosiek, *Dimension-Six Terms in the Standard Model Lagrangian*, *JHEP* **10**, 085 (2010), [arXiv:1008.4884 \[hep-ph\]](#).

- [212] B. Henning, X. Lu, T. Melia, and H. Murayama, *Operator bases, S-matrices, and their partition functions*, *JHEP* **10**, 199 (2017), [arXiv:1706.08520 \[hep-th\]](#).
- [213] C. Cheung, K. Kampf, J. Novotny, C.-H. Shen, and J. Trnka, *A Periodic Table of Effective Field Theories*, *JHEP* **02**, 020 (2017), [arXiv:1611.03137 \[hep-th\]](#).
- [214] P. De Causmaecker, R. Gastmans, W. Troost, and T. T. Wu, *Multiple Bremsstrahlung in Gauge Theories at High-Energies. 1. General Formalism for Quantum Electrodynamics*, *Nucl. Phys. B* **206**, 53–60 (1982).
- [215] F. A. Berends, R. Kleiss, P. De Causmaecker, R. Gastmans, W. Troost, and T. T. Wu, *Multiple Bremsstrahlung in Gauge Theories at High-Energies. 2. Single Bremsstrahlung*, *Nucl. Phys. B* **206**, 61–89 (1982).
- [216] R. Kleiss and W. J. Stirling, *Spinor Techniques for Calculating p anti- $p \rightarrow W^{+-} / Z0 + Jets$* , *Nucl. Phys. B* **262**, 235–262 (1985).
- [217] Z. Xu, D.-H. Zhang, and L. Chang, *Helicity Amplitudes for Multiple Bremsstrahlung in Massless Nonabelian Gauge Theories*, *Nucl. Phys. B* **291**, 392–428 (1987).
- [218] Z.-Y. Dong, T. Ma, and J. Shu, *Constructing on-shell operator basis for all masses and spins*, (2021), [arXiv:2103.15837 \[hep-ph\]](#).
- [219] R. M. Fonseca, *Enumerating the operators of an effective field theory*, *Phys. Rev. D* **101**, 035040 (2020), [arXiv:1907.12584 \[hep-ph\]](#).
- [220] S. D. Chowdhury and A. Gadde, *Classification of four-point local gluon S-matrices*, *JHEP* **01**, 104 (2021), [arXiv:2006.12458 \[hep-th\]](#).
- [221] L. Lehman, *Extending the Standard Model Effective Field Theory with the Complete Set of Dimension-7 Operators*, *Phys. Rev. D* **90**, 125023 (2014), [arXiv:1410.4193 \[hep-ph\]](#).
- [222] C. W. Murphy, *Dimension-8 operators in the Standard Model Effective Field Theory*, *JHEP* **10**, 174 (2020), [arXiv:2005.00059 \[hep-ph\]](#).
- [223] Y. Liao and X.-D. Ma, *An explicit construction of the dimension-9 operator basis in the standard model effective field theory*, *JHEP* **11**, 152 (2020), [arXiv:2007.08125 \[hep-ph\]](#).
- [224] P. Dittner, *Invariant tensors in $su(3)$* , *Commun. Math. Phys.* **22**, 238–252 (1971).
- [225] P. Dittner, *Invariant tensors in $su(3)$. 2.*, *Commun. Math. Phys.* **27**, 44–52 (1972).
- [226] J. A. de Azcarraga, A. J. Macfarlane, A. J. Mountain, and J. C. Perez Bueno, *Invariant tensors for simple groups*, *Nucl. Phys. B* **510**, 657–687 (1998), [arXiv:physics/9706006](#).
- [227] D. Littlewood and A. Richardson, *Group characters and algebra*, *Philos. Trans. Roy. Soc. London Ser. A* **233**, 99–141 (1934).
- [228] G. de B. Robinson, *On the representations of the symmetric group*, *American Journal of Mathematics* **60**, 745–760 (1938).
- [229] C.-N. Yang and R. L. Mills, *Conservation of Isotopic Spin and Isotopic Gauge Invariance*, *Phys. Rev.* **96**, edited by J.-P. Hsu and D. Fine, 191–195 (1954).
- [230] M. E. Peskin and D. V. Schroeder, *An Introduction to quantum field theory* (Addison-Wesley, Reading, USA, 1995).
- [231] D. Liu and Z. Yin, *Gauge invariance from on-shell massive amplitudes and tree unitarity*, (2022), [arXiv:2204.13119 \[hep-th\]](#).

- [232] A. Brandhuber, G. Chen, G. Travaglini, and C. Wen, *A new gauge-invariant double copy for heavy-mass effective theory*, *JHEP* **07**, 047 (2021), [arXiv:2104.11206 \[hep-th\]](#).
- [233] R. K. Ellis, W. T. Giele, Z. Kunszt, and K. Melnikov, *Masses, fermions and generalized D -dimensional unitarity*, *Nucl. Phys. B* **822**, 270–282 (2009), [arXiv:0806.3467 \[hep-ph\]](#).
- [234] S. D. Badger, *Direct Extraction Of One Loop Rational Terms*, *JHEP* **01**, 049 (2009), [arXiv:0806.4600 \[hep-ph\]](#).
- [235] N. Arkani-Hamed, Y. Bai, S. He, and G. Yan, *Scattering Forms and the Positive Geometry of Kinematics, Color and the Worldsheet*, *JHEP* **05**, 096 (2018), [arXiv:1711.09102 \[hep-th\]](#).
- [236] A. von Manteuffel and R. M. Schabinger, *A novel approach to integration by parts reduction*, *Phys. Lett. B* **744**, 101–104 (2015), [arXiv:1406.4513 \[hep-ph\]](#).
- [237] T. Peraro, *Scattering amplitudes over finite fields and multivariate functional reconstruction*, *JHEP* **12**, 030 (2016), [arXiv:1608.01902 \[hep-ph\]](#).
- [238] A. Hodges, *Eliminating spurious poles from gauge-theoretic amplitudes*, *JHEP* **05**, 135 (2013), [arXiv:0905.1473 \[hep-th\]](#).
- [239] S. Badger, *Automating QCD amplitudes with on-shell methods*, *J. Phys. Conf. Ser.* **762**, edited by L. Salinas and C. Torres, 012057 (2016), [arXiv:1605.02172 \[hep-ph\]](#).
- [240] F. A. Berends and W. T. Giele, *Recursive Calculations for Processes with n Gluons*, *Nucl. Phys. B* **306**, 759–808 (1988).
- [241] S. Chang and M. A. Luty, *The Higgs Trilinear Coupling and the Scale of New Physics*, *JHEP* **03**, 140 (2020), [arXiv:1902.05556 \[hep-ph\]](#).
- [242] A. Falkowski and R. Rattazzi, *Which EFT*, *JHEP* **10**, 255 (2019), [arXiv:1902.05936 \[hep-ph\]](#).
- [243] H. Georgi, *An Effective Field Theory for Heavy Quarks at Low-energies*, *Phys. Lett. B* **240**, 447–450 (1990).
- [244] M. E. Luke and A. V. Manohar, *Reparametrization invariance constraints on heavy particle effective field theories*, *Phys. Lett. B* **286**, 348–354 (1992), [arXiv:hep-ph/9205228](#).
- [245] M. Neubert, *Heavy quark symmetry*, *Phys. Rept.* **245**, 259–396 (1994), [arXiv:hep-ph/9306320](#).
- [246] A. Brandhuber, G. Chen, H. Johansson, G. Travaglini, and C. Wen, *Kinematic Hopf Algebra for Bern-Carrasco-Johansson Numerators in Heavy-Mass Effective Field Theory and Yang-Mills Theory*, *Phys. Rev. Lett.* **128**, 121601 (2022), [arXiv:2111.15649 \[hep-th\]](#).
- [247] S. Weinberg, *Infrared photons and gravitons*, *Phys. Rev.* **140**, B516–B524 (1965).
- [248] S. L. Adler, *Axial vector vertex in spinor electrodynamics*, *Phys. Rev.* **177**, 2426–2438 (1969).
- [249] J. S. Bell and R. Jackiw, *A PCAC puzzle: $\pi^0 \rightarrow \gamma\gamma$ in the σ model*, *Nuovo Cim. A* **60**, 47–61 (1969).
- [250] D. C. Dunbar and W. B. Perkins, *Two-loop five-point all plus helicity Yang-Mills amplitude*, *Phys. Rev. D* **93**, 085029 (2016), [arXiv:1603.07514 \[hep-th\]](#).

- [251] D. C. Dunbar, G. R. Jehu, and W. B. Perkins, *Two-loop six gluon all plus helicity amplitude*, *Phys. Rev. Lett.* **117**, 061602 (2016), [arXiv:1605.06351 \[hep-th\]](#).
- [252] W. L. van Neerven, *Dimensional Regularization of Mass and Infrared Singularities in Two Loop On-shell Vertex Functions*, *Nucl. Phys. B* **268**, 453–488 (1986).
- [253] R. Boughezal, K. Melnikov, and F. Petriello, *The four-dimensional helicity scheme and dimensional reconstruction*, *Phys. Rev. D* **84**, 034044 (2011), [arXiv:1106.5520 \[hep-ph\]](#).
- [254] S. Davies, *One-Loop QCD and Higgs to Partons Processes Using Six-Dimensional Helicity and Generalized Unitarity*, *Phys. Rev. D* **84**, 094016 (2011), [arXiv:1108.0398 \[hep-ph\]](#).
- [255] S. Badger, H. Frellesvig, and Y. Zhang, *A Two-Loop Five-Gluon Helicity Amplitude in QCD*, *JHEP* **12**, 045 (2013), [arXiv:1310.1051 \[hep-ph\]](#).
- [256] F. R. Anger and V. Sotnikov, *On the Dimensional Regularization of QCD Helicity Amplitudes With Quarks*, (2018), [arXiv:1803.11127 \[hep-ph\]](#).
- [257] S. Abreu, F. Febres Cordero, H. Ita, B. Page, and V. Sotnikov, *Planar Two-Loop Five-Parton Amplitudes from Numerical Unitarity*, *JHEP* **11**, 116 (2018), [arXiv:1809.09067 \[hep-ph\]](#).
- [258] S. Badger, C. Brønnum-Hansen, H. B. Hartanto, and T. Peraro, *Analytic helicity amplitudes for two-loop five-gluon scattering: the single-minus case*, *JHEP* **01**, 186 (2019), [arXiv:1811.11699 \[hep-ph\]](#).
- [259] S. Abreu, J. Dormans, F. Febres Cordero, H. Ita, and B. Page, *Analytic Form of Planar Two-Loop Five-Gluon Scattering Amplitudes in QCD*, *Phys. Rev. Lett.* **122**, 082002 (2019), [arXiv:1812.04586 \[hep-ph\]](#).
- [260] D. A. Kosower and S. Pögel, *A Unitarity Approach to Two-Loop All-Plus Rational Terms*, (2022), [arXiv:2206.14445 \[hep-ph\]](#).
- [261] F. Wilczek, *Decays of Heavy Vector Mesons Into Higgs Particles*, *Phys. Rev. Lett.* **39**, 1304 (1977).
- [262] M. A. Shifman, A. I. Vainshtein, M. B. Voloshin, and V. I. Zakharov, *Low-Energy Theorems for Higgs Boson Couplings to Photons*, *Sov. J. Nucl. Phys.* **30**, 711–716 (1979).
- [263] W. Buchmuller and D. Wyler, *Effective Lagrangian Analysis of New Interactions and Flavor Conservation*, *Nucl. Phys. B* **268**, 621–653 (1986).
- [264] S. Dawson, *Radiative corrections to Higgs boson production*, *Nucl. Phys. B* **359**, 283–300 (1991).
- [265] D. Neill, *Two-Loop Matching onto Dimension Eight Operators in the Higgs-Gluon Sector*, (2009), [arXiv:0908.1573 \[hep-ph\]](#).
- [266] D. Neill, *Analytic Virtual Corrections for Higgs Transverse Momentum Spectrum at $O(\alpha(s)^2/m(t)^3)$ via Unitarity Methods*, (2009), [arXiv:0911.2707 \[hep-ph\]](#).
- [267] R. V. Harlander and T. Neumann, *Probing the nature of the Higgs-gluon coupling*, *Phys. Rev. D* **88**, 074015 (2013), [arXiv:1308.2225 \[hep-ph\]](#).
- [268] S. Dawson, I. M. Lewis, and M. Zeng, *Effective field theory for Higgs boson plus jet production*, *Phys. Rev. D* **90**, 093007 (2014), [arXiv:1409.6299 \[hep-ph\]](#).

- [269] L. J. Dixon, E. W. N. Glover, and V. V. Khoze, *MHV rules for Higgs plus multi-gluon amplitudes*, *JHEP* **12**, 015 (2004), [arXiv:hep-th/0411092](#).
- [270] S. D. Badger, E. W. N. Glover, and V. V. Khoze, *MHV rules for Higgs plus multi-parton amplitudes*, *JHEP* **03**, 023 (2005), [arXiv:hep-th/0412275](#).
- [271] S. D. Badger, E. W. N. Glover, and K. Risager, *One-loop phi-MHV amplitudes using the unitarity bootstrap*, *JHEP* **07**, 066 (2007), [arXiv:0704.3914 \[hep-ph\]](#).
- [272] S. Badger, E. W. Nigel Glover, P. Mastrolia, and C. Williams, *One-loop Higgs plus four gluon amplitudes: Full analytic results*, *JHEP* **01**, 036 (2010), [arXiv:0909.4475 \[hep-ph\]](#).
- [273] A. Brandhuber, M. Kostacinska, B. Penante, and G. Travaglini, *Higgs amplitudes from $\mathcal{N} = 4$ super Yang-Mills theory*, *Phys. Rev. Lett.* **119**, 161601 (2017), [arXiv:1707.09897 \[hep-th\]](#).
- [274] Q. Jin and G. Yang, *Analytic Two-Loop Higgs Amplitudes in Effective Field Theory and the Maximal Transcendentality Principle*, *Phys. Rev. Lett.* **121**, 101603 (2018), [arXiv:1804.04653 \[hep-th\]](#).
- [275] A. Brandhuber, M. Kostacinska, B. Penante, and G. Travaglini, *$Tr(F^3)$ supersymmetric form factors and maximal transcendentality Part I: $\mathcal{N} = 4$ super Yang-Mills*, *JHEP* **12**, 076 (2018), [arXiv:1804.05703 \[hep-th\]](#).
- [276] A. Brandhuber, M. Kostacinska, B. Penante, and G. Travaglini, *$Tr(F^3)$ supersymmetric form factors and maximal transcendentality Part II: $0 < \mathcal{N} < 4$ super Yang-Mills*, *JHEP* **12**, 077 (2018), [arXiv:1804.05828 \[hep-th\]](#).
- [277] Q. Jin and G. Yang, *Hidden Analytic Relations for Two-Loop Higgs Amplitudes in QCD*, *Commun. Theor. Phys.* **72**, 065201 (2020), [arXiv:1904.07260 \[hep-th\]](#).
- [278] L. V. Bork, D. I. Kazakov, and G. S. Vartanov, *On form factors in $N=4$ sym*, *JHEP* **02**, 063 (2011), [arXiv:1011.2440 \[hep-th\]](#).
- [279] A. Brandhuber, O. Gurdogan, R. Mooney, G. Travaglini, and G. Yang, *Harmony of Super Form Factors*, *JHEP* **10**, 046 (2011), [arXiv:1107.5067 \[hep-th\]](#).
- [280] L. V. Bork, D. I. Kazakov, and G. S. Vartanov, *On MHV Form Factors in Superspace for $\mathcal{N} = 4$ SYM Theory*, *JHEP* **10**, 133 (2011), [arXiv:1107.5551 \[hep-th\]](#).
- [281] T. Gehrmann, J. M. Henn, and T. Huber, *The three-loop form factor in $N=4$ super Yang-Mills*, *JHEP* **03**, 101 (2012), [arXiv:1112.4524 \[hep-th\]](#).
- [282] L. V. Bork, *On NMHV form factors in $N=4$ SYM theory from generalized unitarity*, *JHEP* **01**, 049 (2013), [arXiv:1203.2596 \[hep-th\]](#).
- [283] R. H. Boels, B. A. Kniehl, O. V. Tarasov, and G. Yang, *Color-kinematic Duality for Form Factors*, *JHEP* **02**, 063 (2013), [arXiv:1211.7028 \[hep-th\]](#).
- [284] A. Brandhuber, G. Travaglini, and G. Yang, *Analytic two-loop form factors in $N=4$ SYM*, *JHEP* **05**, 082 (2012), [arXiv:1201.4170 \[hep-th\]](#).
- [285] B. Penante, B. Spence, G. Travaglini, and C. Wen, *On super form factors of half-BPS operators in $N=4$ super Yang-Mills*, *JHEP* **04**, 083 (2014), [arXiv:1402.1300 \[hep-th\]](#).
- [286] A. Brandhuber, B. Penante, G. Travaglini, and C. Wen, *The last of the simple remainders*, *JHEP* **08**, 100 (2014), [arXiv:1406.1443 \[hep-th\]](#).

- [287] D. Nandan, C. Sieg, M. Wilhelm, and G. Yang, *Cutting through form factors and cross sections of non-protected operators in $\mathcal{N} = 4$ SYM*, *JHEP* **06**, 156 (2015), [arXiv:1410.8485 \[hep-th\]](#).
- [288] F. Loebbert, D. Nandan, C. Sieg, M. Wilhelm, and G. Yang, *On-Shell Methods for the Two-Loop Dilatation Operator and Finite Remainders*, *JHEP* **10**, 012 (2015), [arXiv:1504.06323 \[hep-th\]](#).
- [289] A. Brandhuber, M. Kostacinska, B. Penante, G. Travaglini, and D. Young, *The $SU(2/3)$ dynamic two-loop form factors*, *JHEP* **08**, 134 (2016), [arXiv:1606.08682 \[hep-th\]](#).
- [290] F. Loebbert, C. Sieg, M. Wilhelm, and G. Yang, *Two-Loop $SL(2)$ Form Factors and Maximal Transcendentality*, *JHEP* **12**, 090 (2016), [arXiv:1610.06567 \[hep-th\]](#).
- [291] W. Siegel, *Supersymmetric Dimensional Regularization via Dimensional Reduction*, *Phys. Lett. B* **84**, 193–196 (1979).
- [292] Z. Bern, A. De Freitas, L. J. Dixon, and H. L. Wong, *Supersymmetric regularization, two loop QCD amplitudes and coupling shifts*, *Phys. Rev. D* **66**, 085002 (2002), [arXiv:hep-ph/0202271](#).
- [293] Z. Bern and D. A. Kosower, *The Computation of loop amplitudes in gauge theories*, *Nucl. Phys. B* **379**, 451–561 (1992).
- [294] G. 't Hooft and M. J. G. Veltman, *Regularization and Renormalization of Gauge Fields*, *Nucl. Phys. B* **44**, 189–213 (1972).
- [295] T. Dennen, Y.-t. Huang, and W. Siegel, *Supertwistor space for 6D maximal super Yang-Mills*, *JHEP* **04**, 127 (2010), [arXiv:0910.2688 \[hep-th\]](#).
- [296] S. Dawson, I. M. Lewis, and M. Zeng, *Usefulness of effective field theory for boosted Higgs production*, *Phys. Rev. D* **91**, 074012 (2015), [arXiv:1501.04103 \[hep-ph\]](#).
- [297] L. J. Dixon and Y. Shadmi, *Testing gluon selfinteractions in three jet events at hadron colliders*, *Nucl. Phys. B* **423**, [Erratum: *Nucl.Phys.B* 452, 724–724 (1995)], 3–32 (1994), [arXiv:hep-ph/9312363](#).
- [298] J. Broedel and L. J. Dixon, *Color-kinematics duality and double-copy construction for amplitudes from higher-dimension operators*, *JHEP* **10**, 091 (2012), [arXiv:1208.0876 \[hep-th\]](#).
- [299] A. Y. Morozov, *MATRIX OF MIXING OF SCALAR AND VECTOR MESONS OF DIMENSION $D \leq 8$ IN QCD. (IN RUSSIAN)*, *Sov. J. Nucl. Phys.* **40**, 505 (1984).
- [300] J. A. Gracey, *Classification and one loop renormalization of dimension-six and dimension-eight operators in quantum gluodynamics*, *Nucl. Phys. B* **634**, [Erratum: *Nucl.Phys.B* 696, 295–297 (2004)], 192–208 (2002), [arXiv:hep-ph/0204266](#).
- [301] M. B. Green and J. H. Schwarz, *Supersymmetrical Dual String Theory. 2. Vertices and Trees*, *Nucl. Phys. B* **198**, 252–268 (1982).
- [302] J. H. Schwarz, *Superstring Theory*, *Phys. Rept.* **89**, 223–322 (1982).
- [303] A. A. Tseytlin, *Vector Field Effective Action in the Open Superstring Theory*, *Nucl. Phys. B* **276**, [Erratum: *Nucl.Phys.B* 291, 876 (1987)], 391 (1986).

- [304] C. R. Schmidt, $H \rightarrow g g g$ ($g q$ anti- q) at two loops in the large $M(t)$ limit, *Phys. Lett. B* **413**, 391–395 (1997), [arXiv:hep-ph/9707448](#).
- [305] R. Mertig, M. Bohm, and A. Denner, *FEYN CALC: Computer algebraic calculation of Feynman amplitudes*, *Comput. Phys. Commun.* **64**, 345–359 (1991).
- [306] V. Shtabovenko, R. Mertig, and F. Orellana, *New Developments in FeynCalc 9.0*, *Comput. Phys. Commun.* **207**, 432–444 (2016), [arXiv:1601.01167 \[hep-ph\]](#).
- [307] E. D'Hoker and D. Z. Freedman, *Supersymmetric gauge theories and the AdS / CFT correspondence*, in Theoretical Advanced Study Institute in Elementary Particle Physics (TASI 2001): Strings, Branes and EXTRA Dimensions (Jan. 2002), pp. 3–158, [arXiv:hep-th/0201253](#).
- [308] J. A. Minahan and K. Zarembo, *The Bethe ansatz for $N=4$ superYang-Mills*, *JHEP* **03**, 013 (2003), [arXiv:hep-th/0212208](#).
- [309] N. Beisert, *The complete one loop dilatation operator of $N=4$ superYang-Mills theory*, *Nucl. Phys. B* **676**, 3–42 (2004), [arXiv:hep-th/0307015](#).
- [310] N. Beisert and M. Staudacher, *The $N=4$ SYM integrable super spin chain*, *Nucl. Phys. B* **670**, 439–463 (2003), [arXiv:hep-th/0307042](#).
- [311] G. Ferretti, R. Heise, and K. Zarembo, *New integrable structures in large- N QCD*, *Phys. Rev. D* **70**, 074024 (2004), [arXiv:hep-th/0404187](#).
- [312] N. Beisert et al., *Review of AdS/CFT Integrability: An Overview*, *Lett. Math. Phys.* **99**, 3–32 (2012), [arXiv:1012.3982 \[hep-th\]](#).
- [313] B. I. Zwiebel, *From Scattering Amplitudes to the Dilatation Generator in $N=4$ SYM*, *J. Phys. A* **45**, 115401 (2012), [arXiv:1111.0083 \[hep-th\]](#).
- [314] M. Wilhelm, *Amplitudes, Form Factors and the Dilatation Operator in $\mathcal{N} = 4$ SYM Theory*, *JHEP* **02**, 149 (2015), [arXiv:1410.6309 \[hep-th\]](#).
- [315] A. Brandhuber, B. Penante, G. Travaglini, and D. Young, *Integrability and MHV diagrams in $N=4$ supersymmetric Yang-Mills theory*, *Phys. Rev. Lett.* **114**, 071602 (2015), [arXiv:1412.1019 \[hep-th\]](#).
- [316] A. Brandhuber, B. Penante, G. Travaglini, and D. Young, *Integrability and unitarity*, *JHEP* **05**, 005 (2015), [arXiv:1502.06627 \[hep-th\]](#).
- [317] R. Frassek, D. Meidinger, D. Nandan, and M. Wilhelm, *On-shell diagrams, Grassmannians and integrability for form factors*, *JHEP* **01**, 182 (2016), [arXiv:1506.08192 \[hep-th\]](#).
- [318] A. Brandhuber, P. Heslop, G. Travaglini, and D. Young, *Yangian Symmetry of Scattering Amplitudes and the Dilatation Operator in $N = 4$ Supersymmetric Yang-Mills Theory*, *Phys. Rev. Lett.* **115**, 141602 (2015), [arXiv:1507.01504 \[hep-th\]](#).
- [319] E. E. Jenkins, A. V. Manohar, and M. Trott, *Renormalization Group Evolution of the Standard Model Dimension Six Operators I: Formalism and lambda Dependence*, *JHEP* **10**, 087 (2013), [arXiv:1308.2627 \[hep-ph\]](#).
- [320] E. E. Jenkins, A. V. Manohar, and M. Trott, *Renormalization Group Evolution of the Standard Model Dimension Six Operators II: Yukawa Dependence*, *JHEP* **01**, 035 (2014), [arXiv:1310.4838 \[hep-ph\]](#).

- [321] R. Alonso, E. E. Jenkins, A. V. Manohar, and M. Trott, *Renormalization Group Evolution of the Standard Model Dimension Six Operators III: Gauge Coupling Dependence and Phenomenology*, *JHEP* **04**, 159 (2014), [arXiv:1312.2014 \[hep-ph\]](#).
- [322] S. Antusch, M. Drees, J. Kersten, M. Lindner, and M. Ratz, *Neutrino mass operator renormalization revisited*, *Phys. Lett. B* **519**, 238–242 (2001), [arXiv:hep-ph/0108005](#).
- [323] R. Alonso, H.-M. Chang, E. E. Jenkins, A. V. Manohar, and B. Shotwell, *Renormalization group evolution of dimension-six baryon number violating operators*, *Phys. Lett. B* **734**, 302–307 (2014), [arXiv:1405.0486 \[hep-ph\]](#).
- [324] Y. Liao and X.-D. Ma, *Renormalization Group Evolution of Dimension-seven Baryon- and Lepton-number-violating Operators*, *JHEP* **11**, 043 (2016), [arXiv:1607.07309 \[hep-ph\]](#).
- [325] S. Davidson, M. Gorbahn, and M. Leak, *Majorana neutrino masses in the renormalization group equations for lepton flavor violation*, *Phys. Rev. D* **98**, 095014 (2018), [arXiv:1807.04283 \[hep-ph\]](#).
- [326] Y. Liao and X.-D. Ma, *Renormalization Group Evolution of Dimension-seven Operators in Standard Model Effective Field Theory and Relevant Phenomenology*, *JHEP* **03**, 179 (2019), [arXiv:1901.10302 \[hep-ph\]](#).
- [327] M. Chala and A. Titov, *Neutrino masses in the Standard Model effective field theory*, *Phys. Rev. D* **104**, 035002 (2021), [arXiv:2104.08248 \[hep-ph\]](#).
- [328] M. Chala, G. Guedes, M. Ramos, and J. Santiago, *Towards the renormalisation of the Standard Model effective field theory to dimension eight: Bosonic interactions I*, *SciPost Phys.* **11**, 065 (2021), [arXiv:2106.05291 \[hep-ph\]](#).
- [329] S. Das Bakshi, M. Chala, Á. Díaz-Carmona, and G. Guedes, *Towards the renormalisation of the Standard Model effective field theory to dimension eight: Bosonic interactions II*, (2022), [arXiv:2205.03301 \[hep-ph\]](#).
- [330] C. G. Callan Jr., S. R. Coleman, J. Wess, and B. Zumino, *Structure of phenomenological Lagrangians. 2.*, *Phys. Rev.* **177**, 2247–2250 (1969).
- [331] K. Symanzik, *Small distance behavior in field theory and power counting*, *Commun. Math. Phys.* **18**, 227–246 (1970).
- [332] K. Symanzik, *Small distance behavior analysis and Wilson expansion*, *Commun. Math. Phys.* **23**, 49–86 (1971).
- [333] J. Elias-Miro, J. R. Espinosa, E. Masso, and A. Pomarol, *Higgs windows to new physics through $d=6$ operators: constraints and one-loop anomalous dimensions*, *JHEP* **11**, 066 (2013), [arXiv:1308.1879 \[hep-ph\]](#).
- [334] Z. Bern, C. Cheung, R. Roiban, C.-H. Shen, M. P. Solon, and M. Zeng, *Black Hole Binary Dynamics from the Double Copy and Effective Theory*, *JHEP* **10**, 206 (2019), [arXiv:1908.01493 \[hep-th\]](#).
- [335] Z. Bern, J. Parra-Martinez, R. Roiban, M. S. Ruf, C.-H. Shen, M. P. Solon, and M. Zeng, *Scattering Amplitudes, the Tail Effect, and Conservative Binary Dynamics at $O(G^4)$* , (2021), [arXiv:2112.10750 \[hep-th\]](#).
- [336] W.-M. Chen, M.-Z. Chung, Y.-t. Huang, and J.-W. Kim, *Lense-Thirring effects from on-shell amplitudes*, (2022), [arXiv:2205.07305 \[hep-th\]](#).

- [337] J.-W. Kim, *Quantum corrections to frame-dragging in scattering amplitudes*, (2022), [arXiv:2207.04970 \[hep-th\]](#).
- [338] A. Gruzinov and M. Kleban, *Causality Constrains Higher Curvature Corrections to Gravity*, *Class. Quant. Grav.* **24**, 3521–3524 (2007), [arXiv:hep-th/0612015](#).
- [339] B. Bellazzini, C. Cheung, and G. N. Remmen, *Quantum Gravity Constraints from Unitarity and Analyticity*, *Phys. Rev. D* **93**, 064076 (2016), [arXiv:1509.00851 \[hep-th\]](#).
- [340] X. O. Camanho, J. D. Edelstein, J. Maldacena, and A. Zhiboedov, *Causality Constraints on Corrections to the Graviton Three-Point Coupling*, *JHEP* **02**, 020 (2016), [arXiv:1407.5597 \[hep-th\]](#).
- [341] S. Endlich, V. Gorbenko, J. Huang, and L. Senatore, *An effective formalism for testing extensions to General Relativity with gravitational waves*, *JHEP* **09**, 122 (2017), [arXiv:1704.01590 \[gr-qc\]](#).
- [342] N. Sennett, R. Brito, A. Buonanno, V. Gorbenko, and L. Senatore, *Gravitational-Wave Constraints on an Effective Field-Theory Extension of General Relativity*, *Phys. Rev. D* **102**, 044056 (2020), [arXiv:1912.09917 \[gr-qc\]](#).
- [343] H. O. Silva, A. Ghosh, and A. Buonanno, *Black-hole ringdown as a probe of higher-curvature gravity theories*, (2022), [arXiv:2205.05132 \[gr-qc\]](#).
- [344] W. T. Emond and N. Moynihan, *Scattering Amplitudes, Black Holes and Leading Singularities in Cubic Theories of Gravity*, *JHEP* **12**, 019 (2019), [arXiv:1905.08213 \[hep-th\]](#).
- [345] P. van Nieuwenhuizen and C. C. Wu, *On Integral Relations for Invariants Constructed from Three Riemann Tensors and their Applications in Quantum Gravity*, *J. Math. Phys.* **18**, 182 (1977).
- [346] M. H. Goroff and A. Sagnotti, *QUANTUM GRAVITY AT TWO LOOPS*, *Phys. Lett. B* **160**, 81–86 (1985).
- [347] M. Accattulli Huber, A. Brandhuber, S. De Angelis, and G. Travaglini, *From amplitudes to gravitational radiation with cubic interactions and tidal effects*, *Phys. Rev. D* **103**, 045015 (2021), [arXiv:2012.06548 \[hep-th\]](#).
- [348] S. A. Fulling, R. C. King, B. G. Wybourne, and C. J. Cummins, *Normal forms for tensor polynomials. 1: The Riemann tensor*, *Class. Quant. Grav.* **9**, 1151–1197 (1992).
- [349] A. A. Tseytlin, *Ambiguity in the Effective Action in String Theories*, *Phys. Lett. B* **176**, 92–98 (1986).
- [350] R. R. Metsaev and A. A. Tseytlin, *Order alpha-prime (Two Loop) Equivalence of the String Equations of Motion and the Sigma Model Weyl Invariance Conditions: Dependence on the Dilaton and the Antisymmetric Tensor*, *Nucl. Phys. B* **293**, 385–419 (1987).
- [351] D. C. Dunbar, J. H. Godwin, G. R. Jehu, and W. B. Perkins, *Loop Amplitudes in an Extended Gravity Theory*, *Phys. Lett. B* **780**, 41–47 (2018), [arXiv:1711.05526 \[hep-th\]](#).
- [352] D. J. Gross and E. Witten, *Superstring Modifications of Einstein's Equations*, *Nucl. Phys. B* **277**, 1 (1986).
- [353] F. A. Berends and R. Gastmans, *Quantum Electrodynamical Corrections to Graviton-Matter Vertices*, *Annals Phys.* **98**, 225 (1976).

- [354] I. T. Drummond and S. J. Hathrell, *QED Vacuum Polarization in a Background Gravitational Field and Its Effect on the Velocity of Photons*, *Phys. Rev. D* **22**, 343 (1980).
- [355] T. J. Hollowood and G. M. Shore, *The Refractive index of curved spacetime: The Fate of causality in QED*, *Nucl. Phys. B* **795**, 138–171 (2008), [arXiv:0707.2303 \[hep-th\]](#).
- [356] G. Goon and K. Hinterbichler, *Superluminality, black holes and EFT*, *JHEP* **02**, 134 (2017), [arXiv:1609.00723 \[hep-th\]](#).
- [357] M. Accettulli Huber, A. Brandhuber, S. De Angelis, and G. Travaglini, *Note on the absence of R^2 corrections to Newton's potential*, *Phys. Rev. D* **101**, 046011 (2020), [arXiv:1911.10108 \[hep-th\]](#).
- [358] I. I. Shapiro, *Fourth Test of General Relativity*, *Phys. Rev. Lett.* **13**, 789–791 (1964).
- [359] H. Cheng and T. T. Wu, *High-energy elastic scattering in quantum electrodynamics*, *Phys. Rev. Lett.* **22**, 666 (1969).
- [360] M. Levy and J. Sucher, *Eikonal approximation in quantum field theory*, *Phys. Rev.* **186**, 1656–1670 (1969).
- [361] H. D. I. Abarbanel and C. Itzykson, *Relativistic eikonal expansion*, *Phys. Rev. Lett.* **23**, 53 (1969).
- [362] D. Amati, M. Ciafaloni, and G. Veneziano, *Superstring Collisions at Planckian Energies*, *Phys. Lett. B* **197**, 81 (1987).
- [363] D. Amati, M. Ciafaloni, and G. Veneziano, *Higher Order Gravitational Deflection and Soft Bremsstrahlung in Planckian Energy Superstring Collisions*, *Nucl. Phys. B* **347**, 550–580 (1990).
- [364] D. N. Kabat and M. Ortiz, *Eikonal quantum gravity and Planckian scattering*, *Nucl. Phys. B* **388**, 570–592 (1992), [arXiv:hep-th/9203082](#).
- [365] P. Di Vecchia, A. Luna, S. G. Naculich, R. Russo, G. Veneziano, and C. D. White, *A tale of two exponentiations in $\mathcal{N} = 8$ supergravity*, *Phys. Lett. B* **798**, 134927 (2019), [arXiv:1908.05603 \[hep-th\]](#).
- [366] P. Di Vecchia, S. G. Naculich, R. Russo, G. Veneziano, and C. D. White, *A tale of two exponentiations in $\mathcal{N} = 8$ supergravity at subleading level*, *JHEP* **03**, 173 (2020), [arXiv:1911.11716 \[hep-th\]](#).
- [367] R. Akhouri, R. Saotome, and G. Sterman, *High Energy Scattering in Perturbative Quantum Gravity at Next to Leading Power*, *Phys. Rev. D* **103**, 064036 (2021), [arXiv:1308.5204 \[hep-th\]](#).
- [368] Z. Bern, H. Ita, J. Parra-Martinez, and M. S. Ruf, *Universality in the classical limit of massless gravitational scattering*, *Phys. Rev. Lett.* **125**, 031601 (2020), [arXiv:2002.02459 \[hep-th\]](#).
- [369] T. J. Hollowood and G. M. Shore, *Causality and Micro-Causality in Curved Spacetime*, *Phys. Lett. B* **655**, 67–74 (2007), [arXiv:0707.2302 \[hep-th\]](#).
- [370] T. J. Hollowood and G. M. Shore, *Causality Violation, Gravitational Shockwaves and UV Completion*, *JHEP* **03**, 129 (2016), [arXiv:1512.04952 \[hep-th\]](#).
- [371] K. Benakli, S. Chapman, L. Darmé, and Y. Oz, *Superluminal graviton propagation*, *Phys. Rev. D* **94**, 084026 (2016), [arXiv:1512.07245 \[hep-th\]](#).

- [372] T. J. Hollowood and G. M. Shore, *Causality, Renormalizability and Ultra-High Energy Gravitational Scattering*, *J. Phys. A* **49**, 215401 (2016), [arXiv:1601.06989 \[hep-th\]](#).
- [373] C. de Rham and A. J. Tolley, *Speed of gravity*, *Phys. Rev. D* **101**, 063518 (2020), [arXiv:1909.00881 \[hep-th\]](#).
- [374] C. de Rham, J. Francfort, and J. Zhang, *Black Hole Gravitational Waves in the Effective Field Theory of Gravity*, *Phys. Rev. D* **102**, 024079 (2020), [arXiv:2005.13923 \[hep-th\]](#).
- [375] L. Eisenbud, “The formal properties of nuclear collisions”, PhD thesis (Princeton U., 1948).
- [376] D. Bohm, *Quantum theory*, Dover books in science and mathematics (Dover Publications, 1989).
- [377] E. P. Wigner, *Lower Limit for the Energy Derivative of the Scattering Phase Shift*, *Phys. Rev.* **98**, 145–147 (1955).
- [378] D. Nandan, J. Plefka, and G. Travaglini, *All rational one-loop Einstein-Yang-Mills amplitudes at four points*, *JHEP* **09**, 011 (2018), [arXiv:1803.08497 \[hep-th\]](#).
- [379] A. Einstein, *On The influence of gravitation on the propagation of light*, *Annalen Phys.* **35**, 898–908 (1911).
- [380] M. Ciafaloni and D. Colferai, *Rescattering corrections and self-consistent metric in Planckian scattering*, *JHEP* **10**, 085 (2014), [arXiv:1406.6540 \[hep-th\]](#).
- [381] S. L. Adler and W. A. Bardeen, *Absence of higher order corrections in the anomalous axial vector divergence equation*, *Phys. Rev.* **182**, 1517–1536 (1969).
- [382] A. Laddha and A. Sen, *Gravity Waves from Soft Theorem in General Dimensions*, *JHEP* **09**, 105 (2018), [arXiv:1801.07719 \[hep-th\]](#).
- [383] A. Cristofoli, R. Gonzo, D. A. Kosower, and D. O’Connell, *Waveforms from Amplitudes*, (2021), [arXiv:2107.10193 \[hep-th\]](#).
- [384] R. Britto, R. Gonzo, and G. R. Jehu, *Graviton particle statistics and coherent states from classical scattering amplitudes*, *JHEP* **03**, 214 (2022), [arXiv:2112.07036 \[hep-th\]](#).
- [385] A. Cristofoli, R. Gonzo, N. Moynihan, D. O’Connell, A. Ross, M. Sergola, and C. D. White, *The Uncertainty Principle and Classical Amplitudes*, (2021), [arXiv:2112.07556 \[hep-th\]](#).
- [386] D. A. Kosower, *Next-to-maximal helicity violating amplitudes in gauge theory*, *Phys. Rev. D* **71**, 045007 (2005), [arXiv:hep-th/0406175](#).
- [387] R. Lidl and H. Niederreiter, *Introduction to finite fields and their applications*, 2nd ed. (Cambridge University Press, 1994).
- [388] T. Peraro, *FiniteFlow: multivariate functional reconstruction using finite fields and dataflow graphs*, *JHEP* **07**, 031 (2019), [arXiv:1905.08019 \[hep-ph\]](#).
- [389] P. S. Wang, *A p-adic algorithm for univariate partial fractions*, in *Proceedings of the fourth acm symposium on symbolic and algebraic computation*, SYMSAC ’81 (1981), pp. 212–217.